Biopolymer Methods in Tissue Engineering

Edited by

Anthony P. Hollander
Paul V. Hatton

✳ HUMANA PRESS

1

Processing of Resorbable Poly-α-Hydroxy Acids for Use as Tissue-Engineering Scaffolds

Minna Kellomäki and Pertti Törmälä

1. Introduction

1.1. Absorbable Poly-α-Hydroxy Acids

Poly (α-hydroxyacids) were found to be bioabsorble and biocompatible in the 1960s *(1,2)*. They are the most widely known, studied and used bioabsorbable synthetic polymers in medicine. Polyglycolide (PGA) and poly-L-lactide (PLLA) homopolymers and their copolymers (PLGA), as well as polylactic acid stereocopolymers produced using L-, D-, or DL-lactides and rasemic polymer copolymer PLDLA are all poly (α-hydroxyacids) *(3)*. Poly (α-hydroxy acids) can be polymerized via condensation, although only low mol-wt polymers are produced. In order to obtain a higher mol wt and thus mechanical strength and longer absorption time, the polymers are polymerized from the cyclic dimers via ring-opening polymerization using appropriate initiators and co-initiators. The most commonly used initiator is stannous octoate *(2,3)*.

The absorption rate both in vitro and in vivo of the poly (α-hydroxy acids) is dependent on the microstructural, macrostructural, and environmental factors listed in **Table 1**. The degradation mechanism is mainly hydrolysis. Polylactides (PLAs) absorb via bulk erosion—e.g., erosion occurs simultaneously throughout the device. Some studies have revealed an autocatalytic degradation of PLAs. Autocatalysis shows as a more dense surface layer and as faster degradation inside the samples which has also been reported for as-polymerized PLLA *(7)*, for PLLA *(8)*, for PLLA-fiber-reinforced PLDLA 70/30 *(9)*, for PDLLA *(10)*, and for PLA50 samples *(11)*. Li et al. have proposed a degradation model for PLA50 with a faster degrading core and a more slowly degrading shell

Table 1
Factors That Affect Hydrolytic Degradation *(3–6)*

Microstructural factors
    Chemical structure
    Chemical composition
    Distribution of repeat units in multimers
    Presence of ionic groups
    Presence of unexpected units or chain defects
    Permeability to water
    Configurational structure
    Mol-wt and mol-wt distribution (polydispersity)
    Morphology
        Crystalline vs amorphous
        Molecular orientation
        Presence of microstructures
        Presence of residual stresses
        Matrix/reinforcement morphology
    Impurities and additives
    Porosity
    Surface quality
Macrostructural factors
    Size and geometry of the implant (design)
    Weight/surface area ratio
    Processing method and conditions
    Annealing
    Method of sterilization
    Storage history
Environmental factors
    Tissue environment; site of implantation or injection
    pH, ion exchange, ionic strength, and temperature of the degradation medium
    Adsorbed and absorbed compounds (e.g., water, lipids, ions)
    Mechanism of degradation (enzymes vs water)

(11). In general, the autocatalytic phenomenon has been reported in non-fibrillated polylactide samples but not in fibrillated structure *(12)*. This variation may originate from the different processing histories. Because of mechanical deformation *(13)*, the fibrillated (e.g., self-reinforced) materials contain microscopical longitudinal channels or capillaries between fibrils. These channels may absorb buffer solution into the sample and carry degradation products away from the bulk polymer into the surrounding buffer solution, thus preventing the autocatalysis.

The tissue reactions caused by PGA vary from moderate to severe complications, such as local fluid accumulation and transient sinus formation *(14)*. Tissue reactions of PLLA, PLA stereocopolymers, PLDLA, and PLGA copolymers vary from none *(15)* via moderate *(16)* to severe foreign body reactions *(17)*. Tissue reactions caused by PLLA fluctuate according to the degradation stage of the polymer *(18)*, and probably increase when PLLA starts to lose mass substantially *(19)*. No complete explanation for these different reactions has been reported.

PLA and PGA as homopolymers or different copolymer combinations have been studied and used for several applications. Clinically, their uses as implants include sutures, suture anchors, staples, interference screws, screws, plates, and meniscus arrows *(20)*.

1.2. Tissue-Engineering Scaffolds

The main goal of tissue engineering is to produce new tissue where it is needed. Therefore, knowledge of the structure and functional limits of the regenerated tissue is essential. The cell type should be suitable for the implanted site, and preferably the cells should be from the patient—e.g., autologous. The volume of cells that can be transferred into a body and retained functionally is limited to 1–3 μL, for example, if it is injected. The scaffold should thus provide a greater surface area where cells can grow *(21)*.

Biomaterials in tissue-engineered substitutes serve as a structural component and provide the proper three-dimensional (3D) architecture of the construct. The scaffold provides a 3D matrix for guided cell proliferation and controls the shape of the bioartificial device *(22)*. Principally, a scaffold should have high porosity and have suitable pore sizes, and the pores should be interconnected *(21)*.

Scaffolds designed for tissue engineering should mimic the site where they will be implanted as closely as possible, and they should support cell growth. All tissues have their own architecture. Organs, such as liver, kidney, and bone, have parenchymal and stromal components. The parenchyma is the physiologically active part of the organ, and the stroma is the framework to support the organization of the parenchyma *(21,23)*. For example, to provide a bone defect with a stromal substitute, spaces that are morphologically suitable for osteons and vascularization enable the biological response to be supported, and the regenerative process is enhanced *(23)*. For an ideal cortical bone scaffold, several studies have been performed to reveal the optimal pore size, and results vary from 40 μm for polyethylene scaffolds *(25)* to 50–100 μm *(24,26)* and 500–600 μm for ceramic scaffolds *(23)*. In fact, pore size for optimal tissue ingrowth may be material-specific, not only cell-specific. Studies show that different cells prefer differently sized pores. As examples of different cells, fibrovascular tissues appear to require pore sizes greater than 500 μm for rapid vascularization and for the survival of transplanted cells *(27)*, and for

chondrocytes, 20 µm is better than 80 µm *(28)*. Even 90 µm pores are colonized by growing cells, but this does not occur with 200-µm pores *(29)*. For each application the total porosity should be high—for example, for cartilage tissue engineering it should be 92–96% *(30)*.

Several criteria define the ideal material for tissue-engineering scaffolds. The material should be biocompatible, absorbable, and easily and reproducibly processable, and the surface of the material should interact with cells and tissues *(31)*. The material should not transfer antigens, and it should be immunologically inert *(21)*. The most commonly used scaffold materials are the natural polymers (such as chitosan, collagen, and hyaluronic acid with its derivatives), ceramics such as hydroxyapatite and transformed coral, and synthetic bioabsorbable polymers (of these, PGA and PLGA copolymers have been the most studied). A relatively new approach to make biomimetic materials is to introduce biological activity through natural molecules *(32)*. For example, fibrin can be crosslinked with biomimetic characters *(33,34)*. Advantages of synthetic bioabsorbable polymers compared to the others—especially for commercially available poly-α-hydroxy acids—include the reproducibility of the raw polymer, good processability, and existing knowledge of the material behavior in the body.

The scaffolds studied have included gels, foils, foams, membranes, and capillary membranes, non-wovens and other textiles, tubes, microspheres and beads, porous blocks, and specialized 3D shapes. Porosity made by leaching salts or porosity made by fibrous structure has been achieved for polymer scaffolds. Other methods applied have included non-woven technology, freeze drying, rapid prototyping, 3D printing, and phase separation *(15,21,31,35–49)*.

Knitting is one way to manufacture from polymer filaments even large quantities of porous structures with controlled porosity and pore size. The simplest method to produce knitted structures made of bioabsorbable polymers is introduced in this chapter.

2. Materials
2.1. Source of PLAs

For the purposes of this chapter, we will use as an example, the use of a medical-grade polylactide L- and D-stereocopolymer (PLA 96) purchased from Purac Biochem b.v. (Gronichem, The Netherlands). However, exactly the same method can be used with other poly-α-hydroxy acids.

2.2. Characteristics of PLA 96

The initial L/D ratio was 96/4, and it was a medical-grade, highly purified polymer with residual monomer less than 0.5% (by gas chromatography; manufacturer's information). The other characteristics of the polymer were:

1. Mol-wt, 4.2 dL/g (chloroform, 25°C, measured by the raw material supplier).
2. Partially crystalline with melting enthalpy (H_m) 31.8–40.1 J/g.
3. Glass transition temperature (T_g): 57–59°C.
4. Melting range: 144–168°C.
5. Peak value of melting temperature (T_m) 164–166°C (all thermal properties measured using Perkin-Elmer DSC7 equipment under N_2-gas from specimens weighing 6 ± 0.2 mg, heating range 27–215°C and rate 20°C/min, thermal cycle heating–cooling–heating).

3. Methods
3.1. Drying

1. Prior to extrusion, pre-dry PLA96 in vacuum at an elevated temperature to remove the excess moisture from the structure of the polymer granules (*see* **Note 1**). Any vacuum chamber that is large enough to accommodate all of the polymer spread in a thin layer onto a tray and able to reach a 10^{-5} torr vacuum is adequate.
2. Drying temperature can vary between T_g and T_m, and the temperature directly corresponds to the drying time (*see* **Note 2**).
3. Care must be taken to avoid thermally destroying the polymer during drying but still dry the polymer.
4. The polymer can be stored briefly over drying agent before processing, but for no longer than 4 h.

3.2. Extrusion

1. Melt-spin four-ply multifilament yarn from PLA96 (*see* **Note 3**) using a Gimac microextruder ϕ 12 mm (Gimac, Castronno, Italy) and a spinneret with four orifices each ϕ 0.4 mm (*see* **Note 4**).
2. Use a screw with a small compression rate (*see* **Note 5**).
3. At spinning, temperatures must be between 165° and 260°C, and the highest must be the die temperature.
4. The spinning should be performed under protective gas (dry nitrogen) to prevent thermal degradation of the polymer in processing.
5. Orient the yarn by drawing it freely in a three-step process at elevated temperatures between T_g and T_m.
6. The drawing line must consist of three drawing units with adjustable speeds and with heated chambers in between.
7. Temperatures of the chambers will depend on the thickness of the filaments and their initial strength.
8. It is possible to reach a draw ratio (DR) of approx 5 by this method, when DR is calculated as a ratio of the speeds of the first and last drawing units.
9. In order to obtain good quality filaments, no melt fracture on the surfaces of the filaments must be allowed after extruder die.
10. It may be necessary to change the die temperature within a couple of degrees centigrade during the processing. Also, it is best to start with a low DR and

then to increase it gradually because the process is easier to control (*see* **Notes 6** and **7**).

11. Under these conditions, the final diameter of each filament will be between 70 and 120 µm when melt-spun varying these parameters (*see* **Note 8**). The tensile strength of the filaments will be 450–600 MPa and Young's modulus between 6.5 GPa and 8.5 GPa, depending on the DR (4.0–4.8) and the thickness of the fibers.

3.3. Knitting

1. The yarn can be knitted into a tubular mesh using a tubular single jersey knitting machine (for example, Elha R-1s, Textilmaschinenfabrik Harry Lucas GmbH & Co KG, Neumünster, Germany).
2. The knitting machine has a cylinder that varies in size (diameter), which has needles with which knitting is performed (*see* **Note 9**).
3. The quantity of the needles in a cylinder can vary depending on the desired density of the knitting.
4. Knit the PLA 96 yarn to a tubular mesh form using a 19-needle cylinder of 0.5 inches in diameter.
5. Taylor the loop size of the knit using a combination of the position of the needles and the cylinder (e.g., how high the needles rise in knitting procedure) and the pulling force of the ready knit (*see* **Note 10**).
6. The minimum size of the loops in knitting will be determined by the size of the needles (e.g., how small a loop can go through the needle hook). For example, use a loop size of 650–800 µm (width of the loop) and 950–1300 µm (length of the loop) to achieve successful knitting from 80-µm filaments.

3.4. Gamma Sterilization

1. The sterilization method recommended for PLA products is gamma irradiation (*see* **Note 11**) with a ^{60}Co gun as the source of radiation.
2. The process is usually performed by a commercial company, and the minimum dose of irradiation applied should be 25 kGy.
3. All the devices for irradiation should be clean (if necessary, wash with ethanol and dry) before packing into plastic sachets or other containers suitable for gamma irradiation (*see* **Note 12**).
4. Preferably use double packing.

4. Notes

1. Drying the polymer before processing is extremely important. If not done properly, the melt-spinning cannot be performed.
2. Drying temperature and time both depend on the molecular structure of the polymer, and several temperature/time combinations have been found to be suitable.
3. Purified polymers should be used in processing devices. Otherwise, degradation rate is unpredictable, and degradation may occur very rapidly.

4. Standard extruders are not suitable equipment for processing the bioabsorbable polymers. The equipment must be modified for shear and thermally sensitive materials to cause as low shear stresses as possible.

5. Also, extrusion parameters, such as screw speed and temperatures of die and extruder barrel zones, should be carefully selected because even a slight change in parameters cause dramatic loss in degradation rate of the end-product.

6. Optimal processing parameters depend on the polymer used—for example, on the molecular structure of the polymer chain, stereoregularity, crystallinity, and mol wt of the polymer. Again, very small changes influence optimal parameter selection.

7. Virtually all poly-α-hydroxy acids are processable to filaments, but in each case the parameters must be studied and optimized separately.

8. Each separate spun filament should be as thin as possible to enable efficient knitting to small loop size.

9. For knitting, it is essential to have all the filaments running from the spool smoothly and simultaneously.

10. The loop size of the knit influences the pore size of the scaffold.

11. Gamma irradiation is the most commonly used sterilization method for bioabsorbable polymers.

12. The mol wt of the polymer inevitably drops 40–60% as a result of processing and gamma irradiation.

References

1. Kulkarni, R. K., Pani, K. C., Neuman, C., and Leonard, F. (1966) Polyglycolic acid for surgical implants. *Arch. Surg.* **93,** 839–843.

2. Kulkarni, R. K., Moore, E. G., Hegyeli, A. F., and Leonard, F. (1971) Biodegradable poly (lactic acid) polymers. *J. Biomed. Mater. Res.* **5,** 169–181.

3. Vert, M., Christel, P., Chabot, F., and Leray, J. (1984) Bioresorbable plastic materials for bone surgery, in *Macromolecular Biomaterials* (Hastings, G. W. and Ducheyne, P., eds.), CRC Press, Inc., Boca Raton, FL, pp. 119–142.

4. Vert, M. (1989) Bioresorbable polymers for temporary therapeutic applications. *Angewende Makromolekulare Chemie* **166/167,** 155–168.

5. Piskin, E. (1994) Review. Biodegradable polymers as biomaterials. *J. Biomater. Sci., Polym. Ed.* **6,** 775–795.

6. Törmälä, P., Pohjonen, T., and Rokkanen, P. (1998) Bioabsorbable polymers: materials technology and surgical applications. *Proceedings of the Institution of Mechanical Engineers. Journal of Engineering in Medicine Part H* **212–H,** 101–111.

7. Kellomäki, M. (1993) Polymerization of lactic acid and property studies. M.Sc. Thesis (in Finnish), Tampere University of Technology, Materials Department. 131 pages.

8. Li, S. M., Garreau, H., and Vert, M. (1990) Structure-property relationships in the case of the degradation of massive poly-(α-hydroxy acids) in aqueous media, Part 1, Influence of the morphology of poly(L-lactic acid). *Journal of Materials Science: Materials in Medicine* **1,** 198–206.

9. Dauner, M., Hierlemann, H., Caramaro, L., Missirlis, Y., Panagiotopoulos, E., and Planck, H. (1996) Resorbable continuous fibre reinforced polymers for the osteosynthesis processing and physico-chemical properties, in *Fifth World Biomaterials Congress*, Toronto, Canada, p. 270.

10. Ali, S. A. M., Doherty, P. J., and Williams, D. F. (1993) Mechanisms of polymer degradation in implantable devices. 2. Poly(DL-lactic acid). *J. Biomed. Mater. Res.* **27,** 1409–1418.

11. Li, S. M., Garreau, H., and Vert, M. (1990) Structure-property relationships in the case of the degradation of massive aliphatic poly-(α-hydroxy acids) in aqueous media, Part 1, Poly (DL-lactic acid). *Journal of Materials Science: Materials in Medicine* **1,** 123–130.

12. Pohjonen, T. (1995) Manufacturing, structure and properties of SR-PLLA. Licenciate thesis (in Finnish), Tampere University of Technology, 295 pages.

13. Törmälä, P. (1992) Biodegradable self-reinforced composite materials; manufacturing, structure and mechanical properties. *Clin. Mater.* **10,** 29–34.

14. Böstman, O., Hirvensalo, E., Mäkinen, J., and Rokkanen, P. (1990) Foreign-body reactions to fracture fixation implants of biodegradable synthetic polymers. *British Journal of Bone and Joint Surgery* **72–B,** 592–596.

15. Thomson, R. C., Mikos, A. G., Beahm, E., Lemon, J. C., Satterfied, W. C., Aufdemorte, T. B., et al. (1999) Guided tissue fabrication from periosteum using performed biodegradable polymer scaffolds. *Biomaterials* **20,** 2007–2018.

16. Bergsma, J. E., Bos, R. R. M., Rozema, F. R., de Jong, W., and Boerig, G. (1995) Biocompatibility of intraosseously implanted predegraded poly(lactide). An animal study. 12th ESB Conference, Porto, Portugal.

17. Van der Elst, M., Klein, C. P. A. T., de Blieck-Hogervorst, J. M., Patka, P., and Haarman, H. J. (1999) Bone tissue response to biodegradable polymers used for intra medullary fracture fixation: A long-term *in vivo* study in sheep femora. *Biomaterials* **20,** 121–128.

18. Hooper, K. A., Macon, N. D., and Kohn, J. (1998) Comparative histological evaluation of new tyrosine-derived polymers and poly (L-lactic acid) as a function of polymer degradation. *J. Biomed. Mater. Res.* 41, 443–454.

19. Bos, R. R. M., Rozema, F. R., Boering, G., Nijenhuis, A. J., Pennings, A. J., Verwey, A. B., et al. (1991) Degradation of and tissue reaction to biodegradable poly(L-lactide) for use as internal fixation of fractures: a study in rats. *Biomaterials* **12,** 32–36.

20. Maitra, R. S., Brand (Jr) J. C., and Caborn, D. N. M. (1998) Biodegradable implants. *Sports Medicine and Arthroscopy Review* **6,** 103–117.

21. Patrick Jr., C. W., Mikos, A. G., and McIntire, L. V. (eds.), (1998) *Frontiers in Tissue Engineering*. Pergamon, Oxford, UK, p. 700.

22. Nerem, R. M. and Sambanis, A. (1995) Tissue engineering: from biology to biological substitutes. *Tissue Engineering* **1,** 3–13.

23. Shors, E. C. and Holmes, R. E. (1993) Porous hydroxyapatite, in *An Introduction to Bioceramics* (Hench, L. L., Wilson, J., eds.), World Scientific, Singapore, 181–198.

24. Klawitter, J. J. and Hulbert, S. F. (1971) Application of porous ceramics for the attachment of load bearing orthopedic applications. *J. Biomed. Mater. Symp.* **2,** 161.

25. Klawitter, J. J., Bagwell, J. G., Weinstern, A. M., Sauer, B. W., and Pruitt, J. R. (1976) An evaluation of bone growth into porous high density polyethylene. *J. Biomed. Mater. Res.* **10,** 311–323.
26. Eggli, P. S., Müller, W., and Schenk, R. K. (1988) Porous hydroxyapatite and tricalcium phosphate cylinders with two different pore size ranges implanted in the cancellous bone of rabbits. *Clin. Orthop. Relat. Res.* **232,** 127–138.
27. Wake, N. C., Patrick, C. W., and Mikos, A. G. (1994) Pore morphology effects on the fibrovascular tissue growth in porous polymer substrates. *Cells and Transplants* **3,** 339–343.
28. Nehrer, S., Breinan, H. A., Ramappa, A., et al. (1997) Matrix collagen type and pore size influence behaviour of seeded canine chondrocytes. *Biomaterials* **18,** 769–776.
29. Grande, D. A., Halberstadt, C., Naughton, G., Schwartz, R., and Manji, R. (1997) Evaluation of matrix scaffolds for tissue engineering of articular cartilage grafts. *J. Biomed. Mater. Res.* **34,** 211–220.
30. Freed, L. E., Grande, D. A., Lingbin, Z., et al. (1994) Joint resurfacing using allograft chondrocytes and synthetic biodegradable polymer scaffolds. *J. Biomed. Mater. Res.* 28, 891–899.
31. Cima, L. G., Vacanti, J. P., Vacanti, C., Ingber, D., Mooney, D., and Langer, R. (1991) Tissue engineering by cell transplantation using degradable polymer substrates. *Journal of Biomechanical Engineering* **113,** 143–151.
32. Hubbel, J. A. (2000) Biomimetic materials, in *The Art of Tissue Engineering Symposium.* 17.11.2000 Utrecht, The Netherlands (published as a CD-ROM).
33. Schense, J. C. and Hubbel, J. A. (1999) Cross-liking exogenous bifunctional peptides into fibrin gels with factor XIIIa. *Bioconjuctival Chemistry* **10,** 75–81.
34. Schense, J. C., Bloch, J., Aebischer, P., and Hubbel, J. A. (2000) Enzymatic incorporation of bioactive peptides into fibrin matrices enhances neurite extension. *Nat. Biotechnol.* **18,** 415–419.
35. Vacanti, C. A., Langer, R., Schloo, B., and Vacanti, J. P. (1991) Synthetic polymers seeded with chondrocytes provide a template for new cartilage formation. *Plast. Reconstr. Surg.* **88,** 753–759.
36. Chu, C. R., Coutts, R. D., Yoshioka, M., Harwood, F. L., Monosov, A. Z., and Amiel, D. (1995) Articular cartilage repair using allogeneic perichondrocyte seeded biodegradable porous polylactic acid (PLA): A tissue-engineering study. *J. Biomed. Mater. Res.* **29,** 1147–1154.
37. Ma, P. X., Schloo, B., Mooney, D., and Langer, R. (1995) Development of biomechanical properties and morphogenesis of *in vitro* tissue engineered cartilage. *J. Biomed. Mater. Res.* **29,** 1587–1595.
38. Laurencin, C. T., Attawia, M. A., Elgendy, H. E., and Herbert, K. M. (1996) Tissue engineered bone-regeneration using degradable polymers: the formation of mineralized matrices. *Bone* **19,** 93s-99s.
39. Mooney, D. J., Baldwin, D. F., Suh, N. P., Vacanti, J. P., and Langer, R. (1996) Novel approach to fabricate porous sponges of poly(D,L-lactic-co-glycolic acid) without the use of organic solvents. *Biomaterials* **17,** 1417–1422.

40. Mooney, D. J., Mazzoni, C. L., Breuer, C., McNamara, K., Hern, D., Vacanti, J. P., et al. (1996) Stabilized polyglycolic acid fibre-based tubes for tissue engineering. *Biomaterials* **17,** 115–124.

41. Sittinger, M., Reitzel, D., Dauner, M., Hierlemann, H., Hammer, C., Kastenbauer, E., et al. (1996) Resorbable polymers in cartilage engineering: affinity and biocompatibility of polymer fiber structures to chondrocytes. *J. Biomed. Mater. Res.* **33,** 57–63.

42. Wintermantel, E., Mayer, J., Blum, J., Eckert K-L, Lüscher, P., and Mathey, M. (1996) Tissue engineering scaffolds using superstructures. *Biomaterials* **17,** 83–91.

43. Widmer, M. S., Gupta, P. K., Lu, L., Meszlenyi, R. K., Evans, G. R. D., Brandt, K., et al. (1998) Manufacture of porous biodegradable polymer conduits by an extrusion process for guided tissue regeneration. *Biomaterials* **19,** 945–1955.

44. Angele, P., Kujat, R., Nerlich, M., Yoo, J., Goldberg, V., and Johnstone, B. (1999) Engineering of osteochondral tissue with bone marrow mesenchymal progenitor cells in a derivatized hyaluronan-gelatin composite sponge. *Tissue Engineering* **5,** 545–554.

45. Doser, M. (1999) Criteria for the selection of biomaterials for tissue engineering, in *Polymers for Medical Technologies*, 37th Tutzing-Symposon of Dechema e.V. 8–11.3.1999.

46. Kreklau, B., Sittinger, M., Mensing, M. B., Voigt, C., Berger, G., Burmester, G. R., et al. (1999) Tissue engineering of biphasic joint cartilage transplants. *Biomaterials* **20,** 1743–1749.

47. Madihally, S. V. and Matthew, H. W. T. (1999) Porous chitosan scaffolds for tissue engineering. *Biomaterials* **20,** 1133–1142.

48. Redlich, A., Perka, C., Schultz, O., Spitzer, R., Häupl, T., Burmester, G. R., and et al. (1999) Bone engineering on the basis of periosteal cells cultured in polymer fleeces. *Journal of Materials Science: Materials in Medicine* **10,** 767–772.

49. Huibregtse, B. A., Johnstone, B., Goldberg, V. M., and Caplan, A. I. (2000) Effect of age and sampling site on the chondro-osteogenic potential of rabbit marrow-derived mesenchymal progenitor cells. *J. Orthop. Res.* **18,** 18–24.

Fibrin Microbeads (FMB) As Biodegradable Carriers for Culturing Cells and for Accelerating Wound Healing

Raphael Gorodetsky, Akiva Vexler, Lilia Levdansky, and Gerard Marx

1. Introduction

Fibrinogen exerts adhesive effects on cultured fibroblasts and other cells. Specifically, fibrin(ogen) and its various lytic fragments (e.g., FPA, FPB, fragments D and E) were shown to be chemotactic to macrophages, human fibroblasts, and endothelial cells *(1–3)*. Thrombin has also been shown to exert proliferative and adhesive effects on cultured cells *(4–7)*. We previously demonstrated that covalently coating inert Sepharose beads with either fibrinogen or thrombin rendered them adhesive to a wide range of cell types. We employed such coated Sepharose beads to screen or rank normal and transformed cells for their haptotactic responses to fibrinogen *(8,9)*.

Micro-carrier beads made of some plastic polymers or glass provide cells with a surface area on the order of 10^4 cm^2/L for cell attachment, which is one order of magnitude larger than the area available with stack plates or multi-tray cell-culture facilities *(10)*. From the point of view of transplantation biology, the major disadvantage of such cell micro-carriers is that most of them are not biodegradable or immunogenic. Others have prepared microparticles from plasma proteins, such as albumin or fibrinogen, generally using glutaraldehyde to cross-link the proteins. However, glutaraldehyde is not appropriate for preparing cell-culture matrices because such crosslinking slows down degradation of the matrix or blocks the protein epitopes that may attract cells. Consequently, the use of glutaraldehyde crosslinked micro-carriers has been limited to drug release or imaging *(11–17)*.

Based on our experience with the attraction of many normal cell types to fibrin(ogen) with minimal effect on their proliferation *(8,9)*, we fabricated small

microbeads of fibrin (FMB) that could be loaded with cells and grown as a dense suspension. The FMB were found to be haptotactic to a wide range of cell types. These include normal cells such as primary endothelial cells, smooth muscle cells (SMCs), fibroblasts, chondrocytes, and osteoblasts, and osteogenic bone marrow-derived progenitors, as well as several transformed cells, such as 3T3 and mouse mammary carcinoma lines *(18,19)*. FMB minimally attached normal keratinocytes and different cell lines of the leukocytic lineage. Cells could be maintained on FMB in extremely high densities for more than 2 wk and could be transferred to seed culture flasks or to be downloaded without prior trypsinization. Light, fluorescent, and confocal laser microscopy revealed that—depending on the cell type tested—beads could accommodate up to a few dozen cells per FMB, because of their high surface area, with minimized contact inhibition.

In a pigskin wound-healing model, we showed that FMB + fibroblasts could be transplanted into full-thickness punch wounds and by the third day after wounding, only the wounds in which fibroblasts on FMB were added showed significant formation of granulation tissue, compared to other treatment modalities, such as the addition of PDGF-BB *(9)*.

We are interested in developing these new biodegradable fibrin-derived microbeads (FMB), 50–300 µm in diameter, as potent cell carriers. FMB technology enables one to transfer cells in suspension into wounds as "liquid-tissue." The non-trypsinized cells on FMB can download onto the wound bed, repopulate it with cells that can regenerate extracellular matrix (ECM), and stimulate neovascularization. Currently, FMB + cells are being evaluated in a number of animal models in which the intention is to regenerate tissues such as skin or bone *in situ*. We anticipate many uses of the novel FMB technology for cell culturing, wound healing, and tissue engineering.

2. Materials

2.1. Fibrinogen and Thrombin

Fibrinogen prepared by fractionation of pooled plasma is a component of clinical-grade fibrin sealant that is typically virus-inactivated by methods such as solvent detergent (S/D) process *(20,21)* with human thrombin (stock 200 U/mL) as previously described *(20)*. The activity of thrombin is performed by clot time assays calibrated against an international standard (Vitex Inc., New York, NY).

2.2. Culture Reagents

For the experimental work that is described here, the culture-medium components were purchased mainly from Biological Industries (Beit-HaEmek, Israel), and fetal calf serum (FCS) was supplied by GIBCO-BRL (Grand Island, New York, NY). Other equivalents should work the same.
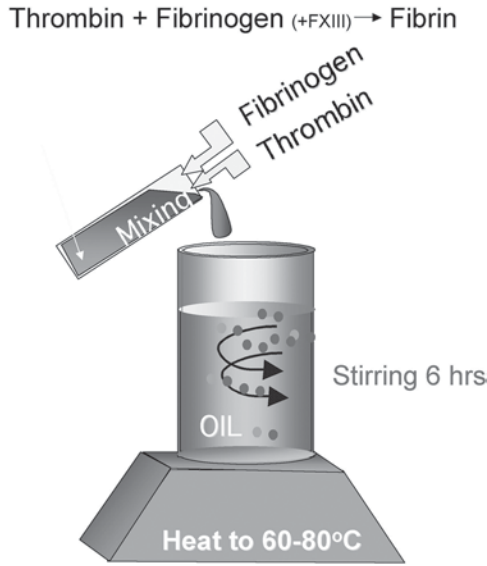
Thrombin + Fibrinogen (+FXIII)→ Fibrin

Fig. 1. Cartoon showing the setup for producing FMB by the oil emulsion method.

3. Methods

3.1. FMB Preparation

A typical preparation of FMB is carried out as described in the following steps *(19)*:

1. Heat 400 mL corn or other type of compatable oil to 60–75°C with high-speed mechanical stirring.
2. Prepare a solution of fibrinogen (25 mL; 35–50 mg/mL) in Tris/saline buffer (pH 7.4) with 5 mM Ca^{+2} and mix it with thrombin to 5 U/mL (final concentration) to initiate the coagulation reaction.
3. Add the protein mixture to the heated oil as a flowing gel, and disperse to droplets by vigorous stirring.
4. Under these conditions, the thrombin will promote fibrin polymerization and activate endogenous, relatively heat-stable factor XIII, which can crosslink the fibrin droplets in the heated oil.
5. Continue the mixing and heating at a temperature of ~65–70°C for 5–7 h.
6. Filter off the crude FMB.
7. Sequentially wash with solvent such as hexane and acetone, then air-dry (**Fig. 1**). The resultant FMB will be highly crosslinked, have a low water content, and will be insoluble in water or organic solvents.

8. Wash and resuspend the FMB in 96% ethanol until their use, preferably for at least 24 h. Before using the FMB, wash extensively in sterile phosphate-buffered saline (PBS).
9. The FMB can also be pre-sterilized by gamma irradiation.

3.2. Solubility, Density, and Sodium Dodecyl Sulfate-Polyacrylamide Gel Electrophoresis (SDS-PAGE)

1. Test the FMB for solubility in Tris/saline or in 4 *M* urea. The Tris buffer nor the 4 *M* urea should not significantly dissolve the FMB, even after 1 wk at room temperature.
2. To carry out SDS-PAGE analysis, partially digest the FMB using 0.1 *N* NaOH for 1 or 2 h and subject to non-reduced 4–12% gradient SDS-PAGE (Nova, Encino, CA), with fibrinogen as a control. The non-reduced SDS-PAGE of NaOH digests of FMB should show that FMB contains many more crosslinks than observed with normally clotted fibrin, which usually show only γ-γ dimers and loss of α and γ bands as well as a-a multimers (**Fig. 2**).
3. Determine the density of the FMB by layering an aliquot of it onto a sucrose solution of known density. After centrifugation, one can observe that the FMB settles to the bottom or remains on top of the sucrose. Carry out this test using a series of sucrose solutions of different concentrations (and densities), and thereby determine the minimal density of sucrose at which the FMB do not settle at the bottom of the tube to determine their density. Typically, FMB have a density of 1.3 ± 0.05 that enables them to settle down in the bottom of the rotating spinning tubes used for cell growth.

3.3. Cell Cultures

1. Isolate normal human fibroblasts (HF) from skin biopsies of young human subjects as previously described *(8)*. These cells can be grown for at least 12 passages.
2. Prepare porcine SMCs by separating them from the thoracic aortas of young animals and grow for up to 10 passages.
3. Other cell lines that were tested include the murine fibroblast line (3T3), murine leukemic cell line (P-388), human ovarian carcinoma line (OV-1063), murine mammary adenocarcinoma cells (EMT-6), and murine macrophage-like cell line (J774.2), all of which should be grown and maintained as previously described *(8,9)*.
4. Maintain all cell cultures at 37°C in a water-jacketed CO_2 incubator, and harvest cells using trypsin/versen solution with 1–2 passages per wk in a split ratio of 1:10 for fast-proliferating transformed cells and 1:4 for normal cell types.

3.4. Assay for FMB Attachment to Cells

Assay for haptotaxis induced by FMB to attached cells in monolayer is done as previously described *(8)*, and is summarized here. It is similar to the test of the response to fibrinogen-coated Sepharose beads (SB-fib) that was previously described *(8)*.
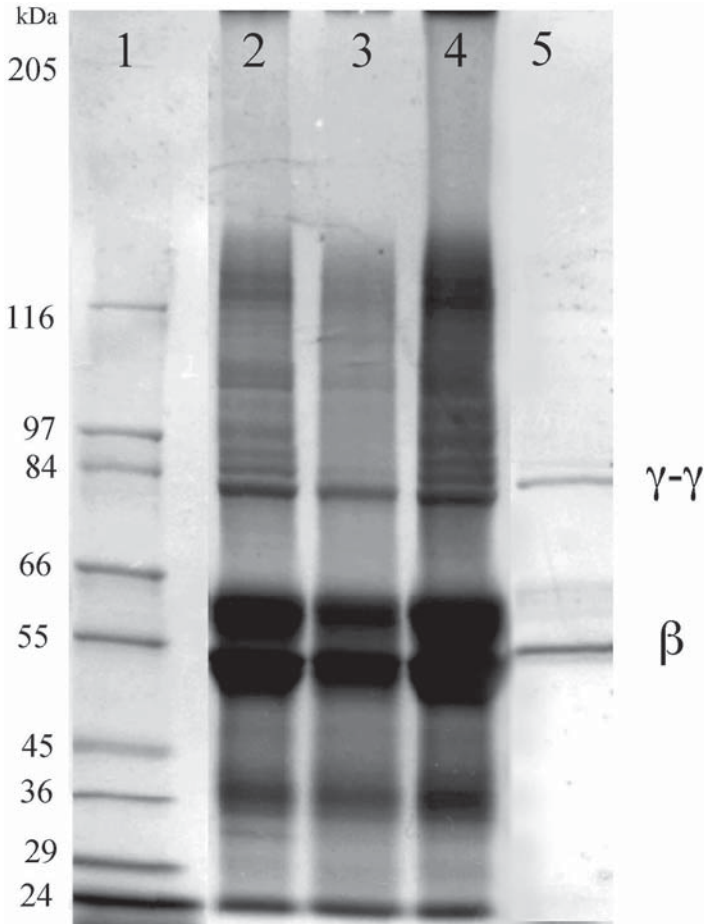
Fig. 2. Non-reduced 4–12% SDS-PAGE of NaOH-degraded FMB *(2–4)* and fibrino-gen *(5)*. Note the prevalence of crosslinked fragments in FMB.

1. Add FMB to a growing culture in a 12-well plate and count the attached beads per well periodically by visual inspection with an inverted phase microscope (typically 300 beads but not less then 200 FMB/well) (*see* **Note 1**). Initially, all FMB roll freely over the near-confluent culture.
2. Count the number of FMB anchored to the cell layer at different time intervals from 4 h onward, and calculate the ratio of FMB bound to the cells, relative to their total number. All experiments are done at least with triplicates.
3. FMB attachment to normal and transformed cells should correspond to the cell interactions with fibrin bound to otherwise nonreactive Sepharose beads (SB-Fib)

Table 1
Cell Attachment to SB-Fibrinogen and FMB (%) *

Primary cells	SB-fibrinogen	FMB
Human fibroblasts	>92	>95
Pig fibroblasts	>92	>95
Normal human keratinocytes	<5	<5
Mouse osteoblasts	>95	>95
Pig smooth-muscle cells	75	>95
Human chondrocytes	ND	>95
Bovine endothelial cells	>95	>95
Pig kidney epithelial cells	ND	>95
Transformed Cell Lines		
3T3/NIH fibroblasts	>90	>95
OV-1063 human ovarian carcinoma cells	0	10
EMT-6 murine mammary carcinoma cells	62	94
4T1 murine mammary carcinoma cells	>90	>90
Human melanoma cells	>90	>90
J-774.2 murine macrophage-like cells	0	0

* Sepharose beads with covalently bound fibrinogen (SB-Fib) or FMB were placed on nearly confluent culture, and the percentage of beads attached to the cells at d 1 was counted. Naked SB did not attach (O%).

(**Table 1**). In previous experiments, the FMB have not shown significant attachment to some cell types that grow in monolayer such as normal keratinocytes, OV-1063, and J-774.2 cells; whereas many normal mesenchymal cell types such as normal fibroblasts (human rat or pig) or transformed (3T3) as well as normal SMCs, endothelial cells, and EMT-6 cell line can attach the FMB with equal or greater degree than SB-Fib.

3.5. Loading Cells on FMB

1. Prior to use, suspend FMB in sterile 96% alcohol for at least a few hours, and then rinse extensively with sterile PBS. FMB can also be presterilized by ionizing radiation
2. The cells to be loaded on the FMB are grown in plastic tissue-culture dishes in their normal growth conditions. Prior to reaching confluence, the cells are trypsinized and collected in their growth medium to 50-mL polycarbonate tubes. Typically, up to 1–10 million cells are added per 100 μL FMB suspended in approx 6–10 mL of medium.
3. The tube should be closed by a perforated stopper that is covered loosely with aluminum foil to enable gas exchange with minimal risk of contamination. All tubes con-

Fig. 3. Rotating cell-culture setup for growing cells on FMB in 50-mL polycarbonate tubes.

taining the FMB + cells should be placed on a rotating device at 10–20 cycles per min at an angle of 20–30°, so that the medium does not reach the stoppers (*see* **Note 2**). The rotating device should be placed in a 7% CO_2 tissue-culture incubator (**Fig. 3**). 48 h after mixing the cells with FMB, the supernatant medium containing unattached cells, as well as small fragments of FMB, should be removed and replaced with fresh medium. The tubes should be kept still for 60–90 s to allow the FMB loaded with cells to sediment before the medium is exchanged. The cells can continue to grow on the FMB in such a rotating device for prolonged periods, up to a few weeks, depending on the cell type and the density of cells on the FMB.

4. Replace the medium frequently, every 2–3 d, depending on cell number on the FMB in the tube.
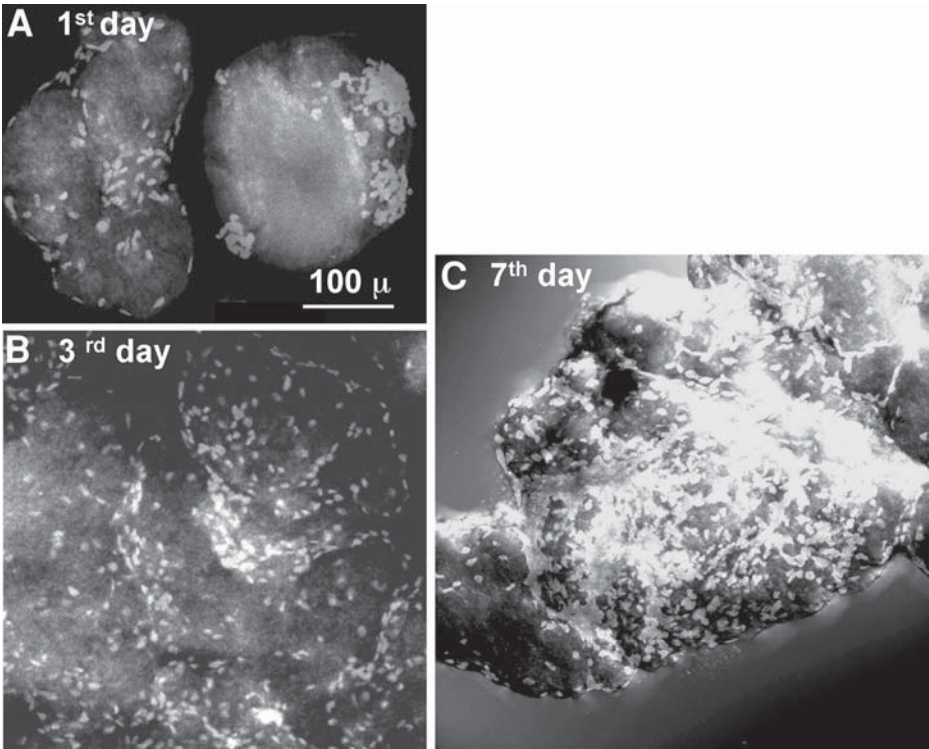
Fig. 4. Endothelial cells seeded and grown on FMB; nuclei fluorescence is seen as light dots. **(A)** 1 d after seeding, **(B)** and **(C)** at 3 and 7 d, respectively. By d 7, the cells secrete ECM that forms aggregates with large number of cells.

3.6. Imaging Cells on FMB

1. Perform light and fluorescent microscopy using a standard fluorescent microscopy system. Micrographs can be taken by single or double (fluorescence and light) exposures.
2. In order to distinguish and localize the cells on FMB, fix the samples in 0.5% buffered glutaraldehyde or 70% alcohol and stain the cell nuclei with propidium iodide (PI) by adding 50 µg/mL PI in darkness for at least 20 min before examination, and rinse with saline.
3. Place the PI stained FMB on a microscope slide with PBS-glycerol 80% and 2% DABCO, and scan with fluorescence microscope or with a computerized confocal laser microscope, typically with double excitation at 410 and 543 nm, to visualize the endogenous fluorescence of the FMB and the PI stained nuclei.
4. For confocal fluorescence microscopy, process the visual composite images (phase and differential interference contrast according to Nomarski) and the
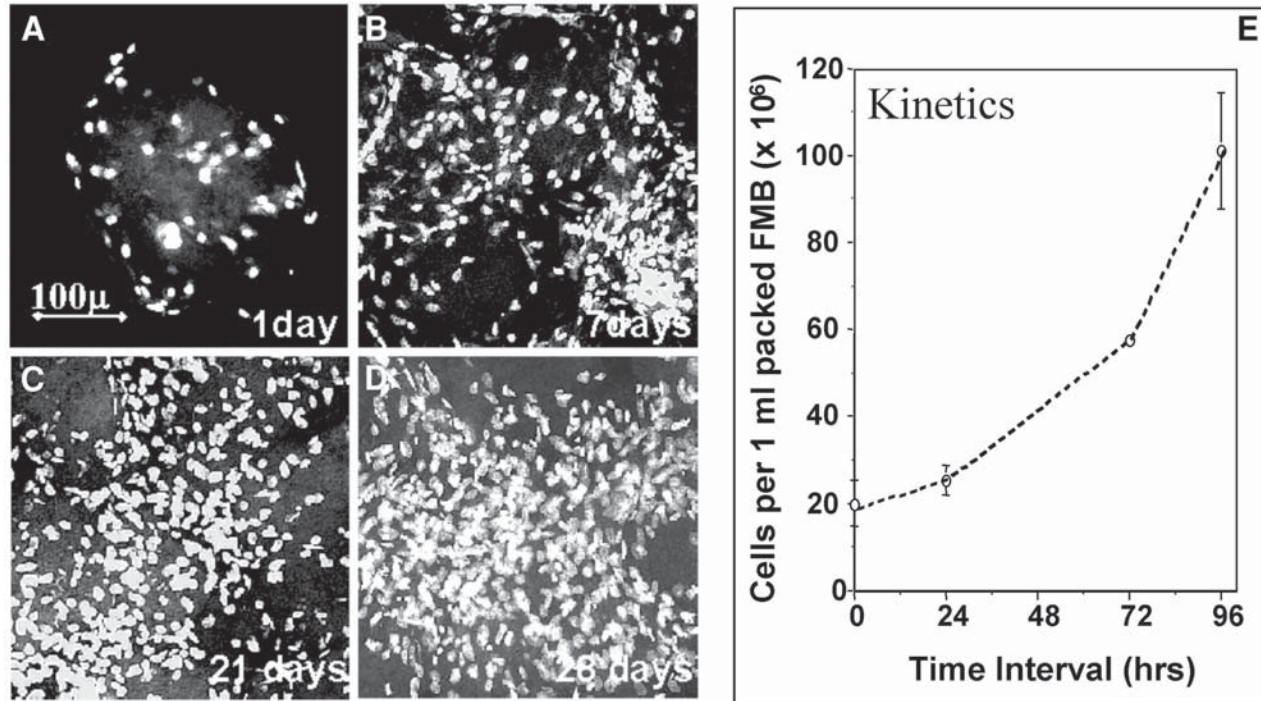
Fig. 5. Human fibroblasts are seeded and grown on FMB as in Fig. 4. About 1 million cells were loaded on 100 µL FMB and cultured in suspension for a period up to 28 d. **(A–D)** Confocal microscopy of samples taken at d 1, 7, 21, and 28 after seeding. The nuclei, revealed by PI (white spots) staining, indicate the increasing cell density over a 4-wk growth period. The Numarsky optics suggest that with time, the single FMB become aggregated and digested to be replaced by secreted new extracellular matrix. **(E)** Cell number on FMB was evaluated by the MTS assay that gave credible results up to d 4–5. Thereafter, the cell number was underestimated because of the inaccessibility of cells buried within the newly synthesized ECM.

fluorescent slice scans for overlap slice summation or three-dimensional (3D) presentation. The cell nuclei are stained with PI, and can be visualized. **Fig. 4** shows such a fluorescence microscopy image of bovine endothelial cells seeded and grown on FMB for 1 wk. **Fig. 5 A–D** shows composite confocal images of FMB loaded with fibroblasts at an estimated cell density of 100 million cells per 1 mL packed FMB. The rate of cell proliferation on the beads is clearly manifested.

3.7. Modified MTS Assay for Cell Number on FMB

Evaluate cell number on FMB by CellTitre 96Aqeous colorimetric assay (MTS assay) as previously described *(8)*. For use with FMB, the assay must be modified as follows:

1. Place 200-µL samples of suspended FMB + cells in 24-well flat bottom plates (in triplicate) and add 200 µL of fresh mixture of MTS/PMS (CellTitre 96 AQueous Assay by Promega, Madison, WI) to each well.
2. After 2–6 h of incubation at 37°C, add 50 µL of dimethyl sulfoxide (DMSO) for 1 h with periodic shaking and transfer 0.1–0.3 mL of the supernatant to a 96-well plate.
3. Measure the optical density (OD) of the supernatant in a computerized automatic microwell-plate spectrophotometer (Anthos HT-II, Salzburg, Austria, or any equivalent) at 492 nm.
4. In a calibration of the procedure, various known amount of cells are seeded in plates, and when they attach they are incubated with the MTS reagents for 2, 4, and 6 h. The OD readings of the MTS should correlate well (r > 0.95–0.99) with the number of seeded cells.
5. Choose the incubation time at which the OD readings are within the optimal range for the assay of cell number on FMB. Depending on the cell types tested, the assay can be used to monitor cell number until a dense extracellular matrix (ECM) is deposited and masks the cells, typically after 4–5 d (*see* **Note 3**).
6. To monitor the proliferation of the cells, vortex for up to 3 s to disperse clumps, remove 100-µL samples of suspended FMB with cells at regular intervals, allow the particulate FMB to settle (1 min), and assay the cell number. **Fig. 5E** shows the proliferation of fibroblasts on FMB. **Fig. 6** shows that the highly populated FMB can be used to transfer seeded cells onto a plastic culture dish.

3.8. Pig Skin Wound-Healing Model

1. Make full-thickness excisional wounds using an 8-mm circular punch into the paravertebral skin of pigs as previously described *(9)*.
2. To each wound space, add a mixture of 150 µL of 3 mg/mL fibrinogen and 2 U/mL human α-thrombin (*see* **Note 4**). However, in some cases, prior to the addition of the fibrin, 2 million of the cultured syngeneic fibroblasts in suspension or on FMB should first be added to the wound (*see* **Note 5**).
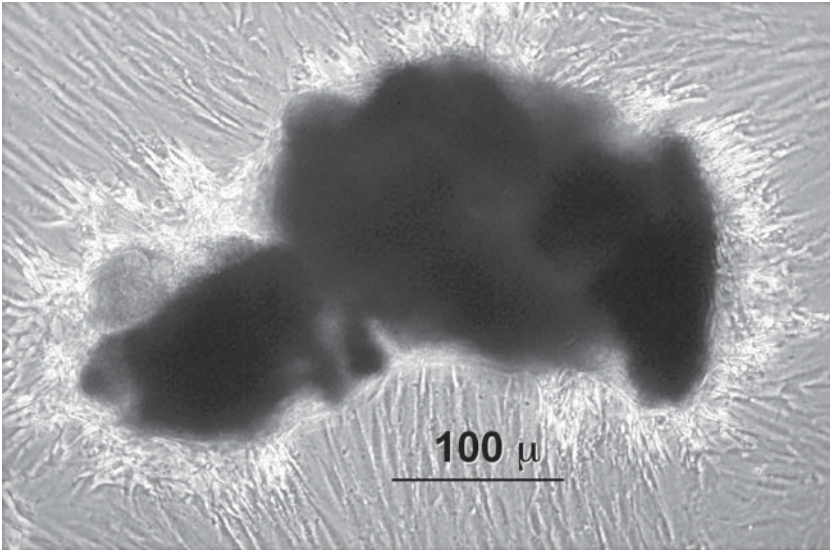
Fig. 6. Downloading of HF grown on FMB. Cells were grown on FMB for 14 d to reach saturation and downloaded from the FMB to plastic culture dish.

3. Dress the wound sites with an occlusive dressing, and harvest after 4 d. **Fig. 7** shows a comparison of wounds filled with fibrin alone (A), fibrin + naked FMB (B), and fibrin with FMB + cells (C), each tested in duplicate. In the control wounds, no granulation can be observed at this time-point; FMB alone seems to initiate vascularization and formation of granulation at the wound bed; FMB + cells fill the wound bed with newly formed granulation tissue (*see* **Note 6**).

4. Notes

1. The ideal size of FMB for cell culturing appears to be between 50 and 300 microns. Below 20 microns, the cells appear to engulf the particles rather than just adhere to them.
2. Cell growth on FMB appears to be optimal under conditions of low shear. Thus, we employ roller bottles or test-tubes made of non-cell-adherent polymers, rather than stirred suspensions in spinner flasks to grow cells on FMB. Experiments not described here demonstrate that the FMB are biodegradable, in vitro as well as in various animal models.
3. It is worth noting that the previously-described modified MTS assay provides good evaluation of the number of cells on FMB for only a few days after seeding. When the cells generate a significant amount of ECM, this tends to clump the FMB, and the cells become embedded within the whole aggregate. Thus, the
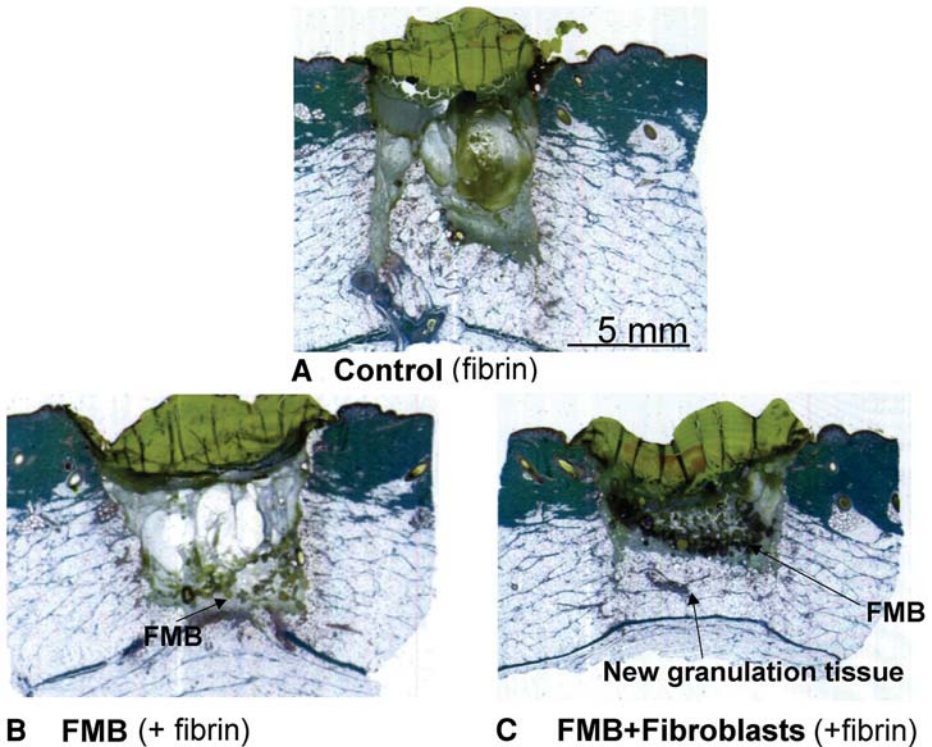
Fig. 7. Pigskin wound healing (d 4): histology of cutaneous wounds implanted with 3 mg/mL fibrin and combinations of FMB, human skin fibroblasts (HF), PDGF-BB, and controls: **(A)** Control wound (no fibrin or cells) shows no evidence of granulation tissue. **(B)** Addition of human fibrin and trypsinized HF shows no evidence of granulation tissue. **(C)** Wound to which syngeneic PF loaded FMB were added in fibrin. We observe FMB along the base of the wound and robust granulation tissue and neovascularization between the FMB and the underlying subcutaneous tissue. Additional PDGF did not further augment granulation tissue formation (not shown). (See color plate 1 appearing in the insert following p. 112.)

    penetration of the MTS reagent into the cells is reduced, thereby underestimating cell number.

4. A major consideration for delivering cells-on-FMB in dilute fibrin glue to a wound site is the use of the appropriate applicator. Thus, for skin repair, a spray-type device may be adequate *(22)*. For internal use, an endoscopic delivery system can be developed. Currently available fibrin glue applicators are not adequate for such delivery of cells on FMB because of internal clogging, clotting, and shear force. We are currently designing applicators to allow the delivery of cells-on-FMB that are convenient for tissue-engineering purposes.

5. The general approach is to implant viable cells-on-FMB to a wound site and fix them in place with a concomitantly formed low concentration of fibrin. Thus, the cells-on-FMB are suspended in fibrinogen (~3–5 mg/mL) and delivered simultaneously with thrombin, equivalent to the use of fibrin glue to seal surgical wounds, but in much lower concentrations *(18,19)*.

6. The issue of immunogenicity is also relevant to materials employed for tissue engineering. Because FMB are composed of human fibrin(ogen) and thrombin, they are not expected to induce immune reactions to these materials in humans.

Acknowledgments

References

1. Brown, L. F., Lanir, N., McDonagh, J., Tignazzi, K., Dvorak, A. M., and Dvorak, H. F. (1993) Fibroblast migration in fibrin gel matrices. *Am. J. Pathol.* **142,** 273–283.
2. Gray, A. J., Bishop, J. E., Reeves, J. T., and Laurent, G. J. (1993) Aα and Bβ chains of fibrinogen stimulate proliferation of human fibroblasts. *J. Cell Sci.* **104,** 409–403.
3. Lorenzet, R., Sobel, J. H., Bini, A., and Witte, L. D. (1992) Low molecular weight fibrinogen degradation products stimulate the release of growth factors from endothelial cells. *Thromb. Haemostasis* **68,** 357–363.
4. Shuman, F. (1986) Thrombin-cellular interactions. *Ann. NY Acad. Sci.* **408,** 228–235.
5. Daniel, T. C., Gibbs, V. C., Milfay, D. F., Garovoy, M. R., and Williams, L. T. (1986) Thrombin stimulates c-cis gene expression in microvascular endothelial cells. *J. Biol. Chem.* **261,** 9579–9582.
6. Dawes, K. E., Gray, A. J., and Laurent, G. J. (1993) Thrombin stimulates fibroblast chemotaxis and replication. *Eur. J. Cell Biol.* **61,** 126–130.
7. Bar-Shavit, R., Benezra, M., Eldor, A., Hy-Am, E., Fenton, J. W., Wilner, G. D., et al. (1990) Thrombin immobilized to extracellular matrix is a potent mitogen for vascular smooth muscle cells: nonenzymatic mode of action. *Cell Regul.* **1,** 453–463.
8. Gorodetsky, R., Vexler, A., An, J., Mou, X., and Marx, G. (1998) Chemotactic and growth stimulatory effects of fibrin(ogen) and thrombin on cultured fibroblasts. *J. Lab. Clin. Med.* **131,** 269–280.
9. Gorodetsky, R., Vexler, A., Shamir, M., An, J., Levdansky, L., and Marx, G. (1999) Fibrin microbeads (FMB) as biodegradable carriers for culturing cells and for accelerating wound healing. *J. Investig. Dermatol.* **112,** 866–872.

10. Griffith, B. and Looby, D. (1996) Scale-up of suspension and anchorage-dependent animal cells, in *Methods in Molecular Biology, Vol. 75. Basic Cell Culture Protocols* (Pollard, J. W. and Walker, J. M., eds.), Humana Press, Inc., Totowa, NJ, pp. 59–76.

11. Arshady R. (1990) Microspheres and microcapsules, a survey of manufacturing techniques. *Polymer Engin. and Science* **30,** 905–914.

12. Yapel, A. F. (1985) Albumin microspheres: heat and chemical stabilization. *Methods in Enzymology* **112,** 3–43.

13. Royer, G. P. (1982) Implants, microbeads, microcapsules, preparation thereof and method for administering a biologically-active substance to an animal. US Pat. #4,349,530.

14. Miyazaki, S., Hashiguchi, N., Takeda, M., and Hou, W. M. (1986) Antitumor effect of fibrinogen microspheres containing doxorubicin on Ehrlich ascites carcinoma. *J. Pharm. Pharmacol.* **38,** 618–620.

15. Gref, R., Minamitake, Y., Peracchia, M. T., Trubetskoy, V., Torchilin, V., and Langer, R. (1994) Biodegradable long circulating polymeric nanospheres. *Science* **263,** 1600–1603.

16. Evans, R. (1972) Biodegradable parental (albumin) microspherules. US Patent #3,663,687.

17. Lee, T. K., Sokolovski, T. D., and Royer, G. P. (1981) Serum albumin beads: an injectable, biodegradable system for the sustained release of drugs. *Science* **213,** 233–235.

18. Gurevitch, O., Vexler, A., Marx, G., Bar-Shavit, Z., Prigozhina, T., Levdansky, L., et al. (2002) Fibrin microbeads for isolating and growing bone marrow derived progenitor cells capable of forming bone tissue. *Tissue Engineering* **8,** 661–672.

19. Marx, G. and Gorodetsky, R. (2000) Fibrin microbeads prepared from fibrinogen, thrombin and factor XIII, US Patent 6,150,505.

20. Marx, G., Mou, X., Freed, R., Ben-Hur, E., Yang, C., and Horowitz, B. (1996) Protecting fibrinogen with rutin during UVC irradiation for viral inactivation. *Photochem. Photobiol.* **63,** 541–546.

21. Sanders, R. P., Goodman, N. C., Amiss, L. R., Pierce, R. A., Moore, M., Marx, G., et al. (1996) Effect of fibrinogen and thrombin concentrations on mastectomy seroma prevention. *J. Surg. Res.* **61,** 65–70.

22. Marx, G. (2000) Fibrin sealant glue gun. US Patent 6,059,749.

3

Synthesis and Characterization
of Hyaluronan-Based Polymers for Tissue Engineering

Carlo Soranzo, Davide Renier, and Alessandra Pavesio

1. Introduction

Hyaluronan (HA) is a naturally occurring, negatively charged high mol-wt glycosaminoglycan (GAG), that is composed of repeated disaccharide units of D-glucuronic acid and N-acetylglucosamine. It is the only GAG that lacks an associated protein moiety and sulfate groups. HA is a highly conserved and widely distributed polysaccharide. In a variety of mammalian tissues, it exerts structural functions because of its peculiar physicochemical properties. Because of its propensity to form highly hydrated and viscous matrices, HA imparts stiffness, resilience, and lubrication to tissues. The unique properties of HA are manifested in its mechanical function in the synovial fluid, the vitreous humor of the eye, and the ability of connective tissue to resist compressive forces, as in articular cartilage.

HA also plays a fundamental role during embryonic development *(1–3)* and in wound healing, both in adult and fetal life stages, favoring cell migration processes. In fact, its extreme hydrophylicity creates an environment that is conducive to cellular motility *(4)*.

These biological properties make HA an ideal candidate for the development of innovative medical devices for a number of clinical applications, ranging from postsurgical adhesion prevention to its use as a viscoelastic agent in intra-ocular surgery or as a synovial fluid adjuvant. Other potential applications of HA are precluded because of its physical nature: HA exists only as an aqueous gel, with a short resident time in vivo, and is rapidly degraded upon application. Therefore, it cannot be used as a solid, multidimensional scaffold, although attempts have been made to use high mol-wt HA to deliver chondrocytes
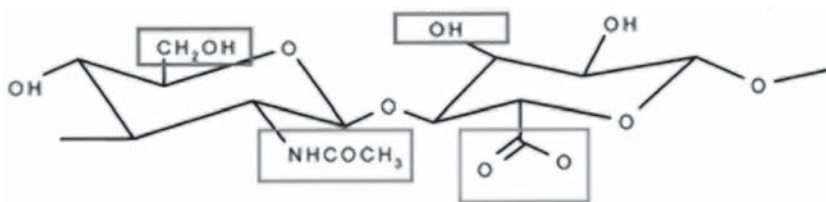
Fig. 1. Reactive groups that can undergo chemical modification on the HA backbone.

for repairing chicken *(5)* or rabbit knee full-thickness lesions, but with variable results *(6)*.

Through the chemical modification of HA, a new class of HA-derived semisynthetic polymers can be obtained that retain some of the features of the parent molecule, such as biocompatibility and cell interaction properties—but which are water-insoluble and therefore, thanks to this property, can be manufactured into a variety of different physical configurations such as films, threads, microspheres, sponges, and woven and non-woven fabrics *(7)*.

1.1. Esters of Hyaluronic Acid (HYAFF® and ACP® Polymers)

Two types of chemical reaction have been investigated to modify the HA backbone: *coupling reactions*, which involve the modification of specific functional groups of HA by subjecting them to chemical reaction such as esterification or amidation, and *crosslinking reactions*, which involve the creation of reticulates between HA polymeric chains through condensation of specific functional groups of HA or through the formation of atomic bridges.

These chemical modifications involve each of the various functional groups of the fundamental disaccharide unit of the polysaccharide in a different manner. **Fig. 1** illustrates groups that are potentially subject to a modification; these are represented by: carboxyls ($-COO^-$), primary hydroxyls ($-CH_2OH$), secondary hydroxyls ($-OH$), and *N*-acetyl ($-NHCOCH_3$) groups.

HA derivatives can be further divided into two classes of compounds: linear and crosslinked. The former are constituted by compounds in which the reaction involves one or more functional groups belonging to the same polysaccharide chain, by the addition of a molecular residue. Crosslinked compounds are those in which several polymer chains are chemically linked by condensation of the same functional groups onto different HA molecules (autocrosslinked HA or autocrosslinked polymers [ACP]®).

Esters of HA are particularly interesting as novel biopolymers for tissue engineering. By esterification of HA with alcohols of different chain lengths, modified biopolymers can be produced with significantly different physico-
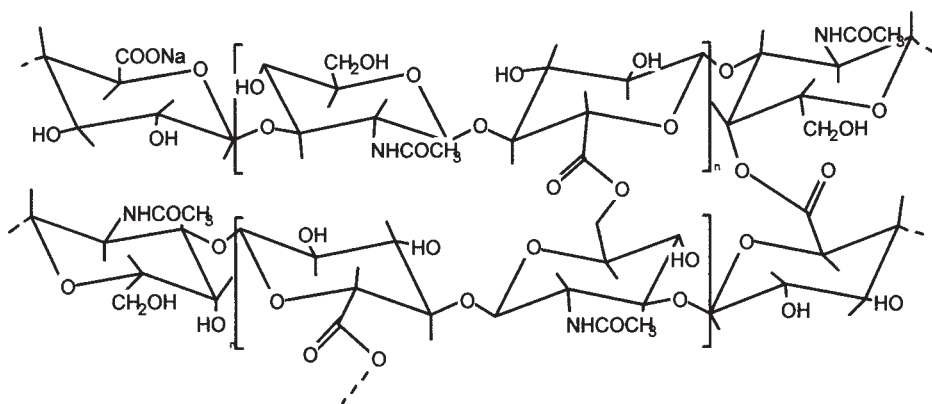
Fig. 2. The inter-chain bonds connect different HA units, thus forming a network of molecules with a much higher mol wt compared to the starting material.

chemical properties with respect to those of the parent molecule *(8,9)*. Two type of esters are described here: the benzyl ester (totally esterified, for which >90% of the carboxyl groups of HA react with benzyl alcohol), and the ACP®.

It is important to note that the esterification reaction may involve all or some of the carboxy groups of HA, giving rise to compounds with quite different physicochemical properties *(8)*. Indeed, an esterification involving more than 50% of the carboxyl groups tends to drastically reduce the product's water-solubility, leading to a virtually water-insoluble polymer for esterification degrees above 70%. This allows the technological transformation into scaffolds of defined three-dimensional (3D) configurations (e.g., sponges, films, threads, fleeces, woven mats), which will still be characterized in their physicochemical properties by the related degree of esterification of the HA-based polymer used *(9)*.

The ACP® is an ester, obtained through a condensation reaction resulting in the formation of inter- and intramolecular ester bonds (**Fig. 2**). During the reaction, a predetermined percentage of carboxyl groups is esterified, with hydroxyl groups of the same molecule thus forming a mixture of lactones and intermolecular ester bonds. Thermodynamic calculations show that the crosslinks preferably involve groups on different chains, thus originating intermolecular bonds *(10)*. No foreign bridge molecules are attached to the HA chain, thus ensuring only the liberation of parental HA upon degradation.

1.2. HA-Derived Polymer Degradation

One of the most interesting features of HYAFF® esters is that, upon degradation, parental HA is released, together with the alcohol moiety involved in the esterification process.

In vitro, the hydrolysis of the ester can be catalyzed by chemical (by adjusting the pH above or below 7, or by increasing the temperature) or biochemical reactions (e.g., linked with the presence of enzymes such as esterases). In vivo, the degradation process is mainly the result of macrophage activation and internalization of the HA derivative into phagosomes, where it is degraded into its components *(7)*. The choice of the alcoholic residue involved in the esterification process becomes decisive in order to reduce the toxicological risks involved with the release of the secondary product, but also in establishing usefulness of the derivative for tissue engineering, for which an in-vitro cultivation phase is very often envisaged.

HYAFF® 11 total ester is a polymer with high hydrophobicity (compared to HA); for this reason in vivo it is normally degraded in about 12–16 wk (depending on the implantation site). Under in vitro cell-culture conditions, this material maintains its structural integrity. It can easily be handled, and does not contract as some collagen-based materials do.

In contrast, ACP® polymer presents significantly improved viscoelastic properties with respect to unmodified HA. Because of its very high hydrophilicity, the in vitro degradation time is quite rapid (2–5 d in culture medium). Therefore, ACP®-based scaffolds can be used as cell delivery systems in which the cell-biomaterial contact time before implantation is very short.

In vivo, as the HA-based scaffold is degraded into its components, released HA is further degraded into oligomers that can still evoke an angiogenic response *(11,12)*. From a tissue-engineering perspective, this is even more important, because this type of scaffold be degraded without eliciting any significant foreign body reaction, providing the space for the developing tissue, and the angiogenic stimulus can facilitate cell-construct maturation and integration within the host.

2. Materials

We will provide two preparation methods for synthesizing two of the HA-derivatives that are best-characterized as scaffolds for TE purposes (HYAFF® 11: HA benzyl ester, totally esterified, and the ACP®), together with methods for manufacturing, on a lab scale, two device configurations: a membrane of HYAFF® 11 and a sponge of ACP®. Both scaffolds have been successfully employed in various TE applications, such as skin *(13)*, cartilage *(14)*, and skeletal tissue reconstruction *(5)*.

2.1. Reagent Preparation

1. We routinely prepare HA-sodium salt by an in-house method with a mol-wt range of 160–200 kDa, but similar material can be purchased from Sigma or other suppliers.
2. All other chemicals are of reagent grade, and have been used without further purification.
3. If Vaseline oil is used, a pharmaceutical-grade type must be selected.

3. Methods

3.1. Preparation of the Tetrabutylammonium Salt of HA

1. Dissolve HA-sodium salt in aqueous solution to a final concentration of 20 mg/mL.
2. Apply the HA solution to a chromatographic column (3 cm in diameter, 50 cm long) filled with Dowex 20 *M* (Dow Chemical) ion-exchange resin, which is activated by tetrabutylammonium hydroxide (TBA-OH). Flow rate is set at 10 mL/min. Generally, the mEq ratio between Dowex 20 M resin and HA is 2:1.
3. Lyophilize the eluate collected from the column in order to obtain the hyaluronic acid tetrabutylammonium salt (HA-TBA), which is highly soluble in non-polar solvents, such as dimethyl sulfoxide (DMSO) or n-methylpirrolidone (NMP).

3.2. Preparation of a Sterile HYAFF® 11 Membrane

3.2.1. Synthesis of HYAFF® 11 Total Ester

NMP is used under strict anhydrous conditions (*see* **Note 1**).

1. Dissolve HA-TBA (12.4 g, corresponding to 20 mEq of a monomeric unit), 4.5 g (25 mEq) benzyl bromide, and 0.2 g of tetrabutylammonium bromide in 620 mL of NMP (*see* **Note 2**).
2. Allow the reaction of these reagents to continue at room temperature for 48 h.
3. Slowly pour the resulting mixture into 3,500 mL of ethyl acetate, with constant agitation.
4. Filter the precipitate through a sintered glass filter.
5. Wash the recovered precipitate 4× with 500 mL/wash of ethyl acetate.
6. This precipitate is washed again several times with water and ethanol until all of the NMP is completely removed.
7. Dry the HA derivative in an oven at 35–45°C under controlled vacuum.

3.2.2. HYAFF®11 Membrane Formation

1. Dissolve the HYAFF®11 powder at 180 mg/mL in DMSO at room temperature.
2. Using a stratifier, gently spread a thin layer of the HYAFF®11 solution onto a glass plate contained inside a large tray (*see* **Notes 3** and **4**).
3. Add ethanol in the proportion of 2 L/25 mL of HYAFF®11 solution. This adsorbs DMSO, but does not solubilize HYAFF®11 which instead becomes solid.
4. Gently remove the polymer sheet, pipetting ethanol to detach it from the coagulation surface.
5. Wash the the film several times with ethanol, with water, and finally with ethanol again.
6. Press-dry the resulting sheet under vacuum at 30°C in an electrophoresis gel dryer for 48 h (*see* **Note 5**). **Fig. 3** shows an HYAFF® 11 membrane.

3.2.3. HYAFF®11 Membrane Preparation for Tissue Culture

1. In order to make film adhere to the bottom of a bacterial Petri dish, use a cell scraper to spread the plastic surface with a few μL of Vaseline oil (200 μL/100 cm² membrane).
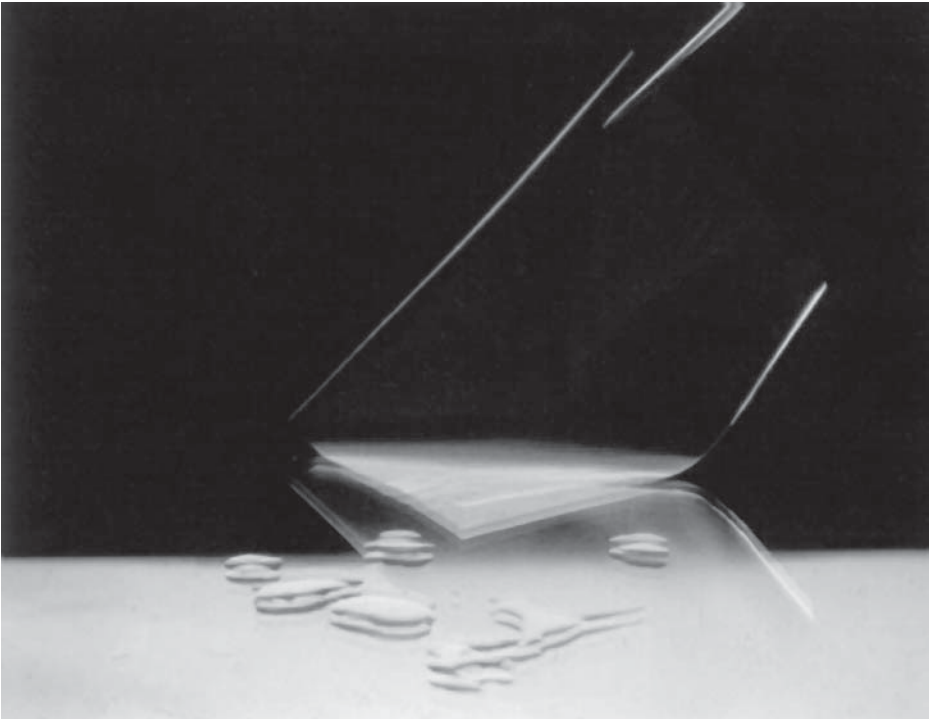
Fig. 3. The HYAFF® 11 membrane is optically transparent and allows microscopic observation of cells cultured on it. The film in the picture has a thickness of 20 μm. Keratinocytes can be cultivated on this substrate for about 20 d without loosing mechanical resistance.

2. Immediately place the film on the oily surface, starting from one side of the membrane. It is important to avoid adjusting the position of the membrane because of a non-central position, as this may cause tearing. Do not entrap air bubbles during film deposition because an uneven surface will result, affecting the subsequent cell seeding and monitoring under the microscope (*see* **Note 6**).
3. Sterilize the entire product (Petri dish + membrane) by γ-irradiation before use in cell cultivation.

   Fig. 4 shows FT-IT spectra for both hyaluronic acid and HYAFF®11. The peak at 1750 nm (stretching of COO-R bond) confirms the presence of ester. **Table 1** reports the product specifications for a HYAFF®11 membrane suitable for human fibroblasts or keratinocyte cultivation.

   Such "plain" films can be further developed, although at an industrial scale, into laser-microperforated HYAFF®11 membranes (Laserskin®), which have been designed to improve transplantation of cultured autologous keratinocyte
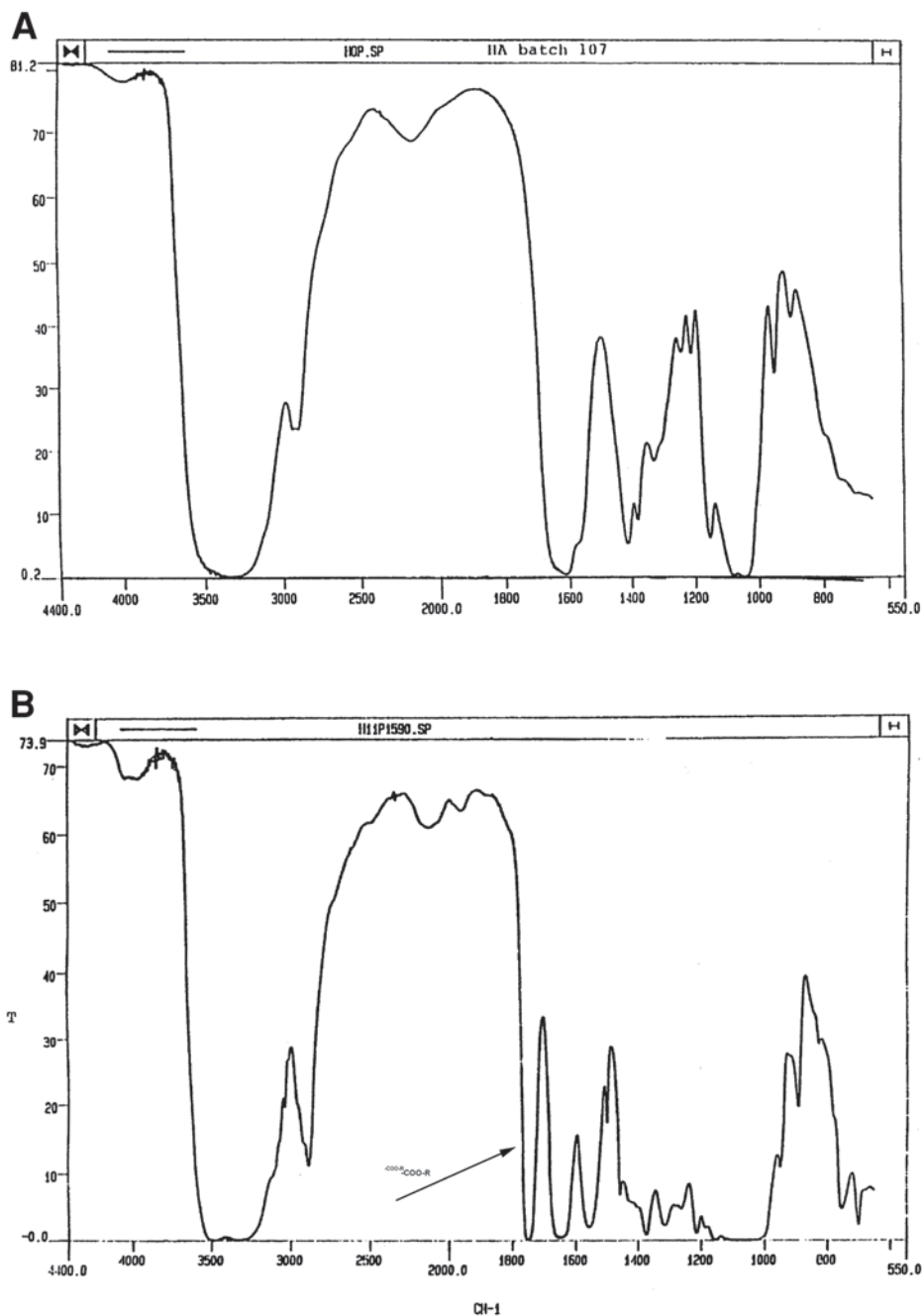
Fig. 4. (**A**) FT-IR spectrum of hyaluronic acid-sodium salt. (**B**) FT-IR spectrum of HYAFF®11 total ester. Arrow points to the 1750 nm peak.

Table 1
Product Specifications for HYAFF®11 Films Suitable
 for Mammalian Adherent-Cell Cultures

Parameter	Unit	Range
Loss on drying	%	5.5–7.5
Percentage of esterification	% w/w o.d.b.	92–98
Free benzyl alcohol	% w/w o.d.b.	<0.1
Methanol	% w/w	<0.1
Ethanol	% w/w	<0.1
Acetone	% w/w	<0.1
Isopropanol	% w/w	<0.1
Ethyl acetate	% w/w	<0.1
DMSO	% w/w	<0.1
Sterility	Ref. Eu/US P	Conform
Endotoxins content	Eu/mg	<0.1

sheets *(15,16)*. In this case, high-density, 40 μm laser-drilled holes have been made on the film. Keratinocyte colonies can set into the pores and migrate to the underneath surface or, when applied onto the wound bed, they can colonize the wound, with a better clinical outcome compared to the traditional technique developed by Rheinwald and Greene *(17)*.

3.3. Preparation of ACP® Sponges

ACP® scaffolds are made through *in situ* synthesis of the crosslinked derivative by an heterogeneous phase reaction, starting from HA-TBA salt, prepared as described in **Subheading 3.1.**

3.3.1 Synthesis of ACP®

1. Dissolve 16 mEq of HA-TBA (corresponding to 10 g) in 500 mL of anhydrous NMP.
2. To the resulting solution, add 0.8 mEq of chloro-methyl-pirydinium iodide (CMPI) and 0.8 mEq of triethylamine.
3. Allow the reaction to proceed at low temperature (–10°C) for at least 8 h.
4. Increase the temperature to 15–20°C.
5. Add 1 vol of NaCl (10% w/w final concentration).
6. Slowly pour the resulting mixture into 1000 mL of ethanol, with constant agitation.
7. Filter the precipitate through a sintered glass filter and washed 4× with 250 mL/ washing of ethanol, until the precipitating solvent has been completely removed.
8. Vacuum-dry the ACP® at 30°C for 96 h.

Fig. 5 illustrates NMR spectra, comparing HA, as starting material and ACP® (5% esterification). Two peaks at 5.12 and 5.01 are detected, which can
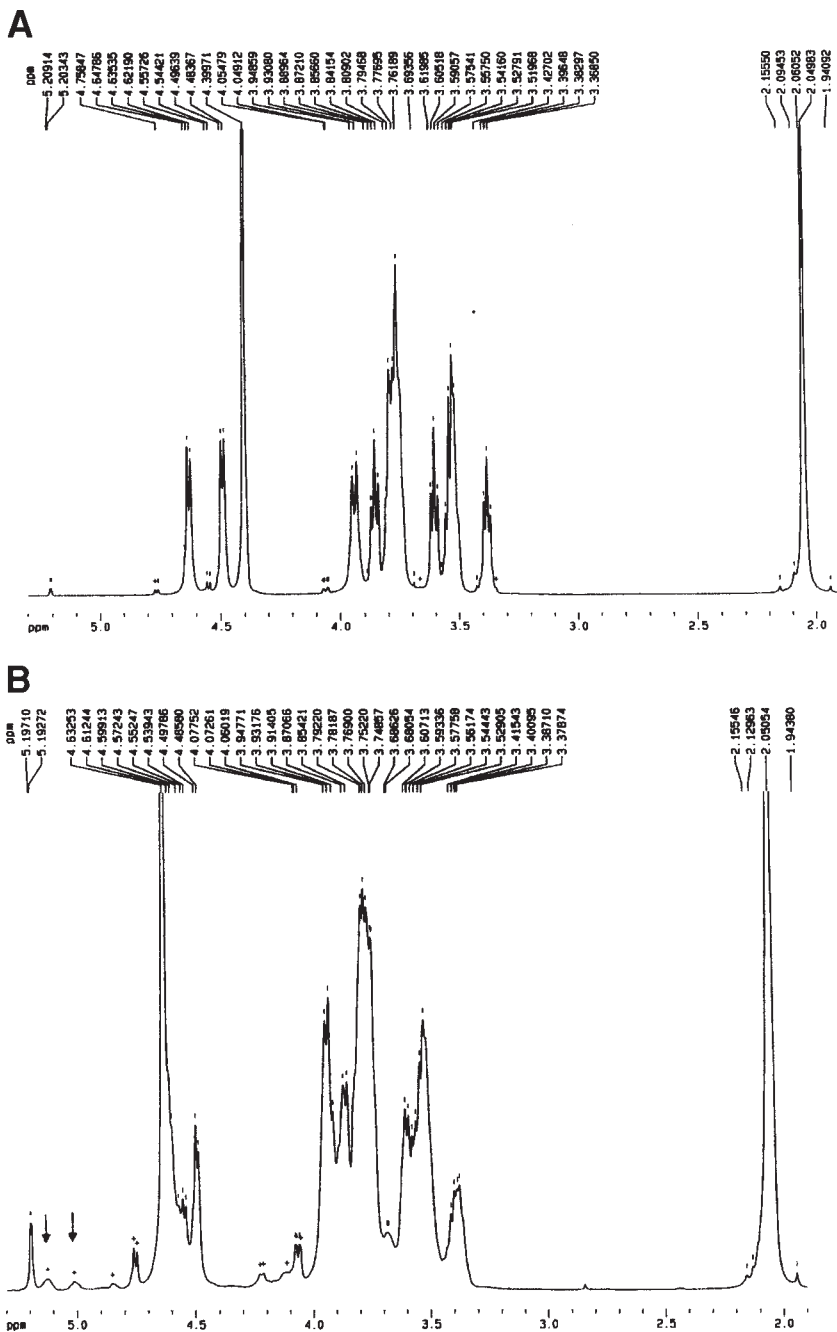
A

B

Figure 5. **(A)** ^{3}H-NMR spectrum of HA-sodium salt. **(B)** ^{3}H-NMR spectrum of ACP®. Arrows point to the 5.12- and 5.01-ppm peaks.
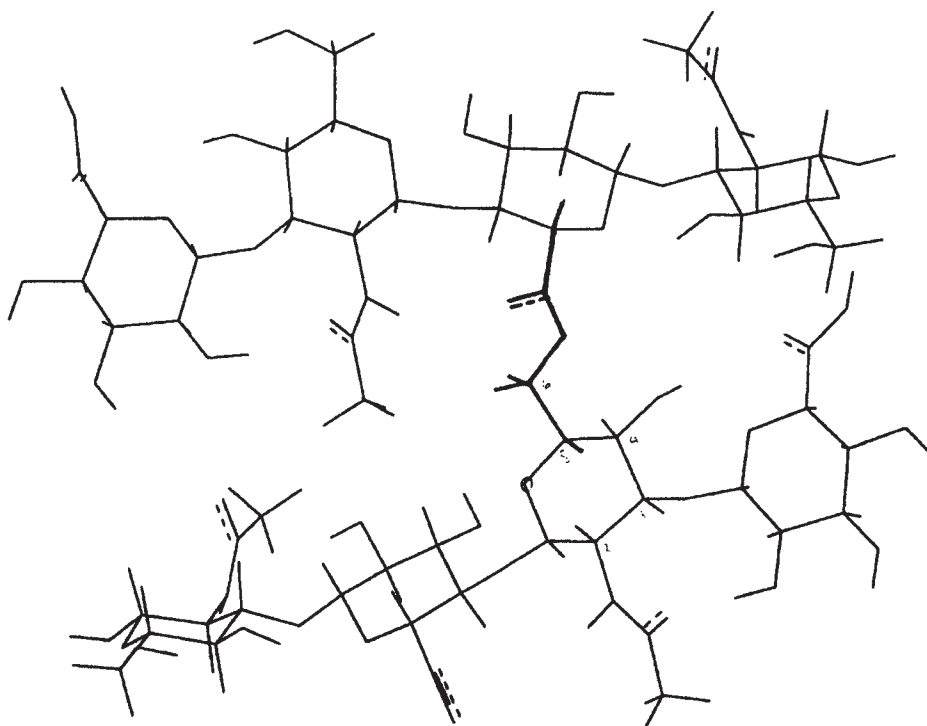
Fig. 6. Molecular conformation of ACP® in water.

be assigned to the carboxyl ester. The 3D spatial chemical conformation of ACP®, in which both carboxyl and primary oxydrilic functions are involved in the formation of a crosslinked derivative, is shown in **Fig. 6**.

3.2.1 Sponge Formation

1. Dissolve ACP® in a solvent consisting of DMSO and water (50/50) in a concentration ranges between 15 and 20 mg/mL, at room temperature.
2. Add to each 10 mL of solution a mixture of 31.5 g of sodium chloride prepared as 300-μm granules, 1.28 g of sodium bicarbonate, and 1 g of citric acid (*see* **Note 7**).
3. Homogenize the entire mixture in a mixer
4. Stratify the paste using a mangle-device consisting of two rollers that turn in opposite directions with an adjustable distance between the two. The optimal depth of the layer is 0.5 cm. By regulating this distance (optimal range 0.8–1.3 cm), the paste is forced between the rollers together with a strip of silicone sheet which acts as a support to the layer of paste just formed.
5. Cut the layer to the desired size (e.g., 1 cm in diameter).
6. Remove from the silicone.

7. Wrap in filter paper and dip in water.
8. In this way the sponges must be washed thoroughly in water, in order to completely dissolve all the salt granules. The resulting spaces left by the dissolved salt confers a specific porosity on the sponge.
9. Freeze-dry the sponge (*see* **Note 7**) and sterilize using γ-irradiation.

Fig. 7 shows an SEM image of the inside surface of a sponge obtained with the method described here; pore diameter ranges from 10 to 300 μm, average porosity is 85%, and the surface area is 7.34 m^2/cm^3. Measurements of porosity and surface area were conducted on the dry materials by mercury porosimetry. **Table 2** reports the analytical production data of ACP® scaffolds suitable for tissue-engineering applications. Among the different in vitro and in vivo characterization studies *(18)*, these scaffolds have been employed as cell-carriers of bone marrow-derived-cultured-expanded mesenchymal progenitor cells, used to repair full-thickness osteochondral defects in adult rabbits *(19,20)*.

3.3. Pretreatment of HA Membranes and Sponges for Cell Seeding

Although HA-derived polymers present good cell-adhesion properties, attachment of cells can be enhanced by coating techniques.

1. Condition HYAFF® 11 membranes in culture medium (Dulbecco's modified Eagle's medium [DMEM] 10% fetal calf serum [FCS]) for 2–4 h before cell addition in order to remove excessive Vaseline oil.
2. Dip ACP® sponges into a 100 μg/mL solution of fibronectin (Collaborative Biomedical Products, Collaborative Research, Bedford. MA) in Tyrode's salt solution.
3. After 1 h at 4°C, remove the sponges and dry overnight at room temperature in a sterile laminar flow hood.
4. Dilute mesenchymal progenitor cells to 5×10^6 cells/mL in DMEM.
5. Combine the cells with an ACP® sponge in a 5-mL tube.
6. Seal the tube with its cap.
7. Apply a negative pressure to the tube using a 20-mL syringe fitted with a 20-gauge needle.
8. This vacuum facilitates the removal of air bubbles from the HA scaffold, thus allowing complete infiltration of the sponge with the cells. Cell constructs are then placed in the incubator at 37°C for the required period of time.

4. Notes

1. NMP is dehydrated by molecular sieve treatment. Reflux the solvent through the bed beads for at least 8 h. Molecular sieves are dried at least overnight at 250°C before use.
2. The molar ratio between HA and the coupling reagent is chosen as a function of the degree of substitution of the ester. For a total esterification (>90% of carboxyl groups esterified), use an excess of 25–30% of benzyl bromide (expressed as molar equivalent).
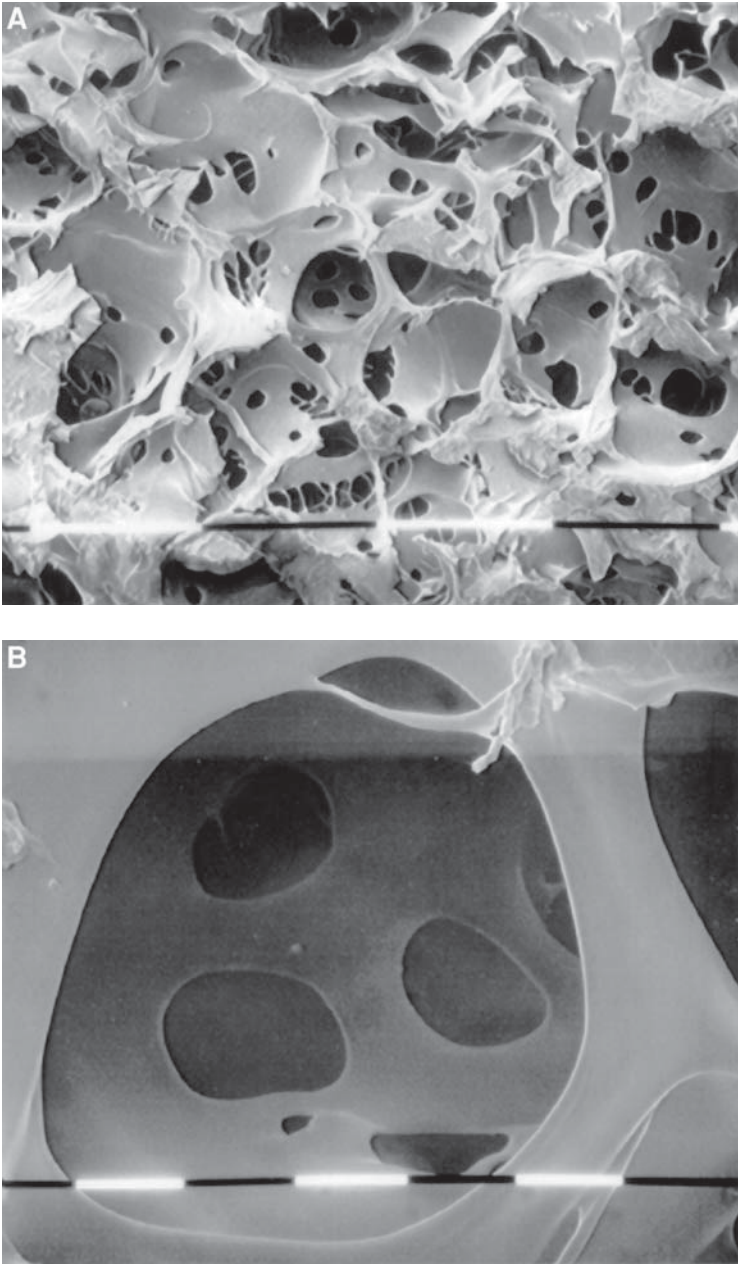
Fig. 7. (**A**) ACP® sponge, cross-section. Note the large pores (100–300 μm), designed for cell seeding and colonization. Smaller pores (10–30 μm) facilitate nutrient exchange within the inner mass of the scaffold (bars represent 100 μm). (**B**) Macropore enlargement to show microchannnels. which allows interconnectivity (bars represent 10 μm).

Table 2
Product Specifications of ACP® Sponges for TE Applications

Parameter	Unit	Range
Loss on drying	%	<10
Percentage of crosslinking	% w/w o.d.b.	30–35
CMPIJ	% w/w	0.1
1-methyl-2-piridone	% w/w	<0.1
Ethanol	% w/w	<0.1
Acetone	% w/w	<0.1
Isopropanol	% w/w	<0.1
TBA residual	% w/w o.d.b.	<0.1
Chloride	% w/w o.d.b.	<0.15
Water adsorbency	% w/w	>2200
Iodide	% w/w o.d.b.	<0.5
Sterility	Ref. Eu/US P	Conform
Endotoxins context	Eu/mg	<0.1

3. The thickness of the layer should be 10× the final thickness of the film.
4. A simple way to obtain a 1-mm-thick layer is by means of an electrophoresis glass plate with two 1-mm spacers at the edges. A third spacer is used to gently level the HYAFF®11-DMSO solution layer once it has been poured on the glass surface. It is essential to have a perfectly leveled glass plate (check with a spirit-level).
5. HYAFF®11 sheets can be stored at room temperature for several months.
6. The membrane is optically transparent, allowing control of culture progression and of cell features (e.g., morphology, growth rates).
7. Sponge porosity is a critical parameter, since it influences cell colonization and nutrient exchange inside the inner mass of the sponge. Porosity is conferred by sodium chloride granules (the porofore agent), citric acid, and sodium bicarbonate (used as a gas producer). During the phase inversion process (organic vs inorganic solvent), the polymer solidifies around NaCl crystals, and CO_2, generated by citric acid and sodium bicarbonate produces holes between pores, allowing interconnection. The following parameters must be carefully controlled: salt granulometry (the particle size determines the size of the air pockets that will characterize device porosity), homogeneity of ACP®-inorganic salt mixture, and the subsequent lyophilization process (the polymer mass must be kept at –30°C for the total duration of the process).

References

1. Kujawa, M. J. and Caplan, A. I. (1986) Hayluronic acid bonded to cell-culture surfaces stimulates chondrogenesis in stage 24 limb mesenchyme cell cultures. *Dev. Biol.* **11,** 504–518.

 2. Wheatley, S. C., Isacke, C. M., and Crossley, P. H. (1993) Restricted expression of the hyaluronan receptor, CD44, during postimplantation mouse embryogenesis suggests key roles in tissue formation and patterning. *Development* **119,** 295–306.

 3. Brown, J. J. and Papaioannou, V. E. (1993) Ontogeny of hyaluronan secretion during early mouse development. *Development* **117,** 483–492.

 4. Iocono, J. A. and Krummel, T. M. (2000) The role of hyaluronan in fetal repair: a review, in *Redefining Hyaluronan* (Abatangelo, G. and Weighel, P. H., eds.), Elsevier Science B.V., Amsterdam, The Netherlands, pp. 289–296.

 5. Itay, S., Abramovici, A., Nevo, Z. (1987) Use of cultured embryonal chick epiphyseal chondrocytes as grafts for defects in chick articular cartilage. *Clin. Orthop.* **220,** 234–300.

 6. Solchaga, L. A., Goldberg, V. M., and Caplan, A. I. (2000) Hyaluronic acid-based biomaterials in tissue engineered cartilage repair, in *Redefining Hyaluronan* (Abatangelo, G. and Weighel, P. H., eds.), Elsevier Science B.V., Amsterdam, The Netherlands, pp. 233–246.

 7. Campoccia, D., Doherty, P., Radice, M., Brun, P., Abatangelo, G., and Williams, D. F. (1998) Semisynthetic resorbable materials from hyaluronan esterification. *Biomaterials* **19,** 2101–2127.

 8. Rastrelli, A., Beccaro, M., Biviano, F., Calderini, G., and Pastorello, A. (1990) Hyaluronic acid esters, a new class of semisynthetic biopolymers: chemical and physicochemical properties. *Clinical Implant Materials (Advances in Biomaterials)* **9,** 199–205.

 9. Barbucci, R., Magnani, A., Baszkin, A., Da Costa, M. L., Bauser, H., Hellwig, G., et al. (1993) Physico-chemical surface characterization of hyaluronic acid derivatives as a new class of biomaterials. *J. Biomat. Sci. Polymer Edition* **4(3),** 245–273.

10. Mensitieri, M., Ambrosio, L., Nicolais, L., Bellini, D., and O'Regan, M. (1996) Viscoelastic Properties modulation of a novel autocrosslinked hyaluronic acid polymer. *J. Material Science: Materials in Medicine* **7,** 695–698.

11. West, D. C., Hampson, I. N., Arnold, F., and Kumar, S. (1985) Angiogenesis induced by degradation products of hyaluronic acid. *Science* **228,** 1324–1326.

12. Deed, R., Rooney, P., Kumar, P., et al. (1997) Early-response gene signalling induced by angiogenic oligosaccharides of hyaluronan in endothelial cells. Inhibition by high molecular weight hyaluronan. *Int. J. Cancer* **71,** 251–256.

13. Myers, S. R., Grady, J., Soranzo, C., Sanders, R., Green, C., Leigh, I. M., et al. (1997) A HA membrane delivery system for cultured keratinocytes: clinical "take" rates in the porcine kerato-dermal model. *J. Burn Care Rehabil.* **18,** 214–222.

14. Brun, P., Abatangelo, G., Radice, M., Zacchi, V., Guidolin, D., Daga Gordini, D., et al. (1999) Chondrocyte aggregation and reorganization into three-dimensional scaffolds. *J. Biomed. Mater. Res.* **46,** 337–346.

15. Andreassi, L., Casini, L., Trabucchi, E., Diamantini, S., Rastrelli, A., Donati, L., et al. (1991) Human keratinocytes cultured on membranes composed of benzyl ester of HA suitable for grafting. *Wounds* **3(3),** 116–126.

16. Harris, P. S., di Francesco, F., Barisoni, D., Leigh, I. M., and Navsaria, H. A. (1999) Use of hyaluronic acid and cultured autologous keratinocytess and fibroblasts in extensive burns. *Lancet* **353(9146),** 35–36.

17. Rheiwald, J. G. and Green, H. (1975) Serial cultivation of strains of human epidermal keratinocytes: the formation of keratinizing colonies from single cells. *Cells* **6,** 331–344.

18. Solchaga, L. A., James, E. D., Goldberg, V. M., Caplan, and A. I. (1999) Hyaluronic Acid-based polymers as cell carriers for tissue-engineered repair of bone and cartilage. *J. Orthop. Res.* **17(2),** 205–213.

19. Solchaga, L. A., Yoo, J., Lundberg, M., Hubregtse, B., Caplan, and A. I. (1999) Hyaluronic acid-based polymers in the treatment of osteochondral defects. *Trans. Orthop. Res. Soc.* **24,** 56.

20. Solchaga, L. A., Yoo, J., Lundberg, M., Goldberg, V. M., and Caplan, A. I. (1999) Augmentation of the repair of osteochondral defects by autologous bone marrow in a hyaluronic acid-based delivery vehicle. *Trans. Orthop. Res. Soc.* **24,** 801.

4

Synthesis and Characterization of Chitosan Scaffolds for Cartilage-Tissue Engineering

Steven H. Elder, Dana L. Nettles, and Joel D. Bumgardner

1. Introduction

Chitin, poly(*N*-acetylglucosamine) is a structural polysaccharide found in the shell of crustaceans and mollusks and is typically isolated from waste produced in food processing. The procedure for extracting chitin from crustacean shells usually involves decalcification, deproteination, and decolorization, which may be accomplished by sequential treatment in 5% HCl solution, 5% NaOH, and 0.5%KMnO$_4$(aq) and oxalic acid. *Chitosan*, poly(*N*-acetyl-2-amino-2-deoxy-D-Gluco-pyranose), is formed through the *N*-deacetylation of chitin, usually by treatment with strong alkalis (e.g., 50% NaOH) at an elevated temperature. It is a linear, polycationic copolymer of *N*-acetylglucosamine and glucosamine (combined by 1-4 glycosidic linkages), with the degree of deacetylation defined as the molar fraction of *N*-acetylglucosamine units. Several studies have linked the biological activity of chitosan to its degree of deacetylation and mol wt *(1–6)*, parameters that may be controlled by varying the time and temperature of the deacetylation reaction.

High-purity grades of chitosan are usually supplied in powder or flake form, with the degree of deacetylation ranging from 50–95% and mol wt from approx 50,000 to over 1 million. Chitosan solubility is pH-dependent, and most forms are insoluble in water or in alkaline solutions at pH levels above about 6.5. However, it dissolves readily in dilute solutions of most organic acids, including formic, acetic, tartaric, and citric acids. Chitosan is often formed into a film by casting a chitosan solution on a glass plate and air- or oven-drying. It is also frequently processed into porous beads by coacervation, which occurs when droplets of a chitosan solution are blown, using a compressed air nozzle, into a

non-solvent such as NaOH. Furthermore, the formation of chitosan fibers produced by forcing a chitosan solution through a viscose-type spinneret into an ammonia coagulating solution has been described *(7)*. As will be discussed in greater detail in this chapter, porous chitosan structures can be prepared by freezing and lyophilization of chitosan solutions.

1.1. Biomedical Applications of Chitosan

Chemically similar to both cellulose and hyaluronate, chitosan is generally considered to be nontoxic *(8)*, biocompatible *(5–6,9–10)*, and biodegradable *(6,11)*. It has several interesting biological properties that make it potentially useful in a wide range of biomedical applications. For example, chitosan agglutinates red blood cells, and is therefore under investigation as a hemostatic agent *(8,12)*. Furthermore, because of its cationic nature and high charge density, orally administered chitosan binds fat in the intestine and may be effective in the treatment of hypercholesterolemia *(13)*. Chitosan also stimulates wound healing, and has been reported to perform better than conventional dressings for skin lacerations *(14)*. Finally, chitosan is being increasingly used for drug delivery, as in the controlled release of hormones over extended periods of time *(15)*.

The potential for this material to serve as a cell scaffolding material for cartilage tissue engineering is currently under investigation, and in this area chitosan has several promising features. Chitosan is a structural analog of the cartilage-specific glycosaminoglycans (GAGs), which are known to be involved in regulating chondrocyte differentiation and biosynthesis and to mediate interactions between cells and between cells and the extracellular matrix. Thus, as noted by Suh and Matthew *(16)*, chitosan may be able to mimic certain biological activities of GAGs, including binding with growth factors and adhesion proteins. The polycationic nature of chitosan facilitates cell adhesion and allows for electrostatic interaction with anionic GAGs. As Madihally and Matthew *(17)* point out, ionic interactions with such negatively charged species could promote retention and organization of cartilaginous matrix constituents within a chitosan scaffold. Another interesting characteristic of chitosan is that oligosaccharide degradation products, liberated primarily by enzymatic hydrolysis of the acetylated residues *(18)*, may stimulate the synthesis of cartilage-specific GAGs or be directly incorporated into these polysaccharides *(19)*. Furthermore, chitosan's reactive amino groups provide sites for the grafting of bioactive factors (e.g., oligopeptides) under mild conditions. Finally, chitosan has antimicrobial properties that could reduce the risk of bacterial infection when used as an implant material *(20–22)*.

1.2. Chitosan Variability

As mentioned previously, the physical properties and biological response to chitosan depend strongly on its degree of deacetylation and mol wt. Therefore, the choice of starting material deserves careful consideration. Because they are more crystalline, chitosan-based materials with a higher degree of deacetylation tend to absorb less moisture *(6)*, degrade more slowly *(6,23)*, and have higher tensile strength than materials that retain more acetamide groups *(6)*. It has also been reported that more highly deacetylated chitosan substrates support cell adhesion better than less deacetylated ones *(1,5)*. Materials made from chitosan of higher mol wt exhibit greater tensile strength and moisture absorption *(4)*, as well as higher fat binding *(3)* capacity compared to lower mol-wt preparations. Mol wt could also influence the release profile of drugs loaded into a chitosan cell scaffold *(2)*. The optimal chitosan formulation for a specific tissue-engineering application can only be determined empirically. Commercial sources of chitosan include Vanson, Inc. (Redmond, WA); Fluka Chemicals (France, Germany, UK, USA); and Showa Chemicals (Tokyo, Japan).

1.3. Experimental Design

One technique for the fabrication of bulk porous chitosan scaffolds has been presented by Madihally and Matthew *(17)*. Ice crystal nucleation and growth, as governed by the magnitude and directionality of thermal gradients, occurs upon freezing of a chitosan-acetic acid solution. Subsequent lyophilization removes the ice phase and generates a porous material, and its overall porosity and mean pore size are modulated by the rate of freezing. The geometry of thermal gradients during freezing regulates pore orientation and connectivity. Thus, scaffold microstructure will depend on the shape of the mold used for freezing and on the freezer temperature.

The following are protocols for the synthesis of bulk porous chitosan scaffolds suitable for tissue engineering applications and for the analysis of their surface morphology and porosity by scanning electron microscopy (SEM) and mercury intrusion porosimetry (MIP), respectively. MIP is based on the premise that a non-wetting liquid such as mercury will only intrude pores under pressure. By increasing the pressure in a stepwise fashion and measuring the volume of mercury intruded at each step, a pore-size distribution may be calculated by applying the Washburn *(24)* equation:

$$p = (-4\gamma cos\theta)/d \tag{1}$$

where p is the pressure required to force mercury into a pore of entry diameter d, γ is the mercury surface tension, and θ is the contact angle between

mercury and the sample. MIP analysis can yield bulk density, apparent density, total intrusion volume, total pore area, average pore diameter, and overall porosity.

2. Materials

2.1. Scaffold Fabrication

1. Powdered chitosan. Results reported herein are for 86% deacetylated chitosan with a mol wt of approx 200,000 (kindly provided by Vanson).
2. 0.2 *M* acetic acid.
3. Magnetic stirrer and Teflon-coated stir bar.
4. Cheesecloth (optional).
5. Polyethylene scintillation vial (O.D. × length: 17 × 54 mm) with screw cap.
6. Waxed paper.
7. Styrofoam insulator with approx 4 cm wall-thickness.
8. Sharp forceps.
9. 37°C water bath.
10. Ultra-low temperature freezer (–80°C).
11. Crushed dry ice and suitable container.
12. 50-mL screw-capped centrifuge tubes.
13. Lyophilizer (e.g., Flexi-Dry Lyophilizer, FTS Systems, Inc.).
14. Lyophilization chamber (to accommodate 50-mL centrifuge tube).
15. Sharp, straight-edged blades such as disposable microtome blades.
16. Circular punch with 5–10-mm diameter.
17. Dessicator.
18. Ethanol, 100% and 50, 60, 70, and 95% in distilled water.
19. Antibiotic-antimycotic solution in phosphate-buffered saline (PBS): 20,000 U/mL penicillin, 20 mg/mL streptomycin, and 50 μg/mL amphotericin B (Sigma A9909 antibiotic-antimycotic solution, 2×).
20. Phenol red-containing cell-culture medium.

2.2. Scaffold Characterization Equipment

1. Scanning electron microscope.
2. Mercury Intrusion Porosimeter (e.g., AutoPore IV 9500 Series, Micromeritics, Norcross, GA).

3. Methods

3.1. Scaffold Fabrication

1. Dissolve chitosan powder in 0.2 *M* acetic acid in a glass beaker at a concentration of 20 mg/mL (2% w/v chitosan/acid solution).
2. Using a magnetic stirrer and Teflon-coated stir bar, mix the solution for at least 48 h to ensure complete dissolution, at which point the pH of the solution should be approx 4.4.

3. Centrifuge the chitosan solution at 20,000×*g* for 3 h or filter through cheesecloth to remove any undissolved particles and debris.
4. Line a scintillation vial with waxed paper, and pipet 5–7 mL of the chitosan/acid solution into the vial.
5. Transfer the vial to the styrofoam cooler and place inside a –9°C freezer.
6. Allow at least 24 h for freezing.
7. Immerse vial containing frozen chitosan/acid solution in a 37°C water bath for 3–5 s to facilitate removal of the ice core using sharp forceps.
8. Immediately place ice cores in 50-mL polypropylene centifuge tubes precooled in crushed dry ice, and store the tubes at –80°C.
9. The lyophilizer should be turned on and allowed to reach at least –40°C before placing samples in the chamber. Lyophilize samples for 24 h or until completely dry.
10. Store dry samples in a dessicator until ready to rehydrate.
11. Rehydrate scaffolds in a graded ethanol series (*see* **Note 1**). Start with 100% ethanol and proceed to 95%, 80%, and 70% (*see* **Note 2**). Equilibrate the scaffolds in two changes of each solution for at least 60 min (*see* **Note 3**).
12. After the first 60-min incubation in 70% ethanol, cylindrical scaffolds may be obtained by cutting perpendicular to the long axis of the sample with parallel sharp blades (e.g., disposable microtome blades) separated by a 2-mm-thick spacer. The ends of the sample should be discarded (*see* **Note 4**).
13. To produce a scaffold consisting only of material from the core of the original tube, use a sharp punch to cut a cylinder of 5–10 mm diameter from the thin slice.
14. Return samples to a fresh 70% ethanol solution and incubate at 4°C for 24 h. After this time, they should be treated as sterile.
15. Continue rehydration in 60% and 50% ethanol solutions. After the final change of 50% ethanol, transfer the scaffolds to the sterile PBS solution (*see* **Notes 5** and **6**).
16. Incubate in antibiotic-antimycotic solution at 4°C for at least 48 h (*see* **Note 7**).
17. Prior to cell seeding for in vitro colonization of scaffolds, incubate scaffolds in phenol-red containing tissue-culture medium overnight at 37°C in a humidified atmosphere of 5% CO_2.
18. Before adding cells, confirm that there is no residual acidity by checking the color of the medium.

3.2. Scaffold Characterization (see **Note 8**)

3.2.1. Scanning Electron Microscopy (SEM)

1. Lyophilized samples require no further treatment. Wet samples should be dehydrated in a graded ethanol series to 100% ethanol (two changes at each concentration × 30 min per change) followed by chemical drying using Hexamethyldisilazane.
2. To analyze the surface characteristics of scaffolds using SEM, mount on specimen holders with carbon tape, and then sputter-coat with gold/palladium to make them conductive. One 3-min coating is sufficient to eliminate charging inside the scope.
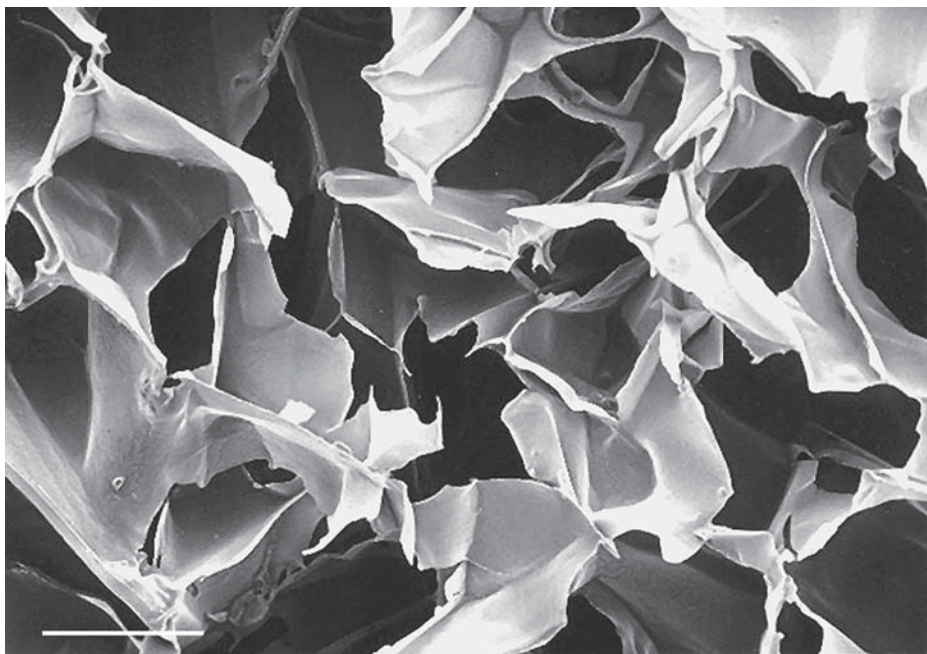3. Scan specimens in secondary electron detection mode.

Fig. 1. Surface morphology of 2% chitosan scaffold as revealed by SEM. Bar = 200 μm.

3.2.2. Mercury Intrusion Porosimetry (MIP)

A detailed protocol for performing mercury intrusion analysis is beyond the scope of this chapter. However, a brief overview is provided.

1. Degas the sample under vacuum and fill penetrometer (sample holder) with mercury.
2. Proceed with low-pressure analysis. Assuming mercury with surface tension of 485 dynes/cm and 130° advancing contact angle, start with a filling pressure of no higher than 3.45 kPa to begin intrusion at 360-μm pore-opening diameter. Allow at least 10 s equilibration time at each pressure step.
3. Continue equilibrated-step analysis to a filling pressure of at least 1 MPa (10 s equilibration) for intrusion of pores down to approx 1 μm opening diameter.

4. Notes

1. A slight amount of shrinkage and distortion may occur during rehydration of lyophilized scaffolds.
2. If lyophilized scaffolds are rehydrated in a neutral aqueous medium, they will become gelatinous and ultimately dissolve.
3. Brief vacuum treatment of scaffolds submerged in 70% ethanol may be employed to remove entrapped air bubbles.

4. Scaffolds will have a more dense microstructure with somewhat smaller pores in a zone extending from the surface to as much as 100 μm in depth.
5. **Fig. 1** is a representative scanning electron micrograph of a porous chitosan scaffold.
6. Hydrated scaffolds are soft, spongy, and highly extensible. The tensile elastic modulus of hydrated samples is in the range of 100–500 kPa *(16)*, and equilibrium compressive modulus is approx 3–4 kPa.
7. The use of ethylene oxide can also be considered as an alternate method of sterilization of lyophilized scaffolds.
8. The interior structure of scaffolds can be investigated using standard histological techniques. The use of hydrated scaffolds is recommended. Sections (5–8 μm) that have been cut using a rotary or sledge microtome can be stained with eosin—an anionic dye—for visualization of scaffold microstrucure. Digitized images of sections prepared in this manner are suitable for quantitative analysis using software such as NIH Image.

References

1. Chatelet, C., Damour, O., and Domard, A. (2001) Influence of the degree of acetylation on some biological properties of chitosan films. *Biomaterials* **22(3),** 261–268.
2. Genta, I., Perugini, P., and Pavanetto, F. (1998) Different molecular weight chitosan microspheres: influence on drug loading and drug release. *Drug Dev. Ind. Pharm.* **24(8),** 779–784.
3. No, H. K., Lee, K. S., and Meyers, S. P. (2000) Correlation between physicochemical characteristics and binding capacities of chitosan products. *J. Food Sci.* **65(7),** 1134–1137.
4. Nunthanid, J., Puttipipatkhachorn, S., Yamamoto, K., and Peck, G. E. (2001) Physical properties and molecular behavior of chitosan films. *Drug Dev. Ind. Pharm.* **27(2),** 143–157.
5. Prasitsilp, M., Jenwithisuk, R., Kongsuwan, K., Damrongchai, N., and Watts, P. (2000) Cellular responses to chitosan in vitro. *J. Mat. Sci.: Mat. in Med.* **11(12),** 773–778.
6. Tomihata, K. and Ikada, Y. (1997) In vitro and in vivo degradation of films of chitin and its deacetylated derivatives. *Biomaterials* **18(7),** 567–575.
7. Hirano, S., Zhang, M., Nakagawa, M., and Miyata, T. (2000) Wet spun chitosan-collagen fibers, their chemical N-modifications, and blood compatibility. *Biomaterials* **21(10),** 997–1003.
8. Rao, S. B. and Sharma, C. P. (1997) Use of chitosan as a biomaterial: studies on its safety and hemostatic potential. *J. Biomed. Mater. Res.* **34(1),** 21–28.
9. Chandy, T. and Sharma, C. P. (1990) Chitosan—as a biomaterial. *Biomater. Artif. Cells Artif. Organs* **18(1),** 1–24.
10. Muzzarelli, R., Baldassarre, V., Conti, F., Ferrara, P., Biagini, G., Gazzanelli, G., and Vasi, V. (1988) Biological activity of chitosan: ultrastructural study. *Biomaterials* **9(3),** 247–252.
11. Varum, K. M., Myhr, M. M., Hjerde, R. J., and Smidsrod, O. (1997) In vitro degradation rates of partially N-acetylated chitosans in human serum. *Carbohydr. Res.* **299(1–2),** 99–101.

12. Klokkevold, P. R., Fukayama, H., Sung, E. C., and Bertolami, C. N. (1999). The effect of chitosan (poly-N-acetyl glucosamine) on lingual hemostasis in heparinized rabbits. *J. Oral Maxillofac. Surg.* **57(1),** 49–52.

13. Muzzarelli, R. A. (1999) Clinical and biochemical evaluation of chitosan for hypercholesterolemia and overweight control *EXS* **87,** 293–304.

14. Stone, C. A., Wright, H., Clarke, T., Powell, R., and Devaraj, V. S. (2000) Healing at skin graft donor sites dressed with chitosan. *Br. J. Plast. Surg.* **53(7),** 601–606.

15. Illum, L. (1998) Chitosan and its use as a pharmaceutical excipient. *Pharm. Res.* **15(9),** 1326–1331.

16. Suh, J.-K. F. and Matthew, H. W. T. (2000) Application of chitosan-based polysaccharide biomaterials in cartilage tissue engineering: a review. *Biomaterials* **21,** 2589–2598.

17. Madihally, S. V. and Matthew, H. W. T. (1999) Porous chitosan scaffolds for tissue engineering. *Biomaterials* **20,** 1133–1142.

18. Hirano, S., Tsuchida, H., and Nagao, N. (1989) N-acetylation in chitosan and the rate of its enzymic hydrolysis. *Biomaterials* **10(8),** 574–576.

19. Lu, J. X., Prudhommeaux, F., Meunier, A., Sedel, L., and Guillemin, G. (1999) Effects of chitosan on rat knee cartilages. *Biomaterials* **20(20),** 1937–1944.

20. Cuero, R. G. (1999) Antimicrobial action of exogenous chitosan. *EXS* **87,** 315–333.

21. Felt, O., Carrel, A., Baehni, P., Buri, P., and Gurny, R. (2000) Chitosan as tear substitute: a wetting agent endowed with antimicrobial efficacy. *J. Ocul. Pharmacol. Ther.* **16(3),** 261–270.

22. Tsai, G. J. and Su, W. H. (1999) Antibacterial activity of shrimp chitosan against Escherichia coli. *J. Food. Prot.* **62(3),** 239–243.

23. Hidaka, Y., Ito, M., Mori, K., Yagasaki, H., and Kafrawy, A. H. (1999) Histopathological and immunohistochemical studies of membranes of deacetylated chitin derivatives implanted over rat calvaria. *J. Biomed. Mater. Res.* **46,** 418–423.

24. Washburn, E. W. (1921) Note on a method of determining the distribution of pore sizes in a porous material. *Proc. Natl. Acad. Sci. USA* **7,** 115–116.

5

Characterization of a Calcium Phosphate-Based Matrix for rhBMP-2

Hyun D. Kim, John M. Wozney, and Rebecca H. Li

1. Introduction

Bone morphogenetic proteins (BMPs) are members of the transforming growth factor-β (TGF-β) superfamily of proteins that have crucial roles in growth and regeneration of skeletal tissues. In particular, recombinant human bone morphogenetic protein-2 (rhBMP-2) has been shown to induce new bone formation by differentiation of mesenchymal progenitor cells into osteoblasts *(1)*. BMPs act locally, and thus for a clinically beneficial outcome, a carrier matrix is required to retain therapeutic levels of BMP at the repair site *(2,3)*. The potent osteoinductive ability of BMP-2 has been demonstrated in numerous preclinical *(4–9)* and clinical studies *(10–14)*. Recent data from clinical trials have reported success in the areas of open fracture repair *(10,14)*, interbody spinal fusion *(11)*, and maxillofacial reconstruction *(12,13)* using rhBMP-2 delivered in an absorbable collagen sponge (ACS). Because rhBMP-2/ACS requires implantation, there is a continuing need for an easily injectable carrier to deliver rhBMP-2 percutaneously to closed fractures. Here, we outline characterization of a calcium phosphate (CaP)-based injectable carrier as a delivery matrix for rhBMP-2.

1.1. Use of CaPs in Orthopedics

Recently, CaP-based cements have been used for orthopedic repairs such as open or closed long bone fractures, comminuted or displaced fractures of the tibial plateau, calcaneal fractures, intertrochanteric fractures of the proximal femur, and Colles fractures of the distal radius *(15)*. These materials have also been used for treatment of other indications such as vertebroplasty, spinal fusion,

and craniofacial trauma *(16–19)*. One such resorbable CaP-based cement that has gained regulatory approval for orthopedic repairs is BSM *(20)* (ETEX Corp., Cambridge, MA). BSM is an amorphous apatitic CaP cement that has currently been approved as a bone substitute for periodontal and craniofacial applications in the United States, as well as orthopedic applications in Europe and Canada. Unique features of this cement are that it sets endothermically, is easily injectable through a small-bore needle, and is remodeled like normal bone through osteoclast action *(21,22)*. This chapter summarizes the methods for evaluation of Calcium Phosphate Matrix (CPM, ETEX Corp), a promising injectable carrier composed of BSM as the base material, and the excipient sodium bicarbonate. CPM was developed in order to facilitate cell infiltration into the matrix after the injection by dispersing the cement into small granules. This matrix also exposes a larger surface area of rhBMP-2 to the host mesenchymal cells, resulting in accelerated bone induction and matrix resorption during the remodeling process. The use of CPM as a carrier also exploits the natural high affinity of rhBMP-2 for CaP materials such as bone. Preclinical animal studies showed that rhBMP-2 combined with a CaP cement was successful in bone repair in both non-critical sized defects *(23,24)* and critical-sized defects *(25)*.

1.2. Objective

The overall goal of this chapter is to describe various characterization techniques for an rhBMP-2 carrier using CPM as an example. In our laboratory, we have developed in vitro formulation methods for rhBMP-2 in combination with CPM. We have also identified several important characteristics of a successful rhBMP-2 matrix, including i) the ability to prolong the rhBMP-2 retention at the local repair site, ii) the ability to maintain the rhBMP-2 bioactivity, iii) the ability to allow cell infiltration, iv) the ability for the combination rhBMP-2/ CPM to form bone. Based on these criteria, we have developed methods to quantify rhBMP-2 bioactivity in combination with the carrier (in vitro), methods to track the local pharmacokinetics of rhBMP-2 released from CPM (in vivo and in vitro using ^{125}I-labeled rhBMP-2), and an in vivo assay of bone formation potential (rat ectopic model). Using these methods, we have begun to study the correlation of specific carrier properties and efficacy in animal models of clinical indications such as fracture healing.

2. Materials

2.1. rhBMP-2 and CPM

1. rhBMP-2 is produced by a Chinese hamster ovary (CHO) cell expression system *(26)*, yielding the secreted glycosylated, dimeric protein (Wyeth BioPharma, Andover, MA).

2. rhBMP-2 is stored at –80°C in an acidic (pH 4.5) glycine-based buffer containing 5 m*M* L-glutamic acid, 2.5% glycine, 0.5% sucrose, 5 m*M* NaCl, and 0.01% polysorbate until use, when it is thawed and stored at 4°C (*see* **Note 1**). This buffer is also used to dilute rhBMP-2 as necessary or used to prepare control carrier-only formulations.

3. BSM is provided by ETEX Corporation (Cambridge, MA).

4. Sodium bicarbonate (J.T. Baker, Phillipsburg, NJ) is used as an excipient. The carrier is comprised of 80% by weight (w/w) BSM and 20% w/w sodium bicarbonate, and is termed CPM. CPM is prepared as a sterile, dry powder in a mixing bulb. CPM powder is supplied in mixing bulbs containing 1.25 g material.

5. Standard 1- or 3-cc syringes are used with 17-gauge epidural Tuohy needles for injections.

2.2. In Vitro Retention Kinetics

1. ^{125}I-labeled rhBMP-2 (^{125}I-rhBMP-2) is obtained from New England Nuclear (Boston, MA). ^{125}I is used to label rhBMP-2 with Iodogen™ reagent in chloroform.

2. For determination of the percentage of non-precipitable (free ^{125}I) counts in the radiolabeled solution, 20% trichloroacetic acid (TCA) (Fisher Scientific) is combined with calcium and magnesium-free phosphate-buffered saline (PBS-CMF) and 10 mg/mL bovine serum albumin (BSA) in PBS-CMF.

3. Release media contains 49.5% (v/v) fetal bovine serum (FBS) (Hyclone, Logan, UT), 49.5% DME media (Sigma), and 1% Penicillin-Streptomycin (Gibco-BRL).

4. Polypropylene cryogenic vials (2-cc size, Corning, Corning, NY).

5. 37°C incubator shaker.

6. Gamma counter calibrated to ^{125}I (Perkin-Elmer, LKB Wallac Wizard Model 1470).

2.3. Morphology Evaluation by Scanning Electron Microscopy (SEM)

1. Colloidal silver paste (Ted Pella Inc., Redding, CA).

2. Sputter coating with Au/Pd (60/40).

3. Amray 3200/C environmental scanning electron microscope (KLA Tencor, Bedford, MA).

2.4. rhBMP-2/CPM Compatibility

A gentle extraction method is used to disassociate rhBMP-2 from the reacted CPM. The recovered protein is tested for bioactivity in a cell-based bioassay. rhBMP-2 is extracted from CPM using 1.0 *M* arginine, 5 m*M* histidine solution (Arg-His buffer), pH 6.5, in polypropylene test tubes (6 mL, 12×75 mm) under sonication (Sonic Dismembrator 60, Fisher Scientific). The rhBMP-2 concentration in the samples is determined by reverse-phase chromatography (RP-HPLC, Waters, Milford, MA). A bioassay to quantitatively evaluate the alkaline phosphatase activity of the extracted rhBMP-2 samples is performed using the W20-C17 mouse bone-marrow stromal cell line *(27)*. Cell-culture

media consists of 85.5% (v/v) Dulbecco's Modified Eagle's (DME) low bicarbonate, 10% heat-inactivated fetal bovine serum (FBS), 4% L-glutamine (200 m*M*), and 0.5% gentamycin.

2.5. Local Pharmacokinetics, Biocompatibility, and Bone Formation

A rat ectopic bone-induction assay is used to evaluate the biocompatibility, efficacy, and pharmacokinetics of rhBMP-2/CPM retention. Subjects are male Long Evans (Charles River) rats, approx 21 d old and 100 g. Bone formation is evaluated using radiographs and histology. Radiographs are taken using a General Electric MST-625II, with settings of 40 cm focal distance, 40 kVp, 200 mA, and 0.2 s exposure time, with Kodak Ektascan *M* film. Pharmacokinetic analysis of ^{125}I-rhBMP-2/CPM to determine local retention is performed using gamma scintigraphy (Siemens ZLC 7500 Orbitor Gamma Camera). Image acquisition is performed using a miniCAP XP electronics rack containing the acquisition processing electronics, disk drive, and network interface coupled to the gamma camera. Image analysis is performed using Picker International Odyssey™ software running on an ODYSSEY 380 workstation. Doses of a phantom control (10–20 µCi ^{125}I-rhBMP-2 in an Eppendorf tube) and the ^{125}I-rhBMP-2 in CPM delivered per site are determined daily by the Capintec® CRC-15R Radioisotope Dose Calibrator. The retention profiles generated from this analysis as a function of time are evaluated for pharmacokinetic parameters using WinNonlin™ Professional, Scientific Consulting, Inc. software.

3. Methods

3.1. Formulation of rhBMP-2 and CPM

Each bulb of CPM is reconstituted with 0.8 mL of rhBMP-2 solution, yielding a paste with a liquid-to-powder ratio of 0.64 (**Table 1**) and a final concentration of rhBMP-2 of 0.1 or 0.2 mg per mL paste (*see* **Note 2**). For the carrier control group, glutamate buffer without rhBMP-2 is added to the CPM powder. The volume of paste created by reconstituting one bulb with 0.8 mL of diluent is determined by completely extruding the paste from the 1.25 g bulb into a 3-cc syringe. This volume is multiplied by 0.1 or 0.2 mg/mL to determine the total mass of rhBMP-2 (in mg) needed for one bulb. For in vivo scintigraphy studies, the volume of radiolabeled rhBMP-2 required is determined by multiplying 25 µCi by the approximately seven 200-µL doses that one bulb provides. 25 µCi has been previously identified as an optimal amount of radioactivity for gamma scintigraphy detection in vivo. This trace amount of ^{125}I-rhBMP-2 is added to unlabeled rhBMP-2 solution to obtain the required dose. For in vitro retention studies, a 250-fold less radiolabel concentration of 0.1 µCi per 200 µL dose is sufficient for detection in a Wallac gamma counter. The volumes of the required rhBMP-2 hot and cold solutions are added together and

Table 1
rhBMP-2 Dilution

Matrix	Bulk rhBMP-2 volume (mL)	^{125}I-rhBMP-2 volume (mL)	Buffer volume (mL)	Total volume (mL)	Wetting volume per bulb (mL)	Estimated final paste volume per bulb (mL)	rhBMP-2 final concentration in matrix (mg/mL)
CPM for in vivo pharmacokinetics	0.300	0.656	2.644	3.600	0.8	1.400	0.200
CPM for in vitro release	0.150	0.003	3.447	3.600	0.8	1.400	0.100
CPM for in vivo efficacy	0.300	0.000	3.300	3.600	0.8	1.400	0.200

then subtracted from the total diluent volume needed for one bulb, and the remainder is the amount of additional glutamate buffer needed for one bulb.

The following example outlines a batch-type formulation for CPM paste. Formulation of CPM is performed with ^{125}I-rhBMP-2 for evaluation of in vitro retention kinetics and in vivo local rhBMP-2 retention profiles. Formulation of CPM is performed with non-radioactive rhBMP-2 for all other studies. The rhBMP-2 bulk liquid at 4.22 mg/mL is diluted to a final concentration of 0.1 or 0.2 mg rhBMP-2/mL matrix according to **Table 1**, in which rhBMP-2 bulk drug substance (4.22 mg/mL stock), ^{125}I-rhBMP-2, and glutamate buffer are added to a 10-mL vial to bring the final solution concentration to 0.35 mg/mL (which becomes 0.20 mg/mL after mixing with matrix assuming the matrix is at a vol of 1.4 mL per bulb after reconstitution). The final volume of this solution is 3.6 mL, enough to provide for four bulbs at 0.80 mL per bulb. Formulation and application of CPM is performed as follows:

1. For all formulations, the corresponding volumes of rhBMP-2, ^{125}I-rhBMP-2 (if required), and buffer solution are injected into the bulbs of the sterile prepackaged CPM powder.
2. The bulbs containing the liquid solution and powder are kneaded by hand for 1 min to obtain a consistent paste.
3. The injection cap is removed from the bulb containing the kneaded paste.
4. The plunger is removed from a 1-cc syringe.
5. Approximately 1 mL of the kneaded paste is then manually extruded from the bulb into the back-end of the 1-cc syringe.
6. For syringes containing ^{125}I-rhBMP-2, the dose is determined in the Capintec® Dose Calibrator.
7. A 17-g epidural Tuohy needle is then placed on the 1-cc syringe.
8. 200 μL of the paste is injected for each corresponding in vitro or in vivo test system.
9. For syringes containing ^{125}I-rhBMP-2, the delivered dose is determined by measuring the residual radioactivity in the syringe with the Capintec® Dose Calibrator.

3.2. In Vitro Retention Kinetics

The in vitro retention assay measures the percentage of rhBMP-2 remaining associated with the CPM as a function of time. ^{125}I-labeled rhBMP-2 is used to quantify the percent of CPM-bound protein. Vials are filled with 1 mL release media. 200-μL aliquots of rhBMP-2/CPM (0.1 mg/mL rhBMP-2, 0.1 μCi) are then dispensed into each vial by syringe. Samples are allowed to set at 37°C for 1 h, then transferred to a 37°C incubator shaker. The initial ^{125}I-rhBMP-2 dose loaded per vial is measured using the gamma counter. The amount of ^{125}I-rhBMP-2 remaining in the CPM is measured at 1, 3, 7, and 14 d by centrifuging the vials for 20 min at 1200 rpm (400 rcf), removing the supernatant, then measuring
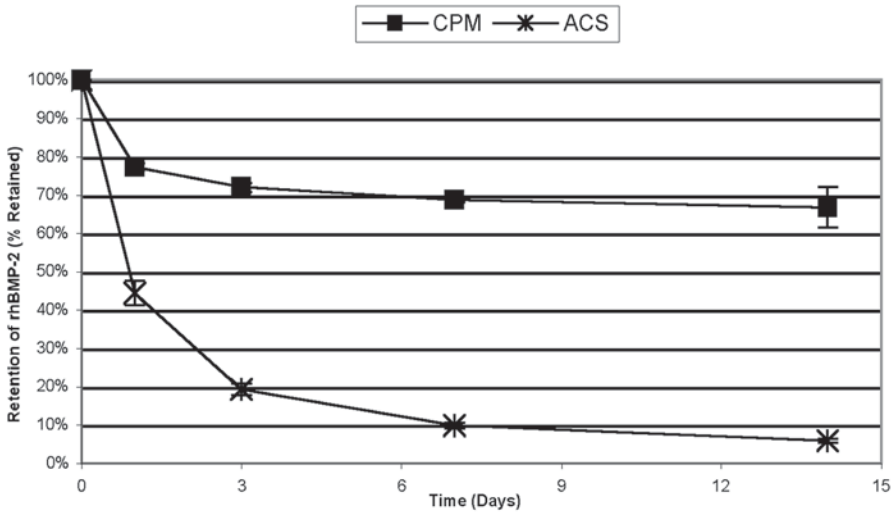
Fig. 1. In vitro retention kinetics of rhBMP-2 from CPM and ACS. Means ($n = 4$) ± standard deviations (S.D.) expressed as percent of initial dose. ACS = absorbable collagen sponge.

the radioactivity of the carrier for retained ^{125}I-rhBMP-2 counts. One mL fresh release media is then added to each vial. A retention profile for CPM as shown in **Fig. 1** can be generated from these data (corrected for radioactive decay and free ^{125}I), which can then be compared to other rhBMP-2 carrier materials (i.e., collagen sponge).

The TCA precipitation method is used to determine the initial free ^{125}I in the radiolabeled rhBMP-2 solution, as well as in the supernatants at each time-point as follows:

1. Prepare two vials containing 295 µL of BSA/PBS (10 mg/mL) and 200 µL PBS-CMF.
2. Add 5 µL of the radioactive sample to one vial of BSA/PBS to create a 500-µL, 100-fold dilution of ^{125}I-rhBMP-2.
3. Add 5 µL of material from the first vial to the second vial to create a 500-µL, 10K-fold dilution of ^{125}I-rhBMP-2.
4. Add 500 µL of TCA into the second vial, and obtain total counts using the Wallac Gamma Counter ("Initial Counts").
5. Allow sample to precipitate for 15 min, then centrifuge at 1200 rpm (400 rcf) for 10 min.
6. After centrifugation, aliquot 500 µL of the supernatant, and obtain counts per sample using gamma counter ("Soluble Counts").
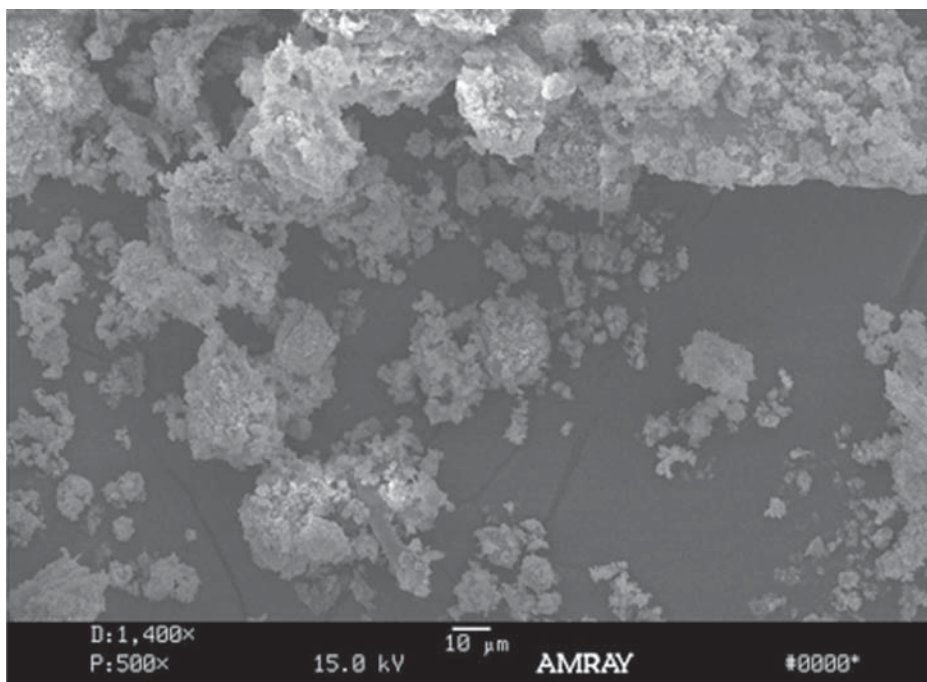7. The percentage of unbound ^{125}I is calculated as follows:

Fig. 2. SEM of CPM (500×). CPM injected into buffer, showing granule formation.

$$\% \text{ unbound } {}^{125}\text{I} = \frac{2 \times [\textit{Soluble Counts}](\textit{CPM})}{[\textit{Initial Counts}](\textit{CPM})} \times 100\% \tag{1}$$

8. The criteria for using initial label in the release assay is that the unbound ^{125}I is ≤5% of the total radioactive counts. If the amount unbound is >5%, the ^{125}I-labeled protein can be concentrated and purified through centrifugal filtration (*see* **Note 3**).

3.3. Morphology

In order to observe the morphology of CPM under simulated in vivo conditions, scanning electron microscopy (SEM) is used. CPM is injected into buffer and hardened at 37°C for 1 h. This example simulates the CPM appearance after injection and is characterized by granulation of the cement into macroparticles ranging from 100 μm to 2 mm in diameter. 200 μL samples are mounted on aluminum stubs with colloidal silver paste and dessicated overnight. Samples are sputter-coated with Au/Pd (60/40) and viewed with SEM (**Fig. 2**).

Table 2
Specific Activity of rhBMP-2 Extracted from CPM In Vitro

% rhBMP-2 yield	Specific activity (U/mg)	% Bioactivity
70	31,360 + 5400	100

*Control and reference samples measured 30,000 U/mg.

3.4. rhBMP-2/CPM Compatibility

CPM powder is reconstituted with rhBMP-2 to form the injectable paste. Once prepared, the rhBMP-2/CPM is dispensed as 200-µL aliquots into the bottom of 6-mL test tubes. The masses of these test tubes are previously measured and recorded. The CPM aliquots are allowed to cure for 60 min at 37°C, after which the masses of the test tube + CPM samples are measured and recorded. The mass of the CPM aliquot is obtained by difference. Extraction of rhBMP-2 is accomplished by addition of 2 mL of 2–8°C Arg-His buffer to each test tube. Samples are sonicated for 25 s in 1-s pulses with a 1-s rest between each pulse to prevent splashing, foaming, and excessive heating. Samples are maintained on ice throughout the procedure. The samples are then placed on a shaker for 3 h, and are then vortexed and centrifuged. Approximately 1.7 mL of supernatant is collected for RP-HPLC and in vitro bioactivity. Actual protein load per sample and percent yield can be determined from the mass of the CPM samples, the liquid-to-powder ratio, the initial rhBMP-2 concentration, and the RP-HPLC results. Two control samples of the rhBMP-2 solution (not mixed with CPM) are treated under the same protocol.

A bioassay to quantitatively evaluate the alkaline phosphatase activity of the extracted rhBMP-2 samples is performed using the W20-C17 mouse bone marrow stromal cell line as previously described *(27)*. W20-C17 cells are exposed to serial dilutions of rhBMP-2 solutions for ~24 h. The cells are then lysed by multiple freeze-thaw cycles in H_2O. The lysate is then tested for alkaline phosphatase activity through the hydrolysis of p-nitrophenyl phosphate to p-nitrophenol. Samples are read at 405 nm using a micro-plate reader (Perkin-Elmer HT5-7000), and nonlinear regression is performed on the OD data. Results are expressed as percent bioactivity compared to a concurrently run rhBMP-2 control. The extracted rhBMP-2 (after mixing, cementing within the CPM, then incubating in 37°C) is comparable in specific activity compared to the reference rhBMP-2 sample (**Table 2**). The 100% specific activity of rhBMP-2 extracted from CPM confirms maintenance of rhBMP-2 bioactivity following formulation and administration.

3.5. Pharmacokinetics, Biocompatibility, and Bone Formation

3.5.1. Local rhBMP-2 Retention in a Rat Ectopic Model

Pharmacokinetic evaluation of ^{125}I-rhBMP-2 local retention in the rat intramuscular site is performed using gamma scintigraphy following injection of ^{125}I-rhBMP-2/CPM. Gamma camera quantitation of retained ^{125}I is achieved through use of a phantom control with a known µCi quantity of the same isotope. The control is positioned in the image during each animal acquisition, and its dose is determined daily by the Capintec®. The Capintec® is utilized to determine the initial injection dose for each animal by measuring syringes containing matrix before and after injection. The Capintec® is calibrated at each time-point of the study for auto zero levels, background, system test, accuracy, and constancy through the use of ^{137}Cs, [57]Co, and [133]Ba of known activity.

Rats are anesthetized by isofluorane. The animals are placed on their right sides in the same position on the gamma camera head and in the same orientation to minimize variability. 200-µL injections are made in the intramuscular space in the right hamstring, with one radiolabeled rhBMP-2 injection per rat (*see* **Note 4**). Gamma camera images of each animal are obtained at initial, 2-h, 1, 2, 3, 4, 7, 14, and 21-d time-points. A low-energy, high-resolution collimator is used to minimize scatter and optimize the image spatial resolution. The gamma camera is peaked to an energy of [57]Co (122 keV) using spot markers that also provide an intrinsic daily quality control image. This intrinsic image allows the characterization of the uniformity of the gamma camera crystal's useful field of view. Background corrected counts per min are determined from a large region of interest drawn around the intramuscular site and the phantom control. Counts per min are then converted to µCi using the control phantom data. Retention data is corrected for ^{125}I radioactive decay. An example of ^{125}I-rhBMP-2 retention profile in CPM is provided (**Fig. 3**), and is compared to that from an absorbable collagen sponge (ACS) which exhibits a faster degradation.

Scintigraphy retention profiles are analyzed using WinNonlin™ software. A noncompartmental analysis is performed on each release profile providing area under the curve (AUC), mean residence time (MRT), and half-life ($t_{1/2}$) data. Noncompartmental parameters are estimated using the linear trapezoidal rule extrapolated to infinity. The AUC is determined from the observed area under the retention-time curve. The mean residence time is determined from the observed retention-time curve, and represents the average amount of time a rhBMP-2 molecule remains at the site of injection. The half-life is determined from the retention-time curve, and represents the rate by which one-half the administered dose leaves the injection site after equilibrium has been reached (terminal half-life). All pharmacokinetic data assumes that a linear ratio exists
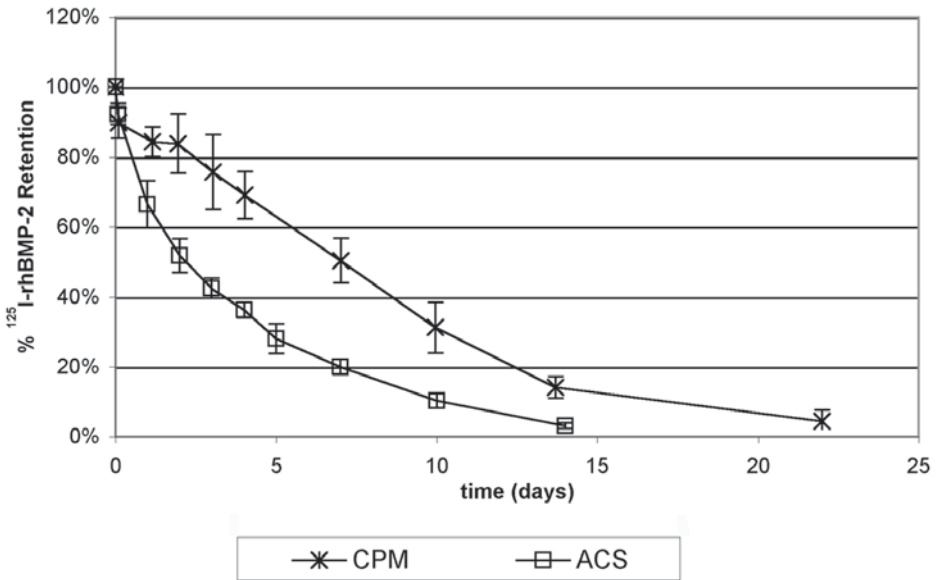
Fig. 3. In vivo local retention of ^{125}I-rhBMP-2/CPM and ^{125}I-rhBMP-2/ACS in the rat intramuscular site. Means ($n = 6$) ± S.D. expressed as percent of initial dose.

between radiolabeled and non-labeled rhBMP-2 throughout the study. Also assumed throughout the study is that radioactivity is only associated with intact rhBMP-2.

In the example provided (**Fig. 3**), the in vivo retention profile of ^{125}I-rhBMP-2 in CPM at the intramuscular site is shown in comparison to a carrier exhibiting faster ^{125}I-rhBMP-2 release kinetics—the collagen sponge implant (ACS). MRT, $t_{1/2}$, and AUC are calculated to be 6.7 ± 1.5, 4.8 ± 1.9, and 8.1 ± 1.1 d, respectively, for the ^{125}I-rhBMP-2/CPM retention profile.

As expected, the in vitro retention kinetics differ significantly from those observed in vivo because of the differing mechanism of rhBMP-2 release in the two environments (**Fig. 1** vs **Fig. 3**). In vivo, the CPM is resorbed, and rhBMP-2 is solubilized and liberated through cellular action. In vitro, very little of the rhBMP-2 is released since the CPM is not soluble, and rhBMP-2 has a high binding affinity for the CaP. As a result, the release of rhBMP-2 from CPM in vivo appears to be coupled to osteoclastic resorption of the carrier in a manner similar to remodeling of normal bone.

3.5.2. Bone Formation in the Rat Ectopic Bone Formation Assay

A rat ectopic model is used to test rhBMP-2/CPM's biocompatibility and bone formation efficacy. Injections are made as in **Subheading 3.5.1** with the
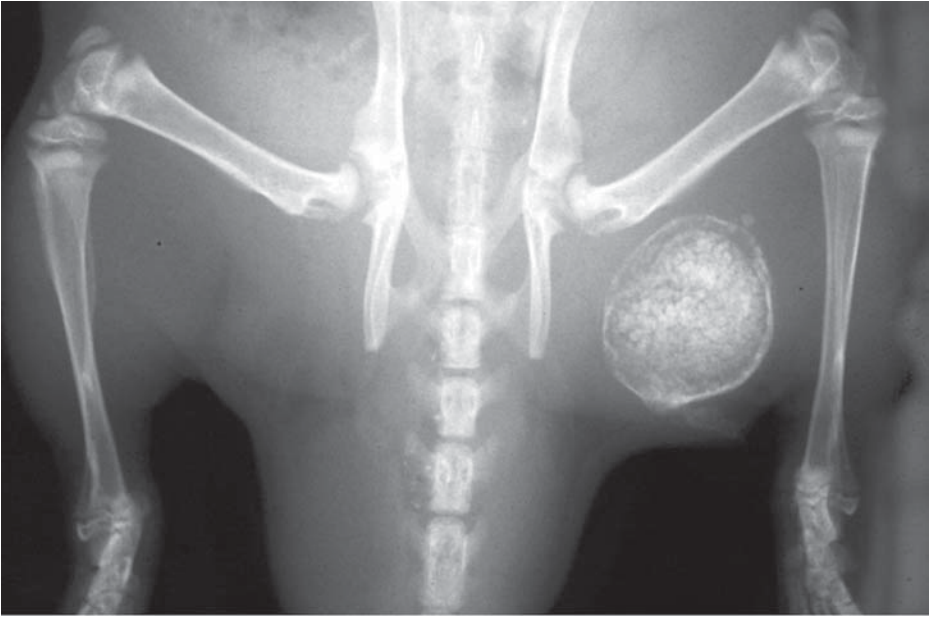
Fig. 4. One-week radiograph in the rat IM ectopic model, 0.2 mg/mL rhBMP-2 in CPM.

exception that non-radiolabeled rhBMP-2 is used to reconstitute the CPM. Radiographs are taken from the antero-posterior view at post-surgery and weekly until the animals are euthanized. By 3 wk post-injection, the animals are euthanized and explants are carefully separated from the surrounding tissue to avoid disrupting the carrier/host tissue interface. Explants are placed in labeled tissue cassettes and placed in 70% ethanol. Samples are embedded undecalcified in methylmethacrylate, cut into 5–7-μ sections, mounted on slides, and stained with Goldner's trichrome stain *(28)*. Samples can then be analyzed for outcome assessments such as biocompatibility, degree of bone formation, degree of matrix degradation, and mechanism of bone formation.

Postoperative radiographs allow visualization of the radiopaque CPM carrier in the intramuscular site and assessment of the timing of bone formation (**Fig. 4**). Histology (**Fig. 5**) shows that after 21 d, the CPM has been largely replaced by new bone formed through both endochondral and intramembranous pathways. Histology also shows minimal inflammatory cells present at the rhBMP-2/CPM site, suggesting that this material is biocompatible.

In this model, the ability of rhBMP-2/CPM to stimulate local bone formation is visualized through histology and radiography results. This ectopic bone induction is presumed to be an effect of rhBMP-2's well-documented ability to
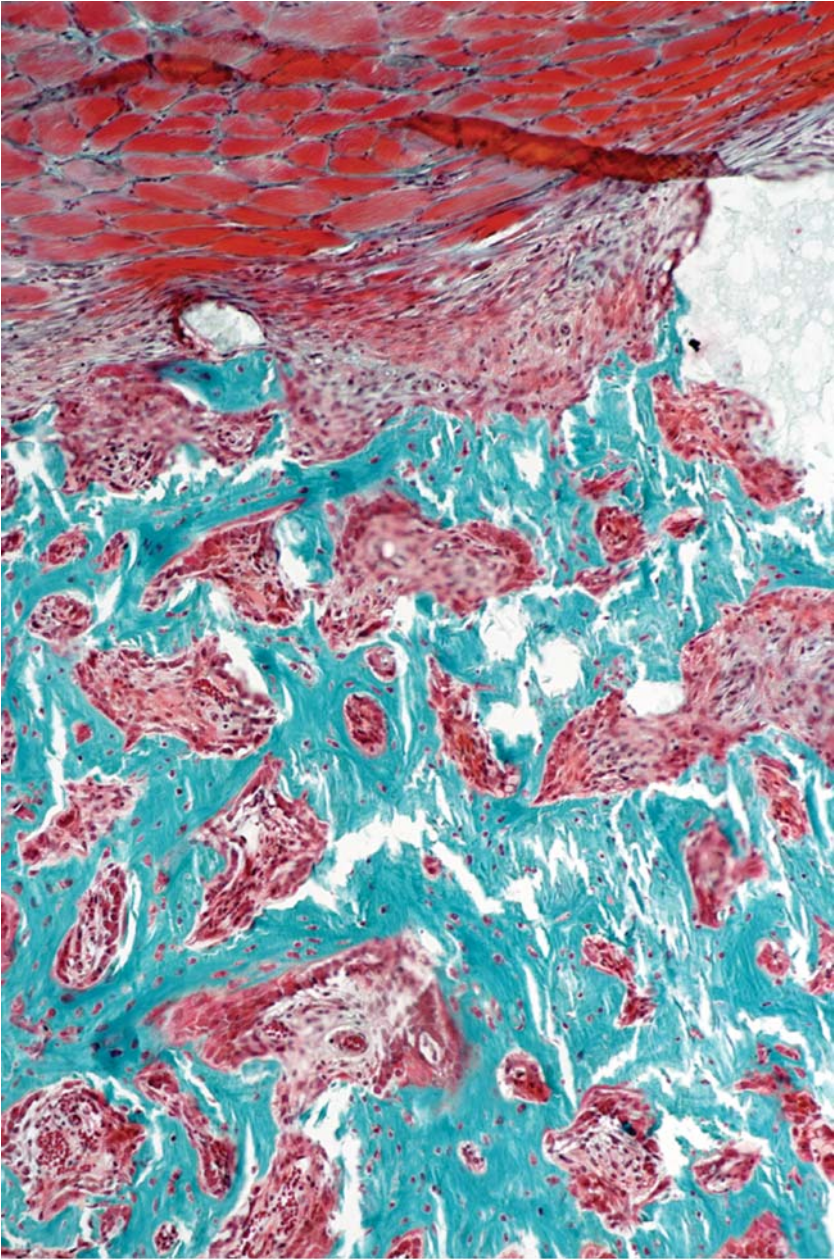
Fig. 5. Bone formation efficacy of rhBMP-2/CPM in the rat ectopic model, $t = 21$ d. Sections are stained with Goldner's trichrome, 10×. (*See* color plate 2 appearing in the insert following p. 112.)

induce the local differentiation of uncommitted mesenchymal and osteoblast precursor cells into osteoblasts *(1,29)*. In addition, the presence of rhBMP-2 accelerates the resorption of the CPM carrier. The use of rhBMP-2 delivered in CPM for acceleration of fracture repair, non-union fractures, bone defect repair, reconstructive surgery, and other orthopedic repairs may hold great promise for clinical orthopedics and tissue engineering.

4. Notes

1. rhBMP-2 is a relatively stable protein, and can be stored at 4°C for several months. However, the stock rhBMP-2 protein should be sub-aliquoted and frozen at –80°C so that only the necessary amounts are thawed and used. Repeated freezing and thawing should be avoided.
2. A range of rhBMP-2 doses for CPM paste can be achieved, depending on the concentration of rhBMP-2 added to the CPM powder. Typically, the working range for various preclinical studies are 0.1–4.0 mg rhBMP-2 per mL paste.
3. If low radioactivity is expected, the PBS-CMF may be exchanged for a greater volume of the radiolabeled sample. In cases in which very low counts are expected, (e.g., d 7 or 14 of an in vitro retention supernatant), a dilution of 200 µL BSA and 300 µL hot sample before the addition of TCA can be done. It is also important to ensure sufficient protein in the samples to be fully precipitated by the TCA.
4. One syringe is used for each injection in order to measure the delivered dose in µCi before and after injection using a Capintec dose calibrator. The CPM carrier is radiodense, allowing the placement of the treament to be visualized with fluoroscopy or radiography during or following injection.

Acknowledgments

References

1. Wozney, J. M. (1990) The bone morphogenetic protein family and osteogenesis. *Mol. Reprod. Dev.* **32,** 160–167.
2. Winn, S. R., Uludag, H., and Hollinger, J. O. (1998) Sustained release emphasizing recombinant human bone morphogenetic protein-2. *Adv. Drug Delivery Rev.* **31,** 303–318.
3. Li, R. H. and Wozney, J. M. (2001) Delivering on the promise of bone morphogenetic proteins. *Trends Biotechnol.* **19(7),** 255–265.
4. Gerhart, T. N., Kirker-Head, C. A., Kriz, M. J., et al. (1993) Healing segmental femoral defects in sheep using recombinant human bone morphogenetic protein-2. *Clin. Orthop.* **293,** 317–326.

5. Hanisch, O., Tatakis, D. H., Rohrer, M.D., et al. (1997) Bone formation and osseointegration stimulated by rhBMP-2 following subantral augmentation procedures in nonhuman primates. *Int. J. Oral Maxillofac. Implants* **12,** 785–792.

6. Muschler, G. F., Hyodo, A., Manning, T., et al. (1994) Evaluation of human bone morphogenetic protein-2 in a canine fusion model. *Clin. Orthop.* **308,** 229–240.

7. Sigurdsson, T. J., Lee, M. B., Kubota, K., et al. (1995) Periodontal repair in dogs: recombinant human bone morphogenetic protein-2 significantly enhances periodontal regeneration. *J. Periodont*. **66,** 131–138.

8. Zegzula, H. D., Buck, D. C., Brekke, J., et al. (1997) Bone formation with use of rhBMP-2 (recombinant human bone morphogenetic protein-2). *J. Bone Jt. Surg. Am.* **79,** 1778–1790.

9. Bax, B. E., Wozney, J. M., and Ashhurst, D. E. (1999) Bone morphogenetic protein-2 increases the rate of callus formation after fracture of the rabbit tibia. *Calcif. Tiss. Int.* **65,** 83–89.

10. Riedel, G. E. and Valentin-Opran, A. (1999) Clinical evaluation of rhBMP-2/ ACS in orthopedic trauma: a progress report. *Orthopedics* **22(7),** 663–665.

11. Boden, S. D., Zdeblick, T. A., Sandhu, H. S., and Heim, S. E. (1999) The use of rhBMP-2 in interbody fusion cages: definitive evidence of osteoinduction in humans, in *Transactions of the Annual Meeting of the American Academy of Orthopaedic Surgeons*, Anaheim, CA, p. 41.

12. Boyne, P. J., Marx, R. E., Nevins, M., et al. (1997) A feasibility study evaluating rhBMP-2/absorbable collagen sponge for maxillary sinus floor augmentation. *International Periodo, J. Resto. Dent.* **17(1),** 11–25.

13. Howell, T. H., Fiorellini, J., Jones, A., et al. (1997) A feasibility study evaluating rhBMP-2/absorbable collagen sponge device for local alveolar ridge preservation or augmentation. *Int. J. Periodontics Restorative Dent.* **17,** 124–139.

14. BESTT (The BMP-2 Evaluation in Surgery for Tibial Trauma Study Group), Govender, S., Csimma, C., et al. (2002) Recombinant human bone morphogenetic protein-2 for open tibial fractures: a prospective, controlled, randomized study in 450 patients. *J. Bone and Jt. Surg.* **84-A(12),** 2123–2134.

15. Frankenburg, E., Goldstein, S., Bauer, T., Harris, S., and Poser, R. (1998) Biomechanical and histological evaluation of a calcium phosphate cement. *J. Bone Jt. Surg.* **80–A(8),** 1112–1124.

16. Lobenhoffer, P., Gerich, T., Witte, F., and Tscherne, H. (2002) Use of an injectable calcium phosphate bone cement in the treatment of tibial plateau bone fractures: a prospective study of twenty-six cases with twenty-month mean followup. *J. Orthop. Trauma* **16(3),** 143–149.

17. Reddi, S., Stevens, M., Kline, S., and Villaneuva, P. (1999) Hydroxyapatite cement in craniofacial trauma surgery: indications and early experience. *Craniomaxillofac, J. Trauma* **5(1),** 7–12.

18. Heini, P. and Berlemann, U. (2001) Bone substitutes in vertebroplasty. *Eur. Spine J.* **10 (Suppl 2),** S205–S213.

19. Spivak J. and Hasharoni, A. (2001) Use of hydroxyapatite in spine surgery. *Eur. Spine J.* **10(Suppl 2),** S197–S204.

20. Schmitz, J. P., Hollinger, J. O. and Milam, S. B. (1999) Reconstruction of bone using calcium phosphate bone cements. *J. Oral Maxillofac. Surg.* **57,** 1122–1126.
21. Lee, D., Tofighi, A., Aiolova, M., et al. (1999) a-BSM: a biomimetic bone substitute and drug delivery vehicle. *Clin. Orthop.* **367S,** S396–S405.
22. Knaack, D., Goad, E., Aiolova, M., et al. (1997) Novel fully resorbable calcium phosphate bone substitute. *J. Bone Miner. Res.* **12(1),** S202.
23. Edwards, I., R., Zabka, A., Hayashi, K., et al. (2000) Accelerated fracture healing by percutaneous injection of rhBMP-2 and alpha-BSM, in *Transactions of the Annual Meeting of the Orthopaedic Research Society*, Orlando, FL., p. 850.
24. Seeherman, H., Aiolova, M., Bouxsein, M., and Wozney, J. (2001) A single injection of rhBMP-2/calcium phosphate paste accelerates healing in a nonhuman primate osteotomy model, in *Transactions of the Annual Meeting of the Orthopaedic Research Society*, San Francisco, CA, p. 251.
25. Hollinger, J., Buck, D., Schmitt, J., et al. (1999) An injectable endothermically-setting calcium phosphate material bridges critical-sized defects in rabbits in combination with rhBMP-2, in *Transactions of the Annual Meeting of the Orthopaedic Research Society*, Anaheim, CA, p. 509.
26. Israel, D. I., Nove, J., Kerns, K. M., et al. (1992) Expression and characterization of bone morphogenetic protein-2 in chinese hamster ovary cells. *Growth Factors* **7,** 139–150.
27. Thies, R. S., Bauduy, M., Ashton, B. A., et al. (1992) Recombinant human bone morphogenetic protein-2 induces osteoblastic differentiation in W-20–17 stromal cells. *Endocrinology* **130(3),** 1318–1324.
28. Schenk, R. K., Olah, A.J., and Herrmann, W. (1984) Preparation of calcified tissues for light microscopy, in *Methods of Calcified Tissue Preparation* (Dickson, G. R., ed.), Elsevier Science, New York, NY, pp. 1–42.
29. Wozney, J. M., Rosen, V., Celeste, A. J., et al. (1988) Novel regulators of bone formation: molecular clones and activities. *Science* **242,** 1528–1534.

6

Methodologies for Processing Biodegradable and Natural Origin Scaffolds for Bone and Cartilage Tissue-Engineering Applications

Manuela E. Gomes, Patrícia B. Malafaya, and Rui L. Reis

1. Introduction

The ultimate goal of tissue engineering is to replace, repair or enhance the biological function of damaged, absent or dysfunctional elements of a tissue or an organ. Engineered tissues are produced by using cells that are manipulated through their extracellular environment to develop living biological substitutes for tissues that are lacking or malfunctioning *(1–5)*. Many different strategies may be used to accomplish this goal. Among the most important factors that determine the selection of the best strategy for developing and utilizing engineered tissues are the technical feasibility, the required properties of the implant, and the interaction of the host with the graft.

The selection of the appropriate approach implies the simultaneous selection of an adequate biomaterial design format, which must be able to induce the desired tissue response *(1–6)*. Three-dimensional (3D) structures have been recognized since the mid-1970s as important components for the development of engineered tissues *(6)*, and in the past few years, the development of matrices to serve as templates for cell attachment/suspension and delivery has progressed at a tremendous rate.

The materials to be used as scaffolds in tissue engineering must fulfill a number of complex requirements, such as biocompatibility, biodegradability (with controlled degradation rate), appropriate porous structure, mechanical properties and suitable surface chemistry. Because of the demand for biodegradability, only biodegradable polymers and some ceramics can be used in tissue engineering. Because ceramics are often difficult to process into porous

matrices with complex 3D shapes and their degradation rates are difficult to control *(7)*, biodegradable polymers have become the most attractive materials to produce tissue-engineering scaffolds, as they are very versatile materials. The selection of the most appropriate polymer to produce the scaffold is a very important step in the construction of the tissue engineered product because its intrinsic properties will determine to a great extent the properties of the scaffold. However, the selected design and method of producing these scaffolds will deeply influence its final characteristics, as it can dramatically change the type and amount of porosity, the mechanical properties and degradation behavior, the surface properties, and even the biocompatibility of the scaffold material.

Therefore, various processing techniques have been and are being developed to fabricate these scaffolds, such as solvent casting *(8–12)*, particulate leaching *(8–13)*, membrane lamination *(10,14)*, fiber bonding *(9,10,14)*, phase separation/inversion *(10)*, high-pressure-based methods *(10,15)*, melt-based technologies *(9,16–19)*, and microwave baking and expansion *(20)*. More recently, highly porous 3D scaffolds have been obtained using advanced textile technologies and rapid prototyping technologies such as fused deposition modeling (FDM) and 3D printing *(21)*. These engineering technologies are highly controllable and reproducible, and facilitate the manufacture of well-defined 3D structures *(22)*.

The optimization and customization of any of these processing technologies to design and manufacture the scaffolds requires a thorough understanding of the materials and equipment that must be used *(22,23)*.

This chapter describes some polymer scaffold-processing methods, particularly developed/optimized to be used with biodegradable—and more specifically, with natural origin—polymers. The described methods include melt-based technologies (using blowing agents or leachable particles), solvent casting and particle leaching, freeze-drying and microwave baking.

1.1. Solvent-Casting and Particle Leaching

The solvent casting and particle leaching method is probably the most well-known process to date for producing scaffolds for tissue engineering.

The solvent casting and particle-leaching method consists of dispersing sieved water (or other "friendly" solvent) soluble particles, such as sugar, gelatin mineral, or sodium chloride (for example) in a polymer solution. This dispersion (polymer/leachable particles) is then processed by casting in order to produce porous 3D supports. The porosity basically results from the selective dissolution of the particles from the polymer/salt composite, although phase separation of the polymer solution can also contribute to the formation of the porous structure *(24)*. Therefore, the porosity and pore size can be controlled independently by varying the amount and size of the salt particles, respectively.

The surface area depends on both initial salt-weight fraction and particle size *(7,9,10,24)*. The main disadvantage presented by this technique is the use of toxic solvents, which may leave residues in the final samples, as well as the typical low stiffness and strength of the developed scaffolds.

1.2. Melt-Based Technologies—Injection Molding and Extrusion With Blowing Agents

To our knowledge, melt-molding has not yet been used by other groups as a single technique to produce scaffolds for tissue engineering. It is normally used in combination with porogen techniques or to produce a pre-shape of the final material—for example, in high-pressure methods. Recently, melt-based technologies, such as injection molding and extrusion, have been proposed as an adequate processing route to produce scaffolds by means of a single step *(16,18,19)*. In these processes, the polymers are previously mixed with blowing agents (BAs), which are previously selected according to factors such as their decomposition temperatures or non-cytotoxicity. The porous structure of the samples obtained by extrusion or injection molding of the polymers combined with BAs results from the gases released by decomposition of the blowing agent during processing. Therefore, with these melt-based methods, it is difficult to have full control over the pore size and the interconnectivity between the pores of the materials obtained by these methods.

The injection molding process is a very reproducible technique, which allows the development of a 3D structure with highly complex designs, in great series.

The extrusion process is very similar to injection molding, but the pressures involved in the former process are usually much lower, which often facilitates the expansion reaction and the achievement of higher porosities. However, the shapes of the samples that can be produced are much more restricted.

1.3. Compression Molding Combined With Particle Leaching

Compression molding and particle leaching are also melt-based methodologies, but in this case there is an additional processing step that consists of the selective dissolution of leachable particles, which are previously mixed with the polymer (as previously described for the solvent casting/particle-leaching method). The most important advantage of this method, regarding the previously described melt-based techniques, is that it makes it possible to control the percentage of porosity and the pore size by simply selecting the appropriate amount and size of the leachable particles used.

1.4. Freeze-Drying

Phase separation of polymer solution may actually be induced by several methods. The basic principle of the freeze-drying process relies on a thermally

induced phase separation, which occurs when the temperature of a homogenous polymer solution, previously poured into a mold, is decreased. Once the phase-separated system is stabilized, the solvent-rich phase is removed by vacuum sublimation, leaving behind the polymer foam. The foam morphology is controlled by any phase transition that occurs during the cooling step—e.g., liquid-liquid or solid-liquid demixing *(7)*.

1.5. Microwave Baking

The microwave baking methodology is an innovative and simple processing route to produce starch (or other natural origin)-based porous materials that have been originally developed in our research group *(20)*. One of the innovative features of this method, that can be very useful in the clinical arena, is that a thermally stable drug (or other bioactive agent) can be loaded during the processing, allowing for a homogeneous dispersion within the polymeric carrier and a controlled release that depends on the porosity of the systems as well as on their swelling and degradation behaviors.

2. Materials

2.1. Solvent Casting and Particle Leaching

1. Leachable particles: sodium chloride particles of different sizes (NaCl) have been widely used as leachable particles because they are easily dissolved in water and can be found in many different sizes. Alternatively, other soluble substances can be used, such as sugar or gelatin, for example. The following text is based on the use of NaCl particles.
2. Starch-based polymer or other natural-based polymer in the powder form.
3. Appropriate solvent for the selected polymers: if it is not known at this time which solvent to use, it will be necessary to perform solubility tests in order to find the less toxic solvent that can dissolve the polymer properly, without degrading its mol wt and compromising its tailored degradation rate.

2.2. Injection Molding With BAs

1. Injection molding machine.
2. Injection mold.
3. Granules of starch-based polymer (or other natural-based polymer) or other biodegradable polymer for example, poly(lactic acid) (PLA), poly(glycolic acid) (PGA), or polycaprolactone that can be processed by melt technologies. Keep in mind that because it will be necessary to use large amounts of polymer, therefore this should be available in large quantities (the optimization trials should not be performed with very expensive medical-grade polymers).
4. Blowing agent. This should be selected according to:
   a. Decomposition/reaction temperature: This should be as close as possible to the melt temperature (T_m), (which will also determine the processing temperatures) of the polymer.

    b. Toxicity: Although it is not possible to find BAs specifically designed/produced for biomedical applications, many have been used—for example, in the food industry—that have low or none toxicity.

2.3. Extrusion With BAs

1. Extrusion machine.
2. Extrusion die.
3. As described in **Subheading 2.2., step 3.**
4. As described in **Subheading 2.2., step 4.**

2.4. Compression Molding With Particle Leaching

1. Hot press.
2. Mold with the desired shape.
3. As described in **Subheadings 2.2.** and **2.3.**
4. Salt (NaCl) particles of the desired size (or other particles, soluble in water or other "friendly" solvents, as stated previously).

2.5. Freeze-Drying-Based Technique

1. Chitosan flakes: The proposed methodology can also be used with other natural and biodegradable polymers. The polymer selection will influence the methodology—namely, the choice of an appropriate solvent—to prepare the polymer solution.
2. Acetic acid (1 *M*) solution.
3. NaOH (1 *M*) solution.
4. Glutaraldehyde.
5. Bioactive filler, in the case of composite scaffold production.
6. Proper mold.
7. Adequate glassware.
8. Liquid nitrogen.
9. Freezer.
10. Lyophilizator.

2.6. Microwave-Based Technique

1. Blend of corn starch with ethylene vinyl alcohol blend (SEVA-C). The proposed methodology can also be used for other blends of starch with synthetic polymers, such as poly(ε-caprolactone (PCL) and PLA, which are being study in our research group.
2. Commercially available baking powder, containing corn starch, sodium pyrophosphate, and sodium bicarbonate or other porifier that releases CO_2.
3. Hydrogen peroxide (H_2O_2 30% v/v).
4. Bioactive filler in case of composite scaffold production.
5. Biologically active agent in the case of drug-delivery systems production or growth factors/other proteins, in the case of scaffolds processing.
6. Proper mold.

7. Adequate glassware.
8. Microwave oven.
9. Conventional oven.

3. Methods

3.1. Solvent-Casting and Particle Leaching

1. Select a solvent capable of dissolving the polymer without affecting its properties and with the lowest possible cytotoxicity.
2. Select the amount of polymer and solvent to use for preparing each sample (or several samples at once), depending on the size of the final samples that is desired. For example, for obtaining a sample in the disk shape using a glass Petri dish of 6 cm of diameter, start by dissolving 8 g of the polymer (in powder form) in 20 mL of solvent. This solution must disclose an adequate viscosity, so that when the salt (or other alternative) leachable particles are added, they can remain uniformly dispersed in this solution while the sample is dried.
3. After preparing the polymeric solution, it is usually necessary to allow the evaporation of the excess solvent (during less than 24 h) before adding the salt particles.
4. Disperse the sieved NaCl particles in the polymer solution. The amount and size of the salt particles to be used will determine the amount and size of the pores in final sample. In general, a salt-weight fraction of about 80% should be added (based on the total mass of polymer and salt). The size of the particles used should range from 50–1000 µm. A variation of this method includes the use of vibration during dissolution of the polymer in the solvent and during solvent evaporation.
5. Pour the mixture of the polymeric solution with the salt particles into a mold (with desired shape) and place it in an oven at 37°C in order to allow the progressive evaporation of the remaining solvent and resulting solidification of the sample, for about 4–5 d.
6. When the samples are completely solidified, immerse them in distilled water (or other solvent, depending on the selected polymer and leachable particles) during a period of several days (optimize for the amount of salt particles used) and change the water daily, for total leaching of the salt particles. This leaching period can be shortened by increasing the number of water changes.
7. Finally, let samples dry.

3.2. Injection Molding With BAs

1. Select appropriate BA to use.
2. Select appropriate mold to use. This should allow the reaction of the BA—e.g., the expansion inside the polymer melt—as much as possible, and therefore must be designed to avoid the development of very high pressures.
3. Pre-mixing of the polymer and the BAs in a bi-axial rotating drum: the range of the amounts of BA that can be used is usually suggested by the BA manufacturer, but this quantity must be optimized according to the desired porosity (minimum 80%). Ideally, the least possible amount of BA should be used in order to avoid any cytotoxicity problems.

4. Injection molding of the polymer BA mixture: This process demands some previous knowledge and experience in order to be optimized, particularly if there is no previous knowledge of the processing conditions to be used for the selected polymer. The expansion reaction during processing will develop additional pressure, which must be balanced with the normal pressures involved in this process. Additional care must also be taken when dealing with natural origin polymers (or other biodegradables), since these are usually very sensitive to thermal degradation.

5. Removal of outer layer of the samples: This process usually leads to the formation of an outer compact layer of polymer, because the first polymer melt that reaches the mold cavity will find the cold wall of this mold and solidify too rapidly to enable the diffusion of the gas generated by the reaction of the BA. Therefore, it is necessary to perform a final machining step to remove this outer layer of the samples, leaving the porous structure exposed. For this purpose, several types of equipments can be used., such as a precision diamond wire saw.

3.3. Extrusion With BAs

1. As described **Subheading 3.2.1.**
2. Selection of the appropriate die: Usually, the larger the die, the better the results. This should be balanced with the availability of material to be processed.
3. As described in **Subheading 3.2.3.**
4. As described in **Subheading 3.2.4.**, although the processing parameters in extrusion are not as many as in the injection molding and are usually easier to understand and optimize.
5. As described in **Subheading 3.2.5.**, but usually in extrusion these layers are thinner and easier to remove.

3.4. Compression Molding—Particle Leaching

1. Select appropriate mold to use. Typically, it cannot be too thick in order to avoid polymer degradation and allow for a proper dissolution of the particles encapsulated on the molded part.
2. Mixing of the polymer and the leachable particles in a bi-axial rotating drum: as in the solvent casting method, the amount and size of the salt particles to be used will determine the amount and size of the pores in the final sample. In general, a salt-weight fraction of about 80% should be added (based on the total mass of polymer and salt). The size of the particles to use should range from 50–1000 μm. Again, other leachable particles can be used, but in this case, they should be thermally stable.
3. Compression molding of the polymer/salt particles mixture: the temperature to use should be very close to the T_m of the polymer, and the pressure must be optimized according to the mold that will be used.
4. Immerse samples in distilled water to remove the leachable particles.

3.5. Freeze-Drying-Based Technique

1. Mill the chitosan flakes (or other flakes/powders of other biodegradable polymers that can also be used) into chitosan powder in order to facilitate the polymer dissolution.

2. Prepare the polymeric solution by dissolving the chitosan powders in the acetic acid solution. The concentration of the polymeric solution will depend on the degree of acetylation of the chitosan used to prepare the scaffolds. This concentration must be maximized before starting scaffold production, and this may require a range of preliminary tests.

3. In order to avoid any extra washing during the materials production (this can be totally undesirable in instances such as the production of scaffolds that incorporate bioactive agents (e.g., drugs, proteins, or growth factors) if the bioactive agents can be loaded during the processing), with the goal of optimizing the scaffold properties, the pH of the polymeric solution is increased to 6.5 with a NaOH solution. This pH increase will prevent any further acidification when immersing the scaffolds in any aqueous medium, avoiding the need for extra washing steps following scaffold production. If the pH is raised, additional care is needed in the crosslinking reaction.

4. If crosslinked samples must be produced, the crosslinking solution should be added at this step in the desired amount. If the pH is higher, the crosslinking reaction will be more rapid, and can take place in a few minutes.

5. Pour the mixture of the polymeric solution into a proper mold (with the desired shape) and the desired amount. Do not forget that these molds must be frozen at –85°C, and in the case of composite scaffold production they will be immersed in liquid nitrogen. For instance, for a cylindrical mold with 3-cm diameter and 5 g of chitosan solution should be cast to produce samples with 3 ± 0.3 cm of diameter 0.5 ± 0.05 cm high. The deviation in the dimensions is dependent on the crosslinking process.

6. If composite samples are desired, the bioactive filler (e.g., hydroxyapatite, bioactive glass, or bi-phasic calcium phosphates [CaPs]) should be added at this point. In order to avoid the sedimentation of the filler, the samples should be immediately frozen in liquid nitrogen. The filler composition and cristallinity should be selected accordingly to the desired level of bioactivity.

7. After the molds are ready, keep them the frozen (at –85°C) overnight.

8. Freeze-dry in a lyophilizator at –85°C and 0.012 Pa to form the porous structures resulting from sublimation of ice crystals.

9. It is possible to improve the material properties of the resulting non-crosslinked samples, namely in terms of swelling behavior. After freeze-drying, the samples should be immersed in a NaOH (1 *M*) solution for a few minutes in order to precipitate the chitosan polymer. Then, go back to **step 7** and repeat the procedure.

10. The samples should be kept in a desiccator until they are used.

3.6. Microwave-Based Technique

1. Select the appropriate mold in terms of material, shape, and dimensions. Do not forget that it must be a proper material that can withstand microwave radiation.

2. Weigh into the mold the correct amount of polymer powders according to the desired final product composition.

3. Weigh into the mold the correct amount of BA according to the desired final product. Typical values are approx 5 and 10% wt of total formulation.

4. Weigh into the mold the correct amount of bioactive filler if composite scaffolds production is the goal. Several percentages can be used in order to achieve different mechanical and morphological properties, as well as different rates of bioactivity.

5. Hydrogen peroxide (H_2O_2) is then added until consistent slurry dispersion is obtained. The adequate quantity of H_2O_2 must first be optimized, depending on the hydrophilicity of the polymeric blend used. Then, the amount of hydrogen peroxide is fixed. For example, in the case of starch-based scaffold production, the amount is typically 1:1 (wt/wt, with respect to the total weight of the polymeric blend), and subsequently the same amount is used for the production of all the samples. The hydrogen peroxide also acts as a BA, and consequently, some samples without any baking powder (only with H_2O_2) are also produced, making it possible to study the effects of the hydrogen peroxide.

6. In the production of drug delivery systems, the drug (or other bioactive agent) is added in amounts up to 20% wt, and dissolved in hydrogen peroxide (H_2O_2) before adding to the solid powders, during the processing route as described, in **steps 4** and **5**.

7. The mixture is then processed in a microwave oven. The microwave oven power setup and treatment time must be optimized as a function of several conditions, such as the presence (and amounts) of baking powder, bioactive filler, and drug. Typical values are between 250 and 400 W for the furnace power, and 1–5 min for the treatment time.

8. The samples are then dried at 50°C for 1 h in a conventional oven.

9. The samples should be kept in a desiccator until they are used.

4. Notes

1. During the extrusion and injection molding with BAs methods, it is also possible to use surfactant agents to obtain a better control of the obtained porosity and its shape, and particularly the interconnectivity between pores.

2. More details about the injection molding with BAs can be found in **refs. *(16,18)***, and more information about the extrusion with BAs, compression molding, and solvent casting and particle leaching can be found in **refs. *(18,19)***. Microwave-baking processing details may also be found on **ref. *(20)***.

References

1. Hardin-Young, J., Teumer, J., Ross, R. N., and Parenteau, N. L. (2000) Approaches to transplanting 1 engineered cells and tissues, in *Principles of Tissue Engineering*, 2nd ed. (Lanza, R., Langer, R., Vacanti, J., eds.), Academic Press, New York, NY, pp. 281–291.

2. Bruder, S. P. and Caplan, A. I. (1997) Bone regeneration thought cellular engineering, in *Principles of Tissue Engineering* (Lanza, R., Langer, R., and Chick, W., eds.), Academic Press, New York, NY, pp. 273–293.

3. Yang, S., Leong, K. F., Du, Z., and Chua, C. K. (2001) The design of scaffolds for use in tissue engineering. Part I. Traditional factors. *Tissue Engineering* **7,** 679–689.

4. Tabata, Y. (2001) Recent progress in tissue engineering. *Research Focus* **6,** 483–487.
5. Freyman, T. M., Yannas, I. V., and Gibson, L. J. (2001) Cellular materials as porous scaffolds for tissue engineering. *Progress in Materials Science* **46,** 273–282.
6. Pachence, J. M. and Kohn, J. (1997) Biodegradable polymers for tissue engineering, in *Principles of Tissue Engineering* (Lanza, R., Langer, R., Chick, W., eds.), Academic Press, New York, NY, pp. 273–293.
7. Thomson, R. C., Wake, M. C., Yaszemski, M., and Mikos, A. G. (1995) Biodegradable polymer scaffolds to regenerate organs. *Adv. Polym. Sci.* **122,** 247–274.
8. Agrawal, C. M., Athanasiou, K. A., and Heckman, J. D. (1997) Biodegradable PLA-PGA polymers for tissue engineering in orthopaedics. *Materials Science Forum* **250,** 115–228.
9. Thomson, R., Yaszemski, M., and Mikos, A. (1997) Polymer Scaffold processing, in *Principles of Tissue Engineering* (Lanza, R., Langer, R., and Chick, W., eds.), Academic Press, New York, NY, pp. 263–272.
10. Lu, L. and Mikos, A. (1996) The importance of new processing techniques in tissue engineering. *MRS Bulletin* **21,** 28–32.
11. Mikos, A. G., Thorsen, A. J., Czerwonka, L. A., Bao, Y., and Langer, R. B. (1994) Preparation and characterization of poly(l-lactid acid) foams. *Polymer* 1068–1077.
12. Langer, R. (1999) Selected advances in drug delivery and tissue engineering. *J. Control. Release* **62,** 7–11 .
13. Mikos, A. G., Sarakinos, G., Leite, S. M., Vacanti, J. P., and Langer, R. (1993) Laminated three-dimensional biodegradable foams for use in tissue engineering. *Biomaterials* **14,** 323–330.
14. Mikos, A. G., Bao, Y., Cima, L. G., Ingeber, D. E., Vacanti, J. P., and Langer, R. B. (1993) Preparation of poly(glycolic acid) bonded fiber structures for cell attachment and transplantation. *J. Biomed. Mater. Res.* **27,** 183–189.
15. Mooney, D. J., Baldwin, D. F., Suh, N. P., and Vacanti, J. P. (1996) Novel approach to fabricate porous sponges of poly (d,l-lactid-co-glycolic acid) without the use of organic solvents. *Biomaterials* **17,** 1417–1422.
16. Gomes, M. E., Ribeiro, A. S., Malafaya, P. B., Reis, R. L., and Cunha, A. M. (2001) A new approach based on injection moulding to produce biodegradable starch-based polymeric scaffolds: morphology, mechanical and degradation behaviour. *Biomaterials* **22,** 883–889.
17. Thompson, R. C., Yaszemski, M. J., and Powders, J. M. (1995) Fabrication of biodegradable polymer scaffolds to engineer trabecular bone. *Journal Biomaterials Science—Polymer Edition* **7,** 23–28.
18. Gomes, M. E., Reis, R. L., and Cunha, A. M. (2002) Alternative tissue engineering scaffolds based on starch: processing methodologies, morphology, degradation behaviour and mechanical Properties. *Materials Science and Engineering: C Biomimetic and Supramolecular Systems* **20,** 19–26.
19. Gomes, M. E. (2002), Godinho, J. S., Reis, R. L., and Cunha, A. M. Design and processing of starch based scaffolds for hard tissue engineering. *Journal of Applied Medical Polymers* **6,** 75–80.

20. Malafaya, P. B., Elvira, C., Gallardo, A., Román, J. S., and Reis, R. L. (2001) Porous starch-based drug delivery system processed by a microwave route. *J. Biomater. Sci.—Polym. Ed.* **12,** 1227–1241.
21. Hutmacher, D. W. (2000) Scaffolds in tissue engineering bone and cartilage. *Biomaterials* **21,** 2529–2543.
22. Hutmacher, D. W., Teoh, S. H., Zein, I., Renawake, M., and Lau, S. (2000) Tissue engineering Research: the engineer's role. *Medical Device Technology* **1,** 33–39.
23. Jiang, G. and Shi, D. (1997) Coating of hidroxylapatite on highly porous Al_2O_3 substrate for bone substitutes. *J. Biomed. Mater. Res.* **43,** 77–88.
24. Maquet, V. and Jerome, R. (1997) Design of macroporous biodegradable polymer scaffolds for cell transplantation, *Materials Science Forum* **250,** 15–42.

7

Alginates in Tissue Engineering

Marcy Wong

1. Introduction

Alginate is a polysaccharide derived from brown seaweed, which has the unique property of being able to form a gel in the presence of certain divalent cations (e.g., calcium, strontium, or barium). Alginate has been of commercial interest in the food industry since the 1930s, when its properties as an emulsifier, thickener, and stabilizer were recognized. Alginate has also long been used for biomedical purposes, particularly in the manufacture of surgical dressings for exuding wounds *(1)*. However, the explosive increase in medical applications for alginate, began with the recognition of its use as a scaffold for the encapsulation and immunoprotection of transplanted cells. The encapsulation of non-autologous islet cells in alginate for the treatment of diabetes is based on the concept that nutrients can diffuse in and insulin out of the alginate construct without triggering an immune response *(2–3)*. Similarly, alginate has been used to immunoprotect recombinant cells delivering tumor-suppressing agents *(4–5)* and growth hormone *(6)*. Stable cultures in alginate beads have been achieved with a number of cell types including chondrocytes, bone-marrow stromal cells, islets, myoblasts, fibroblasts, Schwann cells, kidney cells, epithelial cells, and hepatocytes. For orthopedic purposes, encapsulated bone-marrow stromal cells and chondrocytes have been proposed for the healing bone and cartilage defects *(7–9)*. As a bulking agent, alginate has gained attention as a space-filling material for treating pediatric urinary reflex *(10–12)*.

The methods in this article describe the encapsulation of chondrocytes isolated from articular cartilage in standard alginate. The methods can be generalized to other cell types and other means of gelation. The use of alginate for encapsulation of chondrocytes has become popular, not for its immuno-

protective properties, but because the chondrocytes maintain their phenotype and three-dimensional (3D)-morphology in the gel and do not undergo dedifferentiation even after long culture periods. As seen in **Fig. 1**, chondrocytes cultured in alginate synthesize a pericellar matrix, which is biochemically and structurally similar, although not identical, to that found in native cartilage.

1.1. Properties of Alginate

Alginate is a copolymer of D-mannuronic acid (M) and L-guluronic acid (G). The gelation of alginate occurs as blocks of guluronic acid bind to other G blocks via divalent cations, usually calcium ions (**Fig. 2**). The mechanical properties of alginate are therefore highly dependent on the G content, the length of the G blocks, and the molecular weight of the molecules. Commercially available alginates vary greatly in their composition, and those derived from stems of Laminaria hyperborea have a guluronic-to-mannuronic ratio 3× higher than alginate derived from Durvillea potarum *(13)*. Preparation of the hydrogels can also affect the properties of the gel significantly. The alginate concentration, viscosity, method of sterilization, and the rate of gelation can all be controlled to achieve the desired properties *(14–17)*. Larger structures with more uniform gelation characteristics can be achieved though the use of $CaCO_3$-D-glucono-δ-lactone (GDL) and $CaCO_3$-GDL-$CaSO_4$ during gelation. These substances significantly slow the rates of gelation because of the lower solubility of $CaCO_3$ compared to $CaCl_2$ *(17)*. The use of strontium and barium ions in place of calcium ions can also produce a stronger and more stable gel *(18–19)*. The modification of the chemical structure of alginate in combination with other biopolymers can further extend the properties of this versatile material *(20–22)*. The biological success of alginate-based transplants will also depend on the heavy metal, endotoxin, and protein content of the material, and the trace amounts of bacteria, yeast, and mold present. Important efforts to standardize alginate properties are currently being undertaken by the American Society for Testing and Materials (ASTM) in issuing guidelines for tissue-engineered medical products (TEMPS) *(13)*.

2. Materials

2.1. Isolation of Cells

1. Articular cartilage (*see* **Note 1**).
2. Dulbecco's modified Eagle's medium (DMEM) with glutamax-1 (with 25 m*M* Hepes, without sodium pyruvate, with pyridoxine) to which the following additives are added:
   a. 10% heat-inactivated fetal calf serum (FCS).
   b. 0.35 m*M* proline.
   c. 50 µg/mL gentamycin.
3. Sterile phosphate-buffered saline (PBS) with 50 µg/mL gentamycin.

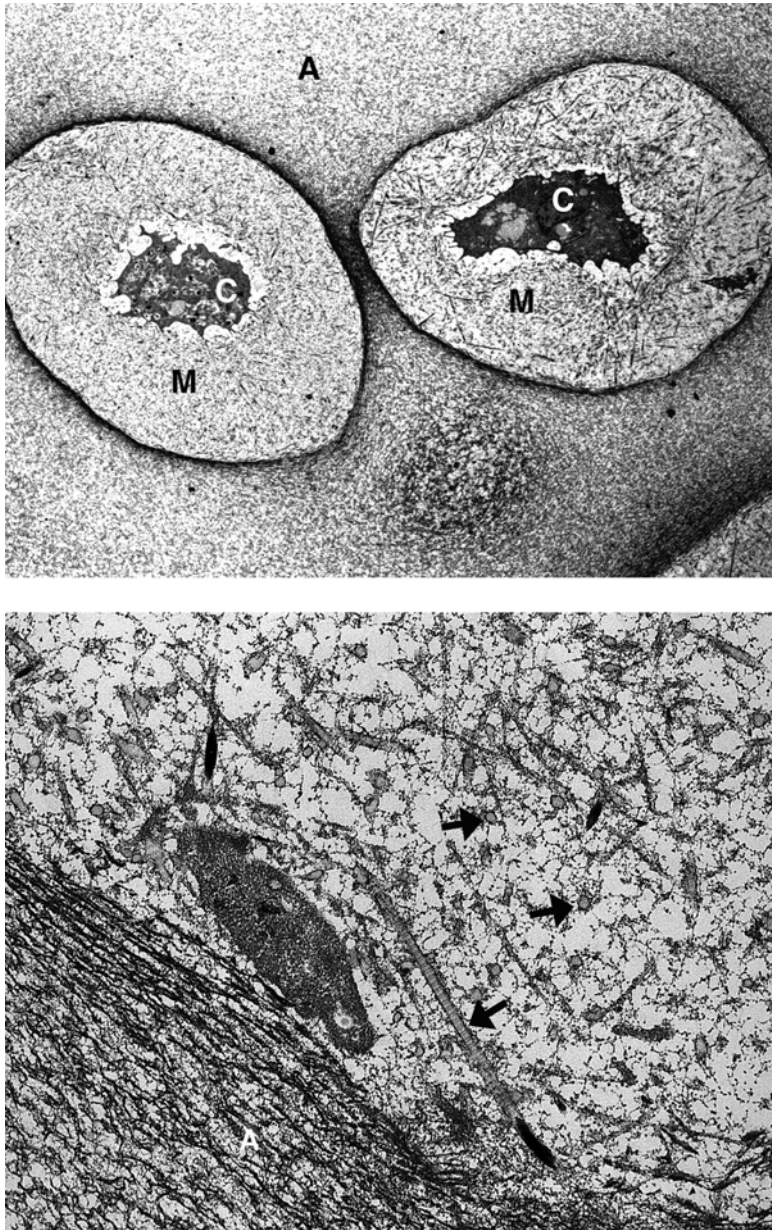Fig. 1. Electron micrographs of chondrocytes in alginate, cultured for 25 d. (*Top*)
The two chondrocytes have synthesized a pericellular matrix that consists of fibrils
and proteoglycans. A = alginate, M = matrix, and C = chondrocyte. (*Bottom*) At higher
magnification, cross-banded type II collagen fibrils are visible in both length and cross-
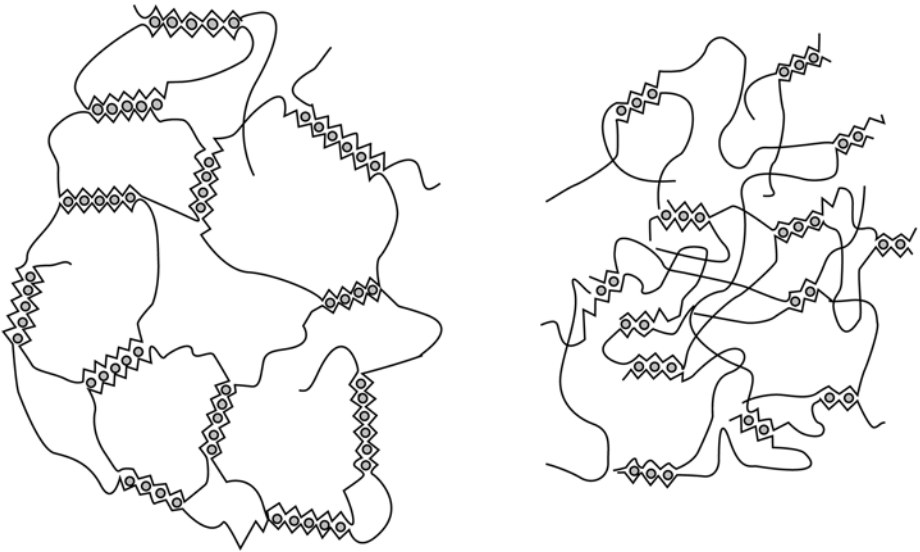section. Proteoglycans appear as tiny condensed black spots.

Fig. 2. A schematic of the structure of alginate based on the egg-box model *(26)*. The gray circles represent calcium ions, which primarily bind to guluronic acid blocks to polymerize the gel. Guluronic-rich alginates (*left*) have a stronger, more open structure than mannuronic-rich alginates (*right*).

4. 1% Pronase solution in DMEM media at 37°C.
5. 0.14% Collagenase solution in DMEM media at 37°C.
6. 0.1% Solution of trypan blue.
7. Hemocytometer.
8. Nylon meshes, 120-μm and 20-μm hole size from Millipore (autoclaved).
9. Stainless steel strainer, e.g., for tea (autoclaved).

2.2. Alginate Bead Culture

1. Alginate (Pronova LVG) with >60% guluronic acid from FMC BioPolymer AS (Drammen, Norway) (*see* **Note 2**). The alginate solution is prepared 2–3 d before use. For a 2% solution, 0.45 g NaCl, and 1.0 g alginate are placed in a 50-mL tube and volume is brought up to 50 mL with distilled water (*see* **Note 3**).
2. 22-gauge needle and syringe.
3. Sterile solution of 50 m*M* CaCl$_2$/0.9% NaCl in 200-mL beaker.
4. DMEM with glutamax-1 (with 25 m*M* Hepes, without sodium pyruvate, with pyridoxine) to which the following additives are added:
   a. 10% heat-inactivated FCS.
   b. 0.35 m*M* proline.
   c. 50 μg/mL gentamycin = 0.5 mL 1000X stock.
   d. 20 μg/mL ascorbate = from 250X stock (made fresh).

    e. 1 m*M* cysteine = from 100 m*M* stock (made fresh).
    f. 1 m*M* pyruvate = from 100 m*M* stock (made fresh).

2.3. Alginate Cylinder Culture

1. Alginate, Pronova LVG with >60% guluronic acid from FMC BioPolymer AS (*see* **Note 2**). The alginate solution is prepared 2–3 d before use. For a 2% solution, 0.45 g NaCl, and 1.0 g alginate are placed in a 50-mL tube and volume is brought up to 50 mL with distilled water (*see* **Note 3**).
2. Stainless-steel casting mold (*see* **Note 4**).
3. Durapore membranes, 5-μm pore size (Millipore).
3. Sterile dermal punches (3- or 5-mm diameter) (Stiefel Laboratories).
4. Nylon meshes (Millipore) lining 6-well culture plates.
5. Size 23-g, 1.25, Nr. 14 needles, and 2-mL syringe (sterile).
6. 200-mL beakers of 70% ethanol, sterile PBS, and sterile solution of 50 m*M* CaCl$_2$/0.9% NaCl.
7. 0.9% NaCl solution (sterile).
8. DMEM with glutamax-1 (with 25 m*M* Hepes, without sodium pyruvate, with pyridoxine) to which the following additives are added:

    a. 10% heat-inactivated FCS.
    b. 0.35 m*M* proline.
    c. 50 μg/mL gentamycin.
    d. 20 μg/mL ascorbate = from 250X stock (made fresh).
    e. 1 m*M* cysteine = from100 m*M* stock (made fresh).
    f. 1 m*M* pyruvate = from 100 m*M* stock (made fresh).

3. Methods

3.1. Isolation of Chondrocytes from Articular Cartilage

1. Remove cartilage from the underlying bone with a sterile scalpel (*see* **Note 5**).
2. Wash pieces of cartilage in PBS supplemented with gentamycin 3 times × 5 min.
3. Transfer tissue to complete temperature- and CO$_2$-equilibrated culture medium until start of digest.
4. Digest tissue in 1% Pronase for 1 h at 37°C. The Pronase is removed and the tissue is washed once with PBS.
5. Digest tissue in 0.14% collagenase solution for at least 17 h at 37°C.
6. On the morning of the following day, the collagenase solution together with the digested tissue is transferred to two 50-mL tubes and the volume of each is brought up to 45 mL with PBS. Tubes are centrifuged for 5 min at 1000*g* and the fluid is decanted. Cells are resuspended in 45 mL of PBS and centrifuged for 5 min at 1000*g*, and the fluid is decanted. The cells are then resuspended in 20 mL of PBS.
7. Filter cell suspension through a 120-μm nylon mesh held in place by a metal strainer.
8. Filter cell suspension through a 20-μm nylon mesh. The volumes of the two tubes

are combined and brought up to 45 mL with PBS.

9. Centrifuge at 700g for 5 min. The fluid is decanted and cells are suspended in 40 mL of PBS.

10. Using a 50-µL aliquot of cell suspension combined with 50 µL of 0.2% trypan blue solution, the total number of cells and the percentage of viability is measured with a hemocytometer.

11. Centrifuge the cell suspension at 500g for 5 min and decant the solution. Filter-sterilized alginate is added to the cell pellet to attain the desired cell density of 4 million cells/mL (*see* **Note 6**). The alginate/cell solution is mixed gently until an even dispersion of cells is attained. At this point, cylinders or beads can be made from the alginate solution.

3.2. Alginate Bead Culture

The alginate solution is drawn up into a 22-gauge needle, and the solution is extruded slowly into the CaCl2/NaCl solution. The beads form spontaneously. Allow gelation to proceed for 15 min, and wash beads in 0.9% NaCl for 5 min to remove remaining $CaCl_2$. Transfer beads to temperature- and CO_2-equilibrated DMEM media + 10% FCS.

3.3. Alginate Cylinder Culture

The casting mold consists of a metal ring and its upper and lower cover. The 22-mm dia × 2-mm high volume in the ring defines the size of the alginate disk that is cast. The top and bottom of the metal ring are spanned by a Durapore membrane and supported by a wire mesh (**Fig. 3**).

1. Soak all metal pieces and filters in 70% ethanol and assemble the mold in a sterile way (*see* **Note 4**).

2. Soak mold in beaker containing 70% ethanol, tapping it to remove air bubbles.

3. Rinse mold in sterile PBS for 3 min and transfer to sterile Petri dish.

4. Inject 1.5 mL of alginate/cell suspension into the mold via a 23-gauge needle.

5. Carefully set entire mold into a beaker of sterile 50 m*M* $CaCl_2$/0.9% NaCl for 30 min to polymerize the alginate.

6. Rinse mold briefly in a beaker of PBS and disassemble in a sterile way.

7. Using the sterile dermal punch, cut up to twelve 6-mm alginate cylinders from the disk. The 6-mm cylinders are washed in 0.9% NaCl for 5 min to remove remaining $CaCl_2$.

8. Transfer cylinders to temperature- and CO_2-equilibrated DMEM media + 10% FCS. The cylinders are cultured in 6-well plates that have been lined with nylon mesh to prevent samples from adhering to the tissue-culture plastic.

3.4. Alginate Construct Characterization

Immunohistochemistry can be performed on alginate beads or cylinders using standard protocols. Fix alginate pieces in 2% glutaraldehyde buffered with
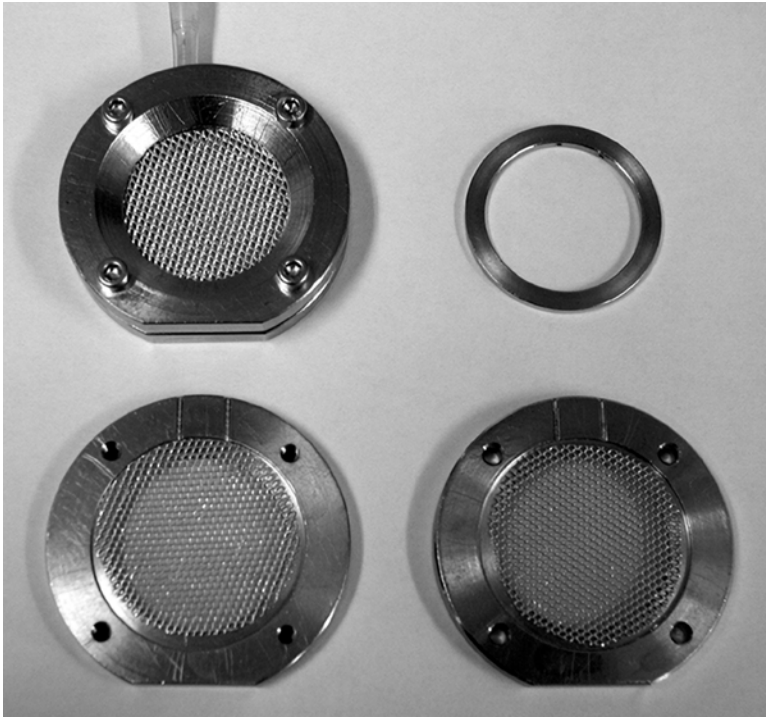
Fig. 3. The stainless-steel casting mold for the gelation of alginate disks, shown assembled (*upper left*) and disassembled with the ring (*upper right*) and top and bottom cover (*bottom left and right*).

0.1 M sodium cacodylate, 10 mM CaCl$_2$ for 3 h followed by incubation in 20% sucrose for 24 h. 10 mM CaCl$_2$ is added to the reagents to prevent destabilization of the alginate.

4. Notes

1. Chondrocytes can survive for several days after sacrifice of the animal if the tissue is stored at 4°C and the joint is not opened until just before cell isolation. The joint should be opened with a sterile scalpel. With a fresh scapula, tissue is removed in small slices and placed into sterile PBS.
2. A sterile version of this alginate is available from FMC Biopolymers. Also available are medium-viscosity alginates and alginates with high mannuronic content. Alginate purchased from Kelco Company and Sigma are not purified. They are derived from Macrocystis pyrifera, and usually have weaker mechanical properties because of the lower guluronic acid content and a lower mean guluronic acid block length.
3. The alginate solution should be made fresh with each encapsulation, as the polymer chains can degrade. The alginate will take up to 3 d to dissolve. Prior to use,

the alginate is sterilized by passing through a 2 µ syringe filter. Sterilization by autoclave should be avoided.

4. An alternative to our mold has been proposed by Hedbom et al. *(23)*. They cut holes from a silicon rubber pad. The bottom of this mold was a nylon filter soaked in calcium chloride. Gelation occurred as the alginate contacted the calcium chloride, and after 2 min, the entire cast was placed in calcium chloride. Gelation in molds using slower gelation rates is also recommended.

5. Articular cartilage is stratified into superficial, transitional, and upper and lower radial zones. The cell morphology and biosynthetic activity vary significantly among the zones *(24–25)*, and a digest from the full thickness of cartilage will contain populations of chondrocytes from each layer. It is possible to remove the upper half of cartilage first and perform separate digestions.

6. Many researchers have had more success producing cartilage-like constructs by increasing the initial chondrocyte cell density to up to 50×10^6 cells/mL *(9)*.

Acknowledgments

References

1. Thomas, S. (2000) Alginate dressings in surgery and wound management—Part 1. *J. Wound Care* **9,** 56–60.

2. Lim, F. and Sun, A. M. (1980) Microencapsulated islets as bioartificial endocrine pancreas. *Science* **210,** 908–910.

3. Soon-Shiong, P., Heintz, R. E., Merideth, N., Yao, Q. X., Yao, Z., Zheng, T., et al. (1994) Insulin independence in a type 1 diabetic patient after encapsulated islet transplantation. *Lancet* **343,** 950–951.

4. Cirone, P., Bourgeois, J. M., Austin, R. C., and Chang, P. L. (2002) A novel approach to tumor suppression with microencapsulated recombinant cells. *Hum. Gene Ther.* **13,** 1157–1166.

5. Joki, T., Machluf, M., Atala, A., Zhu, J., Seyfried, N. T., Dunn, I. F., et al. (2001) Continuous release of endostatin from microencapsulated engineered cells for tumor therapy. *Nat. Biotechnol.* **19,** 35–39.

6. Chang, P. L. (1997) Microcapsules as bio-organs for somatic gene therapy. *Ann. NY Acad. Sci.* **831,** 461–473.

7. Shang, Q., Wang, Z., Liu, W., Shi, Y., Cui, L., and Cao, Y. (2001) Tissue-engineered bone repair of sheep cranial defects with autologous bone marrow stromal cells. *J. Craniofac. Surg.* **12,** 586–593.

8. Fragonas, E., Valente, M., Pozzi-Mucelli, M., Toffanin, R., Rizzo, R., Silvestri, F., et al. (2000) Articular cartilage repair in rabbits by using suspensions of allogenic chondrocytes in alginate. *Biomaterials* **21,** 795–801.

9. Chang, S. C., Rowley, J. A., Tobias, G., Genes, N. G., Roy, A. K., Mooney, D. J., et al. (2001) Injection molding of chondrocyte/alginate constructs in the shape of facial implants. *J, Biomed, Mater, Res,* **55,** 503–511.

10. Loebsack, A., Greene, K., Wyatt, S., Culberson, C., Austin, C., Beiler, R., et al. (2001) In vivo characterization of a porous hydrogel material for use as a tissue bulking agent. *J. Biomed. Mater. Res.* **57,** 575–581.

11. Diamond, D. and Caldamone, A. (1999) Endoscopic correction of vesicoureteral reflux in children using autologous chondrocytes: preliminary results. *J. Urol.* **162,** 1185–1188.

12. Atala, A., Kim, W., Paige, K. T., Vacanti, C. A., and Retik, A. B. (1994) Endoscopic treatment of vesicoureteral reflux with a chondrocyte-alginate suspension. *J. Urol.* **152,** 641–643; discussion 644.

13. Dornish, M., Kaplan, D., and Skaugrud, O. (2001) Standards and guidelines for biopolymers in tissue-engineered medical products: ASTM alginate and chitosan standard guides. American Society for Testing and Materials. *Ann. NY Acad. Sci.* **944,** 388–397.

14. Wong, M., Siegrist, M., Wang, X., and Hunziker, E. (2001) Development of mechanically stable alginate/chondrocyte constructs: effects of gulluronic acid content and matrix synthesis. *J. Orthop. Res.* **19,** 493–499.

15. Draget, K., Myhre, S., Skjak-Break, G., and Ostgaard, K. (1988) Regeneration, cultivation and differentiation of plant protoplasts immobilized in Ca-alginate beads. *J. Plant Physiol.* **132,** 552–556.

16. Martinsen, A., Skjak-Braek, G., and Smidsrod, O. (1989) Alginate as immobilization material: 1. Correlation between chemical and physical properties of alginate beads. *Biotechnol. Bioeng.* **33,** 79–89.

17. Kuo, C.K. and Ma, P.X. (2001) Ionically crosslinked alginate hydrogels as scaffolds for tissue engineering: part 1. Structure, gelation rate and mechanical properties. *Biomaterials* **22,** 511–521.

18. Wideroe, H. and Danielsen, S. (2001) Evaluation of the use of Sr2+ in alginate immobilization of cells. *Naturwissenschaften* **88,** 224–228.

19. Peirone, M., Ross, C. J., Hortelano, G., Brash, J..L., and Chang, P. L. (1998) Encapsulation of various recombinant mammalian cell types in different alginate microcapsules. *J. Biomed. Mater. Res.* **42,** 587–596.

20. Caterson, E. J., Li, W. J., Nesti, L. J., Albert, T., Danielson, K., and Tuan, R. S. (2002) Polymer/alginate amalgam for cartilage-tissue engineering. *Ann. NY Acad. Sci.* **961,** 134–138.

21. Lee, K.Y., Alsberg, E., and Mooney, D. J. (2001) Degradable and injectable poly(aldehyde guluronate) hydrogels for bone tissue engineering. *J. Biomed. Mater. Res.* **56,** 228–233.

22. Halberstadt, C., Austin, C., Rowley, J., Culberson, C., Loebsack, A., Wyatt, S., et al. (2002) A hydrogel material for plastic and reconstructive applications injected into the subcutaneous space of a sheep. *Tissue Eng.* **8,** 309–319.

23. Hedbom, E., Ettinger, L., and Hauselmann, H. J. (2001) Culture of articular chondrocytes in alginate gel—a means to generate cartilage-like implantable tissue. *Osteoarthritis Cartilage* **9,** S123–130.

24. Aydelotte, M. B., Greenhill, R. R., and Kuettner, K. E. (1988) Differences between sub-populations of cultured bovine articular chondrocytes. II. Proteoglycan metabolism. *Connect. Tissue Res.* **18,** 223–234.
25. Aydelotte, M. B. and Kuettner, K. E. (1988) Differences between sub-populations of cultured bovine articular chondrocytes. I. Morphology and cartilage matrix production. *Connect. Tissue Res.* **18,** 205–222.
26. Grant, G., Morris, E., Rees, D., Smith, P., and Thom, D. (1973) Biological interactions between polysaccharides and divalent cations. *FEBS Lett.* **32,** 195–198.

8

Production and Surface Modification of Polylactide-Based Polymeric Scaffolds for Soft-Tissue Engineering

Yang Cao, Tristan I. Croll, Justin J. Cooper-White, Andrea J. O'Connor, and Geoffrey W. Stevens

1. Introduction

Current research in the field of tissue engineering is focused on the development of appropriate strategies for repair and regeneration of biological tissues. Biological tissues consist of cells situated within a complex molecular framework known as the extracellular matrix (ECM) with an integrated vascular system for oxygen or nutrient supply. In soft tissues, native ECMs consist mainly of collagens, proteoglycans, glycosaminoglycans (GAGs), laminins, and fibronection *(1)*.

Artificial three-dimensional (3D) polymeric scaffolds serve as a physical support to provide tissues with the appropriate 3D architecture for in vitro cell culture as well as in vivo tissue regeneration. In addition, 3D scaffolds can be tailored to provide adhesive substrates, which promote signaling pathways that influence cell proliferation, differentiation, and migration. The design and manufacture of 3D polymeric scaffolds that mimic the ECM are crucial to the success of tissue engineering. These scaffolds are expected to be biocompatible and biodegradable, with a controlled porous architecture to allow for rapid and controlled vascularization and tissue growth. Desirable features include ease of fabrication with a range of shapes and the intrinsic capability to communicate with living cells, thereby facilitating controlled and rapid tissue restoration *(2)*.

1.1. Biopolymers Used in Tissue Engineering

Biocompatible, biodegradable polymers have been widely used as scaffold materials for tissue engineering. They can be classified into two categories: naturally derived materials and synthetic materials *(1)*.

1.1.1. Naturally Derived Materials

Naturally derived materials used in the manufacture of synthetic ECMs for tissue engineering include collagens *(1,3–5)*, gelatin (denatured) *(6–8)*, hyaluronic acid *(9)*, chitin/chitosan *(10–13)*, starch *(14,15)*, agarose *(6)*, and alginate *(16,17)*. Such materials are isolated from biological (animal or plant) tissues, and can have intrinsic cell interactions. However, in some cases, their lack of availability in large quantities and batch-to-batch variations presents significant disadvantages. In addition, naturally derived materials lack the mechanical strength required by certain tissues such as bone *(1)*, and in some of these materials, it is difficult to control the scaffold morphology.

1.1.2. Synthetic Materials

Poly(anhydrides) *(18,19)*, poly(phosphazenes) *(1)*, polyorthoesters, poly(trimethylene carbonate), poly(propylene fumarate) (PPF), polyurethane *(20)*, polyurethane amide *(21)*, and polyhydroxyethylmethacrylate *(22)* are just some of the synthetic materials that have been used to fabricate synthetic ECMs in tissue engineering. One important class of synthetic biodegradable polymers is the poly(α-hydroxyesters), such as polyglycolide (PGA) *(23–25)*, polylactide (PLA) *(19,26–33)*, poly(D,L-lactide-co-glycolide) (PLGA) *(34–40)*, and polydioxanone *(41)*. These biodegradable polymers have approval by the US Food and Drug Administration (FDA) for human clinical use. In fact, they have been used for surgical sutures for many years *(42,43)*. Poly(ε-caprolactone) (PCL) *(44,45)* and its copolymers with D,L-lactide *(46)* are frequently used as the base material for scaffolds and for biodegradable sutures throughout Europe *(42)*. Other biodegradable synthetic polymers—including pseudo-poly(amino acid)s such as tyrosine-derived polycarbonates and polyarylates *(1)*, lactide-based polydepsipeptide polymers, poly(L-lactic acid-co-L-aspartic acid), and lactide-based poly(ethylene glycol) copolymers with functional side groups— are proposed as new biomaterials for tissue engineering, but have not yet been approved by the FDA and equivalent bodies, or are not presently commercial products and thus not freely available in the market *(42)*.

1.2. Fabrication Techniques for 3D Polymeric Scaffolds

A plethora of processing techniques are available in the literature for producing 3D scaffolds from various biodegradable polymers. These include fiber

bonding *(24,25,47,48)*, solvent casting and particulate leaching/porogen leaching *(49–56,84)*, membrane lamination *(57–59)*, solvent merging/particulate leaching *(60)*, melt molding *(42)*, solution casting *(61,62)*, gel casting *(63,64)*, thermally induced phase separation/sublimation/lyophilization/emulsion freeze drying *(2,32,33,52,65–76)*, gas foaming/high-pressure processing *(37,77–80)*, a combination of gas foaming and particulate leaching techniques *(81–83)*, biomimetic processes *(85,86)*, co-extrusion techniques *(87)*, 3D printing *(88,89)*, fused deposition modelling (FDM) *(45,90)*, MicroElectroMechanical System (MEMS) microstructure technology *(91)*, and photolithographic techniques *(92)*.

In this chapter, we examine the fabrication of 3D PLGA scaffolds by the techniques of solvent casting and particulate leaching, and thermally induced phase separation (TIPS). Both techniques are often used in constructing 3D polymeric scaffolds in tissue engineering, and are applicable to a range of polymers.

1.2.1. Solvent Casting and Particulate Leaching Technique

Mikos et al. *(49)* first introduced this technique in the early 1990s. Since then, it has become by far the most commonly used technique for manufacturing 3D polymeric scaffolds in tissue engineering. The method consists of dispersing calibrated particles, which may be mineral salts (such as sodium chloride *(49,50,93)*, or ammonium-bicarbonate *(82)*), organic particles (such as saccharose *(20)*, or paraffin spheres *(55)*) or even ice particles *(94)* in a polymer solution. The solvent in this dispersion is then removed either by air-drying or by vacuum-drying. The particles are leached out by selective dissolution to produce a porous polymer matrix. This technique is simple, and allows relatively good control of pore size. The pore size may also be easily changed by using different sizes of the inclusions or particulates *(26,95)*. Unfortunately, the residual salts remaining in the scaffolds, irregularly shaped pores, and poorly interconnected structures have been shown to be problematic for cell seeding and culture *(47)*. Furthermore, this technique is normally used to produce thin wafers or membranes approx 3 mm thick. Thicker sections and complex shapes are difficult to produce because of inherent difficulties in completely removing the dispersed particles and the solvent from the structure.

1.2.2. Thermally Induced Phase Separation

TIPS uses thermal energy as a driving force to induce phase separation *(65)*. This technique has been used commercially to produce microporous membranes for filtration and plasmapheresis *(96)*. Biodegradable polymers (e.g., PLA, PLGA) and their mixtures with bioactive ceramics (e.g., hydroxyapatites) *(70)*, can be dissolved in a variety of pure solvents or solvent/non-solvent mixtures, such as molten phenol *(2)*, naphthalene *(2)*, 1,4-dioxane *(33,70,73,97–99)*,

1,4-dioxane/water *(65–68,73,98,99)* or methylene chloride/water *(71)* mixtures, tetrahydrofuran (THF) *(74,75)*, and benzene *(38,73)*. Solid-liquid or liquid-liquid phase separation is then induced by lowering the solution temperature. Subsequent removal of the solvent is done by sublimation, leaving a highly porous structure. The advantages of the TIPS technique lie in the capability to rapidly produce highly porous, interconnected structures *(98,99)* and to incorporate bioactive molecules into the matrices during processing without denaturation *(73)*. Slight changes in the processing parameters, such as the type of polymer, polymer concentration, solvent/nonsolvent ratio, and the thermal quenching strategy *(99)*, significantly affect the resultant morphology of the porous scaffold. A range of porous structures can thus be easily obtained.

A range of techniques are available for characterizing 3D polymeric scaffolds with scanning electron microscopy (SEM) with image analysis being the most widely used for observing the morphology of 3D macro/micro structures, allowing quantification of pore size, pore shape, structural alignment, and interconnectivity *(66–68,76,98–100)*. Researchers have also used mercury intrusion porosimetry (MIP) to quantify pore distribution and porosity *(97,101)*. However, care should be taken when using this technique to characterize deformable, highly porous (e.g., compressible), polymeric scaffolds, because it can have severe limitations. Scaffold density can be measured by pycnometry *(32)*, gravimetry *(67)* or simply by calculating the volume difference for a particular mass *(55,70,73,102)*. Mechanical properties can be measured via standard mechanical testing methods—for example, using Instron *(85)*, MTS *(81)*, or a texture analyzer *(103)*.

1.3. Surface Modification of PLGA Structures

While the good mechanical properties and processability—as well as the FDA-approved status—of PLA, PGA, and PLGA make them attractive materials for use in tissue engineering *(19)*, their surface properties are not ideal for cell adhesion and growth *(104–106)*. The polymer chains lack functional groups, and each lactic acid residue (**Fig. 1**) contains a pendant methyl group, giving the surface a significantly hydrophobic nature. It is well-known *(107,108)* that adhesion and growth of cells is superior on more hydrophilic surfaces.

Many approaches have been taken for chemically modifying the surfaces of pre-formed PLA and PLGA films and scaffolds. Methods used to date include plasma treatment *(104,106,109,110)*, entrapment of a second functional polymer within the surface *(111–113)*, and partial surface hydrolysis by both acid *(104)* and base *(104,114)* treatments. Although plasma treatment has been shown to work well on two-dimensional (2D) polymer films *(104,106,109,110)*, reliable evidence of modification within a 3D porous structure is lacking. It would
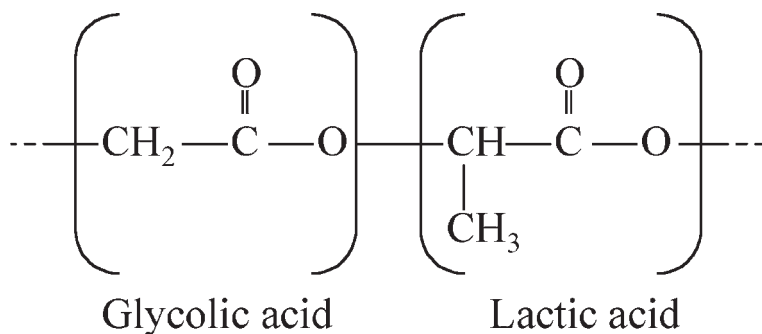
Fig. 1. The backbone structure of PLGA. The methyl group on the lactic acid residues imparts significant hydrophobicity to the polymer.

seem likely that diffusion would be a major limitation in any structure greater than approx 1 mm thick. The entrapment method *(111–113)* appears promising, but again has only been proven on 2D surfaces. In a 3D situation, solvent dilution of the surface and bulk structures can result in collapse of the scaffold. Therefore, surface hydrolysis appears to be the most promising technique presently available for 3D constructs.

Hydrolysis of polyesters such as PLGA proceeds through the addition of a water molecule across a backbone ester bond, yielding a carboxylic acid and a hydroxyl group. While the mechanisms under acidic (**Fig. 2**) and basic (**Fig. 3**) conditions are fundamentally different, the end result is the same—cleavage of the polymer chain to form new hydrophilic end groups. If desired, the exposed carboxyl groups may be used to attach other surface-modifying molecules such as extracellular matrix (ECM) proteins, for example, by carbodiimide coupling *(111)*.

The maximum achievable modification by the hydrolytic method is controlled by the balance between the creation of new end groups and the ablation of the surface by removal of oligomers. Thus, an equilibrium functional group density is quickly reached. Longer treatment times may increase the surface roughness somewhat; however, in a 3D situation; this simply translates to structural degradation.

Although improvements in surface wettability and cell adhesion have been shown for both acid *(104)* and base *(114)* hydrolysis, the treatment conditions used in the past have been quite extreme (70% perchloric acid and 1 N NaOH, respectively). Our results demonstrate, using much thinner films than those previously used, that maximal surface modification can be achieved using concentrations of acid and base up to 100× weaker *(115)*. Thin films—<5 µm as opposed to the >100 µm thickness generally used *(104,114,116)*—are more representative of the thickness of the walls inside a TIPS scaffold, and allow accurate measurement of contact angles with a much lower contribution from surface roughness *(117)*.
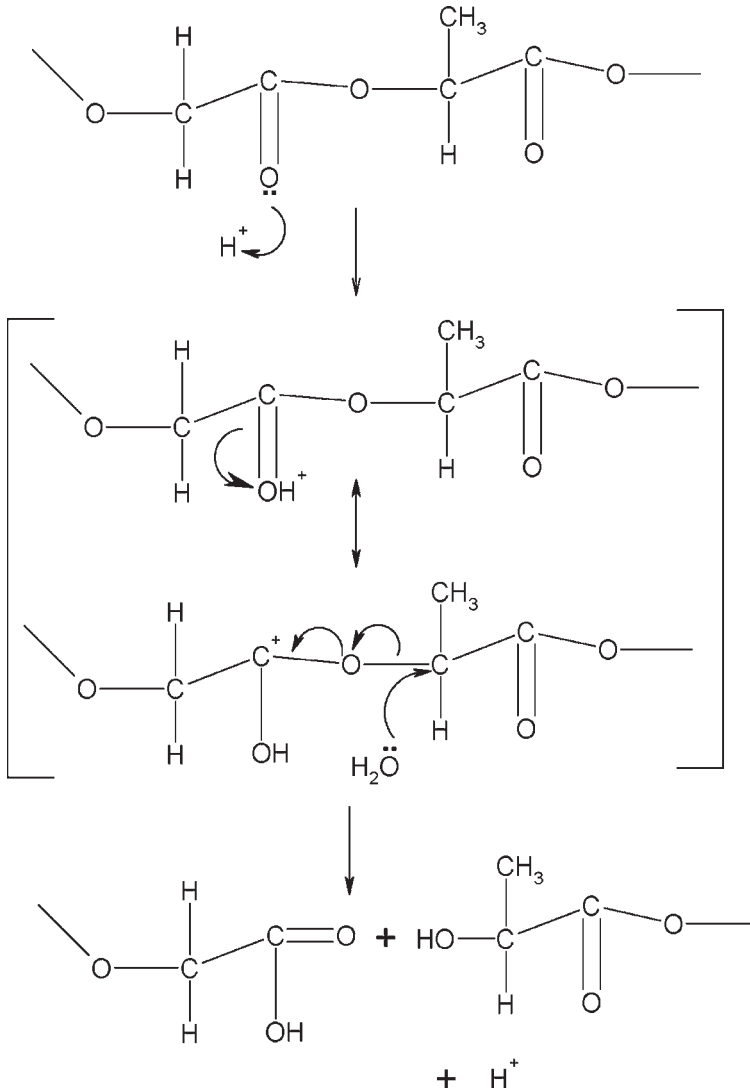
Fig. 2. Mechanism of PLGA acid-catalyzed hydrolysis.

Since the polymer end groups are polar but uncharged under acidic conditions, hydrogen ions diffuse easily into the structure, and thus hydrolysis occurs throughout the bulk. Conversely, under alkaline conditions, the end groups are negatively charged, which helps to prevent hydroxide ions diffusing into the bulk. Thus, degradation of polyesters by alkaline hydrolysis occurs almost entirely at the surface, a highly desirable characteristic.
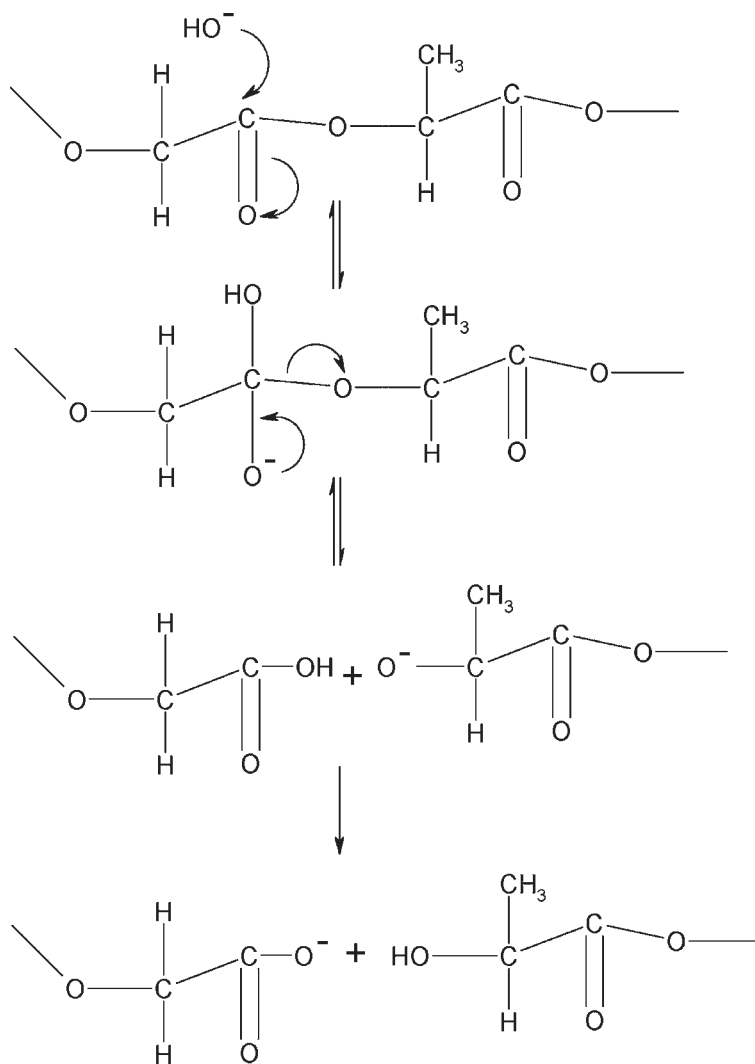
Fig. 3. Mechanism of PLGA hydrolysis in basic solution.

1.4. Surface Characterization by Contact-Angle Measurement

Characterization of surface wettability by contact-angle measurement is a simple procedure that is often poorly understood. The air-water contact angle of a surface is defined as the internal angle formed by the edge of a drop of water sitting horizontally on the surface and the surface itself (**Fig. 4**). It is generally accepted *(117,118)* that the advancing contact angle (**Fig. 4A**) of a
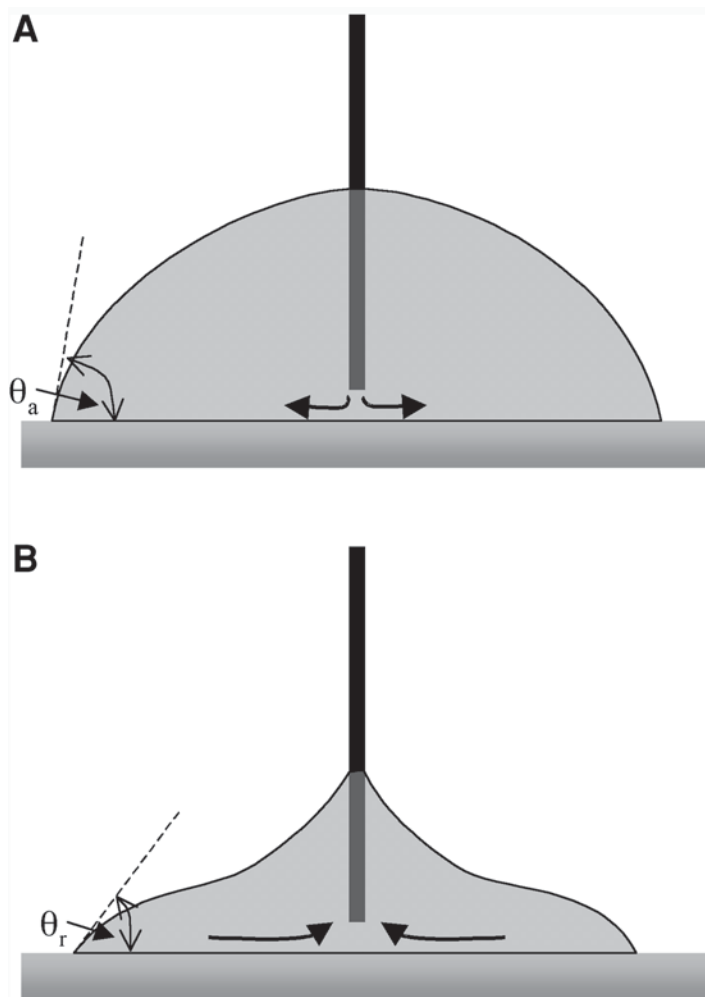
Fig. 4. Measurement of **(A)** advancing and **(B)** receding contact angles by drop-shape anaylsis.

liquid on a heterogeneous surface is mostly dependent on the surface's resistance to wetting—the presence of hydrophobic domains in the case of water. Conversely, the receding contact angle (**Fig. 4B**) is most strongly controlled by the strength of the interaction between the liquid and the surface—that is, the presence of hydrophilic domains. Thus, it is important to measure both the advancing and receding contact angles to reliably characterize the surface. Also, care is needed in interpreting contact-angle results from a rough surface, as both advancing and receding contact angles are strongly affected by surface roughness *(117)*.

Fig. 5. Schematic diagram of a contact-angle goniometer apparatus. The viewer is focused on the needle tip, and inclined 1–2° below horizontal. The needle tip should be ~0.5 mm above the surface of the sample.

The most common method of measuring contact angles is by drop-shape analysis with a contact-angle goniometer *(117,118)* (**Fig. 5**). Some groups choose to measure and report the contact angle of a drop with a constant, slow rate of change of volume *(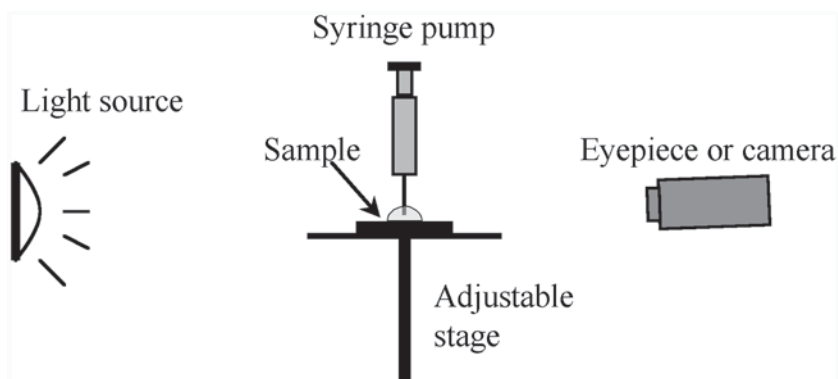118)*. This yields a good result, but requires equipment of very rigid construction to produce reproducible volume flows.

The technique described here is slightly different, and somewhat simpler. In essence, a fixed volume of liquid is quickly pumped onto the surface, and the contact angle followed as the drop relaxes to equilibrium. Liquid is then removed until the interface begins to recede, and once again the contact angle is followed as the drop approaches equilibrium. A typical output trace is shown in **Fig. 6**. This protocol has been found to give results that are reproducible to within approx 0.5–1° *(115)*.

When measuring surface properties by any technique, it is important to remember that any contamination (from dust or silicone grease, for example) can significantly change the results. It is thus important to be extremely careful when preparing and handling samples. Samples should be handled only by their edges with clean tweezers or forceps, and should be stored in an environment that is free of dust and any material (such as silicone grease) that has the capability to form a vapor and deposit on surfaces.

2. Materials
2.1. Scaffold Fabrication
2.1.1. Chemicals

1. Biomedical-grade PLA, PGA, and PLGA are available from Boehringer Ingelheim (Germany), Medisorb Technologies International (Cincinnati, OH),
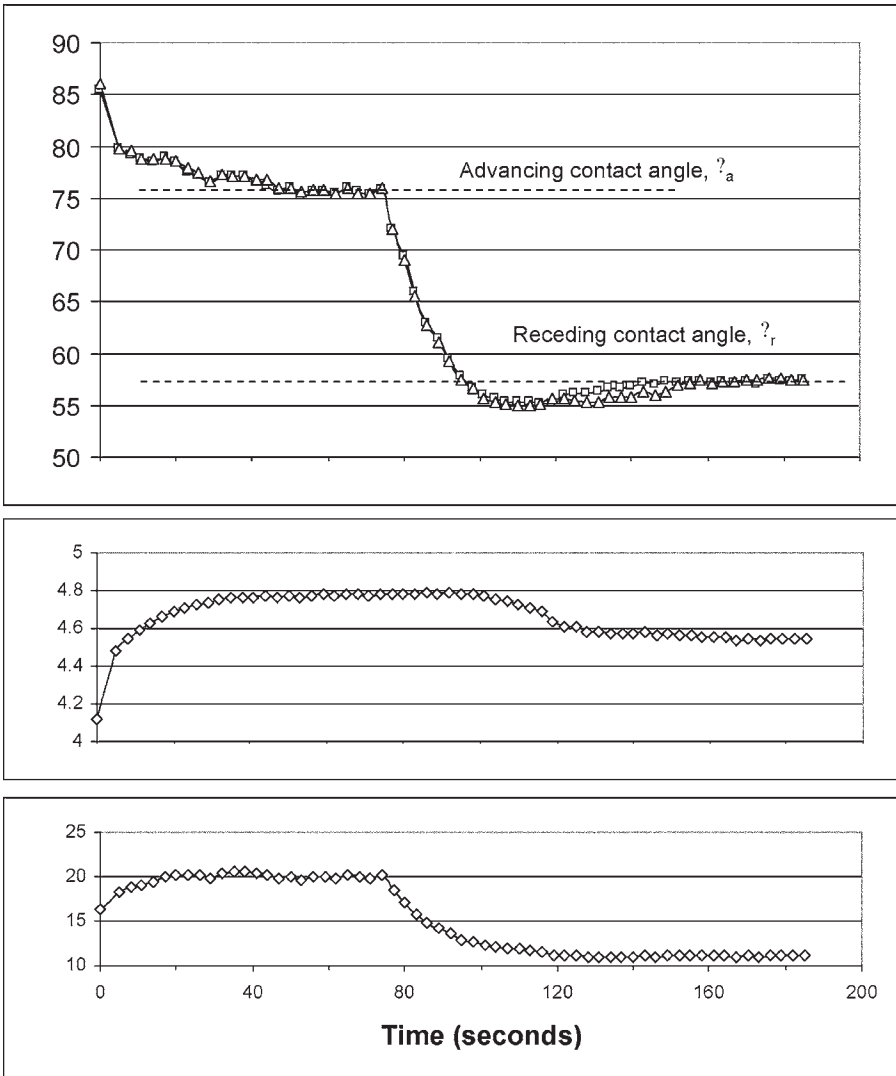
Fig. 6. A typical contact-angle trace (air–water contact angle of 75/25 PLGA). Note that the drop interface keeps moving for some time after the volume stops changing.

Polysciences Inc. (Warrington, PA) and Birmingham Polymers Inc. (Birmingham, AL). For the results presented here, PLGA produced by Birmingham Polymers Inc. was used. In particular, because of the specific mechanical and degradation requirements of the scaffolds in our work, we have used 75/25 PLGA as our base polymer. The inherent viscosity of 75/25 PLGA is 0.69 dL/g in $CHCl_3$ at 30°C, and it is a white to light gold granular solid.

2. Chloroform, AR or high-performance liquid chromatography (HPLC)-grade (toxic).
3. 1,4-dioxane, AR or HPLC-grade (toxic).
4. Sodium chloride, AR.
5. Ethanol, AR.
6. H_2O (high purity, resistivity of at least 18 MΩ cm).

2.1.2. Apparatus

1. 50 mm × 12 mm glass Petri dishes with glass lids.
2. 20-mL, 30-mL, and 250-mL glass beakers.
3. 25 mm × 5 mm stirrer bars.
4. Oven (temperature ranges from 30° to 200°C).
5. Parafilm™.
6. Duraseal™ lab film.
7. Mortar and pestle.
8. 300-μm and 417-μm stainless-steel sieves.
9. 25-mL, 10-mL, and 5-mL measuring cylinders.
10. 500–5000 μL Eppendorf® pipet.
11. Aluminum mold in desired shape (e.g., dome or cylinder).
12. Clear plastic vials with insert lids.
13. Desiccator with silicon gel pellets.
14. Magnetic stirrer/hotplate.
15. pH meter with probe.
16. Cooling bath with programmable temperature controller.
17. Vacuum system capable of achieving at least 10^{-1} mbar.

2.2. Preparation of 2D Films for Surface Modification Testing

2.2.1. Chemicals

1. 1.2 g PLGA or other biomedical-grade polymer (*see* listing under **Subheading 2.1.1.**).
2. 25 mL dichloromethane (DCM), AR or HPLC-grade.
3. Toluene, AR or HPLC-grade.
4. Acetone, AR or HPLC-grade.
5. Ethanol, AR or HPLC-grade.

2.2.2. Apparatus

1. 30-mL beaker.
2. 40 clean (*see* **Note 1**) glass cover slips (preferably silanized (*see* **Note 2**).
3. Glass or stainless-steel rack to hold cover slips upright with minimal surface contact.
4. Magnetic stirrer.
5. Tweezers.
6. Lint-free blotting paper (e.g., Kimwipes™).
7. Neoprene gloves.
8. Grease-free vacuum oven.

2.3. Surface Modification of Scaffolds

1. 0.01 N NaOH solution.
2. Magnetic stirrer.
3. Beaker sized to hold scaffolds.
4. Glass basket to fit inside beaker.
5. Scaffolds, pre-wet with water.

2.4. Contact-Angle Measurement

1. Contact-angle goniometer, preferably with digital camera and drop-shape analysis software. We use a FTÅ-200 goniometer system and analysis software provided by First Ten Angstroms, Inc. Some other suppliers for contact-angle goniometers include Rame-Hart (US), DataPhysics Instruments GmbH (Germany), and Krüss GmbH (Germany). This is not a complete list.
2. Syringe to fit goniometer with flat-tipped needle (21-guage or finer), filled with ultra-pure water.
3. Fine-point tweezers.
4. Tissue paper.

3. Methods

3.1. Scaffold Fabrication

3.1.1. Solvent Casting and Particulate Leaching

1. Dry the salt particles in the oven for at least 24 h at ~50°C (*see* **Note 3**).
2. Sieve sodium chloride particles to desired size range (*see* **Note 4**). Grind larger particles using mortar and pestle as necessary.
3. Line the Petri dish with Duraseal™.
4. Weigh 1 g PLGA into a 30-mL beaker with a stirrer bar.
5. Measure 15 mL of chloroform and add it into the beaker, then cover immediately with Parafilm™.
6. Dissolve the PLGA in the chloroform using a magnetic stirrer/heater at 45°C in a fume cupboard (*see* **Note 5**).
7. Pour the PLGA solution carefully into a Petri dish.
8. Weigh 9 g sieved NaCl and disperse evenly into the Petri dish.
9. Place the lid over the dish and leave for 24 h.
10. Remove the lid and air-dry for an additional 24 h in a fume cupboard.
11. Remove the PLGA/salt matrix from the Petri dish and machine the matrix into the desired shape.
12. Leach the NaCl particles out in 200 mL high-purity H_2O, stirring at room temperature for a minimum of 24 h. Change H_2O approx every 6 h. Remove the scaffold once the resistivity of the water has reached a constant close to 18 MΩ cm.
13. Wash the scaffold in ethanol and vacuum-dry overnight at room temperature.
14. Store the scaffold in a desiccator until needed.

3.1.2. Thermally Induced Phase Separation Technique

1. Accurately weigh 0.5 g PLGA pellets into a 20-mL beaker with a stirrer bar (*see* **Note 6**).
2. Add 10 mL of dioxane to the beaker using a pipet and cover the beaker with Parafilm™ immediately.
3. Dissolve the PLGA in the dioxane by stirring at 45°C for 2 h to obtain a homogeneous polymer solution.
4. Rapidly pour the PLGA solution into an aluminum mold and transfer it into a freezer with a preset temperature of –18°C to solidify the PLGA solution, thereby inducing solid-liquid phase separation (*see* **Note 7**).
5. Keep the solution at –18°C for 2 h, then vacuum-dry the solidified solution at –8°C under at least 10^{-1} mbar for at least 1 d to remove the solvent (*see* **Note 8**).
6. Slowly warm the freeze-drying vessel to room temperature before releasing the vacuum.
7. Carefully remove the scaffold from the aluminum mold and store in a desiccator until needed.

A schematic representation of this procedure for making 3D PLGA scaffolds by the TIPS method is shown in **Fig. 7**. Examples of the morphologies of 3D PLGA scaffolds produced by the methods described here in the Department of Chemical and Biomolecular Engineering at The University of Melbourne are shown in **Fig. 8** *(98)*.

3.2. Coating of Slides (see **Note 9**)

1. Wash the rack and beaker sequentially in toluene, acetone, and then ethanol and allow to dry.
2. Place the PLGA in the 30-mL beaker. Add the DCM while magnetically stirring at medium speed, cover, and leave until the PLGA is fully dissolved (1–2 h).
3. Drop a cover slip into the PLGA solution. Using tweezers, grasp the cover slip as close to the edge as possible and slowly draw it out of the solution, allowing the interface to recede in order to ensure that an even film is formed.
4. Hold the cover slip vertically, with the bottom edge on blotting paper. Use a gloved finger to maintain this position and blot tweezers on paper. This prevents the tweezers from sticking to the film as it dries. Allow approx 10–20 s for the film to dry. At this time, it will turn white and translucent because of crystallization of the polymer.
5. Place the cover slip in the rack.
6. Repeat **steps 3–5** for all coverslips. Approx 40 cover slips can be coated with this amount of solution before the level in the beaker drops too far.
7. Place the rack with the cover slips into a vacuum oven and dry under vacuum at ambient temperature for 24 h.
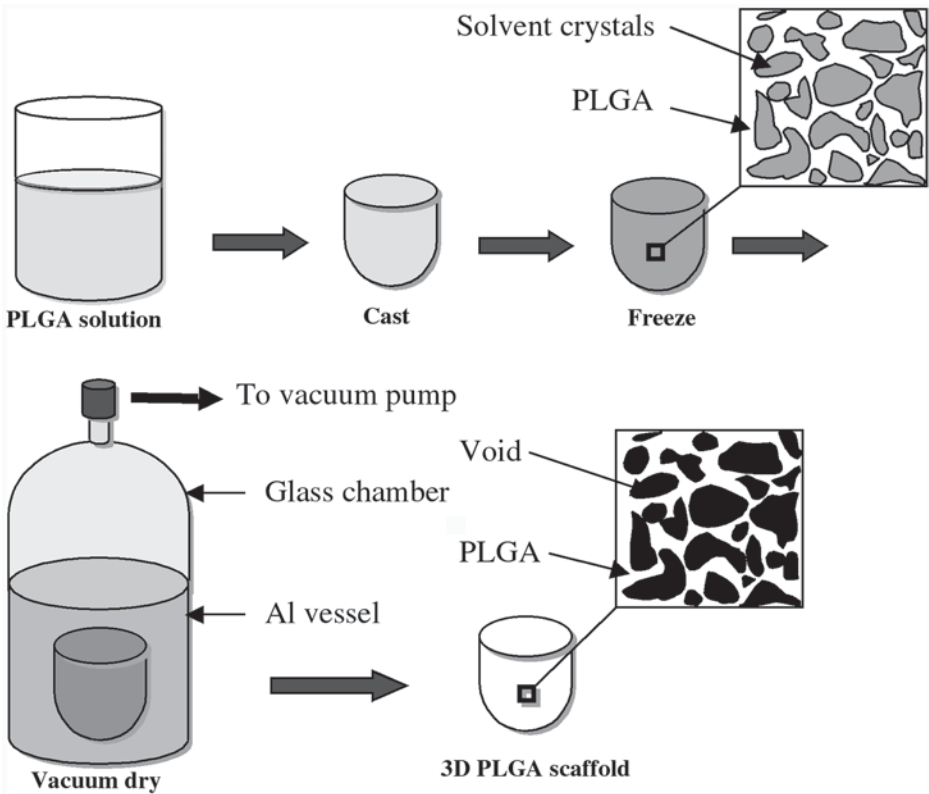
Fig. 7. A schematic illustration of the fabrication procedure for PLGA scaffolds by the TIPS method.

8. Increase the temperature in the vacuum oven to ~75°C and allow to dry for an additional 24 h. During this time the films will turn clear because of relaxation of the crystalline domains.
9. Remove the rack from the vacuum oven, and transfer to a clean, airtight glass storage vessel. If preferred, cover slips can be transferred to individual clean glass vials.

3.3. Surface Modification of Scaffolds

1. Place enough 0.01 N NaOH or 0.07 N HClO$_4$ solution in one of the beakers to cover the surface of the scaffolds when in the basket.
2. Place on a magnetic stirrer at low-medium speed. Add the basket containing the scaffolds and leave for 1 h.
3. Discard the solution, fill the beaker with high-purity water and wash for 1 h on low-medium speed. This step is performed twice.
4. Dry the scaffolds under vacuum for at least 24 h and store in sealed containers away from direct sunlight to avoid ultraviolet (UV) photolysis.
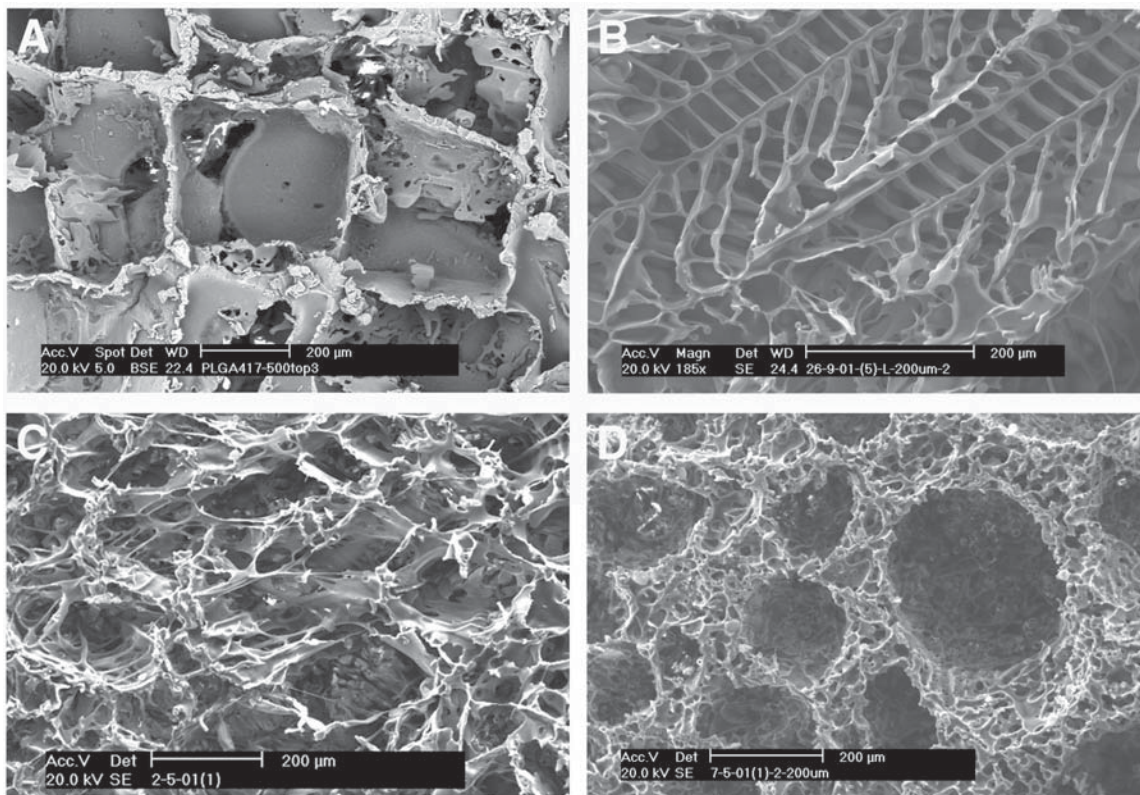
Fig. 8. Morphologies of 3D PLGA scaffolds produced in the Department of Chemical and Biomolecular Engineering at the University of Melbourne. **(A)** The top of a 3-mm disc produced by solvent (chloroform) casting and particulate leaching with salt size 417–500 μm. **(B)** 5%(w/v) PLGA made by TIPS using 1,4-dioxane as solvent. **(C)** 10%(w/v) PLGA made by TIPS using 1,4-dioxane as solvent. **(D)** 10%(w/v) PLGA made by TIPS using 87% 1,4-dioxane as solvent and 13% H_2O as non-solvent.

3.4. Contact-Angle Measurement

1. Place the syringe in the goniometer. Adjust the camera or viewer until the needle tip is in focus, approx 1/5th of the way from the bottom of the viewing area. The width of the viewing area should be at least 5 mm to allow a large drop size in relation to the needle diameter (*see* **Fig. 5**).
2. Push water through the syringe into tissue paper until liquid is flowing freely.
3. Place a sample cover slip on the stage, and adjust to within ~0.5 mm of the needle tip, with the needle tip ~5 mm from one corner.
4. Pump out enough water to make a drop width of approx 5 mm (20–30 µL). This should be done quickly (within 20 s). Watch carefully to determine whether each side of the drop advances without sticking. If one interface sticks (usually because of surface contamination such as dust) discard the measurement for that side of the drop. Wait at least 30 s for the drop to relax. If using a digital system, take images at a rate of at least one per 5 s. Measure the contact angle on each side of the drop. This is the advancing contact angle.
5. Withdraw water from the drop until the interface begins to recede, watching carefully to determine whether both sides recede. Wait at least 30 s for the drop to relax (*see* **Note 10**), and measure the receding contact angle.
6. Pump withdrawn water back onto the surface to avoid a buildup of contaminants, move the sample so the needle is near a different corner of the slide, and repeat **steps 4–5** at least twice for each sample.

A typical contact-angle trace using this method with a digital camera can be seen in **Fig. 6**.

4. Notes

1. One suitable method of cleaning cover slips is by washing for 5 min in a boiling mixture of 1 part by volume 25% ammonia and 9 parts by volume 30% hydrogen peroxide solution, followed by thorough rinsing in high-purity water.
2. Silanization of dry cover slips can be carried out using a 5% solution of trimethylchlorosilane in n-hexane, followed by very thorough rinsing in clean n-hexane. Treatment of ~100 cover slips for 10 min in 50 mL solution yields an air-water advancing contact angle of approx 90°. This prevents the films from detaching from the slides upon exposure to water.
3. It is advisable to leave the salt permanently in the oven if experiments are being carried out regularly.
4. The most frequently used salt particle size is 300–417 µm. However, other size ranges may be used by using different sieves, depending on the application.
5. For safety reasons, all the procedures involving the use of toxic solvents—e.g., chloroform and 1,4-dioxane—must be carried out in a fume cupboard.
6. Different PLGA concentrations can be used, depending on the application. Here, we use 5% (w/v) PLGA as an example.
7. Quenching strategies have significant effects on the morphology of 3D PLGA scaffolds. Different quenching routes and end-point temperatures may be used to achieve desired morphologies *(76,98,99)*.

8. 99% of the solvent will be removed in 1 d, and a constant sample weight will be achieved within 3 d at 10^{-1} mbar.

9. The steps listed in **Subheading 3.2.** should be carried out in a fume hood, or preferably a Type II Class B biological safety cabinet with ducted exhaust, in order to protect the samples from contamination.

10. When measuring the contact angle, try to allow (as closely as possible) the same relaxation time for each sample. If using a digital system, the entire procedure can be carried out automatically, with image analysis as the final step.

References

1. Kim, B.-S. and Mooney, D. J. (1998) Development of biocompatible synthetic extracellular matrices for tissue engineering. *Tibtech* **16,** 224–230.

2. Lo, H., Ponticiello, M. S., and Leong, K. W. (1995) Fabrication of Controlled Release Biodegradable Foams by Phase Separation. *Tissue Engineering* **1(1),** 15–28.

3. Besseau, L., Coulomb, B., Lebreton-Decoster, C., and Giraud-Guille, M.-M. (2002) Production of ordered collagen matrices for three-dimensional cell culture. *Biomaterials* **23(1),** 27–36.

4. Heimburg, D. V., Zachariah, S., Heschel, I., Kuhling, H., Schoof, H., Hafemann, B., and Pallua, N. (2001) Human preadipocytes seeded on freeze-dried collagen scaffolds investigated in vitro and in vivo. *Biomaterials* **22,** 429–438.

5. Hubbell, J. A. (1995) Biomaterials in tissue engineering. *Bio/Technology* **13,** 565–576.

6. Hutmacher, D. W., Goh, J. C. H., and Teoh, S. H. (2001) An introduction to biodegradable materials for tissue engineering applications. *Ann. Acad. Med. Singapore* **30,** 183–191.

7. Shen, F., Cui, Y., Yang, L., Yao, K., Dong, X., Jia, W., and Shi, H. (2000) A study on the fabrication of porous chitosan gelatin network scaffold for tissue engineering. *Polym. Int.* **49,** 1596–1599.

8. Kosmala, J. D., Henthorn, D. B., and Brannon-Peppas, L. (2000) Preparation of interpenetrating networks of gelatin and dextran as degradable biomaterials. *Biomaterials* **21,** 2019–2023.

9. Taguchi, T., Ikoma, T., and Tanaka, J. (2002) An improved method to prepare hyaluronic acid and type II collagen composite matrices. *J. Biomed. Mater. Res.* **61,** 330–336.

10. Mi, F.-L., Ran, Y.-C., Liang, H.-F., and Sung, H.-W. (2002) In vivo biocompatibility and degradability of a novel injectable-chitosan-based implant. *Biomaterials* **23,** 181–191.

11. Lee, J.-Y., Nam, S.-H., Im, S.-Y., Park, Y.-J., Lee, Y.-M., Seol, Y.-J., et al. (2002) Enhanced bone formation by controlled growth factor delivery from chitosan-based biomaterials. *J. Control. Release* **78,** 187–197.

12. Zhang, Y. and Zhang, M. (2001) Synthesis and characterisation of macroporous chitosan/calcium phosphate composite scaffolds for tissue engineering. *J. Biomed. Mater. Res.* **55,** 304–312.

13. VandeVord, P. J., Matthew, H. W. T., DeSilva, S. P., Mayton, L., Wu, B., and Wooley, P. H. (2002) Evaluation of the biocompatibility of a chitosan scaffold in mice. *J. Biomed. Mater. Res.* **59,** 585–590.

14. Gomes, M. E., Reis, R. L., Cunha, A. M., Blitterswijk, C. A., and Bruijn, J. D. D. (2001) Cytocompatibility and response of osteoblastic-like cells to starch-based polymers: effect of several additives and processing conditions. *Biomaterials* **22,** 1911–1917.

15. Gomes, M. E., Ribeiro, A. S., Malafaya, P. B., Reis, R. L., and Cunha, A. M. (2001) A new approach based on injection moulding to produce biodegradable starch-based polymeric scaffolds: morphology, mechanical and degradation behaviour. *Biomaterials* **22,** 883–889.

16. Shapiro, L. and Cohen, S. (1997) Novel alginate sponges for cell culture and transplantation. *Biomaterials* **18,** 583–590.

17. Eiselt, P., Yeh, J., Latvala, R. K., Shea, L. D., and Mooney, D. J. (2000) Porous carriers for biomedical applications based on alginate hydrogels. *Biomaterials* **21,** 1921–1927.

18. Engelberg, I. and Kohn, J. (1991) Physico-mechanical properties of degradable polymers used in medical applications: a comparative study. *Biomaterials* **12,** 292–304.

19. Agrawal, C. M. and Ray, R. B. (2001) Biodegradable polymeric scaffolds for musculoskeletal tissue engineering. *J. Biomed. Mater. Res.* **55(2),** 141–151.

20. de Groot, J. H., Nijenhuis, A. J., Bruin, P., Pennings, A. J., Veth, R. P. H., and Klompmaker, J. (1990) Use of porous biodegradable polymer implants in meniscus reconstruction. 1) preparation of porous biodegradable polyurethanes for the reconstruction of meniscus lesions. *Colloid. Polym. Sci.* **268,** 1073–1081.

21. Spaans, C. J., Belgraver, V. W., Rienstra, O., Groot, J. H. D., Veth, R. P. H., and Pennings, A. J. (2000) Solvent-free fabrication of micro-porous polyurethane amide and polyurethane-urea scaffolds for repair and replacement of the knee-joint meniscus. *Biomaterials* **21,** 2453–2460.

22. Roman, J. S., Gallardo, A., Elvira, C., Vazquez, B., Lopez-Bravo, A., Pedro, J. A. D., et al. (2001) Contribution of polymeric supports to the development of tissue engineering. *Macromol. Symp.* **168,** 75–89.

23. Freed, L. E., Vunjak-Novakovic, G., Biron, R. J., Eagles, D. B., Lesnoy, D. C., Barlow, S. K., et al. (1994) Biodegradable polymer scaffolds for tissue engineering. *Bio/Technology* **12,** 689–693.

24. Mikos, A. G., Bao, Y., Cima, L. G., Ingber, D. E., Vacati, J. P., and Langer, R. (1993) Preparation of poly(glycolic acid) bonded fiber structures for cell attachment and transplantation. *J. Biomed. Mater. Res.* **27,** 183–189.

25. Mooney, D. J., Mazzoni, C. L., Breuer, C., McNamara, K., Hern, D., Vacanti, J. P., et al. (1996) Stabilized polyglycolic acid fibre-based tubes for tissue engineering. *Biomaterials* **17,** 115–124.

26. Cassell, O., Morrison, W., Messina, A., Penington, A., Thompson, E., Stevens, G., et al. (2001) The influence of extracellular matrix on the generation of vascularized, engineered, transplantable tissue. *Ann. NY Acad. Sci.* **944,** 429–442.

27. Dunn, R. L., English, J. P., and Cowsar, D. R. (1990) Biodegradable in-situ forming implants and methods of producing the same, US Patent, US 4,938,763.

28. Elema, H., Groot, J. H. D., Nijenhuis, A. J., Pennings, A. J., Veth, R. P. H., Klomopmaker, J., et al. (1990) Use of porous biodegradable polymer implants in meniscus reconstruction. 2) Biological evaluation of porous biodegradable polymer implants in menisci. *Colloid. Polym. Sci.* **268,** 1082–1088.

29. Lo, H., Kadiyala, S., Guggino, S. E., and Leong, K. W. (1996) Poly(L-lactic acid) foams with cell seeding and controlled-release capacity. *J. Biomed. Mater. Res.* **30,** 475–484.

30. Maquet, V., Martin, D., Malgrange, B., Franzen, R., Schoenen, J., Moonen, G., et al. (2000) Peripheral nerve regeneration using bioresorbable macroporous polylactide scaffolds. *J. Biomed. Mater. Res.* **52,** 639–651.

31. Schugens, C., Grandfils, C., Jerome, R., Teyssie, P., Delree, P., Martin, D., et al. (1995) Preparation of a macroporous biodegradable polylactide implant for neuronal transplantation. *J. Biomed. Mater. Res.* **29,** 1349–1362.

32. Schugens, C., Maquet, V., Grandfils, C., Jerome, R., and Teyssie, P. (1996) Polylactide macroporous biodegradable implants for cell transplantation. II. Preparation of polylactide foams by liquid-liquid phase separation. *J. Biomed. Mater. Res.* **30,** 449–461.

33. Schugens, C., Maquet, V., Grandfils, C., Jerome, R., and Teyssie, P. (1996) Biodegradable and macroporous polylactide implants for cell transplantation: 1. Preparation of macroporous polylactide supports by solid-liquid phase separation. *Polymer* **37(6),** 1027–1038.

34. Singhal, A. R., Agrawal, C. M., and Athanasiou, K. A. (1996) Salient degradation features of a **50,** 50 PLA/PGA scaffold for tissue engineering. *Tissue Engineering* **2(3),** 207.

35. Holy, C. E., Shoichet, M. S., and Davies, J. E. (1998) Bone ingrowth on a novel PLGA 75/25 foam, in *Proceedings of 24th Annual Meeting of the Society for Biomaterials.* San Diego, CA.

36. Eliaz, R. E. and Kost, J. (2000) Characterization of a polymeric PLGA-injectable implant delivery system for the controlled release of proteins. *J. Biomed. Mater. Res.* **50,** 388–396.

37. Hile, D. D., Amirpour, M. L., Akgerman, A., and Pishko, M. V. (2000) Active growth factor delivery from poly(D,L-lactide-co-glycolide) foams prepared in supercritical CO_2. *J. Control. Release* **66,** 177–185.

38. Hasirci, V., Berthiaume, F., Bondre, S. P., Gresser, J. D., Trantolo, D. J., Toner, M., et al. (2001) Expression of liver-specific functions by rat hepatocytes seeded in treated poly(lactic-co-glycolic)acid biodegradable foams. *Tissue Engineering* **7(4),** 385–394.

39. Patrick, C. W., Jr., Zheng, B., Johnston, C., and Reece, G. P. (2002) Long-term implantation of preadipocyte-seeded PLGA scaffolds. *Tissue Engineering* **8(2),** 283–293.

40. Borden, M., Attawia, M., Khan, Y., and Laurencin, C. T. (2002) Tissue engineered microscope-based matrices for bone repair: a design and evaluation. *Biomaterials* **23(2),** 551–559.

41. Hutmacher, D. W. (2001) Scaffold design and fabrication technologies for engineering tissues—state of the art and future perspectives. *J. Biomater. Sci. Polym. Edn.* **12(1),** 107–124.

42. Yang, S., Leong, K.-F., Du, Z., and Chua, C.-K. (2001) The design of scaffolds for use in tissue engineering. Part I. Traditional factors. *Tissue Engineering* **7(6),** 679–689.

43. Ikada, Y. and Tsuji, H. (2000) Biodegradable polyesters for medical and ecological applications. *Macromol. Rapid. Commun.* **21,** 117–132.

44. Corden, T. J., Jones, I. A., Rudd, C. D., Christian, P., Downes, S., and McDougall, K. E. (2000) Physical and biocompatibility properties of poly-E-caprolactone produced using in situ polymerisation: a novel manufacturing technique for long-fiber composite materials. *Biomaterials* **21,** 713–724.

45. Zein, I., Hutmacher, D. W., Tan, K. C., and Teoh, S. H. (2002) Fused deposition modelling of novel scaffold architectures for tissue engineering applications. *Biomaterials* **23,** 1169–1185.

46. Tienen, T. G.v., Heijkants, R. G. J. C., Buma, P., de Groot, J. H., Pennings, A. J., and Veth, R. P. H. (2002) Tissue ingrowth and degradation of two biodegradable porous polymers with different porosities and pore sizes. *Biomaterials* **23,** 1731–1738.

47. Mikos, A. G., Bao, Y., Cima, L. G., Ingber, D. E., Vacanti, J. P., and Langer, R. (1993) Preparation of poly(glycolic acid) bonded fiber structures for cell attachment and transplantation. *J. Biomed. Mater. Res.* **27,** 183–189.

48. Kim, W. S., Vacanti, J. P., Cima, L., Mooney, D., Upton, J., Puelacher, W. C., et al. (1994) Cartilage engineered in predetermined shapes employing cell transplantation on synthetic biodegradable polymers. *Plast. Reconstr. Surg.* **94,** 233–237.

49. Mikos, A. G., Thorsen, A. J., Czerwonka, L. A., Bao, Y., and Langer, R. (1994) Preparation and characterization of poly (L-lactic acid) foams. *Polymer* **35(5),** 1068–1077.

50. Freed, L. E., Marquis, J. C., Nohria, A., Emmanual, J., Mikos, A. G., and Langer, R. (1993) Neocartilage formation in vitro and in vivo using cells cultured on synthetic biodegradable polymers. *J. Biomed. Mater. Res.* **27,** 11–23.

51. Wake, M. C., Gupta, P. K., and Mikos, A. G. (1996) Fabrication of pliable biodegradable polymer foams to engineer soft tissues. *Cell Transplant.* **5(4),** 465–473.

52. Whang, K., Thomas, C. H., and Healy, K. E. (1995) A novel method to fabricate bioabsorbable scaffolds. *Polymer* **36(4),** 837–842.

53. Patrick, C. W., Chauvin, P. B., Hobley, J., and Reece, G. P. (1999) Preadipocyte seeded PLGA scaffolds for adipose tissue engineering. *Tissue Engineering* **5(2),** 139–151.

54. Thomson, R. C., Yaszemski, M. J., Powers, J. M., and Mikos, A. G. (1998) Hydroxy fiber reinforced poly(a-hydroxy ester) foams for bone regeneration. *Biomaterials* **19,** 1935–1943.

55. Ma, P. X. and Choi, J.-W. (2001) Biodegradable polymer scaffolds with well defined interconnected spherical pore network. *Tissue Engineering* **7(1),** 23–33.

56. Murphy, W. L., Dennis, R. G., Kileny, J. L., and Mooney, D. J. (2002) Salt fusion: an approach to improve pore interconnectivity within tissue engineering scaffolds. *Tissue Engineering* **8(1),** 43–52.

57. Mikos, A. G., Sarakinos, G., Leite, S. M., Vacanti, J. P., and Langer, R. (1993) Laminated three-dimensional biodegradable foams for use in tissue engineering. *Biomaterials* **14(5),** 323–330.

58. Wake, M. C., Patrick, C. W., and Mikos, A. G. (1994) Pore morphology effects on the fibrovascular tissue growth in porous polymer substrates. *Cell Transplant.* **3(4),** 339–343.

59. Mikos, A. G., Sarakinos, G., Leite, S. M., Vacanti, J. P., and Langer, R. (1993) Laminated three-dimensional biodegradable foams for use in tissue engineering. *Biomaterials* **14(5),** 323–330.

60. Liao, C.-J., Chen, C.-F., Chen, J.-H., Chiang, S.-F., Lin, Y.-J., and Chang, K.-Y. (2002) Fabrication of porous biodegradable polymer scaffolds using a solvent merging/particulate leaching method. *J. Biomed. Mater. Res.* **59,** 676–681.

61. Schmitz, J. P. and Hollinger, J. O. (1988) A preliminary study of the osteogenic potential of a biodegrada*Clin. Orthop. Relat. Res.*ble alloplastic osteoinductive alloimplant. *Clin. Orthop. Relat. Res.* **237,** 245–255.

62. Athanasiou, K. A., Singhal, A. R., Agrawal, C. M., and Boyan, B. D. (1995) In vitro degradation and release characteristics of biodegradable implants containing trypsin inhibitor. *Clin. Orthop. Relat. Res.* **315,** 272–281.

63. Coombes, A. G. A. and Heckman, J. D. (1992) Gel casting of resorbable polymers 1. Processing and applications. *Biomaterials* **13(4),** 217–224.

64. Coombes, A. G. A. and Heckman, J. D. (1992) Gel casting of resorbable polymers 2. In-vitro degradation of bone graft substitutes. *Biomaterials* **13(5),** 297–307.

65. Nam, Y. S. and Park, T. G. (1999) Porous biodegradable polymeric scaffolds prepared by thermally induced phase separation. *J. Biomed. Mater. Res.* **47,** 8–17.

66. Nam, Y. S. and Park, T. G. (1999) Biodegradable polymeric microcellular foams by modified thermally induced phase separation method. *Biomaterials* **20,** 1783–1790.

67. Hu, Y., Grainger, D. W., Winn, S. R., and Hollinger, J. O. (2002) Fabrication of poly(a-hydroxy acid) foam scaffolds using multiple solvent systems. *J. Biomed. Mater. Res.* **59,** 563–572.

68. Hua, F. J., Kim, G. E., Lee, J. D., Son, Y. K., and Lee, D. S. (2002) Macroporous poly(L-lactide) scaffold 1. Preparation of a macroporous scaffold by liquid-liquid phase separation of a PLLA-dioxane-water system. *J. Biomed. Mater. Res.* **63,** 161–167.

69. Ma, P. X., Zhang, R., Xiao, G., and Franceschi, R. (2001) Engineering new bone tissue in vitro on highly porous poly(a-hydroxyl acids)/hydroxyapatite composite scaffolds. *J. Biomed. Mater. Res.* **54,** 284–293.

70. Zhang, R. and Ma, P. X. (1999) Poly(a-hydroxyl acids)/hydroxyapatite porous composites for bone-tissue engineering. I. Preparation and morphology. *J. Biomed. Mater. Res.* **44,** 446–455.

71. Whang, K., Goldstick, T. K., and Healy, K. E. (2000) A biodegradable polymer scaffold for delivery of osteotropic factors. *Biomaterials* **21,** 2545–2551.

72. Hsu, Y.-Y., Gresser, J. D., Trantolo, D. J., Lyons, C. M., Gangadharam, P. R. J., and Wise, D. L. (1997) Effect of polymer foam morphology and density on

kinetics of in vitro controlled release of isoniazid from compresses foam matrices. *J. Biomed. Mater. Res.* **35,** 107–116.

73. Ma, P. X. and Zhang, R. (2001) Microtubular architechture of biodegradable polymer scaffolds. *J. Biomed. Mater. Res.* **56,** 469–477.

74. Ma, P. X. and Zhang, R. (1999) Synthetic nano-scale fibrous extracellular matrix. *J. Biomed. Mater. Res.* **46,** 60–72.

75. Zhang, R. and Ma, P. X. (2000) Synthetic nano-fibrillar extracellular matrices with predesigned macroporous architectures. *J. Biomed. Mater. Res.* **52,** 430–438.

76. Zmora, S., Glicklis, R., and Cohen, S. (2002) Tailoring the pore architecture in 3–D alginate scaffolds by controlling the freezing regime during fabrication. *Biomaterials* In press.

77. Mooney, D. J., Baldwin, D. F., Suh, N. P., Vacanti, J. P., and Langer, R. (1996) Novel approach to fabricate porous sponges of poly(D,L-lactic-co-glycolic acid) without the use of organic solvents. *Biomaterials* **17(14),** 1417–1422.

78. Holy, C. E., Dang, S. M., Davies, J. E., and Shoichet, M. S. (1999) In vitro degradation of a novel poly(lactide-co-glycolide) 75/25 foam. *Biomaterials* **20,** 1177–1185.

79. Sheridan, M. H., Shea, L. D., Peters, M. C., and Mooney, D. J. (2000) Bioabsorbable polymer scaffolds for tissue engineering capable of sustained growth factor delivery. *J. Control. Release* **64,** 91–102.

80. Maspero, F. A., Ruffieux, K., Muller, B., and Wintermantel, E. (2002) Resorbable defect analog PLGA scaffolds using CO_2 as solvent: structural characterization. *J. Biomed. Mater. Res.* **62,** 89–98.

81. Harris, L. D., Kim, B.-S., and Mooney, D. J. (1998) Open pore biodegradable matrices formed with gas foaming. *J. Biomed. Mater. Res.* **42,** 396–402.

82. Nam, Y. S., Yoon, J. J., and Park, T. G. (2000) A novel fabrication method of macroporous biodegradable polymer scaffolds using gas foaming salt as a porogen additive. *J. Biomed. Mater. Res. (Appl Biomater)* **53,** 1–7.

83. Yoon, J. J. and Park, T. G. (2001) Degradation behaviours of biodegradable macroporous scaffolds prepared by gas foaming of effervescent salts. *J. Biomed. Mater. Res.* **55,** 401–408.

84. Agrawal, C. M., Mckinney, J. S., Huang, D., and Athanasiou, S. A. (2000) The use of the vibrating particle technique to fabricate highly permeable biodegradable scaffolds, in *Synthetic Biosorbable Polymers for Implants* (Agrawal, C. M., Parr, J., and Lin, S., eds.), American Society for testing and materials, Philadelphia, PA.

85. Zhang, R. and Ma, P. X. (1999) Porous poly(L-Lactic acid)/apatite composites created by biomimetic process. *J. Biomed. Mater. Res.* **45,** 285–293.

86. Bigi, A., Boanini, E., Panzavolta, S., Roveri, N., and Rubini, K. (2002) Bonelike apatite growth on hydroxyapatite-gelatin sponges from simulated body fluid. *J. Biomed. Mater. Res.* **59,** 709–714.

87. Washburn, N. R., Simon, C. G., Elgendy, H. M., Karim, A., and Amis, E. J. (2002) Co-extrusion of biocompatible polymers for scaffolds with co-continuous morphology. *J. Biomed. Mater. Res.* **60,** 20–29.

88. Park, A., Wu, B., and Griffith, L. G. (1998) Integration of surface modification and 3D fabrication techniques to prepare patterned poly(L-lactide) substrates allowing regionally selective cell adhision. *J. Biomater. Sci. Polym. Edn.* **9(2),** 89–110.

89. Giordano, R. A., Wu, B. M., Borland, S. W., Cima, L. G., Sachs, E. M., and Cima, M. J. (1996) Mechanical properties of dense polylactic acid structures fabricated by three dimensional printing. *J. Biomater. Sci. Polymer Edn.* **8(1),** 63–75.

90. Hutmacher, D. W., Schantz, T., Zein, I., Ng, K. W., Teoh, S. H., and Tan, K. C. (2001) Mechanical properties and cell cultural response of polycaprolactone scaffolds designed and fabricated via fused deposition modeling. *J. Biomed. Mater. Res.* **55,** 203–216.

91. Terada, S., Sato, M., Sevy, A., and Vacanti, J. P. (2000) Tissue engineering in the twenty-first century. *Yonsei Med. J.* **41(6),** 685–691.

92. Salem, A. K., Stevens, R., Pearson, R. G., Davies, M. C., Tendler, S. J. B., Roberts, C. J., et al. (2002) Interactions of 3T3 fibroblasts and endothelial cells with defined pore features. *J. Biomed. Mater. Res.* **61,** 212–217.

93. Mikos, A. G., Sarakinos, G., Lyman, M. D., Ingber, D. E., Vacanti, J. P., and Langer, R. (1993) Prevascularization of porous biodegradable polymers. *Biotechnol. Bioeng.* **42,** 716–723.

94. Chen, G., Ushida, T., and Tateishi, T. (2001) Preparation of poly(L-lactic acid) and poly(DL-lactic-co-glycolide acid) foams by use of ice microparticulates. *Biomaterials* **22,** 2563–2567.

95. Hofer, S. O. P., Knight, K. M., Cooper-White, J. J., O'Connor, A. J., Perera, J. M., Stevens, G. W., et al. (2002) Increasing the volume of vascularized tissue formation in engineering constructs—An experimental study in rats. *Plast. Reconstr. Surg.* **111(3),** 1186–1192.

96. Lloyd, D. R., Kinzer, K. E., and Tseng, H. S. (1990) Microporous membrane formation via thermally induced phase separation. I. Solid-liquid phase separation. *J. Membrane Sci.* **52,** 239–261.

97. Blacher, S., Maquet, V., Pirard, R., Pirard, J.-P., and Jerome, R. (2001) Image analysis, impedance spectroscopy and mercury porosimetry characterisation of freeze-drying porous materials. *Colloids Surf. A Physicochem. Eng. Asp* **187–188,** 375–383.

98. Cao, Y., Cooper-White, J. J., O'Connor, A. J., and Stevens, G. W. 3D Poly(lactic-co-glycolic acid) scaffolds for soft tissue engineering, in *Proceedings of 12th Annual Conference of the Australian Society for Biomaterials*, March 2002, Canberra, Australia.

99. Cao, Y., Cooper-White, J. J., O'Connor, A. J., Stevens, G. W., and Davidson, M. R. (2003) Controlling macroporous architecture of three dimensional poly(D,L-lactic-co-glycolic) acid scaffolds for tissue engineering. In preparation.

100. Holy, C. E. and Yakubovich, R. (2000) Processing cell-seeded polyester scaffolds for histology. *J. Biomed. Mater. Res.* **50,** 276–279.

101. Maquet, V., Blacher, S., Pirard, R., Pirard, J.-P., and Jerome, R. (2000) Characterization of porous polylactide foams by image analysis and impedance spectroscopy. *Langmuir* **16,** 10463–10470.

102. Yang, J., Shi, G., Bei, J., Wang, S., Cao, Y., Shang, Q., et al. (2002) Fabrication and surface modification of macroporous poly(L-lactic acid) and poly(L-lactic-co-glycolic acid) (70/30) cell scaffolds for human skin fibroblast cell culture. *J. Biomed. Mater. Res.* **62,** 438–446.

103. Cao, Y., Cooper-White, J. J., O'Connor, A. J., and Stevens, G. W. (2003) The influence of morphology on degradation and vascularisation of three dimensional poly(D,L-lactic-co-glycolic) scaffolds in vitro and in vivo. In preparation.

104. Khang, G., Lee, S. J., Jeon, J. H., Lee, J. H., and Lee, H. B. (2000) Interaction of Fibroblast Cell onto physicochemically treated PLGA surfaces. *Polym. Korea* **24(6),** 869–876.

105. Tjia, J. S., Aneskievich, B. J., and Moghe, P. V. (1999) Substrate-adsorbed collagen and cell secreted fibronectin concertedly induce cell migration on poly(lactide-glycolide) substrates. *Biomaterials* **20,** 2223–2233.

106. Yang, J., Bei, J., and Wang, S. (2002) Enhanced cell affinity of poly (D,L-lactide) by combining plasma treatment with collagen anchorage. *Biomaterials* **23,** 2607–2614.

107. De Bartolo, L., Morelli, S., Bader, A., and Drioli, E. (2002) Evaluation of cell behaviour related to physico-chemical properties of polymeric membranes to be used in bioartificial organs. *Biomaterials* **23(12),** 2485–2497.

108. Groth, T., Seifert, B., Malsch, G., Albrecht, W., Paul, D., Kostadinova, A., et al. (2002) Interaction of human skin fibroblasts with moderate wettable polyacrylonitrile-copolymer membranes. *J. Biomed. Mater. Res.* **61(2),** 290–300.

109. Yang, J., Bei, J., and Wang, S. (2002) Improving cell affinity of poly(D,L-lactide) Film modified by anhydrous ammonia plasma treatment. *Polym. Adv. Technol.* **13,** 220–226.

110. Chu, P. K., Chen, J. Y., Wang, L. P., and Huang, N. (2002) Plasma-surface modification of biomaterials. *Mater. Sci. Eng. R.* **36,** 143–206.

111. Cai, K. Y., Yao, K. D., Cui, Y. L., Yang, Z. M., Li, X. Q., Xie, H. Q., et al. (2002) Influence of different surface modification treatments on poly(D,L-lactic acid) with silk fibroin and their effects on the culture of osteoblast in vitro. *Biomaterials* **23(7),** 1603–1611.

112. Quirk, R. A., Davies, M. C., Tendler, S. J. B., and Shakesheff, K. M. (2000) Surface engineering of poly(lactic acid) by entrapment of modifying species. *Macromolecules* **33,** 258–260.

113. Quirk, R. A., Davies, M. C., Tendler, S. J. B., Chan, W. C., and Shakesheff, K. M. (2001) Controlling biological interactions with poly(lactic acid) by surface entrapment modification. *Langmuir* **17,** 2817–2820.

114. Nam, Y. S., Yoon, J. J., Lee, J. G., and Park, T. G. (1999) Adhesion behaviours of hepatocytes cultured onto biodegradable polymer surface modified by alkali hydrolysis process. *J. Biomat. Sci. Polym. E.* **10(11),** 1145–1158.

115. Croll, T. I., Cooper-White, J. J., O'Connor, A. J., and Stevens, G. W., (2003) Controllable surface modification of poly(lactic-co-glycolic acid) (PLGA) by hydralysis or aminolysis. I. Physical, chemical and theoretical aspects. In preparation.

116. Khang, G., Choee, J. H., Rhee, J. M., and Lee, H. B. (2002) Interaction of different types of cells on physicochemically treated poly(L-lactide-co-glycolide) surfaces. *J. Appl. Polym. Sci.* **85(6),** 1253–1262.

117. Good, R. J. (1993) Contact angle, wetting and adhesion: a critical review, in *Contact Angle, Wettability and Adhesion: Festschrift in honor of Professor Robert J. Good* (Mittal, K. L., ed.), VSP BV: Utrecht. pp. 1–36.

118. Vargha-Butler, E. I., Kiss, E., Lam, C. N. C., Keresztes, Z., Kalman, E., Zhang, L., et al. (2001) Wettability of biodegradable surfaces. *Colloid. Polym. Sci.* **279(12),** 1160–1168.

9

Modification of Materials With Bioactive Peptides

Jennifer L. West

1. Introduction

Bioactive polymeric materials can be constructed via the modification of bioinert polymers with bioactive peptides such as cell-adhesion peptides or growth factors. Such materials can be designed to induce specific biological responses desired in applications such as tissue engineering and regenerative medicine. For example, transforming growth factor-beta (TGF-β) has been immobilized to polymeric scaffold materials to increase the synthesis of extracellular matrix (ECM) proteins and thus improve the mechanical properties of the engineered tissue *(1)*, and epidermal growth factor has been immobilized to improve the function of hepatocytes *(2)*. Cell adhesion peptides have been grafted to polymeric scaffold materials in order to enhance and promote cell attachment and spreading *(3–5)*. Alternatively, materials can be designed to be cell-selective, and adhesive for only a particular cell type, by modifying cell non-adhesive polymers with cell-selective adhesion ligands. Examples of cell-selective ligands include the peptide REDV, which interacts with endothelial cells but not platelets, fibroblasts, or smooth-muscle cells (SMCs) *(6)*, and the peptide KRSR, which interacts with osteoblasts but not fibroblasts *(7)*.

Bioactive materials can be designed in several ways, as outlined in **Fig. 1**. For many applications, surface modification is a good approach, especially given the expense associated with bioactive peptides (**Fig. 1A**). This approach usually involves surface modification to create functional groups, such as primary amines formed after ammonia plasma treatment, followed by covalent attachment of the peptides *(8)*. However, surface modification is only appropriate for non-porous, non-biodegradable materials, and thus has limited utility in tissue engineering. Alternatively, peptides can be grafted to functional
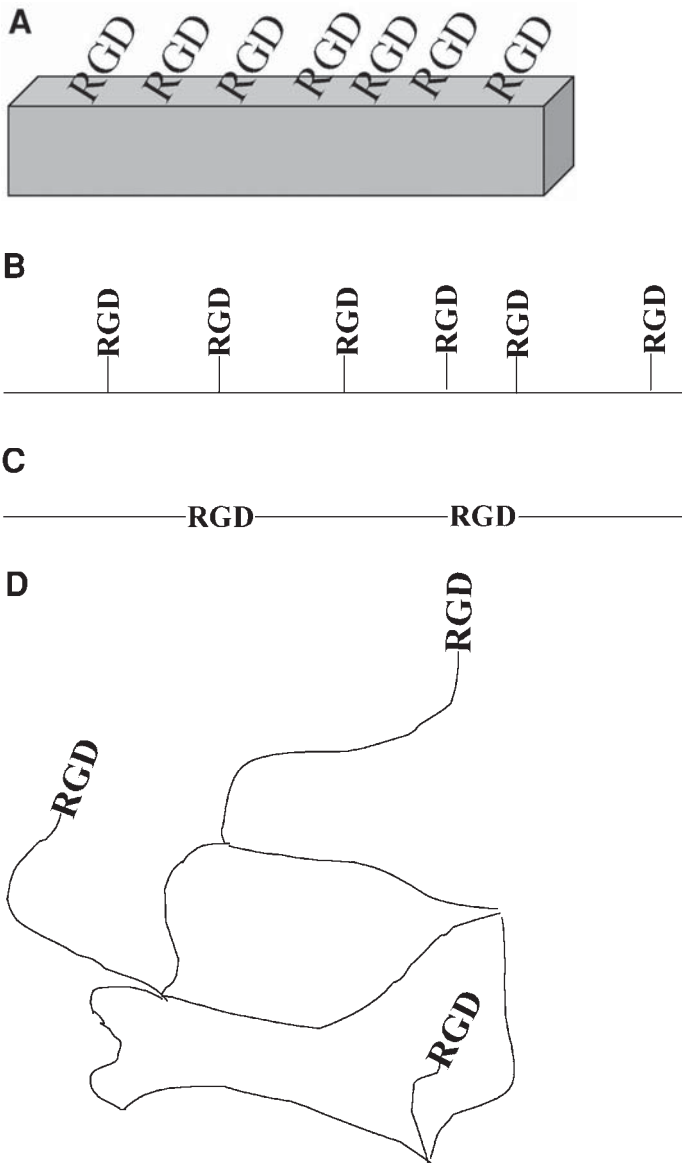
Fig. 1. Design of bioactive polymers with peptide modification. Biopolymers can be modified with bioactive peptides in several ways. As shown in **(A)** surface modification can be used for non-degradable, non-porous materials. Grafting peptides to polymer chains, as depicted in **(B)** or inclusion of peptides in the polymer backbone as shown in **(C)** have been used for bulk modification of biopolymers. Tethering approaches **(D)** have also been successfully utilized. The sequence RGD is shown here as an example of a bioactive peptide.

groups throughout the bulk of the polymer structure, as shown in **Fig. 1B**. This has been accomplished for amine-modified polyvinyl alcohol *(9)* and poly(lactide-co-lysine) copolymers *(10)*. This approach provides uniform peptide density throughout the bulk of the material, thus making the bioactive moiety available to cells as they migrate through pore structures or as new surfaces are exposed during polymer biodegradation. A third approach is to incorporate the peptide into the polymer backbone, as shown in **Fig. 1C**. This approach has been used to synthesize polyethylene glycol copolymers with peptides targeted for proteolytic degradation *(11,12)* and polyurethanes with cell adhesion peptides *(13)*. Additionally, crosslinked hydrogel materials have been designed that contain tethered peptides, as depicted in **Fig. 1D**. In this approach, several polymers with reactive groups such as acrylates or methacrylates are mixed in solution and then chemically crosslinked. One or more components of the polymer mixture can be modified with bioactive peptides. If the peptide-bearing polymer has only one reactive group, the peptide can be tethered into the hydrogel structure during the crosslinking process *(12,14)*. One advantage of this approach is that many hydrogel materials are relatively cell non-adhesive *(15,16)*, making this platform suitable for the development of cell-selective materials. Furthermore, providing the tethering chain has been shown to improve cellular interactions with the incorporated peptides, presumably by increasing the mobility of the peptide and decreasing steric hindrance *(14)*.

In addition to the structural design of the bioactive polymer, it is important to consider and characterize the concentration of the incorporated peptide. In many cases, bioactive peptides can have the desired effects at the optimal concentration, but just the opposite at higher or lower concentrations. For example, many cell adhesion peptides can promote tissue formation by enhancing cell attachment and migration but will inhibit cell growth and ECM protein synthesis when presented at high concentrations *(17,18)*. Another critical consideration is the use of controls for these types of studies. It is crucial to compare results with bioactive polymers, not only to unmodified polymers but also to polymers modified with scrambled amino acid sequences in order to ensure that the observed effects are indeed due to the effects of the bioactive peptide and not simply a change in the surface characteristics of the material.

This chapter describes a model surface—aminated glass—that can be used to investigate the effects of a bioactive peptide on cellular processes such as adhesion, migration, proliferation, and matrix protein synthesis. Using this system, it is easy to vary the peptide surface density, thus making it possible to identify optimal concentrations to use in biopolymer design. Several common chemistries that can be used to modify polymers with bioactive peptides are also described.

2. Materials

2.1. Preparation of Aminated Glass

1. Glass microscope slides.
2. 3:1 (vol/vol) 2 N sulfuric acid:2 N nitric acid mixture.
3. Acetone, dried with molecular sieves.
4. 100% ethanol, USP-grade.
5. Distilled water.
6. Aminopropyl triethoxysilane.
7. Rotary shaker.
8. Centrifuge.
9. Vacuum oven.

2.2. Evaluation of Amine Content Via the Ninhydrin Assay

1. Ninhydrin reagent solution (Sigma).
2. 0.1 M sodium citrate, pH 5.0.
3. 1 mM leucine prepared in 0.1 M sodium citrate.
4. Hot plate and water dish for boiling samples.
5. UV/vis spectrophotometer.

2.3. Coupling Peptides to Amine Groups Using EDC Chemistry

1. Aminated glass or polymer.
2. Bioactive peptide with amine groups blocked or protected (for example, acety-lated via reaction with equimolar acetic anhydride in aqueous buffer, pH 7.4, for 2 h at room temperature).
3. 30 mg 1-ethyl-3-(3-dimethylaminopropyl)carbodiimide hydrochloride (EDC).
4. 0.4 mL ethylmorpholine.
5. 20 mL anhydrous dimethylformamide (DMF).
6. 100-mm glass Petri dish.
7. Oven set at 37°C.
8. Distilled water.
9. 4 M urea, if modifying glass.
10. Ultrasonic bath, if modifying glass.
11. Cellulose dialysis membrane, mol wt cutoff >500 Da, if modifying an aminated poly-mer.
12. Lyophilizer, if modifying an aminated polymer.

2.4. Coupling Peptides to Amine or Hydroxyl Groups Using DCC Chemistry

1. Amine or hydroxyl-bearing polymer, such as polyethylene glycol.
2. Bioactive peptide with amine groups blocked or protected (for example, acety-lated via reaction with equimolar acetic anhydride in aqueous buffer, pH 7.4, for 2 h at room temperature).
3. 2 500-mL round-bottom flasks.

4. Dicyclohexyl carbodiimide (DCC).
5. Anhydrous dichloromethane (DCM).
6. Anhydrous DMF.
7. Anhydrous pyridine.
8. Ethyl ether.
9. Magnetic stir plate and stir bars.
10. Vacuum manifold.
11. Argon or nitrogen gas.
12. Vacuum oven.

2.5. Coupling Peptides to NHS Groups

1. N-hydroxysuccinimide (NHS) functionalized polymer, such as polyethylene glygol-NHS (PEG-NHS, Shearwater Polymers).
2. Bioactive peptide (to couple at N-terminus only, any side-chain amine groups should be protected, to couple at both ends of the peptide, an amine-bearing residue such as a lysine should be added to the C-terminus of the peptide sequence).
3. 0.1 *M* sodium carbonate, pH 8.5.
4. Orbital shaker.

2.6. Coupling Peptides to Isocyanates or Isothiocyanates

1. Isocyanate or isothiocyanate modified polymer, such as a prepolymer formed during polyurethane urea synthesis or polyethylene glycol isocyante.
2. Bioactive peptide (to couple at N-terminus only, any side-chain amine groups should be protected, to couple at both ends of the peptide, an amine-bearing residue such as a lysine should be added to the C-terminus of the peptide sequence).
3. 0.1 *M* sodium carbonate, pH 9.0.
4. Refrigerator.

3. Methods

3.1. Preparation of Aminated Glass

1. Clean glass slides with the sulfuric acid:nitric acid mixture in a chemical fume hood. Rinse thoroughly with acetone, then ethanol, then distilled water. Allow to dry.
2. In a graduated glass cylinder with a stir bar at the bottom, combine 95 mL ethanol and 5 mL distilled water. Stir well. Remove and discard 2 mL.
3. While stirring, add 2 mL aminopropyl triethoxysilane. Stir for 5 min.
4. Pour the ethanol:aminopropyl triethoxysilane mixture over the slides in a glass tray. Place on a rotary shaker and agitate for 10 min.
5. Replace the ethanol:aminopropyl triethoxysilane mixture with pure ethanol. Rinse slides thoroughly with the ethanol.
6. Place slides in a suitable centrifuge holder and spin at 260*g* for 10 min.
7. Place slides in a vacuum oven at 50°C overnight.

3.2. Evaluation of Amine Content Via the Ninhydrin Assay

1. Boil water on hot plate.
2. Put 15 mL of the sodium citrate buffer in a test tube. Add your modified glass or polymer.
3. Prepare serial dilutions of the leucine stock solution with the sodium citrate buffer in test tubes. An appropriate concentration range is often 0, 0.1, 0.05, 0.025, and 0.0125 m*M*.
4. Add 15 mL of ninhydrin reagent solution to each test tube.
5. Place tubes in boiling water and incubate for 15 min.
6. Remove tubes from boiling water and allow to cool to room temperature.
7. Read the absorbance of each sample at 570 nm.
8. Perform linear regression on the readings from the standards. Use this curve to calculate the amine content of your samples. This assay can be performed before and after peptide conjugation to determine the peptide density.

3.3. Coupling Peptides to Amine Groups Using EDC Chemistry

1. Place 30 mg EDC in Petri dish.
2. Add 0.4 mL ethylmorpholine.
3. Add 20 mL DMF.
4. Add an appropriate amount of the bioactive peptide (based on desired material design). Swirl dish to mix.
5. Place in an oven for 30 min.
6. Add the glass or polymer to the Petri dish. Continue to incubate at 37°C for another 3.5 h.
7. If modifying glass, remove slides and rinse with distilled water. Place slides in 4 *M* urea solution and sonicate for 10 min. Rinse again in water and allow to dry.
8. If modifying a polymer, add 20 mL of distilled water. Dialyze against distilled water for at least 12 h. Lyophilize the product.
9. Characterize the remaining amine content of your material using the ninhydrin assay described in **Subheading 3.2.** to determine the peptide density.

3.4. Coupling Peptides to Amine or Hydroxyl Groups Using DCC Chemistry

1. In a round bottom flask, dissolve 16 mmol of the peptide in 10 mL DCM and 2 mL DMF.
2. Add 8 mmol DCC. Stir for 30 min under argon or nitrogen at room temperature.
3. Filter to remove the dicyclohexyl urea that has formed.
4. In another round-bottom flask, dissolve the polymer in DCM.
5. Add the filtered peptide solution to the polymer solution. React for 12 h under argon or nitrogen at room temperature.
6. Precipitate the polymer with cold ether. Filter and wash with additional ether. Dry overnight in vacuum oven.
7. If a removable protecting group was used, the amine groups may be de-protected and further chemical modification can now be conducted.

3.5. Coupling Peptides to NHS Groups

1. Dissolve peptide in buffer at 1 mg/mL.
2. Dissolve polymer in buffer at appropriate concentration based on desired design.
3. Add polymer to peptide solution in a dropwise fashion. Place mixture on an orbital shaker and allow to react for 2 h at room temperature.

3.6. Coupling Peptides to Isocyanates or Isothiocyanates

1. Dissolve peptide in buffer at 1 mg/mL.
2. Dissolve polymer in buffer at appropriate concentration based on desired design.
3. Add polymer to peptide solution in a dropwise fashion. Mix well.
4. Incubate for 8 h at 4°C.

4. Notes

1. When preparing aminated glass, use of high-quality solvents and water is crucial to the success of the procedure.
2. Quantification of peptide density on modified material surfaces is imperative. Techniques such as ESCA/XPS can be used, but quantification of peptide density is generally easier using chemical assays such as the ninhydrin assay. Radiolabeling of peptides—for instance, by iodination of tyrosine residues—can also be used.
3. Glass slides fit well in 50 mL centrifuge tubes. These can be placed in a pyrex dish filled with boiling water during the ninhydrin assay.
4. In designing peptide sequences, performance will often be improved by placing spacer residues between the biologically active sequence and the material, whether it is polymer or glass. Several glycine residues are often used for this purpose.
5. Modified polymers should be characterized using NMR and GPC. FTIR, contact-angle analysis, and reverse-phase HPLC (RPHPLC) may also be useful in characterization. The unmodified base polymer should also be characterized by these methods for comparison.
6. Control peptides should always be used to ensure that any observed changes in cell behaviors are caused by the biological activity of the peptide and not simply a change in surface chemistry. Control peptides may be scrambled amino acid sequences or peptide sequences with one amino acid substitution. In cell adhesion studies, control groups may also be treated with soluble peptide to evaluate the competitive inhibition of cell attachment and spreading.
7. To create biopolymers that allow adhesion of only a particular cell type, a cell-selective peptide sequence can be attached to a cell non-adhesive polymer. Polyethylene glycol- and polyvinyl alcohol-containing materials have shown promise for this type of application.
8. To evaluate the activity of cell adhesion peptides after covalent modification, cell attachment and spreading should be evaluated using the desired cell type. The cell type used must have the receptor for the cell adhesion peptide employed.

In performing these experiments, FlexiPerm membranes can be used to create cell-culture wells on the surface of the modified material. Cell attachment can be assessed by determining the percentage of adherent cells at predetermined time-points over the first 24 h after seeding. Cell spreading can be evaluated by counting the number of spread cells and measuring the spread cell areas (via digital image processing) over the first 24 h after seeding.

9. When modifying materials with growth factors or other proteins, avoid exposure to organic solvents. Good bioactivity has been observed using both NHS and isothiocyanate protocols. Bioactivity of immobilized growth factors should be directly compared to the soluble, unmodified growth factor using a bioassay appropriate to the particular growth factor. For example, fibroblast proliferation may be assessed for materials modified with basic fibroblast growth factor (bFGF), and collagen production is a better bioassay for materials modified with TGF-β.

References

1. Mann, B. K., Schmedlen, R. H., and West, J. L. (2001) Tethered-TGF-β increases extracellular matrix production of vascular smooth muscle cells. *Biomaterials* **22,** 439–444.

2. Kuhl, P. R. and Griffith-Cima, L. G. (1996) Tethered epidermal growth factor as a paradigm for growth factor-induced stimulation from the solid phase. *Nat. Med.* **2,** 1022–1027.

3. Massia, S. P. and Hubbell, J. A. (1990) Covalent surface immobilization of Arg-Gly-Asp- and Tyr-Ile-Gly-Ser-Arg-containing peptides to obtain well-defined cell-adhesive substrates. *Anal. Biochem.* **187,** 292–301.

4. Massia, S. P., Rao, S. S., and Hubbell, J. A. (1993) Covalently immobilized laminin peptide Tyr-Ile-Gly-Ser-Arg (YIGSR) supports cell spreading and co-localization of the 67-kilodalton laminin receptor with α-actinin and vinculin. *Biol, J. Chem.* **268,** 8053–8059.

5. Drumheller, P. D. and Hubbell, J. A. (1994) Polymer networks with grafted cell adhesion peptides for highly biospecific cell adhesive substrates. *Anal. Biochem.* **222,** 380–388.

6. Hubbell, J. A., Massia, S. P., Desai, N. P., and Drumheller, P. D. (1991) Endothelial cell-selective tissue engineering in the vascular graft via a new receptor. *Bio/Technology* **9,** 568–572.

7. Dee, K. C., Anderson, T. T., and Bizios, R. (1998) Design and function of novel osteoblast-adhesive peptides for chemical modification of biomaterials. *J. Biomed. Mater. Res.* **40,** 371–377.

8. Tong, Y. W. and Shoicet, M. S. (1998) Enhancing the interaction of central nervous system neurons with poly(tetrafluoroethylene-co-hexafluoropropylene) via a novel surface amine-functionalization reaction followed by peptide modification. *J. Biomater. Sci. Polym. Ed.* **9,** 713–729.

9. Schmedlen, R. H., Masters, K. S., and West, J. L. (2002) Photocrosslinked PVA hydrogels that can be modified with cell adhesion peptides for use in tissue engineering. *Biomaterials* **23,** 4325–4332.

10. Barrera, D. A., Zylestra, E., Lansbury, P. T., and Langer, R. (1993) Synthesis and RGD peptide modification of a new biodegradable polymer—poly(lactic acid-co-lysine). *J. Am. Chem. Soc.* **115,** 11,010–11,011.

11. West, J. L. and Hubbell, J. A. (1999) Polymeric biomaterials with degradation sites for the proteolytic activities involved in cell migration. *Macromolecules* **32,** 241–244.

12. Mann, B. K., Tsai, A. T., Gobin, A. S., Schmedlen, R. H., and West, J. L. (2001) Synthetic ECM analogs: materials with cell adhesion, growth factor, and proteolytically-degradable domains for use as tissue engineering scaffolds. *Biomaterials* **22,** 3045–3051.

13. Braatz, J. A., Yasuda, Y., Olden, K., Yamada, K. M., and Heifetz, A. H. (1993) Functional peptide-polyurethane conjugates with extended circulatory half-lives. *Bioconjug. Chem.* **4,** 262–267.

14. Hern, D. L. and Hubbell, J. A. (1998) Incorporation of adhesion peptides into non-adhesive hydrogels useful for tissue resurfacing. *J. Biomed. Mater. Res.* **39,** 266–276.

15. Graham, N. B. (1998) Hydrogels: their future, Part 1. *Med. Device Technol.* **9,** 18–22.

16. Graham, N. B. (1998) Hydrogels: their future, Part 2. *Med. Device Technol.* **9,** 22–25.

17. Mann, B. K., Tsai, A. T., Scott-Burden, T., and West, J. L. (1999) Modification of surfaces with cell adhesion peptides alters extracellular matrix deposition. *Biomaterials* **20,** 2281–2286.

18. Mann, B. K. and West, J. L. (2002) Cell adhesion peptides alter smooth muscle cell adhesion, proliferation, migration, and matrix protein synthesis on modified surfaces and in polymer scaffolds. *J. Biomed. Mater. Res.* **60,** 86–93.

10

Isolation and Osteogenic Differentiation of Bone-Marrow Progenitor Cells for Application in Tissue Engineering

António J. Salgado, Manuela E. Gomes, Olga P. Coutinho, and Rui L. Reis

1. Introduction

One of the most widely studied bone-tissue engineering approaches involves the seeding and extended in vitro culturing of cells within a biodegradable scaffold prior to implantation. The bioresorbable scaffold must be biocompatible and porous in order to facilitate rapid vascularization and growth of newly formed tissue *(1–8)*. During the in vitro culture period, the seeded cells proliferate and secrete tissue-specific extracellular matrix (ECM). The selection of the scaffold material, which should exhibit an adequate three-dimensional (3D) porous structure, is a primary consideration in matrix- and cell-based bone-tissue engineering strategies *(9)*.

Another important consideration for tissue-engineering approaches based on culturing cells on polymeric 3D scaffolds is the selection of the source of cells to be used and the ability to generate sufficient amounts of cells of the appropriate type. These cells should be easily expandable to higher passages and non-immunogenic, and should have a protein-expression rate similar to the tissue to be regenerated. For application in bone-tissue engineering, the most obvious choice would be to use cells isolated from the patient's mature bone *(10)*. However, this methodology has several limitations, mainly because relatively few cells are available after the dissociation of the tissue and their expansion rates are relatively low, limiting in this way the number of cells available for seeding into the scaffolds. Moreover, in certain bone-related diseases, the protein-expression profile of osteoblasts is completely

altered and in these cases, it becomes impossible to use cells obtained from the patient *(10)*.

Several studies have demonstrated that mesenchymal stem cells (MSCs) isolated from the bone marrow constitute a potential source of cells for bone-tissue engineering, since it is possible to harvest a small sample of marrow from a patient, select and expand the MSC population, differentiate these cells into osteoblasts, and have them available for transplantation, avoiding a potential immune response because of the autogenous origin of the cells *(11)*. These multipotent cells were first described by Fridestein et al. *(12)*, and are located in the bone marrow surrounding blood vessels (as pericytes), in fat, skin, muscle, and other locations *(13)*. In fact, although they are present in very small amounts (from 0.001% to 0.01%) *(14)*, they have high proliferation rates, which enables them to be expanded over one billion-fold in culture *(12–17)*. The differentiation of the MSCs into the osteogenic lineage is achieved by incubating cells with specific factors, such as dexamethasone, ascorbic acid, and β-glycerophosphate *(11)*. Although the metabolic pathways that are triggered by such factors are not fully understood, ascorbic acid is known to stimulate collagen I production *(18)*. Dexamethasone stimulates the mineralization of the ECM *(16,17)*, which will then lead to bone-nodule formation, and β-glycerophosphate acts as an exogenous source of phosphate groups *(16,17)*.

In this chapter, methods for the isolation of a heterogeneous cell population containing progenitor cells from the bone marrow and methods to induce their osteogenic differentiation are described. These methods are described, as a practical example, for cells obtained from bone marrow collected from both humans and *Wistar* rats. The latter can be used as a model in bone-tissue engineering research, to study the potential of several scaffolds or culturing techniques.

2. Materials

2.1. Human Bone-Marrow Progenitor-Cell Isolation

1. 10–15 mL of human bone marrow.
2. Class II flow hood.
3. Sterile 50-mL centrifuge tubes.
4. 5, 10, and 25-mL sterile pipets.
5. Sterile heparinized syringes.
6. 18-gauge needles.
7. Centrifuge that withstands up to 900*g*.
8. Hemocytometer.
9. 70% (v/v) ethanol.
10. 0.5% acetic acid solution.

11. Sterile Ca^{2+} and Mg^{2+} free phosphate-buffered saline (PBS): 0.14 M NaCl, 2.7 mM KCl, 1.5 mM KH_2PO_4, 8.1 mM Na_2HPO_4, pH 7.2, (Gibco-BRL®, Cat. No. 14200). Store at 4°C.
12. Percol solution (Sigma, P 4937).
13. Basic medium: Dulbecco's modified Eagle's medium (DMEM; high-glucose formula, Gibco-BRL®, Cat No. 10569–010), supplemented with 1% antibiotics/antimycotics and 10% of fetal bovine serum (FBS).

2.2. Isolation of Rat Bone-Marrow Progenitor Cells

2.2.1. Collection of Rat Femurs

1. Young adult male Wistar rats (115–125g).
2. Sterile 50-mL centrifuge tubes.
3. 5, 10, and 25-mL sterile pipets.
4. Sterile scalpels and blades.
5. Sterile pair of scissors.
6. Sterile forceps.
7. Pins.
8. Basic culture medium: α-MEM supplemented with 15% FBS and 1% antibiotics/antimycotics.

2.2.2. Isolation of Rat Bone-Marrow Progenitor Cells

1. Class II flow hood.
2. Sterile 50-mL centrifuge tubes.
3. 5, 10, and 25-mL sterile pipets.
4. 100-mm sterile Petri dish.
5. T75 cell-culture flasks.
6. Syringes.
7. 20-gauge or 21-gauge needles.
8. Hemocytometer.
9. Basic culture medium: α-MEM supplemented with 15% FBS and 1% antibiotics/antimycotics.

2.3. Osteogenic Differentiation and Culture Expansion

1. Basic culture medium: (*see* **Subheading 2.2.2.**)
2. 0.01 M ascorbic acid (stock solution) (Sigma, A 4403).
3. 0.5 M β-blycerophosphate (stock solution) (Sigma, G 9891).
4. 10^{-5} M dexamethasone (stock solution) (Sigma, D 4902).

3. Methods

3.1. Human Bone-Marrow Progenitor-Cell Isolation

1. Collect 10–15 mL of human bone marrow into a 20-mL syringe with an 18-gauge needle.

2. After the collection of the bone marrow, mix it with an equal volume of PBS and homogenize thoroughly until all blood clots are dissociated.

3. Remove a small volume from the resulting cell suspension, mix it with an equal volume of 0.5% acetic acid, and count the cells in the hemocytometer. The acetic acid will burst the erythrocytes so that mononuclear cells can be more easily distinguished.

4. Centrifuge the cell suspension for 10 min at 900g.

5. Carefully aspirate the supernatant and resuspend the pellet in PBS in order to obtain a final density of 4×10^7 nucleated cells/mL.

6. Carefully layer the cell suspension over a 1.073 g/mL Percol solution. The pipetting should be gentle enough to avoid mixing the bone-marrow cell suspension with the percol gradient.

7. After centrifuging at 900g for 30 min, three phases can be distinguished in the percol gradient. Collect the middle phase, also known as interface, and centrifuge it for 10 min at 1000 rpm.

8. Remove the supernatant and resuspend the pellet in 1–3 mL of PBS. Centrifuge again (10 min; 1000 rpm).

9. Aspirate the supernatant and repeat **step 8** using basic culture medium.

10. Count the cells using the trypan blue viability test and plate at a density of 1.2×10^7 nucleated cells/75 cm^2.

11. Incubate the cells at 5% CO_2 and 37°C, and change the medium after 48 h and every 3–4 d thereafter.

12. When cells reach 90% of confluence, subculture them using a 0.25% trypsin/ethylenediaminetetraacetic acid (EDTA) solution and subculture them until they reach the desired number of cells.

3.2. Rat Bone-Marrow Progenitor-Cell Isolation

3.2.1. Dissection Procotocol

1. Sacrifice the rat, shave its back and lower limbs and place it on its stomach on a dissection board.

2. Clean the body parts of the rat that were shaved in **step 1** with 70% ethanol.

3. Pin the rat down by the four limbs on its stomach. Next, make a small incision on the rat's skin. Before cutting it open, and using a pair of scissors, separate the connective tissue from the skin. Next, pin the skin inside-out down for easy access to the femur.

4. Cut the overlying muscle to expose the femur. Once it is exposed, pick up the femur with forceps and clean all the adjacent muscle. When the bone is muscle-free, cut through the hip and knee joint to release the femur.

5. Once the femur is extracted from the rat, place it in antibiotic/antimycotic solution.

3.2.2. Bone Marrow Progenitor Cells Isolation

1. Wash the femurs 3×, 10 min each, in antibiotic/antimycotic solution. After this, the femurs should be placed on basic culture medium.

2. Transfer the femur to a sterile Petri dish and cut off both epiphyses to expose the bone marrow cavity.
3. Fill a 10-mL syringe with basic culture medium, perforate the bone-marrow cavity, and gently flush out its contents into a 50-mL sterile tube. Fill the syringe again with the contents of the tube, and repeat the same procedure for the other end of the femur.
4. Repeat the procedure for the other femur.
5. Add an additional 10 mL of culture medium, and transfer the resulting cellular suspension into T75 cell-culture flasks, pipetting 15-mL/flask.

3.3. Osteogenic Differentiation and Culture Expansion

1. For the osteogenic differentiation of bone marrow progenitor cells, culture medium must be supplemented with ascorbic acid (final concentration 100 μM), β-glycerophosphate (final concentration 10 mM) and dexamethasone (final concentration 10^{-7} M).
2. The medium should be changed every 2 d. The first medium change should be performed carefully, without shaking the culture flask too much. In the following changes, the flasks should be agitated in order to "wash" undesirable cells/residues.
3. The culture period depends on the intended experiments to perform, and therefore must be optimized for each purpose, studying the stage of differentiation/ maturation of the cells during different culture periods.

3.4. Some Comments on the Characterization of the Cultured Cells

One of the problems of using mesenchymal progenitor cells for bone-tissue engineering is the heterogenicity of the cultures, even after exposure to osteogenic differentiation factors. Because of this, it is advisable to make a proper characterization of the cultures, before seeding them on 3D porous structures. This goal can be achieved by standard staining, enzymatic, or immuno-based assays. All data should be compared with data obtained from already differentiated osteoblasts and non-osteogenic cells.

One such assay is designed to detect the activity of alkaline phosphatase (ALP). ALP is a membrane-bounded enzyme, which is commonly associated with the osteogenic phenotype and is believed to be involved in the initial steps of mineralization of bone ECM. This screening can be done either by using staining methodologies or by means of quantifying the levels of ALP present in the supernatant or after lysing the cells. Both of the methodologies are straightforward, and can be easily implemented by using commercially available standard kits.

Although ALP allows for an initial screening of the osteogenic phenotype, a more complete characterization should also be carried out. For this purpose, immuno-based techniques such as immunocytochemistry and Western blot should be conducted, in order to detect bone-matrix proteins such as osteopontin,

bone sialoprotein, or collagen I. The first two are present on the noncollagenous matrix, which is layered down by osteogenic cells known as ciment line, and collagen I is the most abundant protein in the organic part of the bone. The detection of these three proteins is a clear sign of bone ECM deposition, and thus the demonstration that mesenchymal progenitor cells, after exposure to differentiation factors, have an osteogenic phenotype.

Finally, and because the inorganic part of the bone is constituted by calcium-phosphates (CaP), a screening of their presence in the matrix should be conducted. Common histology staining such as von Kossa's can be used for such an application. In alternative quantitative methods for the determination of the concentration of calcium and phosphate can also be used.

References

1. Freed, L. E. and Vunjak-Novakovic, G. (1998) Culture of organized cell communities. *Adv. Drug Delivery Reviews* **33,** 15–30.
2. Thomson, R. C., Wake, M. C., Yaszemski, M., and Mikos, A. G. (1995) Biodegradable polymer scaffolds to regenerate organs. *Adv. Polym. Sci.* **122,** 247–274.
3. Langer, R. (1999) Selected advances in drug delivery and tissue engineering. *J. Control. Release* **62,** 7–11.
4. Lu, L. and Mikos, A. G. (1996) The importance of new processing techniques in tissue engineering. *MRS Bulletin* **21,** 28–32.
5. Langer, R. and Vacanti, J. P. (1993) Tissue engineering. *Science* **260,** 920–925.
6. Chen, G., Ushida, T., and Tateishi, T. (2000) Hybrid biomaterials for tissue engineering: a preparative method for PLA or PLGA-collagen hybrid sponges. *Adv. Mater.* **12,** 455–457.
7. Laurencin, C., Ambrosio, A., Borden, M., and Cooper, J. (1999) Tissue engineering: orthopaedic applications. *Annu. Rev. Biomed. Eng.* **1,** 19–46.
8. Mooney, D. J. and Mikos, A. G. (1999) Growing new organs. *Sci. Amer.* **280,** 38–43.
9. Hutmacher, D. W., Teoh, S. H., Zein, I., Renawake, M., and Lau, S. (2000) Tissue engineering research: the engineer's role. *Med. Dev. Tech.* **1,** 33–39.
10. Heath, C. A. (2000) Cells for tissue engineering. *TIBTECH* **18,** 17–19.
11. Bruder, S. P. and Caplan, A. I. (2000) Bone regeneration through cellular engineering, in *Principles of Tissue Engineering, 2nd ed* (Lanza, R., Langer, R., Vacanti, J., eds.), Academic Press, New York, NY, pp. 683–696.
12. Friedenstain, A. J. (1973) Determined and inducible osteogenic precursor cells, in *Hard Tissue Growth, Repair and Remineralization.* Elsevier, Amsterdam, The Netherlands **11,** 169–185.
13. Caplan, A. I. and Bruder, S. P. (2001) Mesenchymal stem cells: building blocks for molecular medicine in the 21st century. *Trends in Mol. Med.* **7(6),** 259–264.
14. Haynesworth, S. E., Goshima, J., Goldberg, V. M., and Caplan, A. I. (1992) Characterization of cells with osteogenic potential from human marrow. *Bone* **13,** 81–88.

15. Jaiswall, N., Haynesworth, S. E., Caplan, A. I., and Bruder, S. P. (1997) Osteo-genic differentiation of purified, culture-expanded human mesenchymal stem cell *in vitro*. *J. Cell. Biochem.* **64,** 295–312.
16. Pittinger, M. F., Mackay, A.M., Beck, S. C., Jaiswal, R. K., Douglas, R., Mosxca, J. D., et al. (1999) Multilineage potential of adult mesenchymal stem cells. *Science* **284,** 143–147.
17. Bruder, S. P., Jaiwal, N., and Haynesworth, S. E. (1997) Growth Kinetics self renewal, and the osteogenic potential of purified human mesenchymal stem cells during extensive subcultivation and following cryopreservation. *J. Cell. Biochem.* **64(2),** 278–294.
18. Hosseini, M. M., Sodek, J., Franke, R. P. and Davies, J. E. (1999) The structure and composition of the Bone-implant surface, in *Bone Engineering* (Davies, J. E., ed.), Squared Incorporation, Canada, ***26,*** 295–304.

11

Cell Seeding of Polymer Scaffolds

Gordana Vunjak-Novakovic and Milica Radisic

1. Introduction

Engineered tissues could form the basis for novel therapies for millions of patients who suffer from the loss of tissue or its function *(1)*, and be used for in vitro studies of tissue development and normal and pathological function. One approach to tissue engineering involves seeding of a high density of uniformly distributed cells on three-dimensional (3D) polymeric scaffolds, and cultivating the resulting cell-polymer constructs under conditions that permit the formation of functional tissues *(2)*. The scaffold provides a defined structure for cell attachment and tissue development, and the bioreactor provides control over the biochemical and physical factors in the cell environment.

Optimization of cell seeding of polymer scaffolds is essential for the successful in vitro cultivation of functional tissue constructs. General seeding requirements for 3D scaffolds include: high yield, to maximize the utilization of donor cells; high kinetic rate, to minimize the time in suspension culture for anchorage-dependent and shear-sensitive cells; spatially uniform distribution of attached cells, to provide a basis for uniform tissue regeneration; and high initial construct cellularity, to enhance the rate of tissue development *(3)*. Additional seeding requirements may depend on cell type and tissue-engineering application (*see* **Notes 1** and **2**).

This chapter reviews some of the available seeding methods, using articular cartilage and cardiac muscle as two representative examples of engineered tissues that have great clinical relevance but are different in many respects. Once damaged, cartilage and cardiac muscle are unable to regenerate.

Articular cartilage is avascular, and contains only one cell type (chondrocyte) in abundant extracellular matrix (ECM). Chondrocytes are present at a low concentration, and are supplied with oxygen and nutrients by a combination of

diffusion and fluid flow during joint loading. Although the synthesis rates of glycosaminoglycan (GAG) and collagen in a developing tissue in vitro depend on gas exchange *(4)*, cells remain viable under hypoxic conditions, which are inherent for adult cartilage in an articular joint *(5)*.

In contrast, cardiac muscle is a highly differentiated, vascularized tissue that contains several cell types (cardiac myocytes, fibroblasts, and endothelial cells) *(6,7)*. Cardiac myocytes are highly metabolically active, and can not tolerate hypoxia for prolonged periods of time *(8,9)*. These differences in cell metabolism as compared to chondrocytes impose different requirements for mass transfer of oxygen during cell seeding.

We and others have investigated a variety of seeding methods using different cell types (cartilage, cardiac, bone-marrow cells; primary or passaged; genetically transformed), and concentrations (5–50 million cells per cm^3 of scaffold volume), scaffolds (meshes and sponges), seeding vessels (Petri dishes, spinner flasks, rotating vessels, perfused cartridges), mixing conditions (static or mixed cultures), and duration (1 h to several days). The available seeding methods are described in detail, along with some of the underlying principles, and discussed with respect to their impact on the field of tissue engineering. Other related methods (e.g., cell isolation, serial passage in monolayers) are described in detail in other sources, and these references are listed in the text.

2. Materials
2.1. Cells

General requirements for cell sources used for tissue engineering include: cell isolation and/or selection from a tissue; proliferation in vitro to obtain sufficient cell mass for seeding large 3D scaffolds; and a capacity for differentiation into functional tissues. Cartilage can be engineered using either articular chondrocytes or chondrogenic precursors isolated from bone marrow. Both cell sources have been successfully tested in vitro in bioreactors *(10–12)* and in vivo in rabbits *(13,14)*. Cardiac muscle has been engineered using cardiac myocytes obtained from embryonic chicks and neonatal rats and studied in vitro *(15–17a)*, and in vivo *(18,19)*. Seeding studies were also carried out using a cell line (C2C12 mouse myoblasts). Specific protocols used to isolate, amplify, and in some cases genetically modify the cells are summarized here.

1. Articular chondrocytes are obtained as previously described by enzymatic digestion of full-thickness articular cartilage harvested from 2–4-wk-old bovine calves *(20)* and 2–8 mo-old New Zealand white rabbits *(13)*. For both sources, cell yield is 3–5 × 10^7 cells per gm wet tissue.

   Primary chondrocytes can be directly seeded onto scaffolds, or first amplified by subculture in the chondrocyte medium (*see* **Subheading 2.2.1.**) supplemented with 5 ng/mL of fibroblast growth factor FGF-2 *(21)*. Expanded chondrocytes

undergo approx 10 doublings, in two passages.

During monolayer culture, chondrocytes can be transfected—e.g., by human insulin-like growth factor I, as previously described *(22)*.

2. Bone-marrow stromal cells (BMSC) are obtained as previously described from 16-d-old embryonic chicks *(23)* or 2–4-wk-old bovine calves *(24)*. BMSC are selected from the mixed cell population based on their ability to adhere to the dish, and passaged in monolayers (twice, to undergo 10–20 doublings).

3. Primary cardiac myocytes are obtained as previously described by enzymatic digestion of heart ventricles harvested from 1–2-d-old neonatal rats *(15,16)* or 14–15-d-old embryonic chicks *(15)*. Cell yields range from $5 - 7 \times 10^6$ cells/ventricle *(15–17)*. The fraction of cardiac myocytes in the cell preparation can be increased by preplating, which allows preferential attachment of fibroblasts *(16–17)*. After two 1-h periods, the cells that remain unattached are used to seed polymer scaffolds.

4. The C2C12 mouse muscle myoblast cell line is obtained from the American Type Culture Collection (ATCC) (Manassas, VA). The cells are expanded in T175 flasks (Costar, Cambridge, MA) until 80% confluent, rinsed 3× with 25 mL phosphate-buffered saline (PBS, Gibco-BRL, Grand Island, NY), trypsinized for 5 min at 37°C with 10 mL trypsin-ethylenediaminetetraacetic acid (EDTA) solution (1X Trypsin-EDTA, Gibco-BRL) and resuspended in 25 mL of medium, according to the procedures recommended by ATCC.

2.2. Culture Media

1. Chondrocytes are cultured in Dulbecco's Modified Eagle's medium (DMEM) containing 4.5 g/L glucose and 4 m*M* glutamine supplemented with 10% fetal bovine serum (FBS), 10 m*M* N-2-hydroxyethylpiperazine N'-2-ethane sulfonic acid (HEPES), 0.1 m*M* nonessential amino acids (NEAA), 0.4 m*M* proline and 50 mg/L ascorbic acid, 100 U/mL penicillin, 100 mg/L streptomycin, and 0.5 µg/mL fungizone *(25)*. The medium is prepared by adding the following solutions to 500 mL DMEM with 4.5 g/L glucose and 4 m*M* glutamine, and stored at 4°C:
   a. 50 cc of FBS.
   b. 2 mL of filter-sterilized (0.22-µm pore size) 0.1 *M* proline stock (proline stock = 0.575 g of L-proline dissolved in 50 cc DMEM and stored at –20°C.
   c. 2.5 mL of filter-sterilized (0.22-µm pore size) 10 mg/cc ascorbic acid stock (ascorbic acid stock = 0.5 g L-ascorbic acid dissolved in 50 cc DMEM and stored at –20°C).
   d. 5 mL of 1 *M* HEPES stock.
   e. 5 mL of 10 m*M* MEM NEAA.
   f. 5 mL of 100X penicillin/streptomycin (optional).
   g. 1 mL of 1000X fungizone (optional).
2. Neonatal rat cardiac myocytes are cultured in DMEM containing 1 g/L glucose, 110 mg/L pyruvate, 4 m*M* glutamine, and 25 m*M* HEPES and supplemented with 100 U/mL penicillin (optional) and 0.5 µg/mL fungizone (optional) *(15,16)*. The

medium can be further supplemented with 10% FBS or 2% adult horse serum (Hyclone) *(17)*. Embryonic chick cardiac myocytes are cultured in M199 supplemented with 6% FBS *(26)*.

2.3. Scaffolds

General requirements for tissue-engineering scaffolds include: reproducible processing into well-defined 3D structures designed to enhance cell attachment and tissue development, high porosity and large pores to provide unrestricted and spatially uniform cell distribution, chemical properties that allow surface modifications in order to further promote cell attachment and differentiation, and biodegradation at a controlled rate, in order to provide long-term biocompatibility in vivo. A variety of fibrous and porous scaffolds made of synthetic or natural polymers are currently used for tissue engineering *(27)*.

One representative fibrous scaffold is commercially produced at Albany International (Mansfield, MA) through extruding of polyglycolic acid (PGA) into 13-μm-diameter fibers and processing these into a nonwoven mesh with a void volume of 96–97% *(28)*. For cartilage and cardiac tissue engineering, the mesh is punched into 5–10 mm-diameter × 1–5-mm-thick disks. Other shapes are used for other applications (e.g., tubular scaffolds made of 1 mm thick mesh to engineer small-caliber arteries *(29)*. In culture, fibrous PGA loses its mechanical integrity over a period of 12 d *(3)* and degrades to approx 50% of the initial mass over a period of 4 wk *(28)*. PGA mesh can be surface-hydrolyzed to increase hydrophilicity *(30)*, and then coated with laminin to further enhance cell attachment *(17)*.

One representative porous scaffold is the Ultrafoam™ (Davol, Inc., Cranston, RI), a clinically used hemostatic sponge made of a water-insoluble hydrochloric acid salt of purified bovine corium collagen, in the form of 3-mm-thick sheets. For tissue-engineering studies, this sheet is punched into 13-mm-diameter disks; after hydration in culture medium, disks reduce their diameters to approx 10 mm. For rapid cell inoculation, Ultrafoam™ is used in conjunction with Matrigel® (Becton-Dickinson, Bedford, MA), a basement membrane preparation that is liquid at low temperatures (2–8°C) and gels at 22–35°C.

Prior to cell seeding, scaffolds must be thoroughly pre-wetted with culture medium so that all air is displaced. Methods in use include the application of pressure (by a small forceps) or vacuum (by a pipet) on scaffolds immersed in culture medium. Synthetic scaffolds can be first exposed to 70% ethanol to increase wettability *(20)*. In all cases, scaffolds are incubated in culture medium for 2–24 h prior to cell seeding. Incubation in medium that contains serum can further enhance cell attachment.
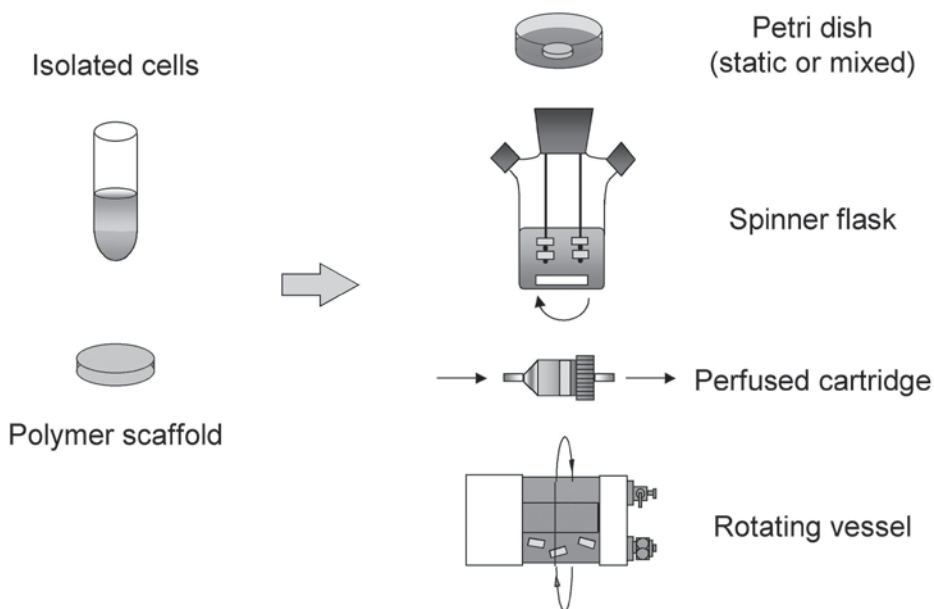
Fig. 1. Seeding vessels. Isolated cells are seeded on polymer scaffolds using static and mixed Petri dishes, spinner flasks, perfused cartridges, and rotating vessel. (Reproduced from ref. *30a*).

2.4. Seeding Vessels

Culture vessels used to seed the cells onto 3D scaffolds include Petri dishes, spinner flasks, rotating bioreactors, and perfused cartridges (**Fig. 1**).

1. Petri dishes are 6-well or 96-well plates (Costar, Cambridge, MA), and contain one scaffold per well seeded with 0.06 mL (96-well plate) to 6 mL cell suspension (6-well plate). Dishes are used either statically *(20)*, on an orbital shaker mixed at 50–75 rpm (Bellco, Vineland, NJ) *(31)*, or on an XYZ gyrator mixed at 60 rpm (Boeker Scientific) *(15)*
2. Spinner flasks (100-mL vol, Bellco) are 6.5 cm in diameter × 12 cm high, filled with 120 mL medium, fitted with a stopper, and mixed at 50–75 rpm using a non-suspended 0.8 cm diameter × 4-cm-long stir bar. Gas exchange is via surface aeration through the side-arms *(2,32)*.
3. Rotating vessels. The Slow Turning lateral Vessel (STLV) and the High Aspect Ratio Vessel (HARV) were developed at NASA and can be obtained from Synthecon (Houston, TX). The STLV is configured as two concentric cylinders that have diameters of 5.75 cm and 2 cm. The annular space, approx 110 mL in

vol, is used for tissue culture, and the inner cylinder serves as a membrane gas exchanger. The HARV is configured as a cylinder 1.3 cm high × 10 cm in diameter, approx 110 mL in vol, with one base serving as a membrane gas exchanger. Both vessels are primed with medium to displace all air, and are mounted on a base that simultaneously rotates the vessel around its central axis at the desired rate (10–45 rpm) and pumps filter-sterilized incubator air over the gas exchange membrane at a rate of about 1 L/min *(2,33)*.

4. Perfused cartridges are small, 10 mm in diameter × 42 mm long, 1.5 mL vol polycarbonate vessels made at the Advanced Tissue Sciences (La Jolla, CA) to culture one scaffold apiece *(2,17a,34)*. For cell seeding, each cartridge is fitted with two stainless-steel screens (with 85% void area) supporting the scaffold during perfusion, each with a silicone gasket (1 mm thick, 10 mm outer diameter [OD], 5 mm inner diameter [ID]) preventing the bypass of medium around the scaffold (**Fig. 2**). Each cartridge is filled with medium to displace all air and connected to a recirculation loop containing two gas exchangers (each configured as a coil of silicone tubing, 80 cm long, 1.6 mm ID, 3.2 mm OD, platinum cured Silicone, Cole Parmer, Vernon Hills, IL), one on each side of the cartridge. Syringes (10 mL, Becton-Dickinson) with three-way stopcocks (Baxter Healthcare, Irvin, CA) are used as medium reservoirs, and for medium sampling and removal of gas bubbles. Medium is recirculated by a Push/Pull syringe pump (PHD 2000, Harvard Apparatus, Holliston, MA), which can operate two loops at a time (**Fig. 2**)

3. Methods

3.1. Cell Seeding of Polymer Scaffolds

After cell inoculation in a laminar hood, cell seeding is done in a humidified, 37°C incubator containing 5–10% CO_2 in air. The duration of seeding ranges from 1 h to 3 d, depending on the cells, scaffold, seeding vessel, and the specific method used. We and others have studied a number of seeding methods for different cell types (chondrocytes, BMSC, cardiac myocytes, C2C12 cell line), initial concentrations (5–50 10^6 cells per cm^3 of scaffold vol), and scaffolds (fibrous and porous; 5–10 mm in diameter × 1–5 mm thick). Thin (<2 mm) scaffolds can be seeded statically; spatially uniform cell seeding of thicker (≥2 mm) scaffolds requires mixing *(31)*. A variety of mechanisms have been utilized to provide mixing and flow of culture medium, in order to suspend the isolated cells and to generate convective motion of the cells into the scaffold interior. Here, we provide an overview of the well-characterized seeding methods for tissue-engineering scaffolds.

3.2. Seeding in Static Dishes

PGA meshes can be seeded statically using small volumes of highly concentrated cell suspension and agarose-coated Petri dishes (*see* **Subheading 3.3., steps 1–3**) *(20)*. Dry PGA meshes (10 mm in diameter × 1.2 mm thick) are
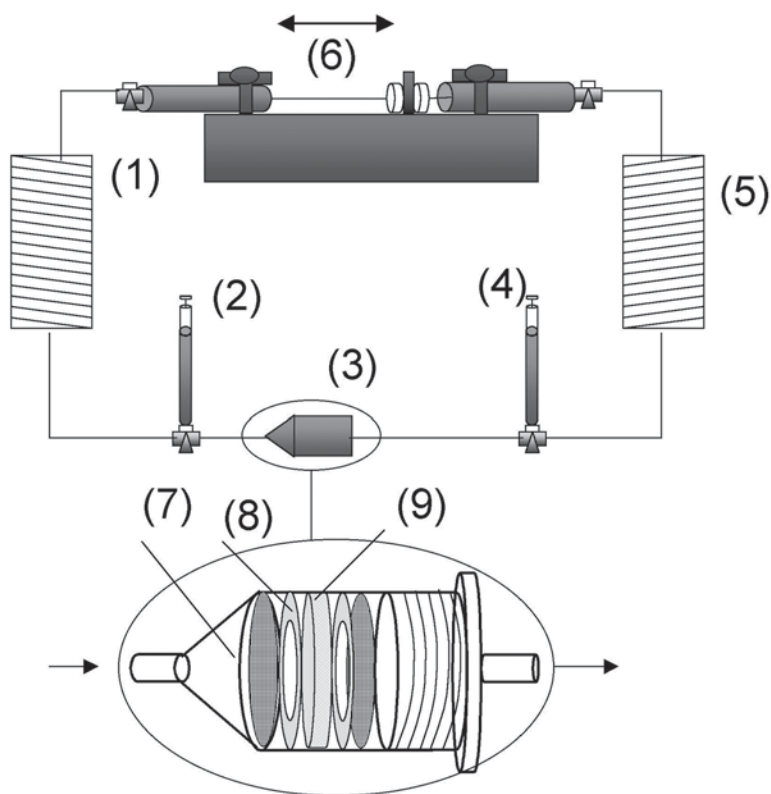
Fig. 2. Experimental setup for scaffold seeding in perfused cartridges. **(1,5)** gas exchangers; **(2,4)** debubbling syringes; **(3)** perfusion cartridge; **(6)** Push/Pull Syringe Pump; **(7)** stainless-steel screen; **(8)** silicone gasket; **(9)** scaffold. (Adapted from ref. *17a*.)

seeded with chondrocytes (0.1 mL of 4×10^7 cells/mL) by repeatedly applying pressure to the mesh with a curved pair of forceps. The dish is cultured statically in a humidified, 37°C/5% CO_2 incubator, with two additions of medium: 1.5 mL after 6 h, and 2.5 mL after 24 h (*see* **Notes 3–5**).

3.3. Seeding in Mixed Dishes

One method for seeding thick (2–5 mm) PGA meshes is to use Petri dishes under mixed conditions *(31,32)*. PGA scaffolds are pre-wetted for 24 h and inoculated with chondrocytes in agarose-coated 6-well (35-mm diameter) Petri dishes, as follows:

1. Heat a sterile solution of 1% (w/v) agarose in water until it melts.
2. Use a sterile 5-mL pipet to transfer 1 mL agarose into each well. Only a thin film should form; remove any excess agarose.

3. Leave dishes in laminar hood for ≥2 h to allow agarose to dry.
4. To each well, add medium (e.g., 4 mL) and one pre-wet polymer (e.g., 10-mm diameter × 5-mm thick disk).
5. To each well, add freshly isolated cells (e.g., 2 mL with $3.5 × 10^6$ cells/mL).
6. Transfer dishes onto an orbital shaker in a 37°C/5% CO_2 incubator. Set shaking speed to 50–75 rpm.
7. After 3 d, transfer seeded scaffolds either into new dishes (not agarose-coated), containing 6 mL medium per well, or into another culture vessel.

To seed cardiac myocytes in mixed dishes, PGA scaffolds (5 mm in diameter × 2 mm thick) were pre-wetted with culture medium for 24 h, and inoculated for 2 h with 1 mL cell suspension containing $8 × 10^6$ cells. One scaffold per well was placed into 6-well (35-mm) dishes mounted on an XYZ gyrator operated at 24 rpm *(15)*. Alternatively, PGA scaffolds can be seeded with a concentrated suspension of cardiac myocytes (0.06 mL of $1.33 × 10^8$ cells/mL) over shorter period of time (1 h) using 96-well (5-mm diameter) dishes mounted on an XYZ gyrator operated at 60 rpm *(17)*.

3.4. Seeding in Rotating Vessels

Rotating vessels (STLVs and HARVs) can be used to seed PGA meshes with articular chondrocytes *(33,35)* and cardiac myocytes *(15,35)*. Scaffolds are pre-wetted as described previously, and transferred into a primed vessel. The vessel rotation speed is adjusted so that each scaffold is maintained freely suspended at a steady position within the vessel. The vessels are inoculated with cells (e.g., $5 – 8 × 10^6$ cells per 5-mm-diameter × 2-mm-thick PGA scaffold). In both cases, vessel rotation maintains a uniform cell suspension and provides a relative velocity between the cells and the scaffolds. The specific steps of the seeding procedure are as follows:

1. Disassemble rotating vessels and clean using distilled water and 70% ethanol (soak in ethanol overnight; rinse thoroughly under running distilled water for 20 min; soak overnight in distilled water; allow to dry in laminar hood). Assemble loosely.
2. Autoclave-sterilize (dry cycle, 30 min of sterilization at 121°C followed by a 30-min drying cycle). Tighten central screws, and allow to cool.
3. Attach disposable sterile stopcocks to needle ports, and bolt on sample port. Attach 10-mL syringes to stopcocks.
4. Add 110 mL medium and pre-wet polymer scaffolds (e.g., $n = 12$ disks, 5 mm in diameter × 2 mm thick) through the 10-mm sample port. Close the sample port.
5. Displace all remaining air using attached syringes (fill one syringe with medium, and push medium into the other syringe while turning the vessel until all bubbles are displaced into the syringes).
6. Attach the vessel to a custom-designed base, in humidified 37°C/5% CO_2 incubator. Set the rotation rate to maintain scaffolds settling at a steady position within the vessel (~15–20 rpm). Leave in incubator ≥12 h.

7. Open sampling port and remove 15 mL medium using a pipet. Add freshly isolated cells (e.g., 12 mL of 5×10^6 cells/mL for $n = 12$ scaffolds).
8. Displace all air with medium, using attached syringes.
9. Transfer the vessel onto the rotating base in a 37°C/5% CO_2 incubator.
10. After 3 d, completely replace medium and continue to culture or transfer into a different culture vessel.

A combination of Petri dishes and rotating vessels can also be utilized to seed cardiac myocytes onto fibrous PGA *(17)*. The cell suspension (8×10^6 cells in 0.06 mL vol) is pipeted onto laminin-coated, surface-hydrolyzed PGA scaffolds (5 mm in diameter × 2 mm thick) in 96-well (5 mm diameter) dishes and placed onto an XYZ gyrator operated at 60 rpm for 1 h. Seeded scaffolds and the unseeded cells are then transferred for 1 additional hr into a HARV rotated at 12 rpm.

3.5. Seeding in Spinner Flasks

Seeding in spinner flasks is the preferred system for seeding chondrocytes on PGA scaffolds. This is a well-characterized method that results in a relatively uniform spatial distribution of attached cells within a period of 24 h at a yield of essentially 100% *(3)*. The main steps of scaffold seeding in spinner flasks are as follows:

1. Autoclave-sterilize a spinner flask, containing a 4-cm-long magnetic stir bar and a 5-cm-diameter silicone stopper into which four, 4-inch-long, 22-gauge needles have been symmetrically placed (*see* **Fig. 1**).
2. Autoclave-sterilize the flask such that the needles extend into the flask and side-arm caps are open.
3. Wearing sterile gloves, thread pre-wetted polymer scaffolds (e.g., 10-mm-diameter × 5-mm-thick disks) onto the needles so that each needle contains $n = 2$ disks (if 5-mm-diameter × 2-mm-thick disks are seeded, $n = 3$ disks are threaded onto each needle).
4. Position disks using 3-mm-long segments of #13 silicone tubing.
5. Place the stopper in the mouth of the flask.
6. Add 120 mL medium, loosen the side-arm caps, and transfer onto a magnetic stirrer in a humidified 37°C/5% CO_2 incubator. Set stirring rate to 50–75 rpm. Leave overnight.
7. When a suspension of freshly isolated cells is prepared, remove 16 cc medium from the flask through the side arm, using a pipet. Flame the side arm after removing the cap.
8. Add cells (e.g., 16 cc of 4×10^6 cells/mL). Flame the side arm and replace the cap (leave loosely capped to allow gas exchange).
9. Transfer flask onto the magnetic stirrer in a 37°C/5% CO_2 incubator.
10. After 1–3 d, completely replace medium. Continue to culture cell-polymer constructs in flasks, or transfer into a different culture vessel.

Dynamic seeding in flasks has been extensively used to seed PGA scaffolds with primary and passaged chondrocytes *(*e.g., *3,11,12,14,22,36)* and embry-

onic chick and bovine BMSCs *(*e.g., *21,23)*. PGA scaffolds are seeded with cardiac myocytes by either inoculating flasks by cell suspension as described previously *(15)*, or by using a concentrated cell suspension *(17)*. In the latter case, 8×10^6 cells in 0.06 mL volume are pipeted onto surface-hydrolyzed PGA scaffolds fixed to needles in spinner flasks and mixed on an XYZ gyrator at 60 rpm for 1 h. The flasks are then filled with 100 mL of medium and stirred at 50 rpm for 1 additional h *(17)*. Spinner flasks are also used to seed porous scaffolds made of poly-lactic-co-glycolyc acid (PLGA) and polyethylene glycol (PEG) with bovine BMSC *(24)* and periosteal cells *(14)*. Seeding yield (percentage of total cells that attached to scaffolds) is essentially 100% for chondrocytes and PGA scaffolds *(3)*, approx 60% for cardiac myocytes on PGA scaffolds *(15)*, and 30–60% for periosteal cells and PLGA-PEG scaffolds *(14)*.

In spinner flasks, mixing during cell seeding maintains the isolated cells in suspension and provides relative velocity between the cells and the scaffolds. The probable mechanism by which cells populate the scaffold interior is convective motion of suspended cells into the scaffold, followed by inertial impacts between the cells and the fibers and cell attachment *(3)*.

The higher cellularities and more uniform cell distributions in 3-d constructs seeded in flasks as compared to dishes could be attributed to differences in flow patterns between the two systems (e.g., turbulent mixing vs orbital fluid motion) *(3)*.

3.6. Gel-Cell Seeding of Porous Scaffolds

Rapid inoculation of metabolically active cells at high initial densities can be achieved using gels as cell-delivery vehicles *(17a)*. Collagen gel can be used to seed mesenchymal stem cells onto biodegradable sutures *(37)*. Fibrin gel can be used for rapid inoculation of PGA scaffolds with bovine articulate chondrocytes *(38)*. We used Matrigel® to inoculate Ultrafoam™ scaffolds (10 mm in diameter × 3 mm thickness) with C2C12 cells or cardiac myocytes at the approximate density of 70×10^6 cells/cm^3 according to the procedure described in **steps 1–6** *(17a)*.

1. Thaw Matrigel® overnight in a 4°C refrigerator (*see* **Note 6**).
2. Pre-wet the scaffolds with culture medium and place into a 37°C/5%CO$_2$ incubator for ≥2 h before inoculation.
3. Blot-dry the scaffolds using sterile Kimwipes, and transfer them to empty Petri dishes (4–5 scaffolds/dish).
4. Centrifuge the cell suspension at 1000 rpm for 10 min in a 15-mL conical tube. Place the tube on ice in the laminar hood and aspirate off the supernatant.
5. Using an automatic pipet, resuspend a cell pellet in Matrigel®. It is advisable to use 5–10 µL of Matrigel® per 10^6 cells.
6. Load the homogeneous cell suspension to a scaffold as uniformly as possible. Place the Petri dish with inoculated scaffolds for 10 min in the 37°C/5%CO$_2$ humidified incubator to allow gelation to occur.

To allow for cell attachment to polymeric support, inoculated scaffolds are further seeded in orbitally mixed dishes or perfused cartridges, as follows.

For seeding in mixed dishes, six-well (35-mm diameter) plates containing gel-cell inoculated scaffolds (one per well in 8 mL of medium) are placed on a 25 rpm orbital shaker in a 37°C/5%CO$_2$ humidified incubator for 1.5–4.5 h, and then transferred into a culture system.

3.7. Perfusion Seeding

To avoid diffusional limitations of mass transfer during scaffold seeding, the scaffolds can be directly perfused with culture medium so that the transport of oxygen from the medium to the cells occurs through both diffusion and convection. For seeding in perfusion, the system shown in **Fig. 2** is used with one scaffold per cartridge (*see* **Note 7**) in an alternating flow regimen according to the following procedure *(17a)*:

1. Autoclave silicone tubing, screens, gaskets, and cartridges (20/20 min dry cycle, 121°C).
2. Assemble the seeding loops according to the scheme in **Fig. 2** using the sterile technique in a laminar flow hood.
3. Using one reservoir syringe, prime one loop with total of 8 mL of culture medium (5.5 mL in perfusion cartridge and tubing; 2.5 mL in one reservoir syringe; the other reservoir syringe is empty). Place the primed loop in the 37°C/5%CO$_2$ incubator for a minimum of 2 h prior to seeding.
4. In the laminar hood, carefully open a perfusion cartridge and using forceps, place the gel-cell inoculated scaffold between two silicone gaskets and stainless-steel screens.
5. Close the perfusion cartridge and remove any air bubbles by injecting culture medium from syringe 2 into the syringe 4 (**Fig. 2**) while holding the cartridge in a vertical position so that bubbles can escape upwards (*see* **Note 8**).
6. Place the seeding loop onto the Push/Pull pump in the 37°C/5%CO$_2$ incubator. Program the pump to perfuse the medium at a desired flow rate (0.5–1.5 mL/min) with flow direction reversal after every 2.5 mL for a period of 1.5–4.5 h.

Perfusion of gel-cell inoculated scaffolds helps maintain viability, metabolic activity, and uniform cell distribution at high initial densities *(17a)*. It is also possible to seed cells directly from suspension (omitting the gel-inoculation step) to a PGA scaffolds in a perfusion loop *(39)*. The procedure yields constructs with a relatively uniform distribution of metabolically active cells, but the cell density and seeding yield are significantly lower than in gel-cell inoculated scaffolds.

4. Notes

1. Cell seeding of polymer scaffolds is the first step in the cultivation of engineered tissues in bioreactors. High initial cell concentration and uniform distribution of the attached cells largely enhance the in vitro development of functional

engineered tissues. In general, it is difficult to compensate for deficiencies in cell seeding during subsequent tissue cultivation. For example, 10-mm-diameter × 5-mm-thick PGA scaffolds seeded with chondrocytes at low initial density (2×10^6 cells per scaffold) lost their mechanical integrity after 12 d of culture. In contrast, the same scaffolds seeded at a higher initial cell density (using $4 - 10 \times 10^6$ cells per scaffold) progressively developed cartilaginous tissue matrix *(3)*.

2. The conditions and duration of cell seeding should be carefully selected, to maximize the kinetic rate, yield, and spatial uniformity of cell attachment. Cell seeding should be evaluated by determining the amount of DNA, cell distribution, and viability on seeded scaffolds, as previously described *(3)*.

3. Static seeding can yield satisfactory results for thin scaffolds (e.g., <2-mm-thick PGA mesh). Flipping the scaffold at timed intervals (e.g., every hour) during static seeding can enhance the uniformity of cell distribution.

4. The static seeding technique has been modified to seed tubular scaffolds made of 1-mm-thick PGA mesh, used to engineer small-caliber arteries. Scaffolds are surface-hydrolyzed, loaded with 1–2 mL suspension (5×10^6 cells/mL) of smooth-muscle cells (SMCs), slowly rotated for 30 min to provide uniform exposure to the cell suspension, and then transferred into bioreactors and exposed to flow *(29)*.

5. PGA scaffolds (13 mm diameter × 3 mm thick, 96% void volume) were pre-wetted in culture medium and seeded statically in 24-well dishes, using 0.38 mL medium with 2.7×10^6 cells in 0.38 mL.

6. For gel inoculation, Matrigel® thawing is best done overnight, at 2–8°C. To ensure homogeneity of cell suspension and avoid premature gelation, all work with Matrigel® must be done using precooled pipet tips (tips are kept at –20°C and transferred to ice 1 h before use, in laminar hood).

7. Perfused cartridges are best primed with one screen and one gasket inside the cartridge. This reduces the amount of medium that will be displaced when the gel-cell inoculated scaffold is placed into the cartridge.

8. If the gel-cell-seeded scaffold offers significant resistance during debubbling, delivering the culture medium in pulsatile mode will help. During this step, care must be taken to avoid displacing cell aggregates from the scaffold.

Acknowledgment

References

1. Langer, R. and Vacanti, J. P. (1993) Tissue engineering. *Science* **260,** 920–926.
2. Freed, L. E. and Vunjak-Novakovic, G. (2000) Tissue engineering bioreactors, in *Principles of Tissue Engineering* (Lanza, R. P., Langer, R., and Vacanti, J., eds.), Academic Press, San Diego, CA, pp. 143–156.

3. Vunjak-Novakovic, G., Obradovic, B., Bursac, P., Martin, I., Langer, R., and Freed, L. E. (1998) Dynamic seeding of polymer scaffolds for cartilage tissue engineering. *Biotechnol. Prog.* **14,** 193–202.

4. Obradovic, B., Carrier, R. L., Vunjak-Novakovic, G., and Freed, L. E. (1999) Gas exchange is essential for bioreactor cultivation of tissue engineered cartilage. *Biotechnol. Bioeng.* **63,** 197–205.

5. Buckwalter, J. A. and Mankin, H. J. (1997) Articular cartilage 1. Tissue design and chondrocyte-matrix interactions. *J. Bone Jt. Surg.* **79A,** 600–611.

6. MacKenna, D. A., Omens, J. H., McCulloch, A. D., and Covell, J. W. (1994) Contribution of collagen matrix to passive left ventricular mechanics in isolated rat heart. *Am. J. Physiol.* **266,** H1007–H1018.

7. Brilla, C. G., Maisch, B., Rupp, H., Sunck, R., Zhou, G., and Weber, K. T. (1995) Pharmacological modulation of cardiac fibroblast function. *Herz* **20,** 127–135.

8. Silverman, H. S., Wei, S., Haigney, M. C., Ocampo, C. J., and Stern, M. D. (1997) Myocote adaptation to chronic hypoxia and development of tolerance to subsequent acute severe hypoxin. *Circ. Res.* **80,** 699–707.

9. Schoen, F. J. (1999) The heart, in *Robbins Pathologic Basis of Disease* (Cotran, R. S., Kumar, V., Collins, T., and Robbins, S. L., eds.), W.B. Saunders, Philadelphia, pp. 543–599.

10. Freed, L. E. and Vunjak-Novakovic, G. (2000) Tissue engineering of cartilage, in *The Biomedical Engineering Handbook* (Bronzino, J. D., ed.), Vol. II, CRC Press, Boca Raton, FL, pp. 124–121 - 124–126.

11. Vunjak-Novakovic, G., Martin, I., Obradovic, B., Treppo, S., Grodzinsky, A. J., Langer, R., et al. (1999) Bioreactor cultivation conditions modulate the composition and mechanical properties of tissue engineered cartilage. *J. Orthop. Res.* **17,** 130–138.

12. Obradovic, B., Martin, I., Padera, R. F., Treppo, S., Freed, L. E., and Vunjak-Novakovic, G. (2001) Integration of engineered cartilage. *J. Orthop. Res.* **19(6),** 1089–1097.

13. Freed, L. E., Grande, D. A., Lingbin, Z., Emmanual, J., Marquis, J. C., and Langer, R. (1994) Joint resurfacing using allograft chondrocytes and synthetic biodegradable polymer scaffolds. *J. Biomed. Mater. Res.* **28,** 891–899.

14. Schaefer, D., Martin, I., Jundt, G., et al. (2002) Tissue engineered composites for the repair of large osteochondral defects. *Arthritis Rheum.* **46,** 2524–2534.

15. Carrier, R. L., Papadaki, M., Rupnick, M., Schoen, F. J., Bursac, N., Langer, R., et al. (1999) Cardiac tissue engineering: cell seeding, cultivation parameters and tissue construct characterization. *Biotechnol. Bioeng.* **64,** 580–589.

16. Bursac, N., Papadaki, M., Cohen, R. J., Schoen, F. J., Eisenberg, S. R., Carrier, R., et al. (1999) Cardiac muscle tissue engineering: toward an in vitro model for electrophysiological studies. *Am. J. Physiol.* **277,** H433–H444.

17. Papadaki, M., Bursac, N., Langer, R., Merok, J., Vunjak-Novakovic, G., and Freed, L. E. (2001) Tissue engineering of functional cardiac muscle: molecular, structural and electrophysiological studies. *Am. J. Physiol. Heart Circ. Physiol.* **280,** H168–H178.

17a. Radisic, M., Euloth, M., Yang, L., Langer, R., Freed, L. E., Vunjak-Novakovic, G. (2003) High density seeding of myocyte cells for tissue engineering. *Biotechnol. Bioeng.* **62,** 403–414.

18. Leor, J., Aboulafia-Etzion, S., Dar, A., Shapiro, L., Barbash, I. M., Battler, A., et al. (2000) Bioengineerred cardiac grafts: a new approach to repair the infarcted myocardium? *Circulation* **102,** III56–III61.

19. Li, R. K., Jia, Z. Q., Weisel, R. D., Mickle, D. A. G., Choi, A., and Yau, T. M. (1999) Survival and function of bioengineered cardiac grafts. *Circulation* **100,** II63–II69.

20. Freed, L. E., Marquis, J. C., Nohria, A., Emmanual, J., Mikos, A. G., and Langer, R. (1993) Neocartilage formation in vitro and in vivo using cells cultured on synthetic biodegradable polymers. *J. Biomed. Mater. Res.* **27,** 11–23.

21. Martin, I., Vunjak-Novakovic, G., Yang, J., Langer, R., and Freed, L. E. (1999) Mammalian chondrocytes expanded in the presence of fibroblast growth factor-2 maintain the ability to differentiate and regenerate three-dimensional cartilaginous tissue. *Exp. Cell Res.* **253,** 681–688.

22. Madry, H. and Trippel, S. B. (2000) Efficient lipid-mediated gene transfer to articular chondrocytes. *Gene Ther.* **7,** 286–291.

23. Martin, I., Padera, R. F., Vunjak-Novakovic, G., and Freed, L. E. (1998) In vitro differentiation of chick embryo bone marrow stromal cells into cartilaginous and bone-like tissues. *J. Orthop. Res.* **16,** 181–189.

24. Martin, I., Shastri, V. P., Padera, R. F., Yang, J., Mackay, A. J., Langer, R., et al. (2001) Selective differentiation of mammalian bone marrow stromal cells cultured on three-dimensional polymer foams. *J. Biomed. Mater. Res.* **55,** 229–235.

25. Sah, R. L. Y., Kim, Y. J., Doong, J. Y. H., Grodzinsky, A. J., Plaas, A. H. K., and Sandy, J. D. (1989) Biosynthetic response of cartilage explants to dynamic compression. *J. Orthop. Res.* **7,** 619–636.

26. Barnett, J. V., Taniuchi, M., Yang, M. B., and Galper, J. B. (1993) Co-culture of embryonic chick heart cells and ciliary ganglia induces parasympathetic responsiveness in embryonic chick heart cells. *Biochem. J.* **292,** 395–399.

27. Freed, L. E. and Vunjak-Novakovic, G. (2001) Cell-polymer-bioreactor systems, in *Methods of Tissue Engineering* (Atala, A. and Lanza, R. P., eds.), Academic Press, San Diego, CA, pp. 97–111.

28. Freed, L. E., Vunjak-Novakovic, G., Biron, R., Eagles, D., Lesnoy, D., Barlow, S., et al. (1994) Biodegradable polymer scaffolds for tissue engineering. *Bio/ Technology* **12,** 689–693.

29. Niklason, L. E., Gao, J., Abbott, W. M., Hirschi, K. K., Houser, S., Marini, R., et al. (1999) Functional arteries grown in vitro. *Science* **284,** 489–493.

30. Gao, J., Niklason, L., and Langer, R. (1998) Surface hydrolysis of poly(glycolic acid) meshes increases the seeding density of vascular smooth muscle cells. *J. Biomed. Mater. Res.* **42,** 417–424.

30a. Freed, L. E., Vunjak-Novakovic, G. (1998) Culture of Organized Cell Communities. *Adv. Drug Deliv. Rev.* **33,** 15–30.

31. Freed, L. E., Marquis, J. C., Vunjak-Novakovic, G., Emmanual, J., and Langer, R. (1994) Composition of cell-polymer cartilage implants. *Biotechnol. Bioeng.* **43,** 605–614.

32. Vunjak-Novakovic, G., Freed, L. E., Biron, R. J., and Langer, R. (1996) Effects of mixing on the composition and morphology of tissue-engineered cartilage. *AIChE J.* **42,** 850–860.

33. Freed, L. E. and Vunjak-Novakovic, G. (1995) Cultivation of cell-polymer constructs in simulated microgravity. *Biotechnol. Bioeng.* **46,** 306–313.

34. Dunkelman, N. S., Zimber, M. P., Lebaron, R. G., Pavelec, R., Kwan, M., and Purchio, A. F. (1995) Cartilage production by rabbit articular chondrocytes on polyglycolic acid scaffolds in a closed bioreactor system. *Biotechnol. Bioeng.* **46,** 299–305.

35. Freed, L. E. and Vunjak-Novakovic, G. (1997) Microgravity tissue engineering. *In Vitro Cell. Dev. B.* **33,** 381–385.

36. Gooch, K. J., Kwon, J. H., Blunk, T., Langer, R., Freed, L. E., and Vunjak-Novakovic, G. (2001) Effects of mixing intensity on tissue-engineered cartilage. *Biotechnol. Bioeng.* **72,** 402–407.

36a. Schaefer, D., Martin, I., Shastri, P., et al. (2000) In vitro generation of osteo-chondral composites. *Biomaterials* **21,** 2599–2606.

37. Awad, H. A., Butler, D. L., Harris, M. T., Ibrahim, R. E., Wu, Y., Young, R. G., et al. (2000) In vitro characterization of mesenchymal stem cell-seeded collagen scaffolds for tendon repair: effects of initial seeding density on contraction kinetics. *J. Biomed. Mater. Res.* **51,** 233–240.

38. Ameer, G. A., Mahmood, T. A., and Langer, R. (2002) A biodegradable composite scaffold for cell transplantation. *J. Orthop. Res.* **20,** 16–19.

39. Kim, S. S., Sundback, C. A., Kaihara, S., Benvenuto, M. S., Kim, B. S., Mooney, D. J., et al. (2000) Dynamic seeding and in vitro culture of hepatocytes in a flow perfusion system. *Tissue Eng.* **6,** 39–44.

Chondrocyte Isolation, Expansion, and Culture on Polymer Scaffolds

Aileen Crawford and Sally C. Dickinson

1. Introduction

The chondrocyte is responsible for maintaining the integrity of the complex extracellular matrix (ECM) of articular cartilage. Therefore, chondrocytes directly control the biomechanical properties of the tissue that enable articular cartilage to bear cyclical compressive loading *(1)*. The ultimate goal of articular cartilage engineering is to produce a cartilage construct with identical structure and properties to native tissue. Although this goal has not yet been achieved, many advances have been made in understanding the biology of the extracellular cartilage matrix *(1–5)*.

The following protocols describe simple methods for the isolation of chondrocytes from bovine nasal and articular cartilage, the expansion of cell numbers in monolayer culture, the subsequent seeding of the cells onto biodegradable polymer scaffolds, and finally, culture of the resulting chondrocyte/ scaffold constructs. A well-documented problem with the use of chondrocytes is that the differentiated phenotype of hyaline chondrocytes is lost during expansion in monolayer culture, as indicated by the decreasing expression of both type II collagen and large aggregating proteoglycans *(6,7)*. However, subsequent transfer of the cells to three-dimensional (3D) culture conditions—e.g., agarose or alginate gel systems *(8–10)*—initiates some re-expression of hyaline cartilage matrix components. In addition, the inclusion of basic fibroblast growth factor (bFGF, FGF-2) during the monolayer expansion of chondrocytes improves re-differentiation and chondrogenesis when the chondrocytes are returned to a 3D environment *(11)*.

The normal growth and differentiation of cartilage is controlled by various growth factors, and there is great interest in the use of growth factors in cartilage repair procedures *(12)*. Prominent among the major cartilage modulating growth factors are insulin-like growth factor-I (IGF-I) and transforming growth factor-β (TGF-β). IGF-I is synthesized by chondrocytes and interacts with the cells to prevent chondrocyte apoptosis *(13)*, to increase production of cartilage matrix components, including collagen, proteoglycans, and hyaluronan (HA) *(14–17)*, and to improve biomechanical properties of the tissue *(18)*. Insulin can also bind to the IGF-I receptor and can mimic many of the actions of IGF-I, including inducing proteoglycan synthesis *(15)*, although much higher concentrations are required. TGF-β is a potent factor in the proliferation and differentiation of mesenchymal cells into chondrocytes in vivo and in vitro *(19)*. The exact role of TGF-β in the regulation of cartilage matrix synthesis remains uncertain, as variable effects have been demonstrated. TGF-β is largely reported to stimulate proteoglycan synthesis and cell proliferation in monolayer cultures and 3D gel systems (e.g., *20,21*), and both stimulation *(22,23)* and inhibition *(24)* of proteoglycan synthesis in cartilage explants have been reported in vitro. Bone morphogenetic proteins (BMPs) are also members of the TGF-β superfamily. BMP 2 and BMP 7 (which is also known as osteogenic protein 1) promote the synthesis and retention of ECM of articular cartilage *(25–28)*.

The model system described in this chapter can be used to further investigate the role of growth factors in cartilage matrix synthesis. Examining possible synergistic/antagonistic interactions of chondrogenic growth factors may aid the formation of an engineered articular cartilage as similar as possible to the natural tissue.

2. Materials

2.1. Dissection of Bovine Nasal and Articular Cartilage

1. Tissue from calves or adult (24- to 30-mo-old) cows transported on ice from a local abattoir and used within a few hours of sacrifice. Obtain nasal septal cartilage with surrounding tissue and the lower leg, incorporating an intact metacarpophalangeal joint.
2. Large dissection tray and aluminum foil.
3. PM40 post-mortem handles and blades.
4. 70% (v/v) ethanol.
5. Sterile Petri dishes (100 mm diameter).
6. Sterile Ca^{2+}/Mg^{2+} -free phosphate-buffered saline (PBS): 0.14 M NaCl, 2.7 mM KCl, 1.5 mM KH_2PO_4, 8.1 mM Na_2HPO_4, pH 7.2 (Gibco-BRL®, Cat. No. 14200). Store at 4°C.
7. Penicillin G (10,000 U/mL) and streptomycin sulfate (10,000 μg/mL) antibiotic mixture (Gibco-BRL® Cat. No. 15140). Store at –20°C in 5-mL aliquots.

8. Class II laminar air hood.
9. Sterile scalpel blades and forceps.

2.2. Isolation of Chondrocytes

1. Class II laminar air hood.
2. Sterile 50-mL centrifuge tubes.
3. Bovine testicular hyaluronidase (E.C. 3.2.1.35, Sigma Cat. No. H3506). Store at –20°C and prepare solution fresh as required.
4. Bacterial collagenase (E.C. 3.4.24.3, Sigma Cat. No. C0130). Store at –20°C and prepare solution fresh as required.
5. 0.25% (w/v) trypsin [(E.C. 3.4.21.4) in 0.4 g/L KCl, 2.2 g/L NaHCO$_3$, 6.8 g/L NaCl, 1.0 g/L glucose, 0.005 g/L phenol red, Gibco-BRL®, Cat. No, 25050]. Store at –20°C in 20-mL aliquots.
6. PBS: *see* **Subheading 2.1.**
7. Sterile syringe-filters (cellulose acetate membrane; 0.2 µm).
8. Rotator.
9. Basic medium: Dulbecco's modified Eagle's medium (DMEM; high-glucose formula containing GLUTAMAX-1, Gibco-BRL®, Cat. No. 61965), containing 10 m*M* Hepes buffer pH 7.4 (Gibco-BRL®, Cat. No. 15630), 100 U/mL penicillin/100 µg/mL streptomycin (Gibco-BRL®, Cat. No. 15140) and 10% (v/v) FCS (heat-inactivated, Gibco-BRL®, Cat. No. 10108). Store at 4°C.
10. 21-gauge needles and 20-mL syringes
11. Hemocytometer.

2.3. Expansion of Chondrocyte Numbers

1. Basic fibroblast growth factor (bFGF [FGF-2], PreproTech Cat. No. 100-18B). Prepare a stock solution of 10 µg/mL in filter-sterilized 5 m*M* Tris-HCL, pH 7.6, containing 1 mg/mL bovine serum albumin (BSA). Store at –20°C in 50-µL aliquots.
2. Expansion medium: Add 1 µL/mL of stock 10 µg/mL bFGF to basic medium (*see* **Subheading 2.2.**) immediately prior to use. The final concentration of bFGF will be 10 ng/mL. Prepare the medium as required, and do not store.
3. Hemocytometer.
4. Tissue-culture dishes.
5. PBS: *see* **Subheading 2.1.**
6. Trypsin-EDTA: 0.05 g/L trypsin/0.2 g/L EDTA in Ca^{2+}/Mg^{2+}-free Hanks balanced salt solution (HBSS) (Gibco-BRL®, Cat. No. 25300).

2.4. Chondrocyte Culture on 3D Scaffolds

1. Sterile 100-mL spinner flask containing a magnetic follower and a single surgical steel wire (0.028 inch diameter) inserted 1 cm off-center into the silicon sealing bung, to leave an exposed wire length of 10 cm, of which the last 5–6 mm is bent slightly upwards.

2. Multi-place magnetic stirrer mounted within a temperature-controlled 37°C incubator with an atmosphere of 95% air/5% CO_2, 95% humidity.
3. Orbital shaker mounted within a temperature-controlled 37°C incubator with an atmosphere of 95% air/5% CO_2, 95% humidity.
4. Hemocytometer.
5. Sterile forceps.
6. PBS: *see* S**ubheading 2.1.**
7. Trypsin-EDTA: *see* S**ubheading 2.3.**
8. Expansion medium: *see* S**ubheading 2.3.**
9. Insulin (Sigma, Cat. No. I5500). Prepare a stock solution of 1 mg/mL insulin in 10 m*M* acetic acid. Filter-sterilize through a 0.2-µm sterile syringe-filter and store aliquoted at –20°C.
10. L-Ascorbic acid (Sigma, A 4544). When required, prepare a filter-sterilized solution of 50 mg/mL in basic medium (*see* S**ubheading 2.2.**). Do not store.
11. Differentiation medium: This is composed of basic medium (*see* S**ubheading 2.2.**) containing 1 µL/mL of the stock 1 mg/mL insulin and 1 µL/mL of the 50 mg/mL stock L-ascorbic acid solution. Prepare as required and do not store.
12. 1% (w/v) melted, sterile agarose solution (1 g agarose/100 mL distilled water).
13. 3D sterile, polymer-scaffold (e.g., nonwoven fibers of esterified hyaluronic acid, HYAFF® 11, Fidia Advanced Biopolymers, Albano Terme, Italy. PGA scaffolds available from Abany International, Bury, Lancashire, UK).

3. Methods (*see* Note 1)

3.1. Dissection of Bovine Cartilage

3.1.1. Nasal Cartilage

1. Dissect bovine nasal septum cartilage free from all surrounding tissue using a post-mortem knife (*see* **Note 2**). Place the isolated cartilage in a Petri dish containing sterile PBS and 10% (v/v) penicillin/streptomycin antibiotic mixture and transfer to a laminar air-flow hood. Leave the cartilage for approx 20 min before rinsing twice with sterile PBS.
2. Using a scalpel blade, cut the cartilage into slices of 2–3-mm thickness, into sterile PBS.
3. Cut each slice into small cubes (approx 40–50 mg wet wt) using a scalpel blade (*see* **Notes 2** and **3**).

3.1.2. Articular Cartilage

1. Wash the lower leg thoroughly with water, particularly around the metacarpophalangeal joint. Place aluminum foil around each end of the lower leg to expose only the required joint and spray with 70% (v/v) ethanol to reduce the risk of contamination.
2. Using a post-mortem knife, remove a large area of skin over the metacarpophalangeal joint, taking care to avoid piercing the joint capsule. Spray the surface of the joint capsule with 70% (v/v) ethanol and transfer the limb to a laminar air hood.

3. Take care to avoid damaging the articular cartilage surface. Open the joint using a sterile scalpel blade by slicing between the bones and cutting through the tendons and ligaments that hold the joint together.

4. Using a scalpel blade, dissect small, full-depth pieces of cartilage (*see* **Note 4**, approx 30–40 mg wet wt) from all articular surfaces and transfer to a Petri dish containing sterile PBS and 10% (v/v) penicillin/streptomycin antibiotic mixture. Leave for approx 20 min before rinsing the cartilage twice with sterile PBS.

3.2. Isolation of Chondrocytes

1. Divide the cartilage dissected from a single nasal septum into three or four 50-mL centrifuge tubes or place all of the articular cartilage from a single metacarpophalangeal joint into one 50-mL centrifuge tube.

2. For each tube, prepare 20 mL hyaluronidase solution by dissolving 1 mg/mL bovine testicular hyaluronidase in warm PBS. Filter-sterilize the solution using a 0.2-µm syringe-filter and incubate with the cartilage for 15 min at 37°C, on a rotator (*see* **Note 5**).

3. Remove the hyaluronidase solution and wash the cartilage 3× with sterile PBS.

4. Add 20 mL 0.25% (w/v) trypsin solution to each 50-mL centrifuge tube and incubate for 30 min at 37°C, on a rotator.

5. Remove the trypsin solution and wash the cartilage twice with basic medium. The fetal calf serum (FCS) present in the medium will inhibit the activity of the trypsin.

6. Prepare 20 mL collagenase solution per 50-mL centrifuge tube by dissolving bacterial collagenase (2 mg/mL) in warm basic medium. Filter-sterilize the solution using a 0.2-µm syringe-filter and incubate with the cartilage for approx 15 h at 37°C on a rotator (*see* **Note 6**).

7. Remove the tubes from the rotator and allow any undigested cartilage to settle to the bottom. Remove the supernatant using a 21-gauge needle and add to a new sterile tube (*see* **Note 7**).

8. Centrifuge at 200g for 7 min and remove the supernatant.

9. Wash the isolated chondrocytes by adding 10 mL sterile PBS to the pellet. Gently resuspend the cells and centrifuge again at 200g for 7 min. If required, combine all chondrocytes isolated from a single nasal septum (*see* **Note 8**).

10. Remove the supernatant and add 10 mL sterile PBS. Resuspend the chondrocytes and count the number of cells (*see* **Note 9**).

3.3. Expansion of Chondrocyte Numbers

1. Centrifuge the chondrocytes at 200g for 7 min and remove the supernatant. Resuspend the cells in expansion medium and add to tissue-culture dishes at a density of 50,000–100,000 cells/cm^2. Incubate the dishes at 37°C in a humidified atmosphere of 5% CO_2/95% air.

2. Allow the chondrocytes to expand until almost confluent. Remove the culture medium and wash twice with warm PBS (*see* **Note 10**).

3. Add a sufficient volume of 0.05% trypsin/0.02% EDTA to completely cover the cell layer and leave to stand for 1 min.

4. Remove the excess trypsin solution and place the culture dish in an incubator at 37°C for 5 min or until the cell-layer becomes detached from the culture dish (*see* **Note 11**).

5. Add an appropriate volume of expansion medium and collect the chondrocytes from the culture dish by gently mixing up and down using a pipet.

6. Centrifuge the cells at 200*g* for 7 min and discard the supernatant. Resuspend in expansion medium and count the cells (*see* **Note 9**).

7. Re-plate the cells as described in **step 2**.

8. Repeat **steps 3–8** for two to three passages until a sufficient number of chondrocytes are available for seeding onto scaffolds.

3.4. Chondrocyte Culture on 3D Scaffolds

Once the required degree of cell expansion has been achieved, confluent chondrocyte monolayers are harvested for seeding onto the polymer scaffold, and the chondrocyte/scaffold constructs are cultured to form a cartilage-like matrix. In the following section, a basic procedure is described for seeding the polymer scaffold using stirred spinner flasks (*see* **Note 12**). Optimal seeding conditions will vary, depending on the polymer type and cell source. A detailed discussion of the various cell-seeding methods is given by Vunjak-Novakovich in Chapter 11 of this book.

1. Allow pieces of the polymer scaffold (7 mm × 7 mm × 2 mm) to equilibrate at room temperature in 10 mL of expansion medium, while preparing the chondrocytes.

2. Remove the culture medium from the chondrocyte cultures, wash the cell monolayers once with PBS, and trypsinize the cells as described in **Subheading 3.3.** using trypsin/EDTA.

3. Aspirate recovered chondrocytes into centrifuge tubes and pellet, using low-speed centrifugation at 200g for 7 min.

4. Decant the supernatant and resuspend the chondrocytes in expansion medium.

5. Use a hemocytometer to determine the total cell number and concentration using an appropriate dilution of the chondrocyte suspension (*see* **Note 9**).

6. Prepare a cell suspension at 0.5×10^6 cells/mL in expansion medium and transfer 60 mL of the cell suspension to each spinner flask.

7. Slot two pieces of scaffold material onto each spinner flask wire using small pieces (4–5 mm) of narrow-bore silicon tubing above, below, and in between the scaffold pieces to keep them in position and separate from each other. Insert the bungs containing the scaffold-laden wires into the spinner flasks.

8. Loosen the side arms of the spinner flasks, position them on the magnetic stirrer in the incubator, and set the stirrer to a slow stirring speed of 75 rpm. Leave the spinner flasks stirring for 72 h to allow the cells to enter the scaffold material.

9. Add 10 mL of melted 1% agarose solution to 100-mm-diameter culture-grade Petri dishes and swirl the dishes to achieve an even coating of agarose. Leave the dishes open until the agarose has set. The coated dishes may then be stored sealed at room temperature until needed. Immediately before use equilibrate the plates with 10–12 mL of culture medium for 5–10 min (*see* **Note 13**).

10. After the cell seeding is complete, use forceps to transfer the chondrocyte/scaffold constructs to the agarose-coated Petri dishes (two constructs/dish). Remove any culture medium and add 25 mL of fresh expansion medium. Place the Petri dishes on the orbital shaker, set at a gentle shaking speed of 50 rpm, and leave the constructs for 72–96 h to allow further expansion of the cells on the scaffold.

11. Remove the culture medium from the culture dishes, taking care to avoid disturbing the agarose coating or the constructs. Replace with 25 mL of the differentiation medium to promote formation of a chondrogenic phenotype in the chondrocytes. Return the construct cultures to the orbital shaker in the incubator, maintaining a gentle shaking speed of 50 rpm.

12. Incubate the constructs for an additional 33 d, replacing the differentiation medium every 2–3 d (*see* **Note 14**).

After culture, the quantity, quality, and structure of the cartilage matrix components of the engineered constructs can be examined using various techniques, including biochemical analyses, histological and immunohistochemical techniques, and electron microscopy. Protocols for various analytical methods are presented elsewhere in this book (*see* Chapter 14 and Chapter 17).

Examples of chondrocyte/polymer scaffold constructs grown by the methodology described here are shown in **Fig. 1**.

4. Notes

1. Unless stated otherwise, all methods should be performed under sterile conditions using a Class II laminar air hood.

2. Surrounding tissue must be completely removed from nasal septum cartilage to prevent the contamination of isolated chondrocytes with other cells. For the same reason, avoid using the outer edges of each slice of cartilage when finely chopping the slices.

3. Although an approximate wet wt of the small cubes of cartilage is suggested, smaller pieces will give a larger surface area, and therefore greater efficiency in the enzymic digestion process that yields isolated chondrocytes.

4. When dissecting articular cartilage, ensure that full-depth cartilage is obtained. Do not cut through to the underlying bone, as the resulting cell culture may become contaminated with osteoblasts. Cutting the cartilage too deeply will be indicated by the appearance of blood.

5. The cartilage pieces require continuous agitation during sequential enzymic digestion. Ideally, a rotator should be used inside a 37°C room. Alternatively, the rotator may be placed inside an oven or incubator set at the same temperature.

6. Incubate the collagenase solution with the cartilage until the cartilage pieces have visibly dissolved. Once digestion is complete, remove the collagenase to prevent any damage to the isolated chondrocytes.

7. Slowly remove the supernatant using a 21-gauge needle to exclude any small pieces of undigested cartilage. Remove the needle from the syringe prior to adding the cell suspension to a new tube, as forcing the cells back through the needle may cause the cells to lyse.
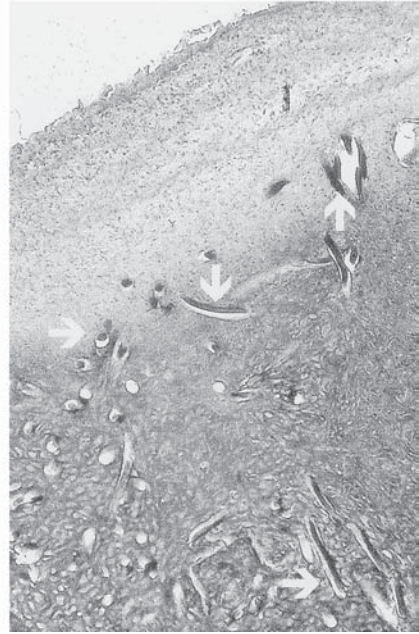
Section A
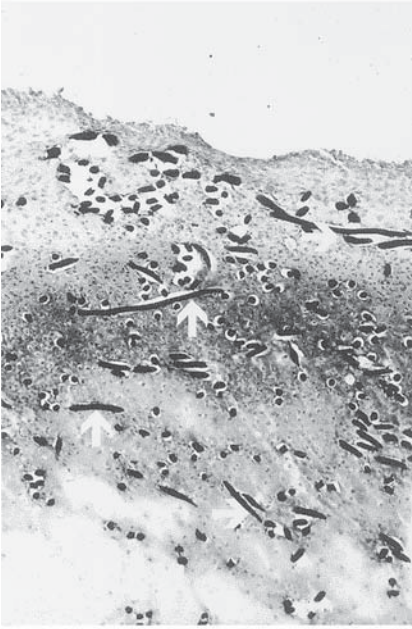
Section B

Fig. 1. Localization of proteoglycan in chondrocyte/scaffold constructs. Bovine articular and nasal chondrocytes were isolated and seeded onto scaffolds of Hyalograft C and cultured for a total of 40 d using methods described in the text. At the end of the culture period, 8 μ frozen sections were prepared and fixed in paraformaldehyde. Proteoglycan was detected by staining with 1% toludine blue. **(A)** was prepared from cell/scaffold constructs of articular chondrocytes and **(B)** from cell/scaffold constructs of nasal chondrocytes. Staining for proteoglycan can be seen within both constructs, with little staining observed at the periphery. Scaffold fibers were still present at the end of the incubation period, as indicated by arrows on the figures. Original magnification ×25.

8. Using this method of sequential enzymic digestion, approx 25×10^6 nasal chondrocytes can be obtained from a single bovine nasal septum and approx 30×10^6 articular chondrocytes from a single metacarpophalangeal joint.

9. To count the number of chondrocytes, ensure that the cells are well-suspended and add small drops of the suspension to both chambers of a hemocytometer. Using a microscope, count the average number of cells per 1 mm square. If the cells are touching or overlapping, dilute the suspension prior to counting. Calculate the number of chondrocytes per mL using the following formula:

$$average \ number \ of \ cells \ per \ 1 \ mm \ square \times 10^4 \times dilution \ factor$$

10. The culture medium must be completely removed, because it contains FCS that would inhibit the activity of trypsin-EDTA.

11. When the chondrocytes become detached from the culture dish, they will appear to be round under the microscope and will be observed to move if the culture dish is tapped vigorously.

12. In comparison to static seeding, where cells and scaffolds are placed together in stationary Petri dishes, dynamic seeding is reported to enhance the colonization of biopolymer scaffolds by chondrocytes and yield a more spatially uniform cell-seeding *(29)*.

13. These culture dishes are used to culture the chondrocyte/scaffold constructs. The agarose coating prevents the attachment of any cells that may be released from the scaffold and would otherwise form monolayers of undifferentiated cells.

14. The culture dishes should be examined regularly for the formation of monolayers beneath the layer of agarose gel. If this occurs, the cell/scaffold constructs should be transferred to fresh agarose-coated Petri dishes.

References

1. Buckwalter, J. A. and Mankin, H. J. (1998) Articular cartilage: tissue design and chondrocyte-matrix interactions. *Instruct. Course Lect.* **47,** 477–486.
2. Cohen, N. P., Foster, R. J., and Mow, V. C. (1998) Composition and dynamics of articular cartilage: structure, function and maintaining healthy state. *J. Orthop. Sports Phys. Ther.* **28,** 203–215.
3. Rosier, R. N. and O'Keefe, R. J. (1998) Autocrine regulation of articular cartilage. *Instruct. Course Lect.* **47,** 469–475.
4. Poole, C. A. (1997) Articular cartilage chondrons: form, function and failure. *J. Anat.* **191,** 1–13.
5. Oloyede, A. and Broom, N. (1996) The biomechanics of cartilage load-carriage. *Connect. Tissue Res.* **34,** 119–143.
6. Poole, A. R. (1993) Cartilage in health and disease, in *Arthritis and Allied Conditions: A Textbook of Rheumatology* (McCarty, D. J. Jr., Koopman, W. J., eds.), Lea and Febiger, Philadelphia, PA, pp. 279–333.
7. Muir, H. (1995) The chondrocyte, architect of cartilage: biomechanics, structure, function and molecular biology of cartilage matrix macromolecules. *Bioassays* **17,** 1039–1048.
8. Benya, P. and Shaffer, J. D. (1982) Dedifferentiated chondrocytes re-express the differentiated collagen phenotype when cultured in agarose gels. *Cell* **30,** 215–224.
9. Liu, H., Lee, Y. W., and Dean, M. F. (1998) Re-expression of differentiated proteoglycan phenotype by dedifferentiated human chondrocytes during culture in alginate beads. *Biochim. Biophys. Acta* **1425,** 505–515.
10. Lemare, F., Steimberg N., Le Greil, C., Demignot, S., and Adolphe, M. (1998) Dedifferentiated chondrocytes cultured in alginate beads: restoration of the differentiated phenotype and of the metabolic responses to interleukin 1 beta. *J. Cell. Physiol.* **176,** 303–313.
11. Martin, I., Vunjak-Novakovic, G., Yang, J., Langer, R., and Freed, L. E. (1999) Mammalian chondrocytes expanded in the presence of fibroblast growth factor 2 maintain the ability to differentiate and regenerate three-dimensional cartilagenous tissue. *Exp. Cell Res.* **253,** 681–688.

12. O'Conner, W. J., Botti, T., Khan, S. N., and Lane, J. M. (2000) The use of growth factors in cartilage repair. *Orthop. Clin. N. Am.* **31,** 399–410.

13. Loeser, R. F. and Gouri, S. (2000) Autocrine stimulation by insulin-like growth factor 1 and insulin-like growth factor 2 mediates chondrocyte survival in vitro. *Arthritis Rheum.* **43,** 1552–1559.

14. Geurne, P. A., Blanko, F., Kaelin, A., Desgeorges, A., and Lotz, M. (1995) Growth factor responsiveness of human articular chondrocytes in ageing and development. *Arthritis Rheum.* **38,** 960–968.

15. McQuillan, D. S., Handley, C. J., Cambell, M. A., Bilis, S., Milway, V. E., and Herington, A. C. (1986) Stimulation of proteoglycan biosynthesis by serum and insulin-like growth factor-I in cultured bovine articular cartilage. *Biochem. J.* **240,** 423–430.

16. Sah, R. L., Chen, A. C., Grodzinsky, A. J., and Trippel, S. B. (1994) Differential effect of bFGF and IGF-I on matrix metabolism in calf and adult bovine cartilage explants. *Arch. Biochem. Biophys.* **308,** 137–147.

17. Pavasant, P., Shizari, T., and Underhill, C. B. (1996) Hyaluronan synthesis by epiphyseal chondrocytes is regulated by growth hormone, insulin-like growth factor-1, parathyroid hormone and transforming growth factor-beta 1. *Matrix Biol.* **15,** 423–432.

18. Sah, R. L. Y., Trippel, S. B., and Grodzinsky, A. J. (1996) Differential effects of serum, insulin-like growth factor 1 and fibroblast growth factor-2 on the maintenance of cartilage physical properties during long-term culture. *J. Orthop. Res.* **14,** 44–52.

19. Hunziker, E. B. and Rosenberg, L. (1994) Induction of repair in partial thickness articular cartilage lesions by timed release of TGF-beta. *Trans. Orthop. Res. Soc.* **19,** 236.

20. Osaki, M., Tsukazaki, T., Yonekura, A., Myazaki, Y., Iwasaki, K., Shindo, H., et al. (1999) Regulation of c-fos gene induction and mitogenic effect of transforming growth factor-β1 in rat articular chondrocyte. *Endocrine J.* **46,** 253–261.

21. Demoor-Fossard, M., Redini, F., Boittin, M., and Pujol, J. P. (1998) Expression of decorin and biglycan by rabbit articular chondrocytes. Effects of cytokines and phenotypic modulation. *Biochim. Biophys. Acta* **1398,** 179–191.

22. Morales, T. I. and Roberts, A. B. (1988) Transforming growth factor-β regulates the metabolism of proteoglycans in bovine cartilage organ culture. *J. Biol. Chem.* **263,** 12828–12831.

23. Iqual, J., Dudhia, J., Bird, J. L., and Bayliss, M. T. (2000) Age related effects of TGF-beta on proteoglycan synthesis in equine articular cartilage. *Biochem. Biophys. Res. Commun.* **274,** 467–471.

24. van der Kraan, P. M., Vitters, E. L., and van den Berg, W. B. (1992) Inhibition of proteoglycan synthesis by transforming growth factor-β in anatomically intact cartilage of murine patellae. *Ann. Rheum. Dis.* **51,** 643–647.

25. van Beuningen, H. M., Glansbeek, H. L, van der Kraan, P. M., and van den Berg, W. B. (1998) Differential effects of local application of BMP-2 or TGF-beta 1 on both articular cartilage composition and osteophyte formation. (1998) *Osteoarthritis and Cartilage* **6,** 306–331.

26. Glansbeek, H. L., van Beuningen, H. M., Vitters, E. L., Morris, E. A., van den Kraan, P. M., and van den Berg, W. B. (1997) Bone morphogenic protein 2 stimulates articular cartilage proteoglycan synthesis in vivo but does not counteract interleukin-1 alpha effects on proteoglycan synthesis and content. *Arthritis Rheum.* **40,** 1020–1028.

27. Nishida, Y., Knudson, C. B., Kuettner, K. E., and Knudson, W. (2000) Osteogenic protein-1 promotes the synthesis and retention of extracellular matrix within bovine articular cartilage and chondrocyte cultures. *Osteoarthritis and Cartilage* **8,** 127–136.

28. Huch, K., Wilbrink, B., Flechtenmacher, J., Koepp, H. E., Aydelotte, M. B., Sampath, T. K., et al. (1997) Effects of recombinant human osteogenic protein 1 on the production of proteoglycan, prostaglandin E2 and interleukin-1 receptor antagonist by human articular chondrocytes cultured in the presence of interleukin-1 beta. *Arthritis Rheum.* **40,** 2157–2161.

29. Vunjak-Novakovic, G., Obradovic, B., Martin, I., Bursac, P. M., Langer, R., and Freed, L. E. (1998) Dynamic cell seeding of polymer scaffolds for cartilage tissue engineering. *Biotechnol. Prog.* **14,** 293–202.

13

Bioreactor Culture Techniques
for Cartilage-Tissue Engineering

David A. Lee and Ivan Martin

1. Introduction

Tissue engineering is a major focus of biotechnological research today, with the expectation that this type of technique will ultimately transform medical practice *(1)*. The most ambitious tissue-engineering schemes assume that specific tissues and organs will be restored, in a multistage fabrication procedure. For example, cells derived from the patient may be processed to increase the total number available, seeded into a suitable three-dimensional (3D) resorbable scaffold and further processed in vitro to induce the elaboration of neo-tissue prior to implantation *(2)*.

For full-depth cartilage repair, tissue-engineered constructs must span the full depth of the tissue, which may be up to 6 mm in thickness *(3)*. In order to maintain cellular viability and activity within a construct of this thickness in vitro, effective delivery of bioactive molecules is required. Indeed, a range of stimuli, both biochemical and biophysical, are required for the induction of appropriate cellular growth, biosynthesis, and tissue remodeling. Simple static tissue-culture techniques are inadequate in this respect, and large necrotic and/or apoptotic regions typically form toward the core of the specimen as a result of limited mass transport through the construct *(4)*. In an attempt to solve this problem, efforts have been made to increase the porosity of the construct, but this may compromise the mechanical integrity of the system. An alternative approach is to enhance mass transport by subjecting the construct to a dynamic fluid environment within a bioreactor system.

A bioreactor is usually defined as a device that provides the transport system for nutrients to cells and allows the efficient withdrawal of toxic or inhibitory
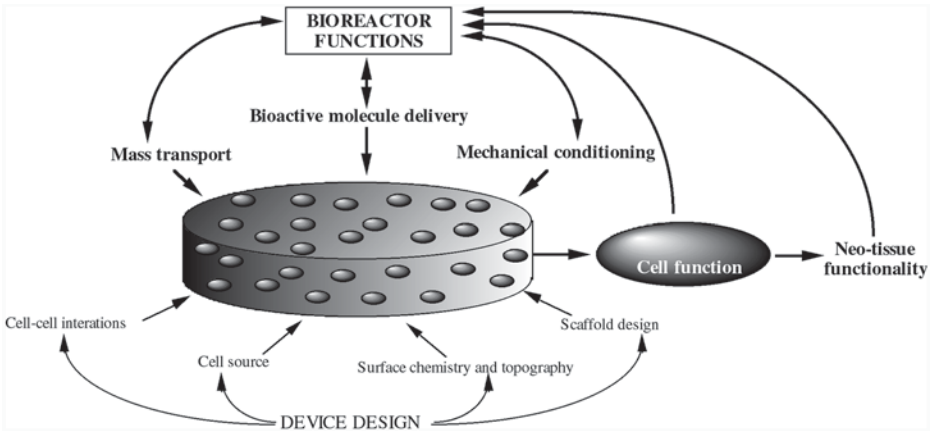
Fig. 1. Schematic indicating the contribution of bioreactors to the development of tissue-engineered constructs.

metabolic byproducts. Bioreactors are commonly used in industry for mass culture, requiring close monitoring of culture conditions and considerable nutrient requirements. The use of smaller bioreactors could offer advantages compared to static culture conditions for cartilage tissue-engineering, for which devices may be as small as 10 mm in diameter with a thickness of 2 mm, and contain less than 1×10^6 cells *(5)*. Uniform and effective mixing is coupled with precise control over mass transport rates, regulation of shear stresses, maintenance of temperature, pH, gas partial pressures (pO_2, pCO_2), and nutrient levels *(6)*. Biophysical stimuli are known to influence the development, maintenance, and remodeling of many tissues, including cartilage, through a process known as mechanotransduction. Several studies have shown that cellular response to physical forces is dependent on various factors such as loading orientation, strain magnitude, and frequency *(7)*. Bioreactors for tissue engineering may also provide appropriate mechanical conditioning, to the developing tissue-engineered construct. Moreover, process-control strategies capable of matching the changing requirements of the developing construct during in vitro cultivation can be provided by bioreactor systems. The contribution of bioreactors to the development of tissue-engineered constructs is portrayed schematically in **Fig. 1**.

In this chapter, methods for the preparation of tissue-engineered constructs for cartilage repair based on two well-characterized scaffolds, nonwoven fibrous meshes of polyglycolic acid (PGA) *(8)* and calcium alginate hydrogels *(9)*, are presented. Methods for the culture of the constructs within two bioreactor systems, the rotating wall vessel (RWV) bioreactor (**Fig. 2**) and
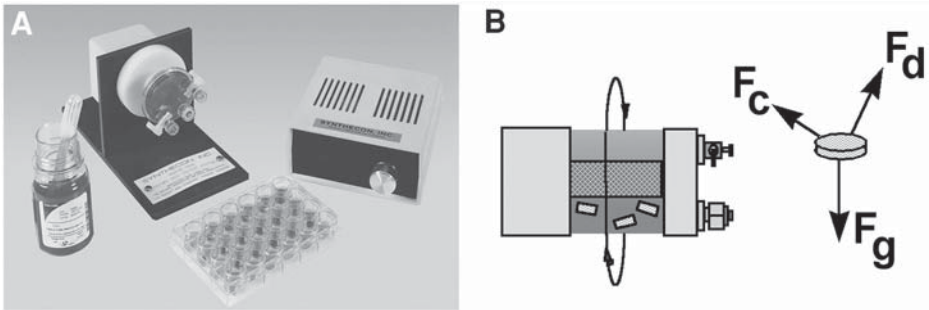
Fig. 2. Photograph **(A)** and schematic representation **(B)** of the rotating wall vessel bioreactor. Because of the balance of the centrifugal (F_c), drag (F_d), and net-gravity (F_g) forces, constructs in the rotating wall vessel are freely settling in a tumble-slide regime and exposed to a dynamic laminar flow.
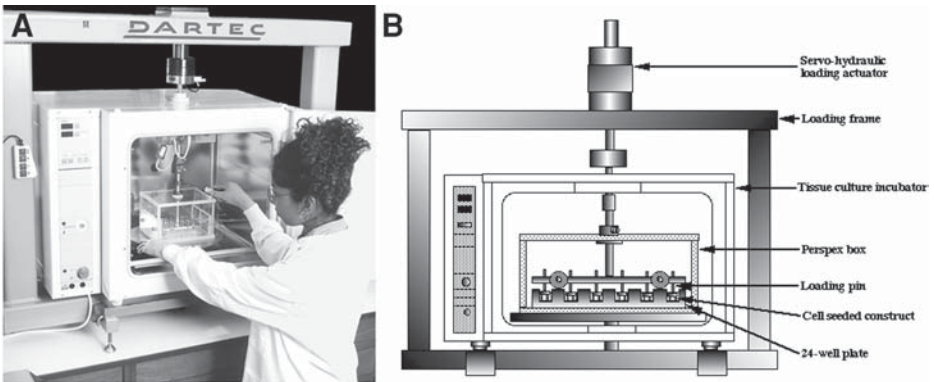
Fig. 3. Photograph **(A)** and schematic representation **(B)** of the Compressive cell strain bioreactor.

compressive cell strain bioreactor (**Fig. 3**), are described. The RWV bioreactor is composed of a family of commercially available systems that embody the same fluid dynamic operating principles. The bioreactors provide solid body rotation about a horizontal axis that is characterized by co-location of particles of different sedimentation rates, extremely low fluid shear stress, and turbulence *(10)*. The systems enhance mass transport by maintaining constructs in a state of continuous free fall within a body of medium. Neo-tissue formation and mechanical properties of tissue-engineered cartilage constructs are enhanced during culture within the RWV compared to static culture conditions or maintenance within a turbulent flow environment, such

as a mixer flask *(11,12)*. The second bioreactor system applies dynamic mechanical compression directly to the constructs, which enhances mass transport and further activates pathways associated with fluid flow-induced shear and cell deformation. The application of dynamic compression to tissue-engineered cartilage constructs within the system has been reported to enhance cell proliferation and proteoglycan synthesis while inhibiting the synthesis of catabolic mediators such as nitric oxide and PGE_2 *(13,14)*. Both of these cultivation methods may be used in conjunction with a full range of molecular, biochemical, histological, and mechanical methods for assessing the metabolic and functional development of the constructs. These methods are described elsewhere in the literature, and are not presented in this chapter. However, simple methods to evaluate mass transport and cell viability within the constructs are described.

2. Materials

2.1. Isolation of Bovine Chondrocytes

1. Front feet from approx 18-mo-old steers (obtain from local slaughterhouse).
2. 70% (v/v) industrial methylated spirits in (IMS) water.
3. Dissection kit: Metal dissection tray, sterile scalpels fitted with No. 20, No. 11, and No. 15 blades.
4. Earle's balanced salt solution (EBSS, Sigma, Poole, UK, cat. no. E-2888 or equivalent).
5. Culture medium: Dulbecco's minimal Essential medium (Sigma cat. no. D-5921 or equivalent) supplemented with 20% (v/v) fetal calf serum (FCS) (Sigma cat. no. F-9665 or equivalent), 2 m*M* L-glutamine (200 m*M* stock solution, Sigma cat. no. G-7513 or equivalent), 20 m*M* HEPES (1 *M* stock solution Sigma cat. no. H-0887 or equivalent), 50 U/mL penicillin/50 µg/mL streptomycin (5000 U/mL penicillin/5 mg/mL streptomycin stock solution, Sigma cat. no. P0906) and 150 µg/mL L-ascorbic acid (Sigma cat. no. A-0278), sterilized by filtration through a 0.2-µm pore size filter. Aliquot and store at –20°C prior to use.
6. Pronase solution: 700 U/mL pronase (Merck, Poole, UK, cat. no. 39052 2P) in culture medium.
7. Collagenase solution: 100 U/mL collagenase type XI (Sigma cat. no. C9407) in culture medium.
8. Trypan blue solution: 0.4% (w/v) trypan blue in 0.81% (w/v) sodium chloride/ 0.06% (w/v) potassium phosphate (Sigma cat. no. T-8154 or equivalent).
9. 35-mm-diameter sterile Petri dishes.
10. 50-mL-capacity sterile polypropylene centrifuge tubes.
11. 70-µm-pore-size cell sieve (Falcon, London, UK, cat. no. 35 2350).
12. Class II safety cabinet.
13. Roller mixer within an incubator or warm room at 37°C.

14. Centrifuge: up to 2000 rpm, compatible with 50-mL centrifuge tubes.
15. Hemacytometer.
16. Inverted microscope with phase-contrast facility.

2.2. Preparation of Chondrocyte/Alginate Constructs

1. Culture medium.
2. Isolated chondrocytes.
3. Alginate suspension: 4% (w/v) alginate (Keltone LV, KelcoNutrasweet, Tadworth, UK) in EBSS, sterilized by autoclaving.
4. Calcium chloride solution: 100 m*M* $CaCl_2$ (Sigma cat. no. C-7902 or equivalent) in culture medium, sterilized by filtration through a 0.2-µm-pore-size filter.
5. Mold for preparing constructs (**Fig. 2**; s*ee* **Note 1**).
6. 150 mL capacity sterile containers.
7. Positive displacement pipet and sterile tips (Gilson Microman M250 or equivalent).

2.3. Preparation of Chondrocyte/PGA Constructs

1. Culture medium.
2. Isolated chondrocytes.
3. PGA nonwoven meshes (Albany International, Mansfield, MA).
4. 95% ethanol (ETOH).
5. Sterile tweezers.
6. Spinner flasks (100 mL) with a 0.8-cm diameter × 4-cm long stir bar, and magnetic stirrer plate (Bellco, Vineland, NJ).
7. 4-in. long, 22-gauge needles (Metropolitan Hospital Supply, Cambridge, MA).
8. Silicone stoppers (No. 10) and silicone tubing (No. 13) (Cole Parmer, Niles, IL), cut into 3-mm-long cylinders.

2.4. Rotating Wall Vessel Bioreactor

1. Rotating vessel (Rotary Cell Culture System; Synthecon, Houston, TX).
2. Hereaus B6060 incubator (Kendro Laboratory Products, Bishop's Stortford, UK).
3. Culture medium.
4. Cell-seeded constructs.
5. 5-mL-capacity sterile syringes.

2.5. Compressive Cell Strain Bioreactor

The equipment comprises the following components, as illustrated in **Fig. 3**:

1. Loading frame to incorporate Hereaus tissue-culture incubator (Zwick Testing Machines Ltd., Leominster, UK).
2. Servo-hydraulic loading actuator incorporating load cell and Linear Variable Displacement Transducer (Zwick Testing Machines Ltd).
3. Hydraulic power supply (Zwick Testing Machines Ltd, Leominster, UK)
4. Digital control unit (Dartec 9610, Zwick Testing Machines Ltd).
5. Hereaus B6060 incubator (Kendro Laboratory Products, Bishop's Stortford, UK).

Table 1
Radiolabeled Molecules Used for Mass Transport Studies

Radiolabeled molecule	Mol wt (Da)	Activity	Source
$^{35}SO_4{}^{2-}$	99	1 µCi/mL	Amersham International[1]
^{14}C-glucose	180	1 µCi/mL	Amersham International[1]
^{3}H-thymidine	242.2	1 µCi/mL	Amersham International[1]
^{125}I-IGF-1	7700	0.1 µCi/mL	ICN Biomedicals[2]
^{125}I-growth hormone	22000	0.1 µCi/mL	ICN Biomedicals[2]
^{125}I-bovine serum albumin	69000	0.1 µCi/mL	ICN Biomedicals[2]

[1]Little Chalfont, UK.
[2]Basingstoke, UK.

6. Custom-designed construct loading assembly and box (Department of Engineering, Queen Mary, University of London, UK).

For culture within the bioreactor, the following are required:

1. 70% IMS.
2. Culture medium.
3. 24-well cell-culture plate (Costar cat. no. 3524, High Wycombe, UK).
4. Cell-seeded constructs.
5. 1-mL capacity sterile syringe with right-angle needle (*see* **Note 2**).

2.6. Assessment of Mass Transport in Constructs

1. Cell seeded or cell-free constructs.
2. Culture medium supplemented with radiolabeled molecules as indicated in **Table 1**.
3. Alginate dissolution buffer: 150 mM sodium chloride, 50 mM sodium citrate in distilled water, pH 7.4. Papain digestion solution: 0.175% cysteine and 0.0125% papain in 100 mM Na_2HPO_4, 10 mM Na_2EDTA, pH 6.5.
4. Scintillation cocktail (Emulsifier Safe, Packard, Pangbourne, UK or equivalent).
5. Scintillation vials, 4-mL capacity (Packard or equivalent).
6. Liquid scintillation counter (e.g., Wallac 1409, Perkin-Elmer, Cambridge, UK).
7. Gamma counter (e.g., VEGA, NE technologies, UK).

2.7. Assessment of Cell Viability in Constructs

1. Scalpel with No. 11 blade or razor blade.
2. Viability testing solution: culture medium supplemented with 5 µM calcein AM (Molecular Probes, Inc., cat. no. C3099) and 5 µM ethidium homodimer (Molecular Probes, Inc., cat. no. E3599).
3. Glass cover slips.
4. Inverted confocal microscope (preferable) or Inverted epifluorescence microscope.

3. Methods

3.1 Isolation of Bovine Chondrocytes

1. Clean bovine front feet with water and immerse in 70% IMS for 5 min to sterilize skin.
2. Within the Class II safety cabinet, expose the metacarpalphalangeal joint and remove full-depth cartilage slices from the proximal articular surfaces of the joint using a no. 15 blade (*see* **Note 3**). Transfer the slices to a 60-mm Petri dish containing 8 mL of EBSS.
3. Aspirate EBSS and dice the tissue into pieces approx 1 mm^3 and transfer to a 50-mL centrifuge tube containing 10 mL of pronase solution (*see* **Note 4**). Incubate on rollers for 1 h at 37°C.
4. Allow the tissue pieces to settle and remove pronase solution. Add 30 mL of collagenase solution and incubate on rollers for 16 h at 37°C (*see* **Notes 4** and **5**).
5. Allow any remaining tissue pieces to settle and carefully remove the collagenase solution containing isolated cells. Filter the solution through a 70-µm-pore-size sieve into a fresh 50-mL centrifuge tube.
6. Centrifuge at 2000*g* for 5 min to pellet cells. Aspirate the supernatant and resuspend the cells in 10 mL of culture medium using a 10-mL sterile graduated pipet. Repeat this process twice.
7. Add 50 µL of cell suspension to 50 µL Trypan blue solution, mix and add resultant suspension to a hemacytometer. Determine total cell number and cell viability and adjust cell concentration to 2×10^7 cells/mL.

3.2. Preparation of Chondrocyte/Alginate Constructs

1. Part assemble the mold used for preparation of alginate/chondrocyte constructs as indicated in **Fig. 4D**.
2. Add the cell suspension, adjusted to 2×10^7 cells/mL, to an equal volume of alginate suspension. Mix thoroughly using a positive displacement pipet.
3. Aliquot the alginate/chondrocyte suspension into individual wells of the mold and complete the assembly by adding a second dialysis membrane and the upper frame and porous support (**Fig. 4D**). Tighten the bolts to ensure that the mold is sealed.
4. Place the mold into a 150-mL capacity sterile container and completely fill the container with calcium chloride solution. Incubate on rollers for 2 h at 37°C.
5. Carefully remove and dismantle the mold to allow removal of the gelled alginate/chondrocyte constructs.

3.3. Preparation of Chondrocyte/PGA Constructs

1. Soak PGA scaffolds in 95% ETOH for 5 min and then rinse them 5× in culture medium.
2. Thread the pre-wetted PGA scaffolds onto needles positioned 5 mm apart using segments of silicone tubing (two to three scaffolds per needle) (*see* **Note 6**).
3. Fix 2–4 needles with threaded scaffolds to the silicone stopper, and place this in the mouth of the flask, containing the magnetic stir bar.

4. Fill the flask with 120 mL of culture medium and place it on a magnetic stirrer (50 rpm) in a humidified incubator at 37°C for 18 h. The side-arm caps of the flask should be loosened to permit gas exchange.
5. Replace the culture medium by a suspension of freshly isolated chondrocytes (5×10^6 cells per scaffold) and place the flask again on the magnetic stirrer for an additional 48 h.
6. Carefully remove the cell-seeded scaffolds from the needles using sterile tweezers. Details on the kinetics of cell seeding using experimental data and a mathematical model may be found in **ref. *15***.

3.4. Culture of Constructs in Rotating Wall-Vessel Bioreactor

1. Assemble the bioreactor according to the manufacturer's instructions; transfer the constructs in the space between the outer and inner cylinder and fill it with culture medium using two syringes connected to the chamber openings (*see* **Note 7**).
2. Adjust the rotation speed of the vessel throughout the the period of cultivation to balance the forces acting on the growing constructs (*see* **Fig. 3B**). Constructs should be settling at a relatively steady position within the vessel.
3. Replace 50–100% of the culture medium every 2–3 d. Details on the structural and functional properties of chondrocyte-PGA constructs cultured in the rotating wall vessel may be found in **refs. *11,16***.

3.5. Culture of Constructs in Compressive Cell-Strain Bioreactor

1. Assemble loading plate, loading pins, and perspex box, ensuring that the outer pins are held in place with plastic collars and the inner pins are clamped. Sterilize in 70% IMS and allow to dry overnight in a tissue-culture hood.
2. Locate constructs at the center of individual wells of a 24-well cell-culture plate and locate within the perspex box.
3. Allow loading pins to drop onto constructs by removing the plastic collars from the outer pins and unclamping the inner pins. Clamp inner pins once they are in position.
4. Introduce 1 mL of culture medium into each well through the medium ports associated with the apparatus using a 1-mL syringe and right-angled needle.
5. Close the box, transfer to the bioreactor, and attach to the loading actuator by means of the central rod. Unlock the central rod to allow free movement.
6. Set the control electronics of the straining apparatus to provide a crosshead movement equivalent to a compressive strain ranging from 0–15% in a sinusoidal waveform at a frequency of 1 Hz.

3.6. Assessment of Mass Transport in Constructs

1. Incubate cell-seeded or cell-free constructs in bioreactor containing culture medium supplemented with radiolabeled molecules as indicated in **Table 1**.
2. Remove constructs from culture after incubation for 0.25, 0.5, 1, 2, 4, 8, 24, and 48 h.
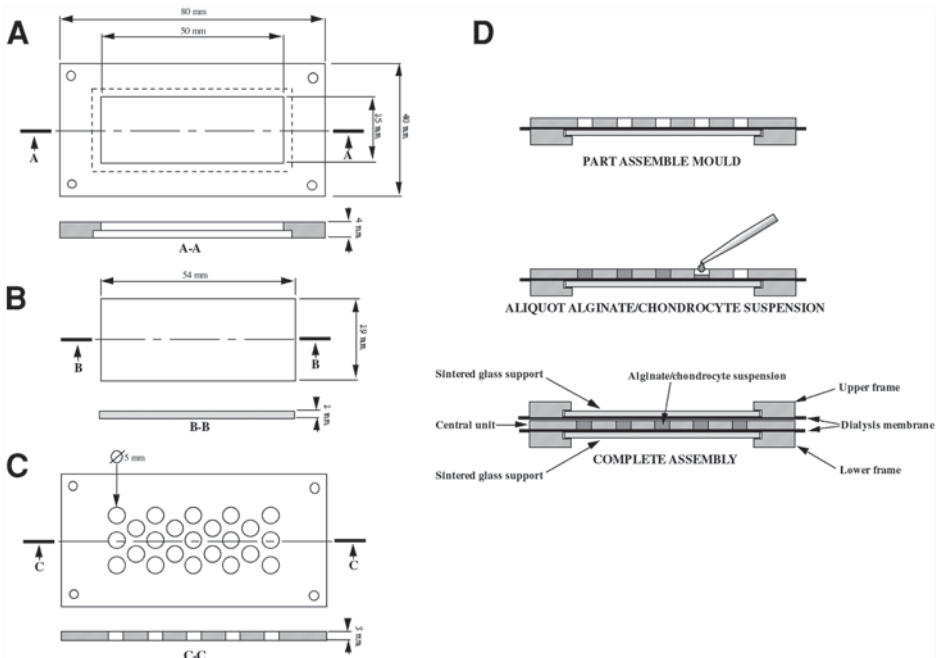
Fig. 4. Diagram of the mold used for the preparation of chondrocyte/alginate constructs, indicating the dimensions of the open frame **(A)**, sintered glass support **(B)**, and central unit **(C)**. Sub-figure **(D)** indicates the assembly and use of the mold.

3. Dissolve constructs as follows. Alginate constructs: Incubate in 1 mL alginate dissolution buffer. PGA constructs: incubate in 1 mL Papain digestion solution at 60°C for 10–16 h, until all the material is in solution.
4. Determine total radioactivity in samples containing ^{125}I directly using a gamma counter. Solutions containing ^{3}H, ^{35}S, and ^{14}C were assessed by mixing 0.5-mL aliquots of sample with 4 mL of scintillation cocktail. Total radioactivity is determined by scintillation counting. An example of a typical result is presented in **Fig. 5** for constructs cultured in the Compressive cell strain bioreactor.

3.7. Assessment of Cell Viability in Constructs

1. Remove cell-seeded construct from culture and cut in half from top to bottom using a razor blade or scalpel.
2. Incubate for 45 min in 1 mL viability testing solution at 37°C.
3. Place the specimen on a glass cover slip with the cut surface adjacent to the glass and mount on the stage of an inverted microscope, associated with a confocal or epifluorescence system. Ensure hydration by immersing the specimen in a drop of viability testing solution.
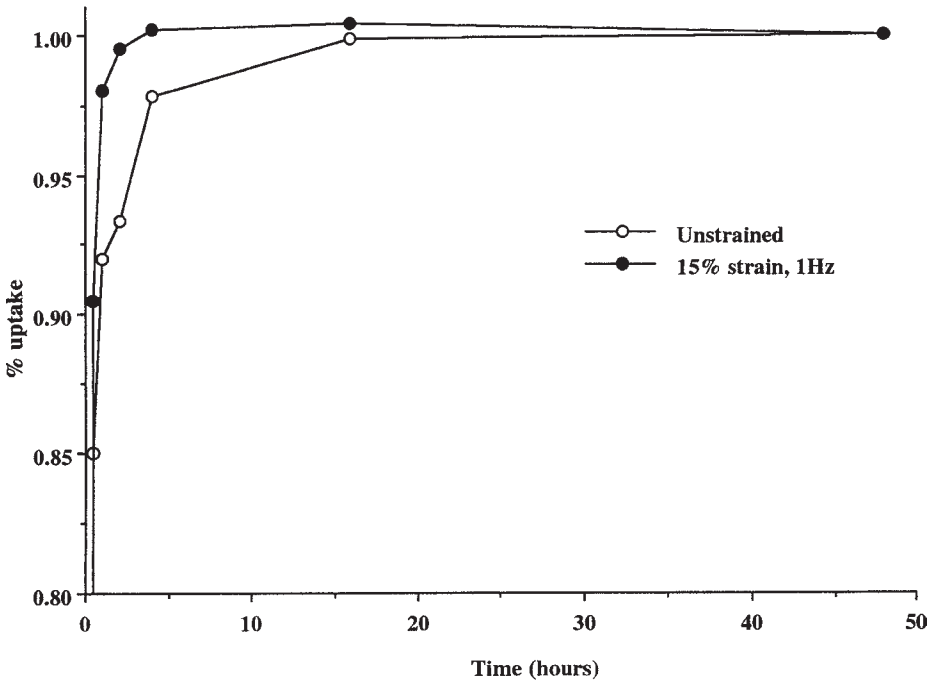
Fig. 5. Uptake of ^{3}H-thymidine by tissue-engineered cartilage constructs cultured for up to 24 h within the compressive cell-strain bioreactor. Constructs were either unstrained (*open circles*) or subjected to 15% dynamic compression at 1 Hz (*closed circles*).

4. Visualize the cells within the construct using epifluorescence or confocal micro- scopy using excitation/emission setting of 488/530 nm and 530/585 nm for calcein AM and ethidium homodimer, respectively (*see* **Note 8**).
5. Determine the numbers of live (green) and dead (orange) cells within a series of fields of view extending across the depth of the specimen.

4. Notes

1. The mold is comprised of two open frames (**Fig. 4A**), which are designed to hold porous sintered glass supports (**Fig. 4B**, R&H Filter Co. Inc., Georgetown, DE), and a central rectangular unit that incorporates a matrix of cylindrical holes (**Fig. 4C**). The frames and central unit are constructed from medical-grade stain- less steel. All three units may be clamped together using four locating bolts and locking nuts. During use, a dialysis membrane is placed between the porous sup- port and the central unit allowing Ca^{2+} diffusion into the alginate/chondrocyte suspension, which is aliquoted into the cylindrical wells formed during partial assembly of the mold (**Fig. 4D**). Detailed design drawings may be obtained from David Lee (D.A.Lee@qmul.ac.uk).

2. The right-angle needle is prepared by taking a sterile 21-gauge, 50-mm-length needle and bending through 90° after partially removing the needle from its sheath.

3. The best method to open the joint is to make a midline incision using a no. 20 blade, taking care to avoid entering the joint space. The skin and digital extensor tendons may then be dissected away from the joint capsule, and the joint may be opened with a no. 11 blade, using the distal surface of the metacarpal bone as a guide.

4. The volumes of pronase and collagenase solution are based on the digestion of tissue from one joint. If digesting tissue from more than one joint, it is recommended that the tissue be digested in additional centrifuge tubes rather than altering the volume of the solutions in each tube. Approximately 1–3 g of tissue can be obtained from a single joint, and this should yield up to 30×10^6 cells.

5. Collagenase batches vary, even when they are purchased from the same supplier. It is highly advisable to test batches prior to use to ensure that all the tissue is digested and that cell viability is maintained. It may be necessary to alter the concentration or incubation times from those stated in order to achieve optimal cell isolation.

6. A convenient way to thread scaffolds and silicone spacers onto the flask needles is to first thread scaffolds and spacers onto a syringe needle (which is sharper), and then sliding them in the flask needles by fitting the two needle gauges.

7. In order to remove air within the rotating vessel, culture medium should be introduced in one syringe until air bubbles emerge from the other one. The operation should be repeated in alternate directions until all the air has been eliminated.

8. When using confocal microscopy, it is recommended to visualize cells approx 50 μm into the specimen, thereby eliminating cells at the cut edge of the specimen, which can be damaged during the cutting process.

References

1. Nerem, R. M. (2000) Tissue engineering: confronting the transplant crisis. *Proc. Inst. Mech. Engrs.* Part H, **214,** 95–99.
2. Bader, D. L. and Lee, D. A. (2000) Structure-properties of soft tissues: articular cartilage, in *Structural Biological Materials: Design and Structure Property Relationships* (Elices, M., ed.), Oxford, UK, Pergamon Press, pp. 73–104.
3. Ateshian, G.A., Soslowsky, L. J., and Mow, V. C. (1991) Quantitation of articular surface topography and cartilage thickness in knee joints using sterophotogrammetry. *J. Biomechanics* **24,** 761–776.
4. Enobakhare, B., Bader, D. L., and Lee, D. A. (2001) Physiochemical, biochemical and mechanical characterisation of chondrocyte/alginate constructs. *Trans. Orthop. Res. Soc.* **26,** 638.
5. Wu, F., Dunkelman, N., Peterson, A., Davisson, T., De La Torre, R., and Jain, D. (1999) Bioreactor development for tissue-engineered cartilage. *Ann. NY Acad. Sci.* **875,** 405–411.

6. Obradovic, B., Carrier, R. L., Vunjak-Novakovic, G., and Freed, L. E. (1999) Gas exchange is essential for bioreactor cultivation of tissue engineered cartilage. *Biotechnol Bioeng*. **63,** 197–205.

7. Huang, D., Chang, T. R., Aggarwal, A., Lee, R. C., and Ehrlich, H. P. (1993) Mechanisms and dynamics of mechanical strengthening in ligament-equivalent fibroblast-populated collagen matrices. *Ann. Biomed. Eng*. **21,** 289–305.

8. Freed, L. E, Vunjak-Novakovic, G., Biron, R.J., Eagles, D. B., Lesnoy, D. C., Barlow, S. K., et al. (1994) Biodegradable polymer scaffolds for tissue engineering. *Biotechnology* **12,** 689–693.

9. Paige, K. T., Cima, L. G., Yaremchuk, M. J., Schloo, B. L., Vacanti, J. P., and Vacanti, C. A. (1996) De novo cartilage generation using calcium alginate-chondrocyte constructs. *Plast. Reconstr. Surg.* **97,** 68–78.

10. Begley, C. M. and Kleis, S. J. (2000) The fluid dynamic and shear environment in the NASA/JSC rotating-wall perfused-vessel bioreactor. *Biotechnol. Bioeng.* **70,** 32–40.

11. Vunjak-Novakovic, G., Martin, I., Obradovic, B., Treppo, S., Grodzinsky, A. J., Langer, R., et al. (1999) Bioreactor cultivation conditions modulate the composition and mechanical properties of tissue-engineered cartilage. *J. Orthop. Res.* **17,** 130–138.

12. Martin, I., Obradovic, B., Treppo, S., Grodzinsky, A. J., Langer, R., Freed, L. E., et al. (2000) Modulation of the mechanical properties of tissue engineered cartilage. *Biorheology* **37,** 141–147.

13. Lee, D. A. and Bader, D. L. (1997) Compressive strains at physiological frequencies influence the metabolism of chondrocytes seeded in agarose. *J. Orthop. Res.* **15,** 181–188.

14. Lee, D. A., Noguchi, T., Frean, S. P., Lees, P., and Bader, D. L. (2000) The influence of mechanical loading on isolated chondrocytes seeded in agarose constructs. *Biorheology* **37,** 149–161.

15. Vunjak-Novakovic, G., Obradovic, B., Martin I., Bursac, P. M., Langer, R., and Freed, L. E. (1998) Dynamic cell seeding of polymer scaffolds for cartilage tissue engineering. *Biotechnol. Progr.* 14,193–202

16. Freed, L. E., Hollander, A. P., Martin I., Barry, J. R., Langer, R., and Vunjak-Novakovic, G. (1998) Chondrogenesis in a cell-polymer-bioreactor system. *Exp. Cell Res*. **240,** 58–65.

14

Microscopic Methods
for the Analysis of Engineered Tissues

Sally Roberts and Janis Menage

1. Introduction
1.1. Range of Microscopic Techniques

Examination of engineered tissues is clearly necessary to evaluate their properties and determine how close they are to those of the original tissue being engineered. Microscopy encompasses a group of techniques that allows the assessment of many parameters, including information on the cells themselves, on their viability, density, proliferation status, morphology, their capacity for protein synthesis, and their cell activity. Microscopy can also be utilized to follow the structure of any scaffold used and to determine whether it is broken down. In addition to examining how the cells interact with it, the scaffold can be examined to establish whether they adhere successfully, which molecules are involved, and whether the cells go on to produce any matrix—and if so, whether it replaces the original scaffold or integrates with it and builds on it.

Different microscopic techniques are best-suited to answer different questions. For example, molecular biology applications such as *in situ* hybridization (ISH), will indicate the cell's gene expression and thus synthetic capabilities, whereas immunohistochemistry demonstrates whether this is put into practice and the cell has actually synthesized specific molecules. Variations of these techniques can be used to undertake cell biology studies in tissue-engineered constructs. For example, by labeling certain proteins with specific antibodies—e.g., Ki67, which are only expressed in certain stages of the cell cycle—proliferating cells can be identified. The most commonly used markers of apoptosis are molecules such as caspase 3, identified by immunohistochemistry, or TdT-mediated dUTP nick-end labeling (TUNEL), which is a modification of *in situ* hybridization. The
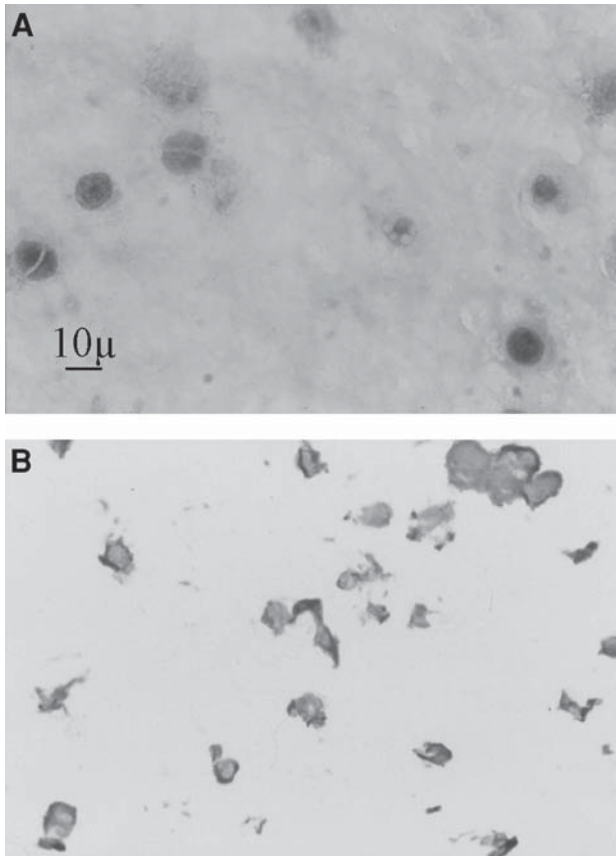
Fig. 1. Alginate beads containing intervertebral disk cells, cultured for 12 d, have been cryo-sectioned and stained with H&E (**A**) and immunostained for keratan sulfate with antibody 5D4 (**B**).

molecules to be studied are many and varied, and can provide information on the cells' ability to produce, and their production of, adhesion molecules, enzymes, cytokines, receptors, and cytoskeletal elements, among others.

Different levels of resolution can be reached, ranging from a magnification of just over 1,—for example, using a dissecting microscope—to 1 million using electron microscopy. In addition, a huge range of possible techniques exist with various potentials, and the directions for these could, and of course do, fill several textbooks *(1,2)*. Thus, this chapter is restricted to what the authors consider to be the most generally applicable and easy-to-implement procedures in a standard laboratory to evaluate tissue-engineered constructs, grown either in vitro (**Figs. 1,2**) or in vivo (**Figs. 3,4**).
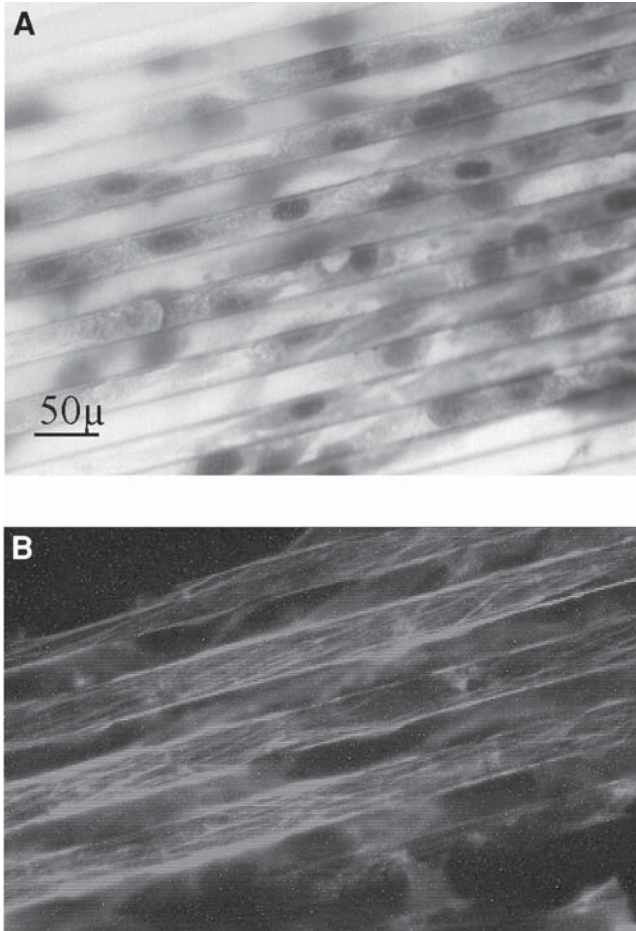
Fig. 2. The morphology of cells—in this case chondrocytes—growing on ridged poly-capralactone can be stained **(A)** with Jenner Giemsa and viewed with normal light and **(B)** for actin in the cytoskeleton, viewed with a fluorescent microscope. (Courtesy of Dr. WEB Johnson, Oswestry, UK.)

Therefore, electron microscopy is not covered at all, because it would only be undertaken by or under the direct guidance of specialized personnel (*see* **Note 1**).

As with any investigation, it is important to define the questions being asked at the outset, and this will help to guide the choice of procedure. For example, the orientation and manner in which the sample is taken may be very important; if so, the sample can be marked with an indelible marker or structure (such as a stitch), so that this information is not lost when the sample arrives in the laboratory in isolation. The sample must then be processed in an appropri-
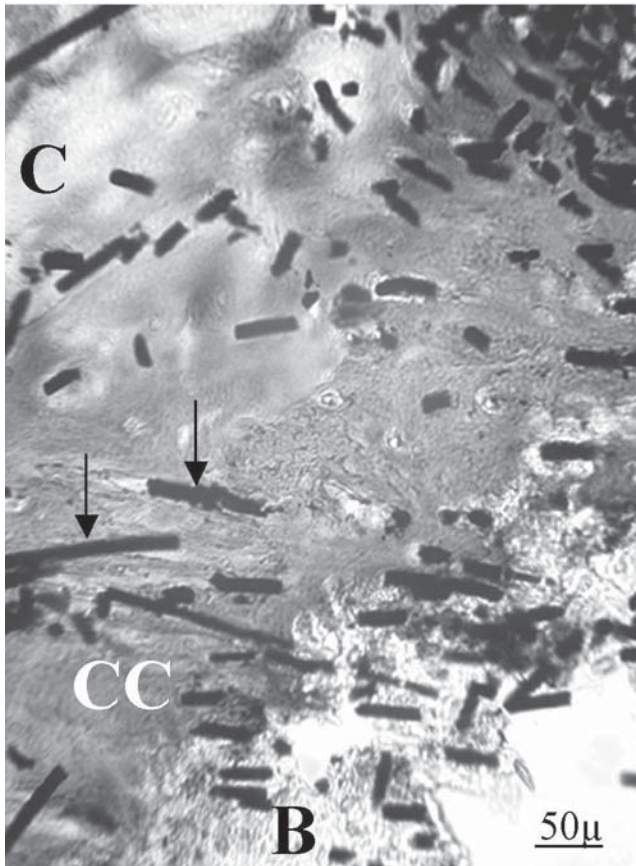
Fig. 3. Frozen sections can be used to cut some very hard material, such as this cartilage (C) with its underlying calcified cartilage (CC) and bone (B) from a knee joint repaired with carbon fiber (*arrows*). The section has been immunostained for type II collagen, and labeled with peroxidase and diamino benzadine tetrachloride (DAB), showing type II collagen to be present in both the calcified and uncalcified cartilage, but not in bone.

ate manner to optimally preserve the feature(s) being investigated. This often involves crosslinking various proteins to fix the molecules in place and retain the structure. Provision of a support medium to allow sectioning and tissue handling may be needed in the form of paraffin wax or plastic resin, which— once its job is done and thin sections of tissue are prepared—must be removed chemically to avoid interference with the staining technique being used. Thus, the physical properties of the structure being evaluated, together with the stability of the protein(s) or molecule(s) being investigated, will help to decide
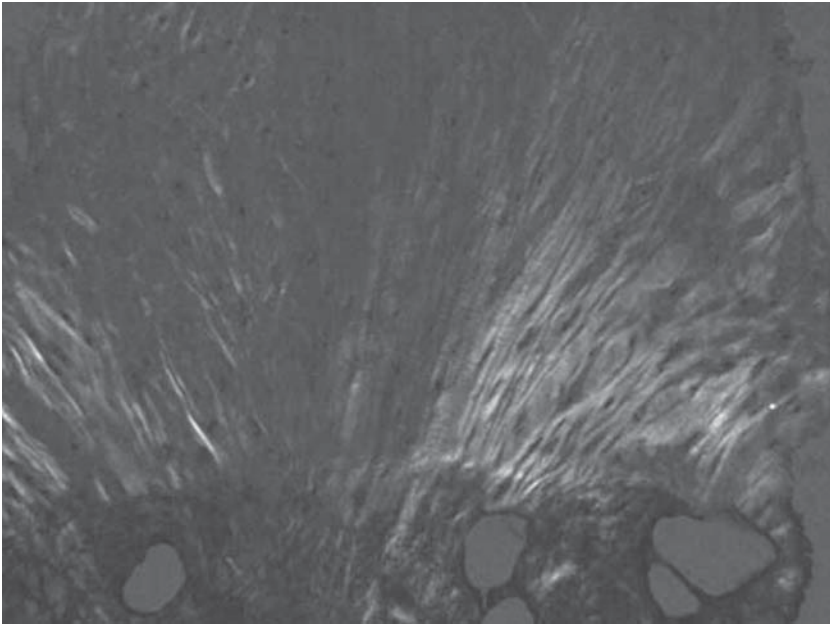
Fig. 4. Biopsy from cartilage repair site treated with autologous chondrocyte transplantation. By viewing with polarized light, it is possible to demonstrate good integration of repair tissue with the underlying calcified tissue of the host by visualizing continuous collagen fibers passing from one region to the other.

which procedures are most appropriate. No knowledge of these will necessitate a trial and error approach! Many commercial preparations are available for several of the chemicals listed. Although these may be convenient, most are relatively simple to make in-house for less money, and the quality or type can be chosen or modified for particular situations.

1.2. Immunohistochemistry

Immunohistochemistry provides an almost limitless capacity for the detection of individual molecules via the use of specific antibodies. Some form of label must be utilized to visualize when the reaction has taken place, and this can be a fluorescent marker such as FITC (fluorescein isothiocyanate) or TRITC (rhodamine), radioactive isotopes (^{14}C or ^{125}I), electron dense materials such as ferritin, or more often, enzymes such as peroxidase or alkaline phosphatase (ALP). The simplest immunohistochemistry method is a direct technique, in which the primary antibody has a label irreversibly attached to it. More often, an indirect technique is used in which the tissue/section/culture is initially reacted with an unlabeled specific antibody and then in a second stage,

a labeled antibody reacts specifically with the first antibody. This method pro-
vides greater sensitivity. Further sensitivity can be obtained with an amplification
layer—for example, using a biotinylated secondary antibody and streptavidin-
linked enzyme system. (Streptavidin binds four molecules of biotin with a very
high affinity.)

Immunohistochemistry can be carried out manually, applying solutions
individually by pipet to each slide. This is preferable if sample numbers are
small or sections are fragile and difficult to handle. The procedure can be
automated to varying extents if appropriate, and this is useful for cytospins
(which are not easy to see on the slide) and homogenous, well-attached sec-
tions, such as alginate bead cultures (**Fig. 1**). It can certainly be advanta-
geous if the antibody steps are carried out with the slides flat. Before adding
antibody to the slides, the slide should be carefully dried around the edge to
prevent excessive dilution of the antibody, but the sections should be kept
moist at all times. Washes should always be thorough. For well-adhered sec-
tions, this process can be carried out in plastic troughs fitted with racks. Fro-
zen sections may be very delicate, especially after some pretreatments, and
require washing each slide individually and with great care to ensure that
sections are not lost.

1.3. In Situ *Hybridization*

ISH allows for the detection and localization of specific nucleic acid
sequences in messenger RNA, and thus expression of specific genes within a
cell; it is estimated that it can detect 5–50 mRNA molecules per cell. The tech-
nique is simple—it uses steps similar to immunohistochemistry, but more of
them—and again, there is room for variation of the conditions, depending on
the probes being used and the questions to be asked *(3)*. As with immunohis-
tochemistry, the results are only as accurate as the probe used initially. ISH is
most commonly carried out on wax sections, but frozen sections can also be
used and the use of cryosections may reduce loss of mRNA during tissue pro-
cessing *(4)*. Paraffin sections of samples that have been processed as for stan-
dard histology are dewaxed and rehydrated prior to permeabilization, which
allows the labeled probe to enter the cell more easily. Sections are then incu-
bated with a chosen probe labeled with, for example, digoxygenin, biotin, or in
the case of fluorescence *is situ* hybridization (FISH), a fluorescent label. (These
labels have mostly now replaced the need to use radioactively labeled probes,
which would need to be demonstrated by autoradiography and are not discussed
here). Bound probe is then detected with the appropriate antiserum labeled
with an enzyme, such as ALP, which is visualized by the addition of the appro-
priate enzyme substrate.

2. Materials

2.1. Dissecting Gear

1. Gloves.
2. Scalpel.
3. Razor blades.
4. Forceps.

These should be clean but not necessarily sterile. When using human engineered tissue, you must take precautions against possible infection of the laboratory personnel, particularly before fixation.

2.2. Fixatives

1. Neutral buffered formalin (NBF, for wax embedding): 100 mL formalin, 900 mL distilled H_2O, 3.5 g sodium dihydrogen orthophosphate, 6.5 g disodium hydrogen orthophosphate, pH 7.4. (NB 40% formaldehyde gas in water is formalin, so 10% formalin, the recipe given here, is equivalent to 4% formaldehyde.)
2. Paraformaldehyde: This contains fewer impurities than NBF, but it is not stable and should be made fresh every 10 d. Heat 4 g paraformaldehyde in 80 mL phosphate-buffered saline (PBS) to approx 60°C, and cool. If not clear, add a few drops of NaOH. Make up to 100 mL and store at 4°C.
   PBS: 2 g KCl, 2 g KH_2PO_4, 80 g NaCl, 11.5 g Na_2HPO_4, make up to 1 L, pH 7.2. Dilute ×10 for use.
3. Alcohol: Alcohols such as ethanol can be used to preserve glycogen and some proteins. They penetrate tissue rapidly, and thus can be used in conjunction with other fixatives, such as formaldehyde, to increase the speed of tissue processing.

Many other fixatives have been modified for preserving specific molecules optimally, for example, Zamboni's fixative for neuropeptides.

2.3. Decalcifying Solutions

These are often necessary for mineralized samples, and the solutions vary in their efficiency and aggressiveness in removing the calcium salts; they are either acids or chelating agents.

The choice of which is used will depend on the type of samples to be studied and how.

1. Formic acid: 10% formic acid in distilled water: 4-mm-thick cancellous bone should decalcify in 48 h. Adjust time according to the size and density of sample.
2. Ethylenediaminetetraacetic acid (EDTA): 15% EDTA, pH 7.3 for 2 wk–3 mo. This is very gentle, and causes little or no tissue damage or loss of staining.
3. EDTA/HCl combined: 0.7 g EDTA, 0.008 g potassium sodium tartrate, 0.14 g Na tartrate; make up to 1 L with distilled water and add 99.2 mL conc. HCl. Decalcify for 10 d maximum.

4. Monitoring systems for decalcification: Ideally, an X-ray setup is used to monitor decalcification (overexposure in decalcifying solution can cause loss of staining by hematoxylin & eosin (H&E), for example. Most pathology laboratories should be able to assist here; alternatively, the texture can be evaluated.

2.4. Equipment for Wax Embedding and Sectioning

The basic facilities needed include:

1. A tissue-processing station.
2. Cassettes to mount the samples in.
3. A microtome for cutting thin sections of tissue (this works best when attached to a highly trained technician!).
4. Water bath (set at temperature just below melting point of wax).
5. Oven for drying slides, 37°–48°C overnight.
6. Storage boxes for microscope slides with sections attached.

2.5. Equipment for Cryopreservation and Sectioning

1. Liquid nitrogen storage vessel for samples.
2. Small stainless-steel Dewar flask for transporting liquid nitrogen and samples.
3. Goggles.
4. Thick insulated gloves.
5. Cryostat (a microtome in a deep-freeze cabinet).
6. Specimen holders or "chucks."
7. Embedding medium (Tissue-tek).
8. Freezing spray.

2.6. Staining Equipment

1. Coplin jars.
2. Flat-ended forceps.
3. Pasteur pipets and a good range of variable volume micropipets, e.g., 1, 50, 100 μL and 1 mL.
4. Plastic racks and troughs.
5. Frosted-ended microscope slides (much easier to label with a pencil than diamond cutter!) and cover slips.
6. Parallel glass rods, 4 cm apart, are very convenient for staining and washing slides manually over a sink.
7. Covered staining trays are required to maintain a humid atmosphere around slides being stained for several hours, such as in immunohistochemistry.
8. Sandwich boxes can be modified easily, but there are very useful, space efficient commercial ones available.
9. Glass rods or a glass syringe can be used for applying mountant to the slides or thin wooden sticks ("applicators") are a very economical, disposable, and "user-friendly" alternative.

10. PAP pens are useful to draw a hydrophobic ring around sections on microscope slides. This retains the solutions around the samples, minimizing the volumes of antibodies and solutions used.

2.7. Enzyme Solutions and Antibodies for Immunohistochemistry

All the enzymes can be made in large quantities and stored as aliquots at –20°C.

1. Hyaluronidase: (sheep testicular, type V), 4800 U/mL in 0.025 *M* sodium chloride (0.145 g), 0.05 *M* sodium acetate (0.41 g) in distilled water, pH 5.0.
2. Chondroitinase ABC: 5 U per vial; add 100 µL of Tris/sodium acetate buffer (1.2 g Tris, 0.8 g sodium acetate in 100 mL distilled water, pH 8.0). Store in 5 µL aliquots at –20°C. For use at 0.25 iu/mL, dilute 5 µL to 1 mL buffer.
3. Trypsin: 0.25% trypsin in PBS when used alone. This can be combined (at 0.2%) with 0.1% hyaluronidase (approx 3000 U/mL in hyaluronidase buffer) for unmasking, e.g., collagen epitopes in wax sections.
4. Pepsin: 0.01% in 0.1 *M* acetic acid.
5. Primary antibody: It is useful to aliquot these (NB: undiluted) in appropriate volumes for the number of slides in a batch and store at –20°C. (As a rough guide, 100 µL of the diluted antibody is sufficient to cover two sections approx 2 cm^2 in area; apply carefully, not touching the section but using the surface tension between the drop on the end of the pipet tip and the slide to "drag" the liquid around.)
6. Secondary antibody: These must have a label attached—usually peroxidase, biotin, or FITC. Care must be taken to choose the appropriate class and species raised against, and to match them to those of the primary antibody. For example, if the primary is a mouse monoclonal IgG$_1$, the secondary antibody must be an anti-mouse IgG$_1$, but can be raised in any species.
7. Controls: Negative, and when possible, positive controls must be routinely carried out with immunohistochemistry. Without these, erroneous interpretation of results can be made. The controls must go through exactly the same process as the test sections. Negative controls should include i) PBS in place of the primary antibody. If there is staining with this, there are major problems—for example, with the detection system. ii) Normal control sera/immunoglobulins. This should be matched to that of the primary antibody in terms of species, immunoglobulin class and concentration. A further check on antibody specificity can be carried out by immunoadsorbing the antibody with the antigen against which it has been raised. This should obliterate the staining.
8. Detection systems: For fluorescent labels, use a non-quenching mountant to prolong the life of the signal. For peroxidase-labeled systems, use either DAB or AEC (AEC is alcohol-soluble, so an aqueous mountant is required and the precipitate fades with time) and for ALP labels use Fast red (also alcohol-soluble) or nitrobluetetrazolium/5-bromo-4-chloro-3-indolyphosphate (NBT/BCIP). The

different colors of these substrates allow dual or triple staining to demonstrate the relative location of more than one antigen at a time.

2.8. In Situ *Hybridization Solutions*

RNA is subject to degradation by the ubiquitous RNases, which are likely to be found on laboratory benches, glassware, and personnel. Thus, great efforts must be made to preserve RNA by inactivating all RNases—e.g., treat all solutions with 0.1% diethylpyrocarbonate (DEPC), treat all glassware in 3% H_2O_2 and bake at 250°C for more than 4 h to destroy the RNases (*see* **Note 2**). Reagents such as Tris buffers (which are destroyed by DEPC), should be made up in inactive DEPC water in RNase-free glassware. Gloves should be worn throughout and changed frequently. Solutions and glassware used for incubations at temperatures other than room temperature should be precooled or preheated.

1. DEPC water: 500 μL DEPC per 500 mL water. Shake, leave overnight at 37°C (this is "active" DEPC water), and autoclave (this is "inactive" DEPC water). Store in a sterile, capped container. No amount of DEPC water can be too great to have in stock when doing ISH!

2. 20X sodium salt citrate (20X SSC): Dissolve 175.3 g NaCl and 88.2 g sodium citrate in 800 mL water and adjust to pH 7. Make up to 1 L. Treat with 1 mL DEPC, shake, leave overnight, and autoclave. Make up various concentrations with DEPC water.

3. Tris-HCl: For 1 *M* Tris-HCl—11.2 g Tris base, 80 mL DEPC water, adjust to pH 7.5 or 9.5 with conc HCl and make up to 100 mL. Alternatively, stock buffers are commercially available that can be diluted with DEPC water. (Tris is damaged by DEPC; therefore, make up with inactive DEPC water—the autoclaving removes the DEPC.)

4. Tris buffer (TBS): 10 mL 1 *M* Tris-HCl pH 7.5, 3 mL 5 *M* NaCl; make up to 100 mL.

5. Modified TBS: 10 mL 1 *M* Tris-HCl, pH 9.5, 2 mL 5 *M* NaCl, 0.406 g $MgCl_2 \cdot 6H_2O$, make up to 100 mL.

6. 10X Modified Denhardt's (PE buffer): 50 mL 1 *M* Tris-HCl, pH 7.5, 1 g tetrasodium pyrophosphate, 2 g polyvinylpyrrolidone, 2 g Ficoll, 10 mL 0.5 *M* EDTA pH 8.0. Make up to 100 mL with inactive DEPC water, dissolve 65°C for 15 min. Store at room temperature. **Caution:** Do not autoclave.

7. Hybridization buffer:
   a. for use with probes: 120 μL 5 *M* NaCl, 100 μL 10X PE, 200 μL 50% dextran, 365 μL DEPC water, 200 μL deionized formamide, 15 μL salmon sperm DNA (boil for 10 min, cool on ice); makes 1 mL. (For riboprobes, 45 μL of water should be replaced with 20 μL dithiothreitol (DTT) (1 *M* in 0.01 *M* sodium acetate, pH 5) and 25 μL tRNA.)
   b. to demonstrate total message: 120 μL 5 *M* NaCl, 100 μL 10X PE, 10 μL salmon sperm DNA, 200 μL 50% polyethylene glycol 6000, 570 μL DEPC water; makes 1 mL.

8. Probes can be oligonucleotides, (many of these are commercially available), cDNA, or complementary RNA (cRNA or riboprobes). Riboprobes are often the most appro-

priate in analyzing tissue-engineered connective tissues for which copy numbers are likely to be low. The following discussion primarily relates to methods using riboprobes. The advantage of riboprobes over DNA probes are: i) their single-stranded nature allows strand-specific probes to be produced, e.g., anti-sense and sense (which can be be used as negative controls). ii) greater sensitivity as probe re-annealing during hybridization is avoided, and the RNA-hybrids are more stable than DNA-hybrids (although this may increase the optimal temperature needed for hybridization and stringency). iii) non-specifically bound probe can be removed by treatment with RNase A, which is very specific for single-stranded RNA *(3)*.

2.9. Chromogens

These are generally substrates for use with enzyme visualization systems in immunohistochemistry or ISH, either in conjunction with i) peroxidase: DAB (brown) or AEC (red-brown) or ii) ALP: Fast red (red) or NBT/BCIP (blue). Because these are toxic, care should be taken to minimize exposure to laboratory personnel. For example, work in a fume cupboard and make in batches that can be aliquoted.

1. 3,3 Diaminobenzidine tetrachloride (DAB): 3 mg in 5 mL PBS; store at –20°C. Add 20 µL of 30% hydrogen peroxide immediately before use, filtering first (millipore filters are convenient). Any surplus must be reacted with H_2O_2 before disposal; soak all glassware in bleach for 24 h before washing.
2. NBT/BCIP: 80 µL of 50 mg/mL BCIP in dimethyl formamide (DMF), 80 µL NBT (75 mg/mL in 70% DMF), 10 µL 1 M levamisole in 10 mL of 0.1 M Tris buffer, pH 9.5.
3. 3-amino-9-ethylcarbazole (AEC): 20 mg dissolved in 5 mL DMF. Mix this with 95 mL of 0.05 M acetate buffer, pH 5.
4. Fast Red: 50 mg fast red, 100 µL of 1 M levamisole, 50 mg naphthol AS-MX in 1 mL DMF. Filter.

2.10. Microscopes

Different microscopes will be required, depending on the task. Inverted microscopes are necessary for viewing cells growing in tissue-culture flasks. They differ from conventional light microscopes because the light source and condensor are above the sample, pointing down, and the objective lenses and the turret are below, pointing up.

1. Darkground illumination or phase contrast are useful for samples and cells that would be transparent and not visible by normal, bright-field methods. Darkground illumination shows up the edges and structures within cells, which shine brightly against a dark background. Phase contrast can provide a large amount of object detail and information by the use of a phase plate that retards some of the light. This, when combined with the rest of the light that has passed through the specimen, forms the images with its "optical staining."
2. Differential interference contrast (Nomarski). Another useful variant is differen-

tial interference contrast (DIC) microscopy when differences in the refractive index and, or the thickness of the specimen alter the light passing through it and give rise to a three-dimensional (3D) or relief image of the sample.

3. Polarized light is a simple modification to normal light microscopy, but one that can provide very useful information—not only precise identification of some individual substances present via their pattern of birefringence, but also how some connective tissues are laid down (**Fig. 4**).

4. A fluorescent microscope is clearly necessary if fluorescent dyes or labels are used as the end point of staining or immunohistochemistry or ISH techniques. The microscope must be fitted with the correct filters to match the appropriate wavelength of the fluorochrome being used. Preferably, it would have special objective lenses, to maximize the light entering them, and low-magnification eye pieces.

5. Confocal microscopes are a recent boon to the microscope field. Most are based on fluorescence, and are a means to optically section through a sample several microns thick. Information gathered from the sequential images at different depths is then used to build a 3D image of the stained features by computer reconstruction.

6. Image analysis. Image capture and quantitative analysis of the images is beyond the scope of this chapter *(5)*. There is a whole spectrum of image-capture systems, ranging from photographic film to digital cameras with a multitude of analytical computer programs to analyze the data *(6–8)*. These will certainly provide many numbers with labels attached: it is important to ascertain exactly what the numbers relate to! Sometimes, more useful, reliable data can still be obtained by carrying out a few manual counts when the filtering systems of the human eye and brain can far exceed the capability of the most sophisticated computer programs.

Treat your microscope as the delicate, precision instrument that it undoubtedly is. Keep it dust free (that's what the dust cover is for) and wipe the lenses regularly, both eye pieces and objectives, with lens tissue (not ordinary tissues off the bench, or worse, from your pocket!) and if using an immersion objective, wipe off all the water or oil following your use and do not leave it to dry for the next person. (Do not use acetone or alcohol to clean the lenses—they can dissolve the cement.)

3. Methods

3.1. Sample Preparation

3.1.1. Fixation

Fixation will be necessary if the sample is to be embedded in paraffin wax or resin.

1. Tissue samples or cultures in 3D scaffolds should be dissected into suitable sizes

depending on their texture and density, and put into the appropriate fixative for 24 h, usually neutral buffered formalin (NBF).

2. Others such as alcohol, acetone or more specialized fixatives can be used, for example, (1) Zamboni's for neural antigens (4–8 h before transferring to sucrose to wash for 24 h ×2, and then snap-freezing *(9)*; or (2) ruthenium hexaammine trichloride for proteoglycans *(10)*.

3. If decalcification is necessary, it is carried out after fixing. The time needed varies widely (from hours to weeks), depending on the sample and decalcifying solution used.

4. If cryosections will be used, initial fixation is not usually done (although it may be necessary in a few cases). Instead, samples are simply cut directly onto microscope slides and then fixed, prior to staining, when the slide is flooded with formalin, paraformaldehyde, acetone, or methanol/acetone mix for 10 min, the first two at room temperature, and the acetone or alcohol at 4°C. Monolayer cultures or cytospins can be treated similarly.

3.1.2. Embedding Procedures (see **Note 3**)

3.1.2.1. WAX EMBEDDING

Equipment for wax embedding is fairly specialized—the services of a histopathology department are recommended. Failing that, an average protocol might be as follows:

1. Take samples out of the formalin.
2. Place in sample cassettes and take through increasing alcohol solutions (70%, 90%) each for 1 h.
3. Take through four changes of industrialized methylated spirits (IMS), two of chloroform, one of xylene and four of melted paraffin wax, under vacuum at 60°C.
4. The samples are set in wax ready for sectioning on a microtome.

3.1.2.2. SNAP-FREEZING (*see* **Note 4**)

1. Cool hexane or isopentane in a small beaker standing in solid CO_2-cooled IMS (*see* **Note 5**), or in liquid N_2 (more difficult to control), until just becoming solid on the bottom.
2. Drop a small piece of sample in cooled hexane for approx 30 s.
3. Blot dry quickly while keeping cold, put into a cold cryovial and store in liquid N_2.
4. To mount the frozen sample onto a metal chuck for sectioning: place a small amount of tissue-tek on the chuck, which is standing in a dish of liquid nitrogen. As the mountant starts freezing (and going opaque), orientate the sample in the mountant and leave to freeze solid.

3.1.3. Coating of Slides (see **Note 6**)

1. Lysine: Wash microscope slides in alcohol and rub dry, preferably until they are "squeaky" clean! Fill a slide rack with clean slides. Immerse in 10% poly-l-lysine

(in distilled water) for 5 min. Drain and air-dry, and keep covered and dust-free at room temperature until needed.

2. APES (aminopropyltriethoxysilane): Fill a metal staining rack with microscope slides. Wash each rack in IMS for 5 min. Air-dry for 5 min (*see* **Note 7**).
   a. Cover with 3% APES in acetone (9 mL in 300 mL) for 5 min. Drain.
   b. Rinse in acetone; dip three times, and drain.
   c. Rinse in distilled water; dip three times, and drain.
   d. Loosely wrap the racks in foil and dry at 37°C overnight. Store at room temperature. They are suitable for use as long as the hydrophobicity is retained.

3.1.4. Sectioning: Wax and Frozen (see **Note 8**)

3.1.4.1. WAX SECTIONING

1. Cut ribbons of wax sections and float them on the surface of the water bath to remove any wrinkles.
2. Tease off individual sections and catch them on microscope slides.
3. Dry the slides overnight at 37°–48°C and store in a dust-free box before use.
4. Wax blocks may be stored long-term, providing a useful archive of material (*see* **Note 9**).

3.1.4.2. FROZEN SECTIONING (see **Notes 10–12**)

1. Cut frozen sections and collect onto slides individually.
2. Several sections may be collected onto 1 slide.
3. Ready cut sections can be stored (after drying for 1 h at RT°C) for several weeks at – 20°C for many stains.

3.2. Standard Staining Procedures

Wax-embedded sections must be deparaffinized and hydrated before staining, whereas frozen sections need no such preparation because the tissue-tek is water-soluble; they can simply be brought to room temperature and air-dried before staining.

3.2.1. Mayer's Hematoxylin and Eosin (H&E) (see Notes 13 and 14)

1. Make stain:
   a. Dissolve 1 g hematoxylin, 50 g K or NH_4 alum, and 0.2 g Na iodate in distilled water, stand overnight at room temperature.
   b. Add 1 g citric acid and 50 g chloral hydrate.
   c. Boil 5 min, cool, and filter; it is then ready for use.
2. Hematoxylin 1–2 min.
3. Wash in tap water.
4. "Blue" in tap water for 2–3 min (*see* **Note 15**).
5. 1% eosin (aqueous) for 30 s.
6. Rinse very quickly in tap water
7. Dehydrate for 2 min in each of 70%, 90%, 100% × 2 alcohol.
8. Clear in xylene ×2.
9. Mount in Pertex, DePeX, or other suitable mountant (*see* **Note 16**).

3.2.2. Toluidine Blue

This is a very useful stain for a quick "look see" and for demonstrating the presence of proteoglycans.

1. Flood slide with toluidine blue (1% aqueous) for 30 s.
2. Wash in tap water.
3. Air-dry (as stain washes out in alcohols).
4. Mount in Pertex.

3.2.3. Safranin O (see **Note 17**)

1. Flood slide with 0.5% safranin O in 0.1 *M* sodium acetate, pH 4.6.
2. Leave on slide for 30 s.
3. Dehydrate very rapidly through the alcohols (*see* **Subheading 3.2.1., step 7**).
4. Clear and mount.

3.2.4. Alcian Blue (see **Note 18**)

1. Stain for 5 min with freshly filtered stain (1.0% in 3% acetic acid, pH 2.5).
2. Wash in water briefly.
3. Dehydrate, clear, and mount in Pertex.

3.2.5. von Kossa

This is a very useful but simple stain to demonstrate mineralization within tissue or constructs.

1. Flood slide with 5% silver nitrate.
2. Put under an ultraviolet (UV) light until brown (approx 3–4 min).
3. Wash with distilled water followed by two quick washes with 2% sodium thiosulfate in water (approx 30 s, taking care not to remove the brown precipitate).
3. Dehydrate, clear, and mount.

3.2.6. van Gieson (see **Note 19**)

1. Make stain:
   a. To 10 mL of 1% aqueous acid fuschin add 100 mL of saturated picric acid.
   b. Boil for 3 min.
   c. Cool and filter.
2. Take sections to water.
3. Stain for 5 min.
4. Rinse in distilled water.
5. Dehydrate and mount.

3.2.7. Acridine Orange

This is used as a nuclear stain and, as with all in this category, care must be taken in handling these chemicals.

1. Stain for 15 min with 50 µL acridine orange in 1 mL medium.
2. Rinse and mount in PBS/glycerol (50:50).

3.2.8. Propidium Iodide

This demonstrates that nucleic acids and can be used as a vital or nuclear stain.

1. Flood slide with 0.1 mg/mL propidium iodide (PI) in PBS.
2. Leave for 15 min.
3. Rinse off before mounting in aqueous mountant.

3.2.9. Trypan Blue

This is a viability stain for cell suspensions, being taken up by dead cells but excluded by the intact membranes of living cells (unless left in trypan blue for a long time!).

1. Prepare 0.4 mg/mL trypan blue in PBS.
2. Mix with equal volumes of cells in culture medium.

3.2.10. Fluorescein Diacetate/Ethidium Bromide

This stains live cells green and dead cells red. It is more sensitive than trypan blue, and supposedly not toxic to the cells, in the short term at least **(12)**.

1. Prepare stock fluorescein diacetate: 5 mg/mL in acetone.
2. Prepare stock ethidium bromide (EB): 200 µg/mL in medium.
3. Mix 5 µL fluorescein diacetate stock solution with 1 mL EB stock.
4. A fresh mixture must be prepared each time, as fluorescein diacetate is only stable for a few minutes in aqueous solution.

3.3. Preparation of Specimens for Immunohistochemistry

3.3.1 Pretreatment Using Enzymes (see **Note 20**)

Tissue sections often need some pretreatment to unmask antigens with epitopes that are unavailable for reactions with the antibody. Culture preparations, especially monolayer, will probably require none.

1. Hyaluronidase is useful for the staining of collagens, as it improves antibody accessibility, for example, by removing glycosaminoglycan (GAG) chains. Use at 4800 U/mL for 2 h at room temperature.
2. Hyaluronidase/trypsin is useful for staining collagens in wax sections. Use 0.1% hyaluronidase and 0.2% trypsin in hyaluronidase buffer at 37°C for 1 h.
3. Chondroitinase ABC for 90 min at room temperature removes the chondroitin sulfate chains.
4. Trypsin for 15 min at 37°C. This can be a useful enzyme to unmask epitopes in wax sections.

3.3.2. Pretreatment Using Reduction and Alkylation

1. Treat with DL-dithiothreitol (DTT; 10 mg/mL in H_2O) for 2 h at 37°C.
2. Wash twice at 2-min intervals with the same volume of sodium iodoacetate (30 mg/mL).

3.3.3. Microwave Pretreatment (see **Note 21**)

This is often necessary to expose antigens in paraffin-embedded samples that have been crosslinked by the formalin fixation.

1. Put slides into a microwaveable plastic rack and staining trough and cover with citrate buffer (0.1 *M*, pH 6.0).
2. Cover with cling film.
3. Puncture holes in film.
4. Microwave on high, for example, for 250 mL for 10 min (800 W); during this time it must have reached a rapid boil.
5. Top up with buffer.
6. Microwave for an additional 10 min (times can be varied according to sample and antigen).
7. Allow to cool.

3.4. Model Immunostaining Protocols

There are endless variations that can be used with immunohistochemistry, depending on the antigen to be investigated, the form of primary antibody (whether mono- or polyclonal) and whether the section is wax embedded or frozen. The following are examples that may be used as a starting point if the investigator has no guidelines (*see* **Notes 22–27**).

3.4.1. Protocol for Polyclonal Antibodies, Such as Collagens, on Frozen-Tissue Sections

1. Cut sections (7 μm thick) onto poly-L-lysine coated slides; store at –20°C and allow to come to room temperature when ready to immunostain. Ensure that the slides are dry before starting. Most steps are carried out at room temperature with washes (at least three) in between each step using PBS for 5 min.
2. Treat sections with hyaluronidase for 2 h.
3. Fix in 10% formalin in PBS for 10 min.
4. Incubate with primary antibody (titer to be established individually)—for example, raised in rabbit—diluted in PBS for 30 min (or normal serum or PBS for negative controls).
5. Incubate with peroxidase-labeled secondary antibody—for example anti-rabbit, (dilution 1 in 50 in PBS) and 10% normal serum, of the same species as the sample being tested for 30 min.
6. Develop color with DAB for 6 min. Dehydrate through a series of isopropyl alcohols (70, 90, and 100% × 2), clear in xylene × 2 and mount in Pertex.

3.4.2. Protocol for Monoclonal Antibodies on Wax Sections With Biotin-Streptavidin Amplification

1. Prepare, process, and paraffin-embed formalin-fixed tissue.
2. Cut into 5-μ-thick sections and collect onto uncoated slides.

3. Dewax before staining in two changes of xylene and rehydrate through a series of alcohols to PBS.
4. Pretreat—for example, for collagen antibodies—with hyaluronidase and trypsin for 1 h at 37°C.
5. Incubate with primary antibody diluted in PBS for 30 min (or normal Ig or PBS for negative controls).
6. Incubate with biotinylated secondary antibody for 30 min, with normal serum of the same species in which this antibody is raised.
7. Block endogenous peroxidase with 0.3% hydrogen peroxide in methanol for 30 min.
8. Incubate with peroxidase-labeled streptavidin (often called ABC complex in kits, which has been previously mixed in PBS and left to stand for 30 min).
9. Stain with DAB for 6 min. Dehydrate through series of isopropyl alcohols, clear in xylene, and mount in Pertex.

3.5. In Situ *Hybridization*

3.5.1. Sample Fixation

Fixation varies depending on the sample and subsequent treatment. Isolated cells need only approx 20 min fixation, compared to 2–3 h or 24 h for samples greater than 1 mm or 1 cm thickness, respectively. mRNA can be lost because of fixation. A good starting point is 4% paraformaldehyde, as the tissue usually requires no permeabilization after that. Ten percent NBF is also suitable, but then permeabilization will be necessary.

3.5.2. Permeabilization

Permeabilization must be optimized for each probe. The extent of permeabilization will depend on the type and extent of fixation, the tissue and section thickness, and the length of the probe. Various methods include acid treatment (e.g., 0.2 M HCl), detergent (e.g., 0.1–0.3% Triton X), alcohols or proteases (such as Proteinase K, 1–100 µg/mL in 50 mM Tris-HCl, pH 7.5). Following permeabilization, the tissue must be re-fixed to maintain tissue structure.

3.5.3. Pre-Hybridization

This is designed to decrease background, nonspecific binding of the probe. Incubation of the sections is carried out as for hybridization, but without the probe added. Thus, any "sticky" sites are blocked by sodium pyrophosphate or unlabeled nucleic acids—e.g., salmon sperm DNA. The value of prehybridization is a matter of debate, but it may depend on the individual system. If nonspecific binding is a problem, further treatment—such as with 0.25% acetic anhydride in 0.1 M triethanolamine, pH 8.0—may be used to block the basic groups on the nucleic acids.

3.5.4. Hybridization

Hybridization occurs when two complementary strands of DNA or RNA come together to form a stable double helix. This begins with nucleation, when there is an initial association between two short complementary regions, followed by a rapid association of adjacent sections, known as "zippering." Many factors affect the efficiency of this process, including the probe concentration and length and the stringency of the hybridization (e.g., temperature, or concentration of formamide or salt). For example, a greater probe size enhances the rate of hybridization and affects the melting temperature (T_m) of the probe. As the temperature is raised, the rate of hybridization increases until T_m is approached, when the rate drops off rapidly. Salt (such as SSC or NaCl) controls the stringency of the probe, and a high salt concentration favors binding. Formamide is a denaturing agent that destabilizes double-stranded nucleic acids by disrupting hydrogen bonds. This reduces the temperature required for optimal re-annealing of the probe, and thus minimizes damage to the sample, which can occur at high temperatures. Hybridization mixes can also include accelerators such as dextran sulfate or polyethylene glycol 6000. These large molecules increase the rate of hybridization by increasing the chance of probe/target interactions because of the space they occupy (*see* **Note 28**).

3.5.5. Post-Hybridization

Unlike hybridization, which is usually carried out at low stringency conditions (so allowing nonspecific binding), post-hybridization is carried out with greater stringency (by controlling the temperature and/or salt and formamide concentration) to reduce the nonspecific binding.

3.5.6. Signal Amplification and Indicator Systems

Amplification can be achieved as in immunohistochemistry—for example, with anti-biotin antibodies, followed by enzyme-linked streptavidin label and indicator systems using ALP or peroxidase.

3.5.7. Model Protocol for Riboprobes

As with immunohistochemistry, endless variations can be used, depending on factors such as the tissue or probe. Thus, the following serves only as a guide, which may be modified in many different ways such as the permeabilization (e.g., concentration of proteinase K), the temperature for hybridization with the probe, and the stringency of post-hybridization washes (by varying the strength of SSC of washing buffers from 0.1–2X SSC, or the levels of formamide or the heat of the washes [37–45°C]). It is extremely easy to misinterpret information from ISH studies. The use of controls is therefore very

important, for example the comparison between sense and anti-sense probes on serial sections is essential when using riboprobes.

1. Collect 4-μ-thick paraffin sections onto APES-coated slides and dry overnight at 60°C.
2. Dewax the sections as follows: 3×5 min in xylene, 4×2 min in IMS, 10 min DEPC water, 20 min 0.2 *N* HCl, 2×3 min in 2X SSC.
3. Place slides in 0.05 *M* prewarmed Tris for 3 min at 37°C before incubating with 1–100 μg/mL of proteinase K in 0.05 *M* Tris for 1 h at 37°C to permeabilize the sections (the optimal proteinase concentration must be established for each probe).
4. Rinse slides in PBS or 0.2% glycine to inactivate the proteinase K for 2×3 min at room temperature before re-fixing in 0.4% paraformaldehyde for 20 min at 4°C and washing in PBS for 3 min.
5. Cover sections with pre-hybridization buffer (e.g., hybridization buffer without the probe) for 1 h at 37°C before adding the digoxygenin-labeled probe in buffer to the slide, placing a cover slip on top. This can be sealed carefully with a thin layer of nail varnish (although in our experience this has proved unnecessary) and incubating overnight at T_m in a moist box (the temperature should be optimized to maximize binding).
6. Soak slides in 4X SSC at room temperature until the varnish is soft (not necessary if varnish is not used). Carefully remove the cover slip, tip off the hybridization solution and incubate the slides with 3×10 min washes of the appropriate SSC (2–0.2 SSC), prewarmed at 37°C before rinsing for 10 min at room temperature in 2X SSC. (These temperatures and times can be varied according to the probe.)
7. Block with 3% BSA, 0.1% Triton X in TBS, pH 7.6 for 30 min at room temperature and rinse with TBS for 5 min.
8. Incubate sections with enzyme-labeled (e.g., ALP) anti-digoxygenin antibody made up in blocking solution (as in **step 7**), for 60 min at room temperature.
9. Wash in blocking solution diluted 1:30 in TBS for 2×5 min.
10. Wash in ALP buffer (0.1 *M* Tris-HCl, pH 9.5, 50 m*M* MgCl$_2$·6H$_2$O, 0.1 *M* NaCl).
11. Add fresh substrate for 1 h before washing, air-drying, and mounting in Pertex as for immunohistochemistry.

3.5.8. Model Protocol for Total Message

It is advisable to carry out this procedure to check on the preservation of RNA during sample fixation, particularly if using archive material. The procedure is basically as in **step 2–5** in **Subheading 3.5.7.**, i.e., sections are dewaxed, treated with proteinase K (approx 10 μg/mL), washed and fixed before hybridizing and post-labeling all mRNA with a digoxygenin-labeled polydT. An ALP-labeled antibody to digoxygenin can also be used to visualize labeling. (TUNEL [TdT-mediated dUTP nick-end labeling] is a variation on this method, in which DNA fragments are stained by using terminal deoxynucleotidyl transferase [TdT] to polymerize labeled nucleotides onto the ends of "nicked" DNA.)

Labeling for total message is as in the previous protocol except:

1. A different hybridization buffer is used (*see* **item 7** in **Subheading 2.9.**).
2. Label the poly dT probe with digoxygenin using TdT: 10 µL 5XTdT buffer (provided in kit), 3.5 µL dTTP, 1 µL digoxygenin-11-dUTP, 5-µL probe (10 pmol), 30 µL DEPC water, 1 µL TdT; incubate at 37°C for 15 min Stop the reaction with 5 µL 0.2 *M* EDTA (this is sufficient hybridization solution for 1 mL—e.g., add 950 µL hybridization buffer).
3. Hybridize with labeled probe overnight at 37°C.
4. Carry out the post-hybridization washes with 2X SSC at 37°C and then 10 min with 2X SSC at room temperature.
5. Block with 0.1% bovine serum albumin (BSA); 0.1% Triton X in modified TBS with $MgCl_2$.
6. Wash and incubate with ALP labeled anti-digoxygenin antibody and continue as in **Subheading 3.5.7.**

4. Notes

1. Many of the protocols included here are personal experiences—they do not come with guarantees, but hopefully will be helpful as starting points! Each setup, particularly for immunohistochemistry and ISH, needs "tweaking" to optimize—for example, unmasking the antigen or nucleic acids, blocking nonspecific staining, and establishing the ideal antibody titer or stringency conditions.
2. Take care with storing glassware, as when used for ISH and keep it RNase-free. For example, keep it all in a specified area, and wear gloves when handling. If possible, store deep-frozen items on the top shelf of the deep-freeze, keeping them exclusively for ISH reagents and away from where tissue is stored.
3. The choice of embedding medium depends on the physical properties and analyses to be carried out on the samples. Snap-freezing is the quickest and simplest procedure and the method of choice for immunohistochemistry of most antigens. However, samples should be stored at at least –80°C and preferably at –180°C in liquid nitrogen, and the quality of morphological preservation is not as good as when samples are embedded in paraffin wax. However, paraffin-embedding may damage some antigens, rendering them unsuitable for immunological recognition. Embedding with either epoxy or acrylic resin is the method of choice for harder materials, and has the added advantage that the same sample is sometimes able to be viewed at both the light and electron microscope level. It takes many days to resin-embed, and limited details have been included on this process as it is likely that specialized help would be needed and those carrying it out could provide the necessary expertise.
4. During snap-freezing, care must be taken to keep everything in contact with the sample very cold—if it warms up inadvertently, water crystal formation can result and damage the morphology of the samples (freezing damage).
5. Small quantities of solid CO_2 can be obtained using a cylinder of CO_2 with a special adapter.

6. Carry out this coating procedure in a fume cupboard. **Caution:** care must be taken when handling APES, and particularly with its disposal.

7. If doing this procedure for ISH, the slides should be baked in metal racks, covered with foil, at 250°C for 3 h before coating. (Remember to wear gloves to avoid RNase contamination.)

8. Section thickness varies, and depends on what one is looking at. As a rough guide, however, wax sections are usually cut at 5 μ, frozen at 7–10 μ, and resin at 2–8 μ. For some structures such as blood vessels or nerves, or when using confocal microscopy, it can be useful to cut thicker sections—for example, up to 30 μ—to obtain more three-dimensional information. Different microtomes are required for each medium. For all, the sharpness (and the angle) of the knife is critical to obtain satisfactory sections.

9. If you have problems with section cutting, the most common cause with both wax and frozen sections is the knife getting blunt. Move the knife along to a sharper edge. (It is useful to always go in the same direction to prevent using previously blunted areas.) It is important to keep the knife free of debris. Other difficulties may occur because the knife angle or anti-roll bar is in slightly the wrong position. A pattern of alternating thick/thin sections indicates that something is loose, either on the microtome itself or in the specimen, which may not be firmly set in the mountant. Many problems may arise during embedding and sectioning. The best advice is to get someone skilled to do it if you can.

10. Frozen sections can be prepared from many substances used in tissue engineering, including alginate (**Fig. 1**), agarose, carbon fiber, PLA, hyaluronan, and collagen gels and capralactone (**Fig. 2**). It is often useful to start investigations with frozen sections; they can be obtained with surprisingly hard and mineralized material without decalcification (**Figs. 3,4**). As long as there is access to a cryostat, the other equipment is minimal, and is available in most laboratories. It is quick, results can be obtained within minutes or hours, and it is generally the best technique for antigen preservation.

11. The temperature for cutting frozen sections varies from one tissue to another, and the ideal temperature depends on the consistency of the sample and fat content. Highly collagenous and firm connective tissues, for example, are cut –28 to –30°C, whereas the ideal for softer tissues or samples such as alginate beads may be –15 to –20°C. Cutting is more difficult with mixed textures and densities—for example, cells on a rigid scaffold.

12. Ensure that frozen sections are dry before storage; keep in a deep-freeze in sealed boxes to avoid ice crystal formation.

13. H&E is the most widely used histological stain because it clearly demonstrates many different tissue structures. Hematoxylin stains cell nuclei blue-black, and eosin is an anionic dye that stains cell cytoplasm and connective tissue fibers pink, red, or orange.

14. Variation in "standard" techniques can be vast; for example H&E is very widely used. However, there are a multitude of different hematoxylins such as Harris's, Ehrlich's, or Mayer's, which can exist at different stages of ripening. The shelf

life, which can be extended dramatically by careful storage in many cases, is very important with hematoxylin—it *does* go off!

15. Blueing with tap water is another variable, which is dependent on the pH of the local water supply! It can be substituted with Scott's solution (7 g sodium bicarbonate, 40 g magnesium sulfate in 1 L) in areas with tap water of a low pH. Differentiation in acid alcohol (10 mL of 1 *N* HCl and 70% alcohol, made up to 1 L) may be necessary for some hematoxylins.

16. These times are a starting point only. They will vary if a different hematoxylin is used, or wax sections, or, for example, if the hematoxylin is to be used as a counterstain, when the time of exposure is minimal—the slide flooded and then tipped off immediately before washing in water for approx 1 min. The eosin can be washed out by the inexperienced—if difficulties arise, omit the wash and go straight to 70% alcohol.

17. In our experience, this is a very unreliable stain, varying not only from batch to batch, but even between different sections on the same slide. Thus, it is not recommended, but is included because it is so often mentioned in the literature.

18. This cationic dye links with sulfate and carboxyl radicals in sections; by varying the pH between 0.2 and 2.5 the level of sulfation can be differentiated. Further modification of the ionic strengths of the dye can differentiate between sulfate and carboxyl groups in the critical electrolyte concentration technique *(11)*.

19. Microwaving is commonly used in connective tissue histology because it stains collagen fibers red (but not immature collagen; for that, use trichrome stain). It can be used in conjunction with hematoxylin and other stains.

20. There are many other enzyme cocktails that are used with specific antibodies. For example, a chondroitinase and keratanase mixture is used for some proteoglycan epitopes.

21. Microwaving works reasonably well for many antigens, but can damage the structure of the sample. Modifications include carrying it out in a plastic pressure cooker inside the microwave or varying the pH of the buffer. Use a Tris-based buffer for high pH or glycine-based for low pH .

22. Immunohistochemistry is only as specific as the antibody being used—at best! Choosing a reliable, well-characterized antibody is of paramount importance. Commercially available antibodies may or may not fit into this category.

23. Immunohistochemistry troubleshooting: Immunohistochemical staining is a lengthy process, lasting a few hours or being carried out over a period of two days. Each step is inherently simple. With care and patience it need not be daunting. Establish a protocol that works and maintain it to minimize variation between batches of slides. If you have no staining: i) remember that processing of the sample to wax embedding may destroy or mask the antigen or epitope that you are looking for. Recent advances in unmasking techniques such as microwaving may be useful. ii) During storage of frozen sections, some epitopes may be subject to breakdown, especially if they undergo freeze-thawing cycles. A "frost-free" deep-freeze should be avoided. Likewise, primary antibodies can lose activity if incorrectly stored; it is advisable to aliquot and store them in the deep-freeze,

retaining only a small volume at 4°C. Alternatively add sodium azide. iii) It is always advisable to check that the correct secondary antibody has been used, e.g., reacting against the correct species and class of immunoglobulin. iv) If you have nonspecific staining: try blocking, filtering or making fresh solutions.

24. In designing these protocols, it is always important to match species and controls. Ensure adequate coverage of the sections, and do not allow them to dry out during any incubation. These can be carried out at 37°C, which sometimes improves reactivity. The level of blocking depends on what you are staining. For example, monolayer cultures need very little (although there are kits available for blocking biotin in tissue-culture systems if using a biotin label at all), whereas tissue containing bone marrow with much endogenous peroxidase requires a lot of blocking.

25. If staining is weak, it could be improved by:
    a. Antibody concentration. Ideally, set up a range of dilutions initially to find the optimum concentration.
    b. Length of incubation time. Thirty minutes is often adequate but it can be 1–2 h or overnight.
    The temperature at which incubation is carried out can also be varied from 4–37°C. If long incubation times are required, such as overnight, it is often carried out at 4°C. If incubating at a higher temperature, take measures to ensure that the sections do not dry out (it may thus be more expensive in terms of antibody use).

26. If there is nonspecific staining:
    1. Try alternative blocking steps. For example:
       a. Block endogenous peroxidase with 0.3–3% hydrogen peroxide (usually 0.3%) in methanol or PBS for 30 min at room temperature. For monoclonal primaries, this may be best carried out after the incubation of the primary antibody; with polyclonals it can be before or after incubating with the primary.
       b. Add 2–10% normal serum of the same species as the sample. This can be done as a separate step for 10 min at room temperature before the secondary antibody incubation, or added in with the secondary antibody.
       c. 2–10% normal serum of the same species in which the secondary antibody is raised can be added in a similar manner.
       d. Bovine serum albumin (BSA) immunohistochemical grade can be added similarly, or antibodies can be made up in 0.3% BSA.
    2. Avoid an "edge effect" by ensuring adequate coverage of the section, and make sure that the slides have not dried out at any stage.
    3. Keep dehydrating and clearing solutions clean.

27. "Advanced" immunohistochemistry: Further complexities can be added to the staining protocol by counterstaining. Nuclear stains, such as hematoxylin or PI or EB if using a fluorescent system, can be very useful. It is important to keep them light and distinct, so that they do not interfere with the interpretation of the

immunostaining. Dual or even triple labeling is another useful modification, but it has difficulties. Of course, it is always necessary to choose different colored substrates for each label. Even so, be warned: dark brown, red, and blue can all look surprisingly similar on a microscope slide!

28. T_m can be calculated for RNA:RNA hybridization by the following equation:

$$T_m = 79.8 + 58.4(FGC) + 11.8(FGC)^2 + 18.5 \log m - (820/L) - 0.35\% \, f - \% \text{ mismatch} \quad (1)$$

where: FGC = mole fraction GC; L = length of probe; m = mole valent cation; % f = % of formamide; and 1% mismatch lowers T_m by 1°C, 10% by 10°C.

References

1. Bancroft, J.D. and Cook, H.C., eds. (1994) *Manual of Histological Techniques and their Diagnostic Application.* Churchill Livingstone, Edinburgh, UK.
2. Bancroft, J. D. and Stevens, A., eds. (1982) *Theory and Practice of Histological Techniques.* 2nd ed. Churchill Livingstone, Edinburgh, UK.
3. Durrant, I. and Cunningham, M. (1995) Synthesis of riboprobes, in *Gene Probes 1. A Practical Approach* (Hames, B. D. and Higgins, S. J., eds.), Oxford University Press, pp. 190–210.
4. Decimo, D., Georges-Labouesse, E., and Dollé, P. (1995) In situ hybridisation of nucleic acid probes to cellular RNA, in *Gene Probes 2. A Practical Approach.* (Hames, B. D. and Higgins, S. J., eds.), Oxford University Press, pp. 183–210.
5. Russ J.C., ed. (1994) *The Image Processing Handbook*. 2nd ed. CRC Press, Boca Raton, FL.
6. Barker, N. J., Zahurak, M., Olsen, J. L., Nadasdy, T., Racusen, L.C., and Hrusan, R. H. (1998) Digital imaging of black and white photomicrographs. *Am. J. Surg. Path*. **22,** 1411–1416.
7. Bradbury, S. (1990) Photomicrography, in *In Situ Hybridization: Principles and Practice* (Polak, J. M. and McGee, J. O'D., eds.), Oxford University Press. Oxford, UK.
8. Cruz-Orive, L. M. and Weibel, E. R. (1990) Recent stereological methods for cell biology: a brief survey. *Am. J. Physiol.* **258,** L148–L156.
9. Ashton, I. K., Roberts, S., Jaffray, D. C., Polak, J. M., and Eisenstein, S. M. (1994) Neuropeptides in the human intervertebral disc. *J. Orthop. Res*. **12,** 186–192.
10. Hunziker, E. B., Ludi, A., and Herrmann, W. (1992) Preservation of cartilage matrix proteoglycans using cationic dyes chemically related to ruthenium hexaammine trichloride. *J. Histochem. Cytochem.* **40,** 909–917.
11. Scott, J. E. and Dorling, J. (1965) Differential Staining of Acid Glycosaminoglycans (mucopolysaccharides) by Alcian Blue in Salt Solutions. *Histochemistry* **5,** 221–233.
12. Gray, D. W. R. and Morris, P. J. (1987) The use of fluoroscein diacetate and ethidium bromide as a viability stain for isolated islets of langerhans. *Stain Techn.* **62,** 373–381.

15

Transmission Electron Microscopy
of Tissue-Polymer Constructs

Paul V. Hatton

1. Introduction

Numerous publications have described the histology of tissue-engineered constructs and tissue-biomaterial interfaces observed with the light microscope *(1–5)*. Indeed, this approach has become a routine method for the evaluation of the biological quality of engineered tissues. Additional microscopical techniques, including immunohistochemistry and confocal microscopy, have also been described. These methods have enabled the localization of important biological molecules in the tissue-engineered construct. However, all of these techniques are limited to describing relatively gross structural features, and they give little insight into the ultrastructural relationships between cells and biomaterials within a construct. Scanning electron microscopy (SEM) has been applied more recently to the study of constructs, but it too provides only limited information and not the "fine detail" of cell-biomaterial interaction *(6,7)*. Despite the limitations noted here, relatively little research has been reported in which the transmission electron microscope (TEM) has been used to study the ultrastructure of cell-polymer constructs. This may be partly because of the difficulties associated with specimen preparation when living tissues and materials are both present. However, these difficulties are not insurmountable. Studies of the cell-biomaterial interface using electron microscopy have been reported in the general field of biomaterials and medical devices *(8–11)*. Here, they have enabled researchers to gain a greater understanding of the response of cells and tissues to biomaterial surfaces. This pioneering work has also contributed to the development of methods to prepare tissue-material "composites" for study with the TEM.

Electron microscopy takes advantage of the superior resolving power of the electron compared to light. Electrons do not travel far through air or other substances, and work with the TEM must therefore be performed under a high vacuum. Although this has not proved particularly problematical in the study of many materials, wet and fragile biological specimens present a particular challenge. Specific techniques have been developed during the last half-century to enable biologists to prepare tissues for examination in the TEM. First, the tissue must be stabilized, usually via treatment with a chemical fixative. The water must then be removed, and finally the specimen must be infiltrated with a resin that, following polymerization, allows the cutting of ultra-thin (< 200 nm) sections that are stable in the environment of the TEM. The principal challenge in the preparation of tissue-polymer constructs is generally the treatment of the biological component, and the risk of artefact creation. Fortunately, many of the established methods for preparing biological materials may be applied to constructs after appropriate modification, and the latter has in turn been informed by experiences gained from the study of composite tissue-biomaterial specimens in the areas of medical devices and biomaterials research. The goal of this chapter is to describe methods that allow the preparation of tissue-polymer constructs for examination with the TEM, and illustrate the value of these to the emerging interdisciplinary field of tissue engineering. The reader is referred to standard electron microscopy textbooks for additional techniques or background information on methodology *(12,13)*.

As a result of the adaptation of established methods and the application of techniques developed in the area of biomaterial research, several papers describing TEM studies of engineered cell-polymer constructs have appeared in recent years. These have all used methods similar to those described in this chapter to gain new insights into the relationship between cultured tissues and scaffold biomaterials. Van Dorp and colleagues have evaluated Polyactive® as a substrate for fibroblast and keratinocyte culture related to skin tissue engineering *(14)*. Marra et al. have investigated engineered bone-like tissues on composite scaffold biomaterials using a range of techniques including TEM *(15)*. In addition, an application of TEM in the evaluation of tissue engineering using non-degradable scaffolds has been reported recently *(16)*. These studies are described in **Table 1**, along with comments on the methods employed to prepare tissue-polymer constructs. It should be noted that published papers rarely provide sufficient details of laboratory methods for repetition of the work. Our own laboratory methods for the preparation of cell-polymer constructs for TEM studies are therefore described here in detail.

Table 1
Comparison of Methods to Prepare Tissue-Polymer Constructs for TEM

Author	Study	Notes on methods different to those described here
Hatton et al. *(10)*	Rat bone marrow stromal cells (BMSC) cultured in poly(glycolic acid) (PGA)-woven scaffolds.	As described in this chapter.
Van Dorp et al. *(14)*	Human fibroblasts and epidermal keratinocytes cultured on Polyactive® copolymer.	Fixed in 2% formaldehyde and 1.5% glutaraldehyde in 0.2 M cacodylate buffer for 2–4 h at 4°C. Secondary fixation in OsO_4 (1%) and $K_4Fe(CN)_6$ (1.5%) for 1 h.
Marra et al. *(15)*	Poly(caprolactone) (PCL) and poly(D,L-lactic acid-co-glycolic acid) (PLGA) blends and homopolymers were combined with hydroxyapatite and evaluated for bone-tissue engineering using rabbit BMSC.	No details given of primary fixation. Postfixed in 1% OsO_4 in phosphate buffer for 1 h.
Springer et al. *(16)*	Human and porcine chondrocytes cultured on range of polymer scaffolds including expanded poly(tetrafluorethylene) and PGA.	Fixation 2.5% glutaraldehyde/ 1.5% formaldehyde in sodium cacodylate buffer. Secondary fixation in 1% OsO_4

2. Materials

2.1. Fixation and Dehydration

1. Tissue-engineered cell-polymer construct.
2. Scalpel and fine forceps.
3. Sodium cacodylate buffer (0.1 M). This buffer contains arsenic, and should be handled with care.
4. Glutaraldehyde (3% v/v) in 0.1 M sodium cacodylate buffer. Glutaraldehyde is an irritant and should be handled with care, using gloves and a fume cabinet.
5. Solution (1% w/v) of osmium tetroxide (OsO_4) in water. **Caution:** Note that this agent is toxic, and has the potential to cause damage to the cornea and blindness. It should only be used in a fume cabinet.

6. Absolute ethanol (dried over anhydrous calcium carbonate).
7. Distilled water.

2.2. Infiltration and Embedding

1. Propylene oxide (1,2-epoxy propane).
2. Embedding resin (e.g., Spurr's resin). **Caution:** Note that many resins contain irritants and/or toxic substances, and they should always be prepared and handled in a fume cabinet until polymerized.
3. Rotating specimen holder.
4. Paper and pencil to make labels.
5. Mold or capsules (gelatin or polypropylene).
6. Polymerization oven (60°C).

2.3. Sectioning and Staining

1. Diamond knife.
2. Ultramicrotome.
3. Fresh distilled water.
4. Copper grids.
5. Saturated solution of uranyl acetate in methanol.
6. Lead citrate solution.
7. Fine EM forceps.

3. Methods

Caution: Many chemicals described here present a potential health hazard. It is strongly recommended that all stages up to and including polymerization are conducted in a fume cabinet with appropriate protective clothing, including latex gloves.

3.1. Fixation and Dehydration

1. Dissect out small (1 mm^3) pieces of engineered tissue construct, using scalpel, and transfer to specimen pot containing 0.1 *M* sodium cacodylate buffer (*see* **Note 1**). The same pot may be used for all the following procedures up to embedding.
2. Wash in fresh buffer (1 min) and then replace with fixative (3% v/v glutaraldehyde in 0.1 *M* sodium cacodylate buffer). Fix for 1 h at room temperature and wash with fresh buffer (15 min).
3. Replace buffer wash with small volume of 1% osmium tetroxide (OsO$_4$) solution (sufficient to cover the specimen) for 1 h. Wash with distilled water (15 min, *see* **Note 2**).
4. Replace with graded series of ethanol-water mixtures according to the following schedule:

   30% (v/v) ethanol   15 min
   50%   15 min
   70%   15 min
   90%   15 min

100%   15 min
100%   15 min

Alternative dehydration sequences may be based on other solvents (*see* **Note 3**).

3.2. Infiltration and Embedding

1. If ethanol was used to dehydrate tissues, replace this with propylene oxide (15–30 min).
2. Prepare embedding resin. Epoxy resins are the material of choice, and Spurr's resin has worked well in our laboratory (*see* **Note 4**):
   Epoxide 1, ERL 4206   10 g
   Epoxide 2, DER 736   6 g
   Hardener, NSA   26 g
   Accelerator, DMAE   0.4 g
   Mix thoroughly before use.
3. Replace propylene oxide with 50:50 (v/v) mixture of propylene oxide:resin. Leave for 8–16 h (overnight) on rotating specimen holder with cap on specimen pot.
4. Replace 50:50 mixture with fresh resin. Change for freshly prepared resin every 24 h for 3 d.
5. Place specimen in fresh resin for 1 h. Transfer specimens to capsule or mold to be used for polymerization. Add label as appropriate (*see* **Note 5**). Fill capsule or mold with fresh resin.
6. Transfer the specimens to an oven and polymerize for 16 h at 60°C (or according to instructions for resin used).

3.3. Sectioning and Staining

1. Remove blocks from capsules/molds.
2. Trim excess resin with sharp blade (scalpel or razor blade) to expose specimen.
3. Mount in ultramicrotome and prepare specimen for sectioning by further trimming with glass knives. Specialized technical assistance or training will be required to use the ultramicrotome.
4. Using a diamond knife, cut ultra-thin sections and float these onto water bath on knife (*see* **Note 6**).
5. Collect sections on copper grids (*see* **Notes 7** and **8**) and allow to air-dry.
6. Stain sections on grid using a saturated solution of uranyl acetate in methanol. Wash in distilled water (3×) and stain using lead citrate. Rinse in distilled water and air-dry (*see* **Note 9**).

The sections are now ready to view in the TEM. Examples of engineered tissue-polymer constructs prepared using the methods described here are given in **Figs. 1–3**.

4. Notes

1. Small (1 mm^3) pieces of construct are ideal for fixation and dehydration. It may be possible to achieve good results with larger specimens, although to a large
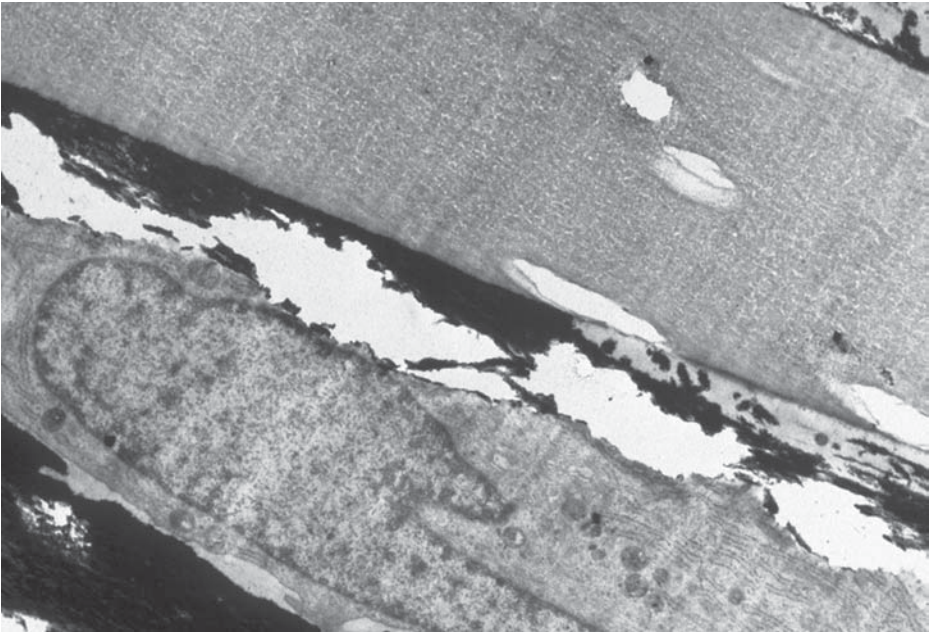
Fig. 1. Bone-like tissue-polymer construct formed by culture of mesenchymal stem cells (MSC) (rat bone marrow) with woven poly(glycolic acid) (PGA) membrane (Biofix®, Tampere, Finland). An osteocyte-like cell is separated from adjacent PGA fiber by a mineralised collagenous extracellular matrix (ECM). Note slight damage caused during sectioning, most likely caused by mineralization of the ECM. Field width = 30 μm.

    degree this depends upon the porosity and density of the construct. If sufficient material is available, then experimentation with various sizes of specimens and fixation times is suggested. When orientation is important, marking the specimen with a small incision is advised.

2. Use fresh distilled water throughout to avoid the risk of contamination with microorganisms.

3. Some polymers are readily solubilized by solvents commonly used in electron microscopy. It is possible to substitute a graded series of acetones or methanol for the alcohols described in **Subheading 3.**, although the former is often the more aggressive with respect to the polymer component. One alternative that has not yet been described for preparation of tissue-polymer constructs is 2,2-dimethoxypropane (DMP), in which methanol and acetone are generated to replace water *(17,18)*. Again, experimentation is recommended for individual materials and constructs.

4. Numerous resins have been described for the infiltration of biological specimens. In general, tissue-polymer constructs benefit from low viscosity to maximize
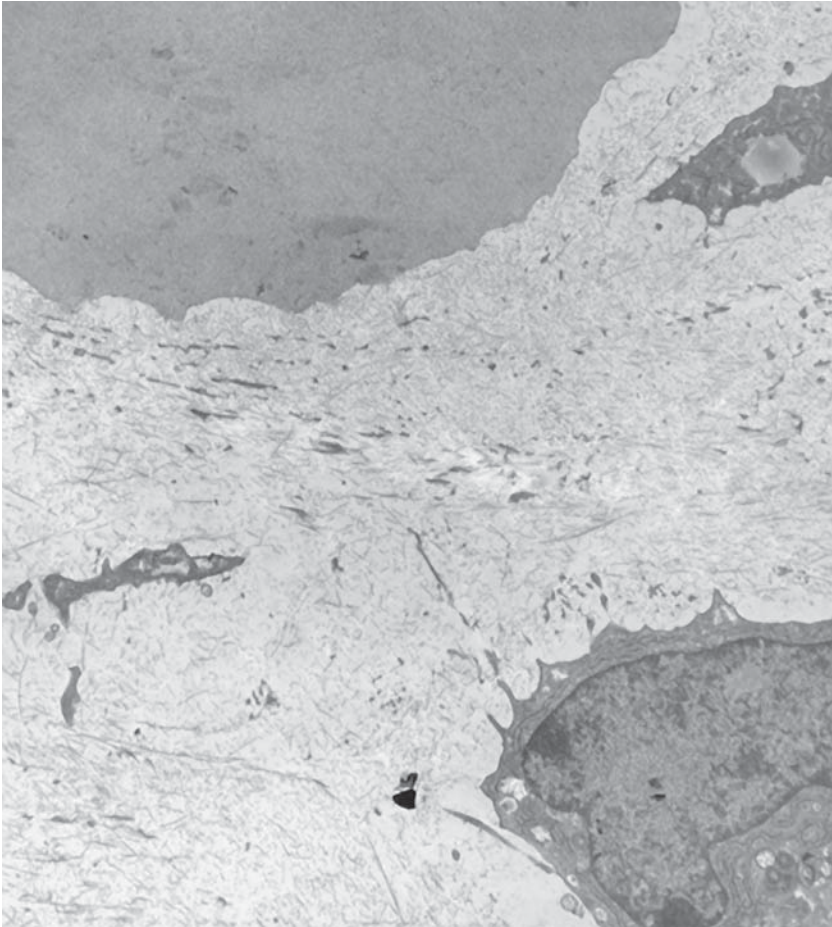
Fig. 2. Bovine chondrocyte adjacent to polymer fiber in Hyaff-11 fiber construct after culture for 40 d. Healthy cell shows distinct nucleus and endoplasmic reticulum. Note extensive biological matrix surrounding cell, and irregular surface of fiber. Field width = 30 μm.

rapid infiltration. When constructs contain mineralized tissues, it is useful to employ a modified Spurr's resin where the resulting block is harder (and therefore a better match to the mineralized tissue properties). Modifications to the ratio of components and polymerization time can be used to alter the properties of the final block *(13)*.

5. Use a sharp pencil to produce paper labels that you embed in the mold or capsule with the tissue. Many types of ink are easily "washed out" during processing and polymerization of the resin.
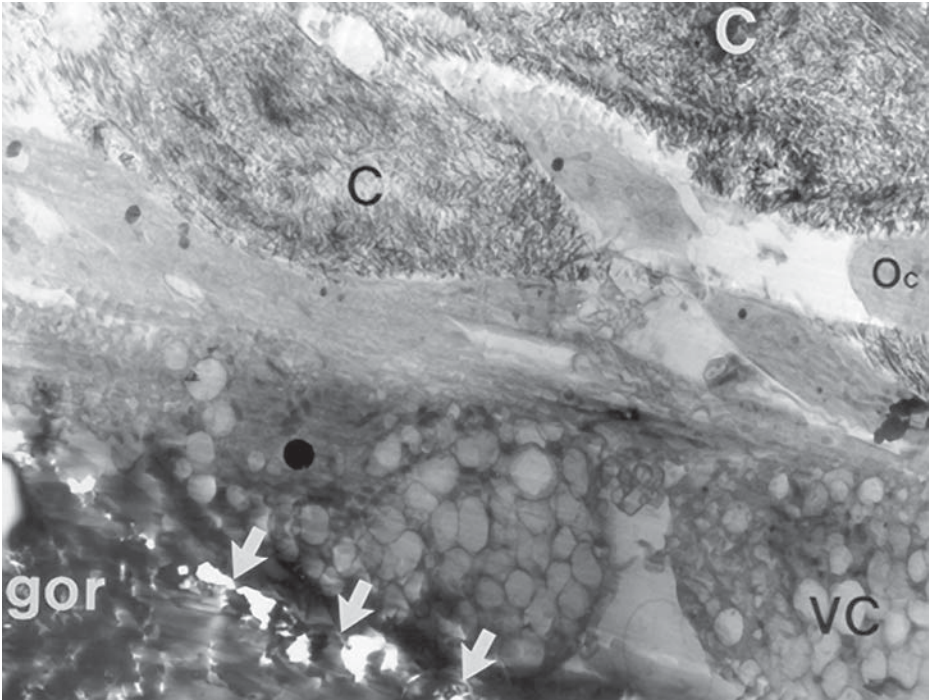
Fig. 3. Interface (*arrows*) between cultured tissues and expanded poly(tetrafluoro-ethylene). Note that cells (VC at interface are highly vacuolated, and the production of collagenous ECM (C). Field width = 40 μm.

6. Glass knives do not generally work well for tissue-polymer constructs. Diamond knives perform best, and a "histo" knife may be sufficient for researchers with a limited budget. Technical assistance/expertise will be required to cut sections.
7. A useful "tool" for pushing sections around after cutting is an eyelash attached to a cocktail stick with some molten wax.
8. Ideally, sections should be placed on a grid without a support film, as support films can reduce contrast and/or contain additional artifacts. Smaller grid sizes (300–400 mesh) work best at supporting sections without a film. Where sections are very fragile, a support film may be essential. Nitrocellulose (collodion) and Formvar have been used in our laboratories, and the reader is referred to a standard text for further information *(13)*.
9. It is vital that the sections are rinsed thoroughly between the staining stages. Minute quantities of residual lead citrate may form insoluble, dense lead carbonate in air, or crossreact with uranium salts to form electron-dense artefacts on the section. Take care to avoid breathing on the sections during staining (again to avoid precipitation of lead carbonate); some people advise placing a few sodium hydroxide pellets (0.5 g) near the section while staining to "scrub" local CO_2.

References

1. Puelacher, W. C., Kim, S. W., Vacanti, J. P., Schloo, B., Mooney, D., and Vacanti, C. A. (1994) Tissue-engineered growth of cartilage: the effect of varying the concentration of chondrocytes seeded onto synthetic polymer matrices. *Int. J. Oral Maxillofac. Surg.* **23,** 49–53.
2. Rotter, N., Aigner, J., Naumann, A., Planck, H., Hammer, C., Burmester, G., et al. (1998) Cartilage reconstruction in head and neck surgery: comparison of resorbable polymer scaffolds for tissue engineering of human septal cartilage. *J. Biomed. Mater. Res.* **42,** 47–56.
3. Martin, I., Vunjak-Novakovic, G., Yang, J., Langer, R., and Freed, L. E. (1999) Mammalian chondrocytes expanded in the presence of fibroblast growth factor 2 maintain the ability to differentiate and regenerate three-dimensional cartilaginous tissue. *Exp. Cell Res.* **253,** 681–688.
4. Holy, C. E., Shoichet, M. S., and Davies, J. E. (2000) Engineering three-dimensional bone tissue in vitro using biodegradable scaffolds: investigating initial cell-seeding density and culture period. *J. Biomed. Mater. Res.* **51,** 376–382.
5. Salata, L. A., Hatton, P. V., Devlin, A. J., Craig, G. T., and Brook, I. M. (2001) *In vitro* and *in vivo* evaluation of e-PTFE and alkali-cellulose membranes for guided bone regeneration. *Clin. Oral Implants Res.* **12,** 62–68.
6. He, Q., Li, Q., Chen, B., and Wang, Z. (2002) Repair of flexor tendon defects of rabbit with tissue engineering method. *Chin. J. Traumatol.* **5,** 200–208
7. Caterson, E. J., Li, W. J., Nesti, L. J., Albert, T., Danielson, K., and Tuan, R. S. (2002) Polymer/alginate amalgam for cartilage-tissue engineering. *Ann. NY Acad. Sci.* **961,** 134–138.
8. Bakker, D., van Blitterswijk, C.A., Hesseling, S. C., Daems, W. T., and Grote, J. J. (1990) Tissue/biomaterial interface characteristics of four elastomers. A transmission electron microscopical study. *J. Biomed. Mater. Res.* **24,** 277–293.
9. Hatton, P. V., Craig, G. T., and Brook, I. M. (1992) Characterization of the interface between bone and glass-ionomer (polyalkenoate) cement using transmission electron microscopy and X-ray microanalysis. *Advances in Biomaterials* **10,** 331–336. (Doherty, P. J., ed.), Elsevier Science Publishers B.V.
10. Hatton, P. V., Walsh, J. and Brook, I. M. (1995) The response of cultured bone cells to resorbable polyglycolic acid and reinforced membranes for use in orbital floor repair. *Clinical Materials* **17,** 71–80.
11. Da Rocha Barros, V. M., Salata, L.A., Van Noort, R., and Hatton, P. V. (2002) *In vivo* bone tissue response to a canasite glass-ceramic. *Biomaterials*, **23,** 2895–2900.
12. Glauert, A. M. (1975) *Practical Methods in Electron Microscopy* (Glauert, A. M., ed), Elsevier, Amsterdam, The Neterlands.
13. Hayat, M. A. (1989) *Principles and Techniques of Electron Microscopy: Biological Applications* (Hayat, M. A., ed.), MacMillan Press, London.
14. van Dorp, A. G., Verhoeven, M. C., Koerten, H. K., van Blitterswijk, C. A., and Ponec, M. (1999) Bilayered biodegradable poly(ethylene glycol)/poly(butylene terephthalate) copolymer (Polyactive) as substrate for human fibroblasts and keratinocytes. *J. Biomed. Mater. Res.* **47,** 292–300.

15. Marra, K. G., Szem, J. W., Kumta, P. N., DiMilla, P.A., and Weiss, L.E. (1999) *In vitro* analysis of biodegradable polymer blend/hydroxyapatite composites for bone tissue engineering. *J. Biomed. Mater. Res*. **47,** 324–335.

16. Springer, I. N., Fleiner, B., Jepsen, S., and Acil, Y. (2001) Culture of cells gained from temporomandibular joint cartilage on non-absorbable scaffolds. *Biomaterials* **22,** 2569–2577.

17. X Muller, L. L. and Jacks, T. J. (1975) Rapid chemical dehydration of samples for electron microscopic examinations. *J. Histochem. Cytochem*. **23,** 107–112.

18. Y Conway, K. and Kiernan, J. A. (1999) Chemical dehydration of specimens with 2,2-dimethoxypropane (DMP) for paraffin processing of animal tissues: practical and economic advantages over dehydration in ethanol. *Biotech. Histochem.* **74,** 20–26.

16

Application of Microscopic Methods for the Detection of Cell Attachment to Polymers

John Hunt and Deborah Heggarty

1. Introduction

Visualizing and quantifying cellular contact with materials is a critical step in the evaluation of cell-material interaction both in vitro and in vivo. To achieve this, a number of techniques are available. The focus of this chapter is the presentation of staining techniques for use with light microscopes, including transmitted, reflected, fluorescence, or laser-scanning confocal. Other visualization techniques and the potential of techniques such as transmission electron microscopes (TEM), scanning electron microscopy (SEM), and atomic force microscopy (AFM) should not be ignored. But the subject becomes too broad and complex to enable a single protocol to be all-encompassing. However, many of the protocols described can be modified easily for use with TEM and SEM visualization.

Cells can interact in many different ways both with and within materials. Some interactions are easy to observe and analyze using quick and simple techniques, and others require a more detailed analysis.

The temptation when looking at cells is to probe with the highest-resolution tool available from today's current technology—for example, *in situ* hybridization (ISH) or *in situ* polymerase chain reaction (PCR). Although these techniques will yield very detailed and useful information about specific cell functions and therefore interactions, quicker, easier, and cheaper techniques can often be used to determine and evaluate more fundamental events. In practice, initial screening analysis using the simpler techniques can be followed up by a more careful and high-tech investigation when this is appropriate.

Many well-practiced classic histopathology stains make an excellent start point for investigating cell material interactions. A basic hematoxylin (Sigma

cat. no. HHS-32) and eosin (Sigma cat. no. E6003) stain *(1)* can yield valuable information about cells, their very presence, and their distribution and number. An "old classic" stain like a van Gieson's (Fuchsin Acid Merck cat. no. 343192E) stains *(2)* collagen fibers in an extracellular matrix (ECM) very quickly and simply, and determines very clearly whether collagen is being formed in or around a material. However, it does not answer the question of which type of collagen is formed. To achieve this, techniques such as immuno-histochemistry and PCR are required. But an initial van Gieson stain could be used to demonstrate that collagen has been formed, and that more detailed analysis might be worthwhile.

Whatever the cell type and whatever the experimental time periods of an in vivo or in vitro model, certain fundamental questions should be considered when looking at cells on or in materials. These may be particularly relevant to the use of cells on polymers because their physical properties lend them to post-fixation processing with good retention of morphology and tissue reactivity.

1.1. The Material

The following key points outline some aspects to consider when determining which protocols are practical for different types of materials.

1. Is the material clear or opaque? If it is clear, transmitted light could work to visualize cells on or in the material. If it is opaque, will it allow the diffuse passage of light without a significant loss that cannot be compensated for? If so, transmitted light microscopy visualization could be possible.
2. Is the material smooth, flat, rough, porous, or three-dimensional (3D)?
3. Does the material autofluoresce? If so, at particular wavelengths or across a broad range of the spectrum?
4. Will the material preferentially absorb specific proteins? Is protein adsorption nonspecific?
5. Which chemicals (including water) will react with the material? Which chemicals could cause damage/changes to the material by swelling, dehydrating, cracking, or even dissolving the material completely into solution?

1.2. The Cell

A second series of fundamental points follow, which address the information that is required from examining cell attachment to a material.

1.2.1. Cell Attachment

1. Number and proliferation.
2. Morphology.
3. Nuclear and cytoplasmic shape.
4. Cytoskeleton orientation.
5. Focal contacts; points of cell-substrate interaction.

6. Receptor expression; expression of specific proteins, in terms of adherence most often on the plasma membrane, but in terms of function also within the cytoplasm. Includes integrin molecules, ligands, and activation molecules.

1.2.2. Infiltration

A structure with three dimensions is almost always the case, but the third dimension is often very small (microns). Is the distance cells can infiltrate within a matrix a variable? Is the rate of infiltration a question? Which parts of a matrix do the cells utilize to migrate through the matrix? What stimulates a cell to move through a matrix?

1.2.3. Phenotype

Phenotype is appearance- and function-dependent. Relating to the formed protein molecules found on and in the cell. Specific proteins have been found to be uniquely associated in some cases with specific cell types. Most often, they are shared between a number of different cell types. A specific cell phenotype and thus cell type is identified by looking for a combination of a number of molecules. Alternatively, but by the same argument, if function can be determined, then phenotype can often be determined or at least implied; many functions confirm or identify phenotype. Phenotype is determined at the product protein level and at the mRNA level. The combination of the two complementary points of cell function add significant detailed information about cell phenotype and function.

1.2.4. Cell–Material Interactions

In most in vitro models this is the usual assumption and goal, but in reality this is very difficult to achieve at a single-cell level in a cultured population environment. Cells communicate with each other and expect to. In many cases they seek out cell–cell interactions, and in all cases they are sensitive to cell-derived signals and glean information about their environment from each other. A population of cells on a surface, regardless of cell density, are in constant communication with each other, either directly by contact (touch) or indirectly by soluble molecules (odor). Cell material experiments always include *cell–cell interactions* and should therefore describe the effects of a material on a cell population; these would be more correctly termed *cell–material–cell–cell interactions*.

2. Materials
2.1. Fixatives

1. Acetone.
2. Ethanol.

3. Glutaraldehyde.
4. Formaldehyde.
5. Paraformaldehyde.

There are many more fixatives than the examples shown here, and many methods for their application.

2.2. For Immunostaining

1. Acetone.
2. Phosphate-buffered saline (PBS).
3. Normal serum (from the appropriate species).
4. Primary (specific) antibody.
5. Bovine serum albumin.
6. Secondary antibody.
7. Vectastain ABC-AP kit.
8. Levamisole solution.
9. Tris-HCl.

3. Methods

Experiments should fundamentally address exactly what information is required from the analysis and select appropriate techniques. Experiment with test samples first and then scale up to parallel processing with both positive and negative controls. All experimental protocols require some trial and error, as materials will react, swell, crack or disintegrate, and some will autofluoresce.

Immunohistochemistry has been practiced for many years, and the list of available primary antibodies is as endless as the list of companies that can supply them. Fundamentally, the procedure utilizes the most specific biological reaction currently known—the interaction between antibody and antigen. The theory behind antibody production can be found in any standard cell biology or immunology textbook. Using this specific interaction, specific molecules can be targeted and labeled, and an amplification step is included to increase this label (usually based around the molecules biotin and avidin because of their extremely high affinity for each other) and to add reaction sites/molecules for a colorizing agent.

3.1. Fixation

The list of fixatives for preserving cells and tissue is extensive, and particularly in the area of polymeric materials, there is no single fixative that can be recommended. In general, fixation involves removing the water and preserving by crosslinking the cellular and extracellular components. Many polymers have a high water content, and thus for analysis of cell attachment, fixation is

actually where the analysis fails. Some fixation systems can work well to preserve cells and tissues, but will actually dissolve, crack, swell, and ultimately destroy the polymer the cells are located on.

A useful experiment to perform before a material even comes into contact with a cell is to prepare a selection of different types of fixative and evaluate what happens to the material. Materials are significantly easier to investigate in material terms without cells, and thus, this strategy works easily and well. The simple option is to fix very gently with an aqueous fixative. The drawback to this approach is that the fixative may kill and hold the cells in suspended animation for a period of time, but it will not actually preserve the cells or tissue long-term.

If possible, understand the chemistry of the material/polymer and investigate the chemistry of potential fixatives for potential problems.

Example protocol using a gentle fixative:

1. Prepare 4% w/v paraformaldehyde and 2% w/v sucrose made up in PBS (Sigma cat. no. P-4417).
2. Fix by immersion or flooding for 10 min.
3. Wash for 5 min in PBS.
4. Store short-term, hydrated in fresh PBS in the dark.
5. Preferably use samples in staining protocols as soon as possible to safeguard against degradation of cellular information.

3.2. Immunostaining Protocol

This method is applicable for use to target any molecule for which a specific antibody is available.

1. Fix in acetone (Merck cat. no. 15296 6P) for 5 min (*see* **Note 1**).
2. Rinse in PBS buffer (Sigma cat. no. P-4417) for 5 min.
3. Incubate with normal serum (Serotec cat. no. C12SBZ) (three drops of stock + 10 mL PBS) for 20 min (*see* **Note 3**).
4. Incubate with primary antibodies diluted with PBS containing 1% BSA (Sigma cat. no. A3912) for 30 min (*see* **Notes 3–6**).
5. Rinse in PBS buffer for 5 min.
6. Incubate with secondary antibody (Dako) prepared at an appropriate dilution for 30 min (*see* **Notes 3–5**).
7. Rinse in PBS buffer for 5 min.
8. Incubate with Vectastain ABC-AP kit (Vector cat. no. AK-5000) (2 drops of reagent A to 10 mL PBS, mix, add two drops of reagent B) for 30 min.
9. Rinse in PBS buffer for 5 min.
10. Incubate with AP (Vector cat. no. SK-5100). Prepare immediately before use 20–30 min before use.
    Add one drop of Levamisole solution (Vector cat. no. SP-5000) to every 5 mL of buffer (*see* **Note 7**).
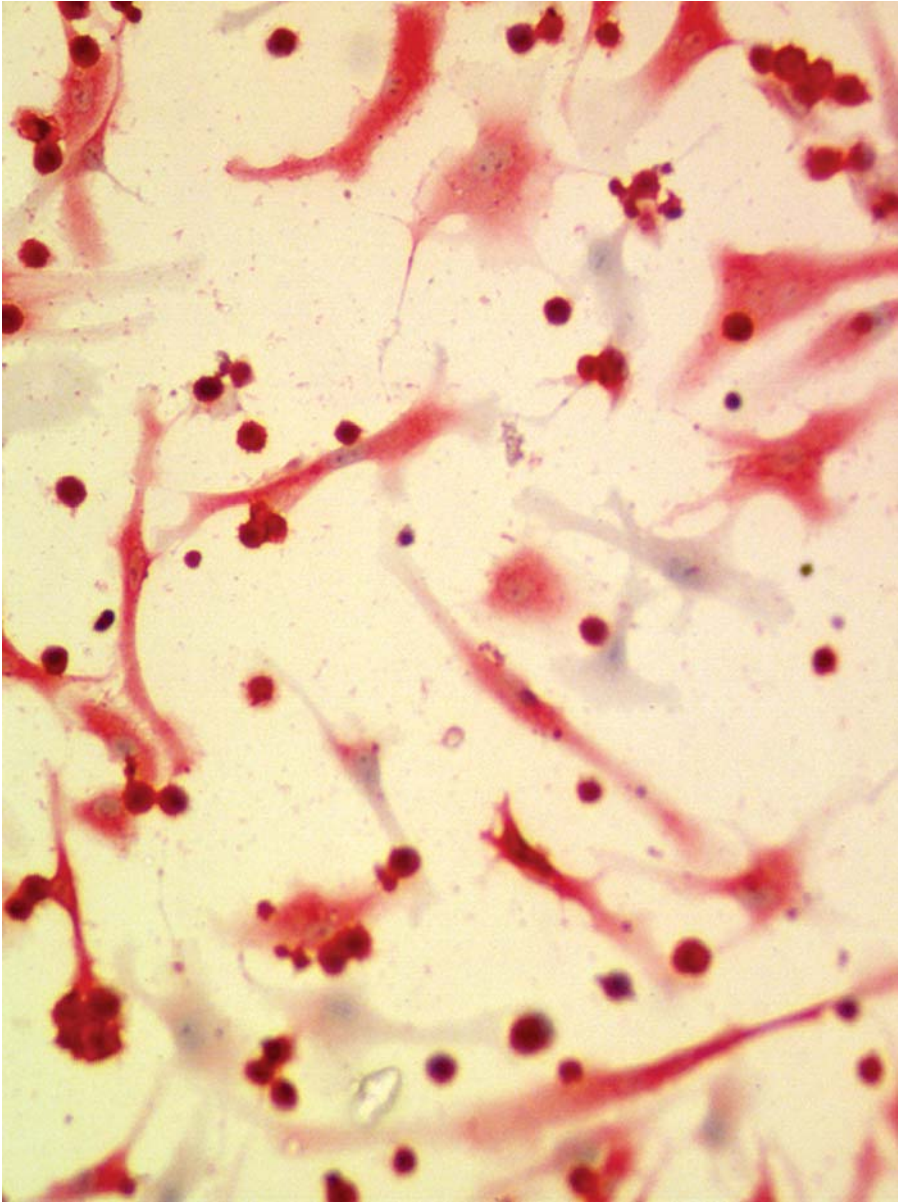
Fig. 1. ICAM-1 (CD54) positive staining of a co-culture of endothelium and macrophages. The positive immunostaining is red, and the sample has been counterstained lightly with Hematoxylin. (F. Pu. *Clinical Engineering*). (*See* color plate 3 appearing in the insert following p. 112.)
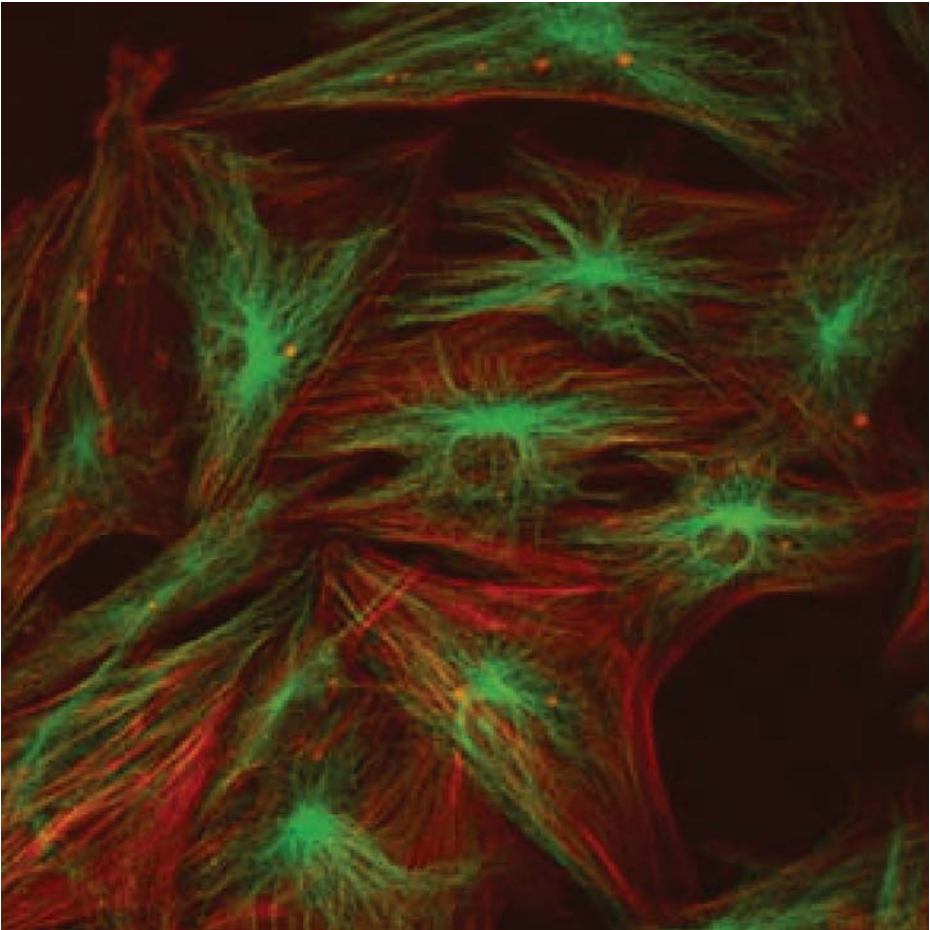
Fig. 2. Cytoskeleton (F-actin) (red) and Microtubule (β tubulin) (green) visualization in cultured human osteoblasts (J.M. Rice *Clinical Engineering*). (*See* color plate 4 appearing in the insert following p. 112.)

11. To 5 mL of 100 m*M* Tris-HCl (Sigma cat. no. T-1503), pH 8.2 buffer, add two drops of vectastain kit reagent 1 and mix well. Add two drops of vectastain kit reagent 2 and mix well. Add two drops of vectastain kit reagent 3 and mix well.
12. Wash in distilled water.
13. Visualize either by transmitted visible light (*see* example, **Fig. 1**) or reflected fluorescence microscopy using excitation wavelength 543 nm (*see* **Notes 9** and **10**).

Table 1
Selected Adhesion Molecule Markers
Useful for Determining the Detail of Cell Adhesion

Cluster designation number	Full name	Catalog number*
CD62E	E-selectin	33361A
CD62L	L-selectin	32231A
CD62P	P-selectin	31791A
CD54	ICAM-1	31621A
CD50	ICAM-3	36011A
CD31	PECAM-1	30881A
CD106	VECAM-1	33351A
CD11a	LFA-1 α chain	30421A
CD11b	Mac-1	30451A
CD11c	Gp150	30481A
CD18	LFA-1β chain Mac-1β chain	35651A
CD41b	GpIIb	31091A
CD61	GpIIIa	33821A
CD162	PSGL-1	36771A

*Pharmingen

3.3. Controls (see *Notes 11–13*)

1. Positive: Slide or sample known to express or contain targeted molecule.
2. Negative 1: Isotype control for primary antibody (**step 4, Subheading 3.2.**).
3. Negative 1a: Good isotype parallel control is to stain for more than one molecule in the staining procedure in parallel, so repeat protocol on numerous samples but use different primary antibodies in **step 4, Subheading 3.3.** on each sample.
4. Negative 2: Use PBS in place of primary on one sample (**step 4, Subheading 3.2.**)
5. Negative 3: Use PBS in place of secondary on one sample (**step 6, Subheading 3.2.**)

This protocol is very specific, but can be broadened and applied to any molecule that an antibody is available for. A third, fourth and fifth primary could be applied in series-dependent on changing the final visualization color and changing the host animal for the primary—and therefore the host and target—for the secondary antibody. For cell adhesion and function, **Table 1** provides details of the most clearly useful primary antibodies.

3.4. Immunostaining Protocol to Label Components of Intracellular Cytoskeleton

1. Fix in acetone for 5 min or substitute other preferred fixative (not all fixatives preserve the antigenicity of cells and tissue).

2. Wash cells in PBS 5 min.
3. Permeabilize cells: 0.05% Triton X-100 (Sigma) 21123 (50 μL Triton X-100+9.95 mL PBS). 4°C, 5 min.
4. Wash 5 min 37°C 1% BSA: PBS.
5. Add primary antibody (Talin (Serotec cat. no. MCA725S) or paxillin (Zymed Lab. Inc. cat. no. 03-6100) for focal contacts) (β tubulin (Zymed Lab. Inc. cat. no. 08-0093) for microtubules) (diluted 1:100 1% BSA:PBS), incubate 60 min at 37°C. Titrate for optimum concentration.
6. Wash 2× at 3 min intervals: 0.01% Tween 20 (ICN Biomedical Inc. cat. no. 103168) (100 μL Tween 20+99.9 mL PBS) in the dark.
7. Add secondary antibody (rhodamine-conjugated [Molecular Probes cat. no. R-6393]) dilution 1:100 with 1% BSA:PBS; incubate 60 min, at 37°C. Titrate for optimum concentration. Emits light by excitation by light at λ 543 nm.
8. Wash twice for 3-min intervals: 0.01% Tween 20 (100 μL Tween 20+99.9 mL PBS) in the dark.
9. Incubate for 30 min fridge Oregon Green Phalloidin (Molecular Probes cat. no. O-7466) (5 μL stock: 200 μL PBS). Titrate for optimum concentration. Oregon Green Phalloidin labels F-actin, and therefore visualizes the cell cytoskeleton. It emits light by excitation by light at λ 488 nm.
10. Wash 2× 3 min intervals: 0.01% Tween 20 (100 μL Tween 20+99.9 mL PBS) in the dark.
11. Mount, using photostabilizing mounting agent (vector Vectorshield cat. no. H1000) (reduces the effects of photobleaching during visualization) and cover slip.
12. Examine using the Confocal laser scanning microscope for good quality sharp visualization from three dimensions (*see* **Fig. 2**) or use fluorescent microscopy for overall visualization. Both techniques must excite and detect from 488 and 543 nm excitation wavelengths independently, or separate samples must be used for each fluorochrome.

4. Notes

1. Incubation times are *not* approximate, particularly the washing steps. Washing for too long results in poor staining—a problem if too many samples are stained in the same protocol. Well-practiced a maximum of 30 samples should stained in any one procedure.
2. Rabbit serum blocks nonspecific binding of antibodies. Any species of serum could be used, and some testing with different ones could enhance the result.
3. Ensure that the solution from the previous step has been completely removed, either by flicking the sample during inversion or by edge or blotting the sample with filter paper/tissue.
4. The primary and secondary incubation times can be lengthened or shortened depending on antibody concentration.
5. Specificity of antibodies can be improved by performing these steps at 4°C with a low antibody concentration for an extended incubation period. A set of samples

in which the variables are adjusted will determine the optimum.

6. A series of titration controls should be run for each primary to determine its optimum working concentration in a protocol for a particular material.

7. Levamisole blocks endogenous alkaline phosphatase (ALP) activity.

8. The pH of the Tris buffer is critical and should be checked just prior to use; avoid precipitate.

9. Edge effects occur on most samples, and are caused by surface tension and accumulation of molecules at edges. Do not take results close to the edges of samples. Edge effects are obvious.

10. A good stain can often be improved and perfected with some controlled experiments to adjust and determine the effects of varying each step in the protocol.

11. When using fluorescence, expose an edge or sacrificial area to set up visualizing equipment for photography. This will avoid photobleaching valuable areas of samples.

12. Optimize the staining procedure for a specific cell type on glass or some other adhesive but inexpensive substrate, then further fine-tune on fewer and more valuable actual test materials.

13. Do not attempt to do too much when learning to handle and control the technique. It is much better to do only few samples, which will be mainly controls, and become confident with the results before wasting many valuable samples.

Many of the terms discussed in this chapter have other meanings in other contexts. The principles and techniques discussed here relate terms in the context of visualizing cells and their function on or in materials. Terms are *not* definitions.

References

1. *Theory and Practice of Histological Techniques* (1977) Bancroft, J. and Stevens, A., eds.), Churchill Livingstone, London, pp. 85–94.

2. *Theory and Practice of Histological Techniques* (1977) Bancroft, J. and Stevens, A., eds.), Churchill Livingstone, London, pp. 95–112.

17

Biochemical Methods for the Analysis of Tissue-Engineered Cartilage

Wa'el Kafienah and Trevor J. Sims

1. Introduction

There have been significant advances in cartilage-engineering methodology in recent years, particularly in the production of biodegradable scaffolds and the use of bioreactors to improve the outcome of the engineering process. To date, engineered cartilage studies have mostly relied on histochemical and immunohistochemical methods for the characterization of the engineered cartilage matrix. The detection of various matrix components using these methods may not be sufficient to judge the quality of engineered cartilage and compare it objectively to natural cartilage. In order for cartilage tissue engineering to progress to the clinic, quantitative methods for the analysis of different matrix components will be required to monitor and ensure the quality of engineered cartilage.

1.1. Sample Preparation

For various assay purposes, it is essential to solubilize the cartilagenous matrix before applying the sample to any of the assays described here. This can be done using a potent proteolytic enzyme such as Proteinase K that has broad substrate specificity and can fully solubilize cartilage after overnight incubation at 56°C. Furthermore, this enzyme can selectively extract the intact epitope from type II collagen alpha-chains for use in an inhibition enzyme-linked immunosorbent assay (ELISA) for quantifying levels of type II collagen *(1)*.

1.2. GAG Assay

Proteoglycans comprise a large number of distinct molecules, all containing a protein core to which sulfated glycosaminoglycans (GAG) are covalently attached. Proteoglycans enable cartilage to bind water molecules and account for the property of compressive stiffness important for the correct functioning of articular joints and intervertebral disks. GAG levels in solution can be quantified by binding of the acidic polymer to the basic dye, 1,9-dimethylmethylene blue (DMB) *(2)*. The resulting metachromatic shift peaks at A_{525} and can thus be adapted for a spectrophotometric assay in a cuvet or a microwell plate.

1.3. Type II Collagen Assay

Type II collagen is the major structural macromolecule of hyaline cartilage. It confers tensile strength to the cartilage matrix, and is thus, a marker of good quality, tissue-engineered hyaline-like cartilage. Specific assay of the individual α-chains of type II collagen can be achieved using antibodies raised against specific linear amino acid sequence(s) of the α-chains. The detected sequence by the antibody can selectively be extracted from the α-chains and quantified by inhibition ELISA. The method described in this chapter utilizes an antibody, Col2–3/4m, raised against a synthetic peptide (CB11B) *(3)*. If alternative anti-collagen antibodies are to be used, then the appropriate method of proteolytic extraction of specific epitope(s) must be established before the procedure can be adapted.

1.4. Hydroxyproline Assay

Hydroxyproline (Hyp) is a post-translational product of proline hydroxylation, catalyzed by the enzyme prolylhydroxylase (E.C. 1.14.11.2). The occurrence of this imino acid is believed to be confined almost exclusively to collagen, the connective tissue protein. The metabolism of total collagen can therefore be studied conveniently by measuring the Hyp content. Measurement of Hyp is possible by colorimetric methods, high-performance liquid chromatography (HPLC), mass spectrometry and enzymatic methods. Here, we describe a simple and sensitive colorimetric microassay system for measuring Hyp *(4)*. The method utilizes the ability to oxidize this amino acid to a pyrrolic compound that reacts with *p*-dimethylaminobenzaldehyde to form a chromophore that can be measured spectrophotometrically.

1.5. Collagen Crosslink Assay

The primary function of collagen in developing and mature tissues is to provide a supporting matrix that confers mechanical strength and functional integrity on the tissue. This is achieved by a network of intermolecular crosslinks

between individual collagen molecules within the fiber at highly specific points (*see* **ref. 5**).

The crosslinks are initiated by the oxidation of specific lysyl or hydroxylysyl residues in the non-helical telopeptide region of the molecule to produce lysyl or hydroxylysyl aldehydes. Because of the precise end-overlap alignment of the collagen molecules in the fiber, the lysyl or hydroxylysyl aldehydes can condense with a lysine or hydroxylysine in an adjacent collagen molecule to form a divalent crosslink. In cartilage collagen, the telopeptidyl and helical lysines are usually hydroxylated so that the resulting crosslink is the keto-imine, hydroxylysino-keto-norleucine (HLKNL). This divalent crosslink is only an intermediate and as the tissue matures, and turnover decreases, the keto-imine crosslink reacts with a further hydroxylysyl aldehyde to form the mature crosslink, hydroxylysyl-pyridinoline (OH-Pyr). A small amount of lysyl-pyridinoline can also be formed if the helical residue is lysine rather than hydroxylysine.

A valuable measure of the development of tissue-engineered cartilage can therefore be obtained by measuring the ratio of the intermediate-to-mature crosslinks. Here, we describe a method for the accurate measurement of both of these crosslinks using a minimal amount of material. The method could therefore be used to monitor the maturation of the engineered cartilage after implantation from a single biopsy of the implanted cartilage.

2. Materials

2.1. Sample Preparation

1. Tris-HCl, pH 7.6. Prepare at 50 mM and add sodium azide to a final concentration of 0.05% w/v. It is useful to make up a large volume (10–20 L) for use over a period of days.
2. Proteinase inhibitors (all from Sigma): Prepare EDTA and iodoacetamide, each as a 200 mM stock solution in water and store at –20°C; prepare pepstatin A as a 2-mg/mL stock solution in 95% v/v ethanol and store at –20°C.
3. Proteinase K (E.C. 3.4.21.1) (Sigma): prepare as a 1-mg/mL stock solution in 50 mM Tris-HCl, pH 7.6, containing proteinase inhibitors: 1 mM EDTA, 1 mM iodoacetamide, and 10 µg/mL pepstatin A. Store in 5 mL aliquots at –20°C.

2.2. GAG Assay

1. DMB color reagent: prepare by dissolving 16 mg DMB in 1 L water containing 3.04 g glycine, 2.37 g NaCl, and 95 mL 0.1 M HCl, to yield a solution at pH 3.0, with A_{525} 0.31. The reagent may need up to 2 h of mixing before being ready for use. It can be stored in a brown (or foiled) bottle at room temperature for 3 mo.
2. Chondroitin sulfate (or other GAGs when appropriate): prepare a stock solution in water at 50 µg/mL and keep refrigerated.

2.3. Type II Collagen Assay

1. 50 m*M* Tris-HCl, pH 7.6.
2. Phosphate-buffered saline (PBS): Prepare as a large volume stock solution of 0.85% (w/v) NaCl, 0.16% (w/v) Na_2HPO_4, 0.054% KH_2PO_4, and 0.05% (w/v) sodium azide. Adjust the pH to 7.4.
3. Carbonate buffer: Prepare 1 L of 0.1 *M* $NaHCO_3$ and 200 mL of 0.1 *M* Na_2CO_3. Gradually add the Na_2CO_3 to the $NaHCO_3$, with mixing, until the pH is 9.2.
4. Proteinase inhibitors (*see* **item 2** of **Subheading 2.1.**).
5. Proteinase K (*see* **item 3** of **Subheading 2.1.**).
6. Bovine type II collagen (Sigma): Store the lyphilized powder at –20°C (not at 4°C as suggested on the bottle label).
7. Heat-denatured type II collagen (HDC), prepared immediately before use: Dissolve native bovine type II collagen in carbonate buffer, pH 9.2, to a final concentration of 1 mg/mL in a screw-capped 1.5-mL centrifuge tube. At this concentration, it will be partly in suspension. Place the tube in a water bath at 80°C for 20 min, but remove it for brief periods of mixing over the first 2 min, to ensure complete dissolution of the collagen. Dilute the HDC in carbonate buffer to a final concentration of 40 µg/mL.
8. Bovine serum albumin (BSA), Sigma: Prepare a stock solution of 1% (w/v) BSA in PBS and store at 4°C.
9. PBS/Tween: add Tween-20 (Sigma) to PBS to a final concentration of 0.1% (v/v).
10. Antibody Col2–3/4m or equivalent.
11. Peptide CB11B or equivalent.
12. Second antibody: goat anti-mouse Ig labeled with ALP (available from many sources).
13. Diethanolamine buffer: prepared as 8.9 m*M* diethanolamine and 0.25 m*M* $MgCl_2$. Store at ambient temperature.
14. ALP substrate solution: Prepared immediately before use as 0.5-mg/mL *p*-nitrophenyl phosphate (Sigma) in diethanolamine buffer.

2.4. Hydroxyproline Assay

Caution: the assay reagents include strong solvents and acids, and should therefore be weighed and handled in a fume hood.

1. Stock buffer: prepare by dissolving 5.04 g citric acid, 11.98 g sodium acetate trihydrate, 7.22 g anhydrous sodium acetate, 3.4 g sodium hydroxide, and 1.26 mL of glacial acetic acid in 80 mL of distilled water. Adjust the pH to 6.1, and then adjust the volume to 100 mL. Keep the reagent refrigerated.
2. Assay buffer: prepare fresh before assay by mixing n-propanol, distilled water, and stock buffer in a vol ratio of 3:2:10, respectively. Each assay plate requires 2 mL of assay buffer.
3. Chloramine-T reagent: prepare fresh before assay by mixing 0.141 g chloramine-T with 0.5 mL distilled water until chloramine-T goes into solution. Add 0.5 mL *n*-propanol and 4 mL stock buffer to finish preparing the reagent. Each assay plate requires 4 mL of this reagent.

4. DMBA reagent: prepare fresh before assay by dissolving 4 g *p*-dimethylamino-benzaldehyde in 8 mL of *n*-propanol/perchloric acid solution (2:1 v/v).
5. Hydroxyproline stock solution: prepare in distilled water at 50 μg/mL and keep refrigerated.

2.5. Collagen Crosslink Assay

1. A number of pieces of specialized equipment are required for the crosslink analysis. These are as follows:
   a. A freeze-drier (lyophilizer), preferably equipped with a chemical trap to afford protection of the vacuum pump against acid corrosion.
   b. A centrifugal evaporator.
   c. An Amino Acid Analyzer equipped with a post-column ninhydrin detection system, and ideally with a computing integrator or with computer-based chromatography data-handling software.
2. Filters for sample preparation and amino acid analyzer buffer filtration are commercially available from numerous suppliers, and 4-mm PVDF syringe filters are used for sample filtration.
3. Fibrous cellulose, CF-1, is a commercially available product from Whatman (Maidstone, Kent, UK).
4. PBS: 0.15 *M* sodium chloride, 0.025 *M* di-sodium hydrogen orthophosphate adjusted to pH 7.4 with potassium di-hydrogen orthophosphate.
5. Sodium borohydride should be dissolved in 1 m*M* sodium hydroxide solution at 5°C immediately prior to use. **Caution:** The dry solid is deliquescent, producing an explosive gas (hydrogen) when wet, and thus, care with storage and handling is essential.
6. Reagents and buffers for use with the amino acid analyzer are best purchased from the equipment supplier. Any alteration to the concentration or pH of such buffers should be done with great care, and any buffers modified in this way should be passed through a 0.2-μm filter prior to use to remove particulate matter. The buffers should incorporate 0.01% phenol to prevent bacterial spoilage and should be stored at 15–20°C.
7. An organic mixture consisting of butan-1-ol:acetic acid:water, 4:1:1 v/v.

3. Methods

3.1. Sample Preparation

1. Cut the engineered cartilage into small pieces and weigh. Distribute the weighed pieces into 1.5-mL centrifuge tubes with a V-shaped bottom and a screw-cap lined with an O-ring.
2. To each tube, add 500 μL of 1 mg/mL proteinase K (including proteinase inhibitors, as described previously). Put the cap on tightly and tap the tube until all the cartilage is submerged in the solution.
3. Incubate overnight in an oven or water bath at 56°C. Then increase the temperature to 100°C and allow the samples to boil for 10–15 min (*see* **Note 5**) to inactivate any remaining proteinase K (*see* **Note 1**).
4. The sample(s) are now ready for different assays as described here.

3.2. GAG Assay

1. Dilute samples as appropriate, with distilled water, into labeled tubes (a minimum of 50 µL/sample is required).
2. Dilute chondroitin sulfate stock with water to make up standards in the range of 0–5 µg/tube with increments of 0.5 µg (total = 11 standards).
3. To a round-bottomed microplate, add 20 µL of distilled water, as a blank, in the first column of wells (A1-H1).
4. Add 20 µL of standards 1–11 to wells A2-F4, in duplicate.
5. Add 20 µL of samples, diluted as appropriate, to wells G4-H12 in duplicate.
6. Add 250 µL of DMB to each well, using a multichannel pipet. Do not mix, as this accelerates the undesirable formation of GAG-DMB precipitates.
7. Measure the optical density (OD) using a pre-programmed microplate reader, at 525 nm (*see* **Note 2**). Most modern plate-readers will be able to construct the best-fit standard curve with a correlation coefficient of 0.99.

3.3. Type II Collagen Assay

1. Distribute HDC in carbonate buffer at 50 µL/well in all except the outermost wells of Immulon-2 ELISA plates. Wrap in cling-film and store at 4°C for 72 h.
2. Wash the plates 3× in PBS/Tween (*see* **Note 3**) and shake them dry. Incubate at room temperature with 1% w/v BSA for at least 30 min. Wash the plates once in PBS/Tween, shake them dry, and dry them further in an oven set to 50–60°C for 15 min or until fully dry. Wrap in cling-film and store at 4°C until required (the HDC-coated plates are usable even after several months of storage).
3. Immediately before assay, prepare a 96-well round-bottom microtiter plate by blocking the plastic with BSA (100 µL/well) for at least 30 min at ambient temperature. Wash it once with PBS/Tween. This is the preculture plate.
4. Add 100 µL of Tris-HCl to each of six nonspecific binding (NSB) wells in the preculture plate. Add 50 µL of Tris-HCl to each of six maximum binding (MB) wells. Add 50 µL of antibody Col2–3/4m at an appropriate dilution (*see* **Note 4**) to all wells except NSB. Do not use the outermost wells, as these are prone to excessive evaporation during the incubation stages. Prepare standard peptide CB11B in Tris-HCL at nine different concentrations within the range of 2–10 µg/mL. These standards can be stored at 4°C for several weeks, but they lose reactivity with time, so the standard curve must be monitored and the standards replaced as necessary. Add 50 µL of each standard to duplicate wells that already contain antibody. Prepare appropriate dilutions of sample in Tri-HCl and add 50 µL of each one to duplicate wells that already contain antibody. Note that a complete standard curve should be set up on each of the plates to be used.
5. Cover the preculture plate tightly with Parafilm and place in a humidified incubator at 37°C overnight. The humidity helps to minimize evaporation of the samples.
6. The most challenging part of the assay is to transfer all the samples from the preculture plate to the ELISA plate within 45 s. This timing is important because the subsequent incubation time on the ELISA plate is short (30 min), and so

small variations in the transfer time can lead to very large variations in the assay result. In practice, the best method is to use a multichannel pipet to transfer from 10 wells at a time. First, transfer row B from one plate to the other, then row C, and so on. It is important to use just one set of pipet tips for each plate during this transfer. There is no time to change tips in between transferring each row of the plate. As soon as the last row has been transferred, begin timing the 30 min incubation time, leaving the plate at ambient temperature, uncovered. If more than one plate is being used, transfer all samples on the next one and then write down the time interval between plate 1 and plate 2 and so on. When 30 min have elapsed, immediately wash plate 1 3× in PBS/Tween and start the timer again so that subsequent plates can be washed at the appropriate time intervals. Note that if the 30-min incubation period is extended, there is generally a significant loss of reactivity in the assay (presumably because of dissociation of the solution phase antigen-antibody complex in favor of antibody binding to the solid-phase antigen).

7. Prepare a commercial second antibody such as ALP-labeled goat-anti-mouse Ig, at the dilution recommended by the manufacturer. In some cases, the required dilution must be optimized in the assay. The antibody should be diluted in PBS-Tween containing 1% (w/v) BSA. Add 50 µL to all wells of the ELISA plate being used in the assay. Incubate at 37°C for 1–2 h (humidity is not necessary at this stage).

8. Wash the plates 3× in PBS/Tween, then once in water and shake them dry. Add 50 µL/well of ALP substrate solution and leave the plates at ambient temperature to allow color to develop.

9. Read the OD at 405 nm in a plate reader. The OD of the MB wells should be in the range of 0.4–1.2 for optimal calculation of the percentage of inhibition values. The mean NSB value should be subtracted from all others prior to calculation. Most modern plate-readers will be able to construct the best-fit standard curve (usually a log-log plot) and calculate specific values from each sample.

10. Calculate type II collagen content.

3.4. Hydroxyproline Assay

1. Hydrolyze prepared samples by adding 2:1 vol ratio of 6 *N* HCl to sample, respectively, in an O-ring screw-top Eppendorf. Incubate overnight at 110°C.

2. Dry the samples in a heating block set to 65°C in a fume hood with the lids open. This may take a few hours to a few days, depending on the initial hydrolysis volume.

3. Dissolve in 200 µL distilled water and vortex. The solution should be clear, but it may appear brown if the sample contains non-collagenous debris. This can be removed by treating the sample with worth 100 µL of charcoal and mixing well.

4. Centrifuge the samples at high speed (13,000 rpm for 5–10 min) to pellet hydrolysis byproducts.

5. Make up hydroxyproline standards from stock by diluting with the sample buffer (Tris-HCl). Prepare 1-mL standards in the following concentrations: 0, 0.1, 0.2, 0.5, 1, 2, 3, and 5 µg/mL.

6. Dispense 60 µL in duplicate to wells of a round-bottomed microplate of the following: distilled water as a blank (A1-H1), hyrdoxyproline standards (A2,3-H2,3), and samples starting from A4,5. A single microplate can accommodate up to 32 test samples.
7. Add 20 µL assay buffer and 40 µL chloramine-T reagent to every well using a multichannel pipet.
8. Incubate 15 min at room temperature to allow hydroxyproline oxidation to complete.
9. Add 80 µL DMBA reagent to all wells using a multichannel pipet. Once added, DMBA will cause the solution in each well to become cloudy. It is essential to mix the contents of each well, using the pipet until the solution in each well becomes clear.
10. Cover the plate with parafilm and incubate in a water bath at 60°C for 20 min with the bottom of the plate just sitting in water. Alternatively, the plate can be incubated in an oven set to 60°C.
11. Allow the plate to cool for 5–10 min before reading the OD in a plate reader at 570 nm. Hydroxyproline levels in the samples can be estimated from the standard curve. Re-dilute samples in distilled water for re-assay if necessary.

3.5. Collagen Crosslinks Assay

3.5.1 Reduction and Hydrolysis of Sample

1. The tissue must first be solubilized with proteinase K (as described in **Subheading 3.1.**). However, before inactivation of proteinase K by boiling, remove 150 µL for crosslink assay (*see* **Note 5**) and pipet this into a borosilicate glass tube with a plastic screw cap with Teflon liner.
2. Add 350 µL of PBS and cool to 5°C.
3. Add 15 µL of a freshly prepared, cold stock solution of sodium borohydride (2 mg/mL) in 1 mM sodium hydroxide to each sample.
4. Raise the temperature of this reduction mixture to 20°C and allow reduction to proceed for 1 h (*see* **Note 6**).
5. Add 500 µL concentrated hydrochloric acid to each tube. This stops the reduction and effectively places the sample in 6 N hydrochloric acid, ready for acid hydrolysis.
6. Seal the tubes and hydrolyze the samples by heating to 110°C for 24 h in a heating block (*see* **Note 7**).
7. After hydrolysis, bring the sample temperature to –20°C and lyophilize to remove all residual hydrochloric acid (*see* **Note 8**).
8. After drying, re-hydrate the sample in 500 µL distilled water.
9. Remove a 50-µL aliquot for measurement of hydroxyproline (*see* **Note 9**).
10. To the remaining 450-µL add an additional 450 µL glacial acetic acid and 1800 µL of butan-1-ol and mix thoroughly in preparation for CF1 chromatography (*see* **Note 10**).

3.5.2. Preparation of a CF1 Pre-Fractionation Column

The CF-1 fractionation step described here is based on the original method of Black et al (1988) *(6)*, and has been subsequently modified for the analysis of intermediate and mature collagen crosslinks *(7)*.

1. Weigh 25g of CF-1 cellulose powder into a 1-L measuring cylinder. Add 200 mL of distilled water to the CF-1 and shake thoroughly to ensure complete hydration of the CF-1 powder. Add 200 mL of glacial acetic acid followed by 800 mL of butan-1-ol. Shake the resulting thin slurry to ensure complete mixing of the cellulose suspension, and then leave to settle for about 15 min until the bulk of the cellulose falls below the 250-mL mark. Pour off the supernatant containing suspended cellulose fines, leaving approx 250–300 mL of the organic mixture containing the bulk of the 25 g of CF-1. Top up the slurry to 500 mL with fresh 4:1:1 organic mixture of butan-1-ol:acetic acid:water to yield a slurry of approx 5%. Decant this into a screw-capped container and store at room temperature until needed (*see* **Note 11**).

2. The pre-fractionation procedure requires the production of a mini-column of CF-1 and is prepared as follows:
   Cut the top off a 3-mL plastic Pasteur pipet bulb and introduce a very small plug of glass wool or non-absorbent cotton wool into the tip of the pipet. Thoroughly mix the CF-1 slurry and pour it into the pipet through the cut bulb. Allow the cellulose to settle, adding more slurry as required to produce a settled bed height of 8 cm. The 3-mL graduation mark on the pipet is a useful guide. Care should be taken to avoid fluid-filled cavities in the column bed, as this will adversely affect the chromatographic properties of the column. Condition the column by passing 2×3 mL of fresh 4:1:1 organic mixture through the column. CF-1 columns made in this fashion do not readily dry out, although precautions should be taken to guard against this.

3.5.3. CF-1 Pre-Fractionation

1. Once the sample is re-hydrated in 4:1:1 organic mixture as indicated in **step 10** of **Subheading 3.5.1.** (*see* **Note 12**), apply the sample to the CF-1 column.

2. Wash the containment vessel with 2×1 mL of fresh 4:1:1 organic mixture, and apply this to the column after the initial sample load has run to waste.

3. Elute the column with an additional 6×3 mL of 4:1:1 organic mixture, allowing the eluate to run to waste. The bulk of the standard non-crosslinking amino acids are eluted by this process, and the crosslinked amino acids remain adsorbed to the CF-1 cellulose.

4. After the 4:1:1 eluant has passed through the column place a collection vessel under the Pasteur pipet and pass an additional 3×3 mL of distilled water through the column to desorb the crosslinks from the cellulose.

5. This aqueous phase should now be taken to dryness (*see* **Note 13**).

3.5.4. Ion-Exchange Chromatography

1. Reconstitute the dried aqueous phase from the CF-1 column in 100 µL 0.01 *M* hydrochloric acid by thorough agitation on a vortex mixer to ensure complete dispersion of the solution around the walls of the vessel.

2. Centrifuge the tube briefly (30 s) to bring the solution to the bottom of the tube and to maximize recovery. Working carefully to minimize loss of fluid, pass
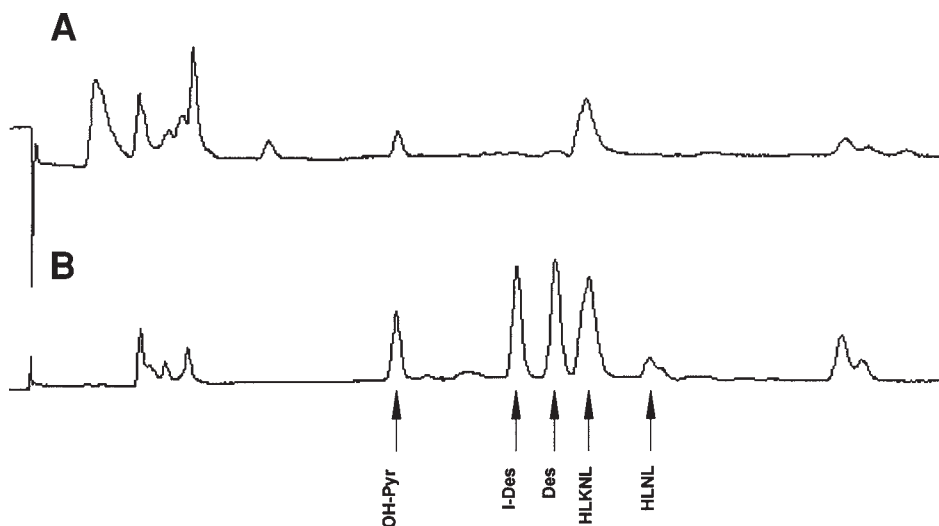
Fig. 1. **(A)** Typical crosslink profile of tissue-engineered cartilage from an amino acid analyzer using the method described here. The two crosslink peaks hydroxylysyl-pyridinoline (OH-Pyr) and hydroxylysino-keto-norleucine (HLKNL) are indicated. **(B)** Profile of crosslink standards run using the same analysis program. Additional crosslink standards to those above are Isodesmosine (I-Des), Desmosine (Des), and hydroxylysinonorleucine (HLNL).

    the sample through a 4-mm, 0.2-μm syringe filter to remove particulate matter. The sample is now ready for amino acid analysis (*see* **Note 14**).

3. The analytical column we use for the analysis is the high-resolution column (Amersham Pharmacia Biotech, Little Chalfont, Bucks, UK), filled with polymeric cation exchange resin in the sodium form. The column should be maintained at 90°C throughout the analysis.

4. Before applying the sample (80–90 μL), equilibrate the column in 0.2 *M* sodium citrate buffer, pH 4.25.

5. After the sample has been applied, elute the column with 0.4 *M* sodium citrate buffer, pH 5.31 (*see* **Note 15**) for 45 min (or to the point in the chromatogram when lysine is expected to elute). During this time, data should be collected by an integrator/data handling system.

6. Upon completion of the analytical run, wash the column in 0.4 *M* sodium hydroxide and then regenerate the resin in 0.2 *M* sodium citrate buffer pH 4.25 when it is ready for running the next sample.

7. From the collected data, compute the area under each peak and use this to calculate the concentration of each crosslink by comparison with the peak area of a leucine external standard of known concentration, taking into account the ninhydrin leucine equivalence value for each crosslink (*see* **Note 16**).

8. Typical elution profiles of a tissue-engineered cartilage and a mixture of crosslink standards are shown in **Fig. 1**.

4. Notes

1. Digestion of cartilage by proteinase K generally results in complete solubilization of the tissue, which is necessary for an accurate estimate of various components of the engineered cartilage matrix. However, in some instances, proteinase K fails to solubilize the tissue. We have found two different reasons for this. The first is that too much cartilage can be added to the centrifuge tube. In this case, the remaining undigested residue can be transferred to fresh proteinase K. The second is that calcified cartilage is resistant to proteolysis. This is a rare problem with good-quality engineered cartilage, but might be expected depending on the level of the hypertrophy of chondrocytes in the construct. In order to resolve this problem, increase the concentration of EDTA in the proteinase-K solution to 400 m*M*.

2. The GAG-DMB complex is unstable. Aggregates form and precipitate with time, and it is therefore advisable to read the absorption at the earliest convenient fixed time period. Preferably, the reading should be taken immediately (within 60 s) after adding DMB. Furthermore, the sensitivity of the assay can be increased by the use of wavelength = 590 nm. However, interference from other polyanions is more pronounced than at 525 nm.

3. Plate washing: A number of techniques have been used to wash ELISA plates. In the method outlined here, speed of washing is essential at the point when samples are being removed following a 30-min incubation time. Whereas plates can be rapidly immersed in a large bowl of washing buffer, this usually leaves the entire plate rather slippery from the detergent, making it difficult to handle. Automated plate-washers can be unreliable and are often rather slow. In our experience, the best method is to use a large reservoir (10–15 L) with a tap at the bottom. The reservoir should be positioned above a sink (e.g., on a shelf top), and a flexible tube should be attached to the outlet and allowed to run down into the sink. When the tap is opened, the washing buffer will run out onto the ELISA plate under the force of gravity. The flow-rate can be adjusted by squeezing the tube, either directly or using a clip.

4. Optimal antibody dilution: The anticollagen antibody must be used at an appropriate dilution. If it is too dilute, the MB value will be too low and inhibition will be difficult to detect. If it is too concentrated, higher concentrations of epitope will be needed to inhibit its binding to HDC on the ELISA plate. For optimal conditions, the antibody should be bound to HDC at a range of dilutions over a 30-min incubation time period at ambient temperature. After washing the plate, bound antibody can be detected using the second antibody/ALP detection system. A plot of log-dilution against OD 405 nm that is approx 40% of maximal OD is optimal for use in the assay. However, note that when the antibody is added to the preculture plate, it is diluted 1:1 with sample (or buffer), so it should be prepared initially at 2X the chosen concentration.

5. It is important to remove the aliquot for crosslink analysis before inactivation of the proteinase K by boiling, as the intermediate crosslinks are heat-labile and may be destroyed by boiling.

6. It is necessary to reduce with sodium borohydride, as this stabilizes the intermediate crosslinks to the next step in the procedure—i.e., acid hydrolysis.

7. It is customary to perform acid hydrolysis under a barrier of nitrogen gas (to eliminate oxygen); however, the presence of oxygen is not known to influence collagen crosslink assays.

8. The freeze-drying apparatus must be rigorously defended from attack by hydrochloric acid vapor that will destroy seals, welds, and pump valves very rapidly. Regular oil changes are essential to the long-term functioning of the dryer. A chemical trap placed between the dryer chamber and the vacuum pump will help to extend the pump life.

9. Determination of hydroxyproline is crucial to subsequent measurements, since the final crosslink quantification is expressed as moles of crosslink per mole of collagen. The most accurate method is by amino acid analysis, using the same ion-exchange column used for crosslink analysis and an analysis program appropriate for hydroxyproline. However, other analytical techniques are available—for example, automated flow analysis (Burkard Scientific, Uxbridge, UK) based on the method of Grant (1964) *(8)* or the microtiter plate method described here. This employs the same chemistry as the Grant method, and can be used for rapid determination of multiple samples.

10. Collagen crosslinks represent about one mole of crosslink per mole of collagen; thus, locating these novel amino acids among the excess of normal amino acids has historically proved difficult. Pre-fractionation using CF-1 cellulose is therefore carried out to remove the bulk of the non-crosslinking amino acids, thereby enhancing the relative proportion of the crosslinking amino acids.

11. It is important to record the date of the slurry production, because prolonged storage—e.g., longer than 2 mo, gives rise to an aggregated product that is unusable and must be discarded. During long-term storage, the 4:1:1 organic mixture also tends to separate into two layers and must not be used once this has occurred, as the two layers will not re-mix into a single phase.

12. Rehydration in this fashion prevents the formation of an "oily" residue that occasionally occurs if the samples are hydrated with the 4:1:1 organic mixture directly.

13. Evaporation is best achieved in a centrifugal evaporator, as the sample is then maintained as a small volume at the bottom of the tube. However, if such an evaporator is not available, then the sample can be freeze-dried, although poor recovery from the vessel walls then becomes an issue.

14. The technique is based on the use of an amino acid analyzer; we use an AlphaPlusII (Amersham Pharmacia Biotech) equipped with ninydrin detection as previously described *(9)* but the technique can be applied to other models of amino acid analyzers. The supplier of such equipment obviously provides instructions on its use, so detailed explanations will not be provided here except for information that is specific to the analysis of collagen crosslinks.

15. This can be prepared by dilution of Amersham Pharmacia's 1.2-*M* sodium citrate buffer, pH 6.45, to a molarity of 0.4 *M* with water containing 0.1% phenol, fol-

lowed by adjustment to pH 5.31 with concentrated hydrochloric acid. The modified buffer should then be passed through a 0.2-μm filter prior to use.

16. Ninhydrin leucine equivalence values for the crosslinks are as follows: Hydroxylysyl pyridinoline (OH-Pyr) 1.7; Lysyl pyridinoline (Lys-Pyr) 1.7; Hydroxylysyl-keto-norleucine (HLKNL) 1.8.

References

1. Hollander, A. P. (2001) Collagen degradation assays. *Methods Mol. Biol.* **151,** 473–484.
2. Handley, C. J. and Buttle, D. J. (1995) Assay of proteoglycan degradation. *Methods Enzymol.* **248,** 47–58.
3. Hollander, A. P., Heathfield, T. F., Webber, C., Iwata, Y., Bourne, R., Rorabeck, C., and Poole, A. R. (1994) Increased damage to type II collagen in osteoarthritic articular cartilage detected by a new immunoassay. *J. Clin. Investig.* **93,** 1722–1732.
4. Creemers, L. B., Jansen, D. C., van Veen-Reurings, A., van den Bos, T., and Everts, V. (1997) Microassay for the assessment of low levels of hydroxyproline. *Biotechniques* **22,** 656–658.
5. Knott, L. and Bailey, A. J. (1998) Collagen cross-links in mineralizing tissues: A review of their chemistry, function, and clinical relevance. *Bone* **22,** 181–187.
6. Black, D., Duncan, A., and Robins, S. P. (1988) Quantitative analysis of the pyridinium crosslinks of collagen in urine using ion-paired reversed-phase high-performance liquid chromatography. *Anal. Biochem.* **169,** 197–203.
7. Sims, T. J. and Bailey, A. J. (1992) Quantitative analysis of collagen and elastin cross-links using a single-column system. *J. Chromatogr.* **582,** 49–55.
8. Grant, R. A. (1964) Application of the auto-analyser to connective tissue analysis. *Clinical Pathology* **17,** 685–691.
9. Sims, T. J., Avery, N. C., and Bailey, A. J., eds. (2000) Quantitative determination of collagen crosslinks. *Extracellular Matrix Protocols* (Streuli, C. and Grant, M., eds.), Humana Press: Totowa, NJ.

18

Real-Time Quantitative RT-PCR Assays

Ivan Martin and Oliver Frank

1. Introduction

Analysis of gene expression at the mRNA level may be used, together with other structural and functional evaluations, to characterize the quality of engineered tissues. In turn, engineered tissues may be used as model systems of developing tissues to investigate how mRNA gene expression is modulated by a variety of factors, including structural (e.g., type of three-dimensional [3D] scaffold), biochemical (e.g., combination of bioactive molecules), and physical (e.g., regime of bioreactor cultivation). In order to reliably evaluate mRNA levels, Northern blotting and *in situ* hybridization (ISH) methods are not sensitive enough to detect low-level gene expression, and not accurate enough to quantify the full range of expression. An amplification step is thus often required to quantify mRNA amounts from engineered tissues of limited size. Quantification of mRNA using conventional reverse-transcriptase polymerase chain reaction (RT-PCR) techniques may be of limited accuracy, both because of the detection method used (e.g., semi-quantitative image analysis), and because analysis is often performed using a constant number of amplification cycles, after which the system could be in a saturation phase. The recently established real-time RT-PCR technology has made mRNA quantitation more reproducible, precise, and sensitive than conventional RT-PCR, because it allows measurement of the amount of amplified product using a quantitative laser-based method and in the early exponential phase of the PCR reaction, when none of the reagents is rate-limiting *(1)*. Furthermore, real-time RT-PCR does not require post-reaction processing, and therefore has a high sample throughput.

1.1. Theoretical Basis of Real-Time RT-PCR

Real-time quantitative RT-PCR monitors the degradation of a sequence-specific, dual-labeled fluorescent probe after each cycle of PCR amplification. During the extension phase, the 5'-exonuclease activity of Taq DNA polymerase cleaves the probe, separating the 5'-reporter fluorescent dye from the 3'-quencher fluorescent dye, and resulting in an increase in the emission spectra of the reporter fluorescent dye. After subtraction of the background fluorescence, typically calculated during the first 15 amplification cycles, the measured fluorescence is graphed as an amplification plot. Each reaction is characterized by a value—Ct—defined as the fractional number of cycles at which the reporter fluorescent emission reaches a fixed threshold level in the exponential region of the amplification plot. The Ct value is correlated to the amount of target mRNA: a larger starting quantity of mRNA target results in a lower number of PCR cycles required for the reporter fluorescent emission to reach the threshold, and therefore a lower Ct value. Thus, the method is not based on the measurement of the total amount of amplified product after a fixed number of cycles, as in conventional PCR, and does not require post-PCR processing of the product *(1)*.

2. Materials

The materials listed have been used to establish the protocols described here. Similar commercially available products or kits could also be used.

2.1. Extraction of Total RNA

1. Phosphate buffered saline (PBS).
2. Ice bucket or tray.
3. Trizol Reagent (Life Technologies, CH).
4. Sonicator (e.g., Sonic dismembrator 550, Fisher Scientific, CH).
5. Tissue homogenizer (e.g., Polytron PT 1200, Kinematica AG, CH).
6. Refrigerated high-speed centrifuge, centrifuge with vacuum system.
7. Chloroform.
8. Isopropanol.
9. 75% ethanol.
10. 20 µg/µL glycogen.
11. Silica gel-based membranes (e.g., RNeasy kit, Qiagen, CH).

2.2. Synthesis of cDNA

1. DNase (e.g., DNA-free kit, Ambion).
2. Spectrometer, PCR heating block or water bath.
3. RT (e.g., Stratascript kit, Stratagene, NL), 500 µg/mL random hexamers (e.g., Catalys AG, CH), RNase-free double-distilled water.

2.3. Design of Primers and Probes

1. Primer Express™ software (Applied Biosystems, CH).

2.4. Real-Time PCR Amplification

1. Universal PCR Master Mix (Applied Biosystems).
2. Primers and FAM-TAMRA or VIC-TAMRA labeled probes (Applied Biosystems).
3. 96-well optical reaction plate and caps.
4. ABI Prism 7700 Sequence Detection System (Taqman®, Applied Biosystems).
5. Sequence Detector software (Applied Biosystems).

3. Methods

The protocols described here have been established for mRNA analysis of human cartilage explants *(2)*, applied for the evaluation of engineered cartilaginous tissues starting from human chondrocytes *(3)* and extended to the evaluation of mineralized bone-like layers generated using human mesenchymal progenitor cells from the bone marrow *(4)*. The technique is virtually adaptable to any engineered tissue, although the properties of the extracellular matrix (ECM) and of the cell type may introduce specific changes in the protocol, as detailed in the Notes section.

3.1. Extraction of Total RNA

3.1.1. Extraction from Cell Layers or Tissues With Little ECM (see **Note 1**)

1. Rinse the cell layer/tissue with phosphate-buffered saline (PBS). Keep the specimen on ice for all the steps described, unless otherwise stated.
2. Solubilize the cell layer (one confluent 10-cm-diameter dish) or the tissue (100 mg) in 1 mL Trizol. Transfer the content in a RNase-free tube. In case the layer/tissue contains mineralized matrix, sonicate at medium intensity for 1 min.
3. Add 0.2 mL chloroform, vortex, and incubate on ice for 10 min. Centrifuge at 1.4*g* at 4°C for 15 min.
4. Transfer the upper phase (about 0.5 mL) to a new tube; add 2 μL of 20 μg/μL glycogen at the bottom of the new tube in order to better visualize the RNA pellet after precipitation. Add 0.5 mL of isopropanol and incubate on ice for 15 min. Centrifuge at 1.4*g* at 4°C for 20 min.
5. Discard the isopropanol by gentle inversion or aspiration and add 1 mL of 75% ethanol. Centrifuge at 1.4*g* at 4°C for 5 min.
6. Discard the ethanol and repeat **step 5** twice.
7. Air-dry or centrifuge with vacuum pump to evaporate all the remaining ethanol. Dissolve the RNA pellet in double-distilled RNase-free water.

3.1.2. Extraction from Tissues With Abundant ECM (see **Note 1**)

1. Chop the tissue specimen in 2–3-mm side pieces using a surgical blade. Keep the specimen on ice for all the steps described, unless otherwise stated.

2. Collect 100 mg of tissue in a RNase-free tube.
3. Add 1 mL of lysis buffer (RNeasy kit).
4. Homogenize the tissue and follow the instructions of the RNeasy Kit.

3.2. Synthesis of cDNA

1. If necessary, treat the extracted RNA with DNase (*see* **Note 2**), following the instructions of the DNA free kit.
2. Measure the absorbance of a diluted aliquot of the extracted RNA at 260 nm and 280 nm. An absorbance of 1 U at 260 nm corresponds to 40 µg of RNA per mL. The ratio between the absorbance values at 260 and 280 gives an estimate of RNA purity, and should be higher than 1.5.
3. Synthesize the cDNA starting from 5 µg of RNA, following the instructions of the Stratascript kit and using random hexamers as primers (*see* **Note 3**).
4. Dilute the cDNA up to 250 µL using double-distilled water.

3.3. Design of Primers and Probes

1. For each gene of interest plus the selected housekeeping gene (*see* **Note 4**), design primers and probes with the assistance of the Primer Express computer program. The sequences should display minimal internal structure (e.g., primer-dimer formation) and similar melting temperatures (e.g., T_m of primers = 58°–60°C and T_m of probes = 68°–70°C) (*see* **Note 5**).

3.4. Real-Time RT-PCR

1. Prepare the reaction mix by adding into each reaction well the following: 12.5 µL of 2X Master Mix; the required amount of primers and probe (*see* **Note 6**); double-distilled water, for a total reaction volume of 20 µL; 5 µL of cDNA (*see* **Note 7**).
2. Close the wells with the cap strips and centrifuge the plate at 320*g* for 1 min.
3. Run the PCR with typical settings: at 95°C for 10 min, then up to 45 cycles consisting of a denaturation step at 95°C for 15 s and an extension step at 60°C for 1 min.
4. The Ct value of a real-time PCR reaction corresponds to the cycle number at which the fluorescence intensity reaches a threshold (usually in the range 0.03–0.06). The threshold level must be selected for each set of primers and probe, so that at this level all amplification curves are in their exponential phase.

3.5. Real-Time PCR Validation

1. Determine the optimal concentrations for the designed primers and probes as the lowest ones giving the highest fluorescence levels and the lowest Ct values (PE-ABI; Sequence Detector User Bulletin 2).
2. Determine the efficiency of the amplification by measuring Ct values after serial dilutions of the cDNA template. The amplification efficiency is calculated as the slope of the best linear fit of the expected increase in Ct (e.g., the logarithm in base 2 of the dilution factor) plotted vs the measured increase in Ct. A slope of 1

corresponds to one additional cycle to reach the threshold after a 1:2 dilution, indicating a 100% efficiency (**Fig. 1**). An acceptable set of primers and probe should yield an efficiency not lower than 90%

3.6. Data Analysis

1. For each cDNA sample, subtract the Ct value of the target gene to the Ct value of the housekeeping gene, to derive ΔCt.
2. Repeat step 1 using the cDNA of a reference sample, to derive Δ'Ct. Determine $\Delta\Delta$Ct = ΔCt – Δ'Ct.
3. Calculate the amount of target mRNA, normalized to the housekeeping gene, either as $2^{\Delta Ct}$ (unitless number) or as $2^{\Delta\Delta Ct}$ (fold difference as compared to the reference sample; *see* **Note 8**).

4. Notes

1. Large amounts of ECM proteins, particularly abundant in cartilage and other connective tissues, may interfere with the extraction procedure and/or inhibit the DNA polymerase in the PCR assays. This problem is solved by purifying the RNA on silica-gel membranes—e.g., those included in the RNeasy Kit by Qiagen. Purification membranes may be used to extract and purify RNA from any tissue type or cell culture, but generally they result in lower RNA yields, particularly when starting from mineralized cell layers. Therefore, we recommend the use of purification membranes only starting from tissues with high amounts of ECM.
2. Treatment with DNase may be performed routinely, in order to minimize the risk of amplifying contaminating genomic DNA sequences. The treatment is essential if the primers and probe sets used in the PCR assays do not cover different exons, and thus recognize the genomic sequences. Thus, DNase treatment is also essential when a ribosomal RNA (rRNA) sequence (e.g., 18s), which is identical to the genomic one, is introduced as a housekeeping gene.
3. The use of random hexamers for the cDNA synthesis is essential when a rRNA sequence is introduced as housekeeping gene. Otherwise, if only mRNA sequences are to be amplified, it is possible to use oligo dT as primers.
4. The choice of the housekeeping gene should depend on the cell system under investigation, although very little is currently known about which housekeeping gene is most consistently expressed in specific cell types *(5)*.
5. Whenever possible (e.g., when the position of introns and exons in the genomic sequence is known), the middle third of the probe sequence should be placed at the junction between two exons. This eliminates the risk of nonspecific detection of products amplified from contaminating genomic DNA.
6. Before the optimal concentrations of primers and probes are determined, the system can be tested using 1-µ*M* primers and 300-n*M* probes. Typically, 10X working solutions can be prepared, so that 2.5 µL can be added to each reaction well.
7. In order to amplify the target and an endogenous reference (housekeeping gene) in the same well, it is possible to use more than one primer/probe set (multiplexing) in the same reaction mix. The conditions for this are that the reporter dyes
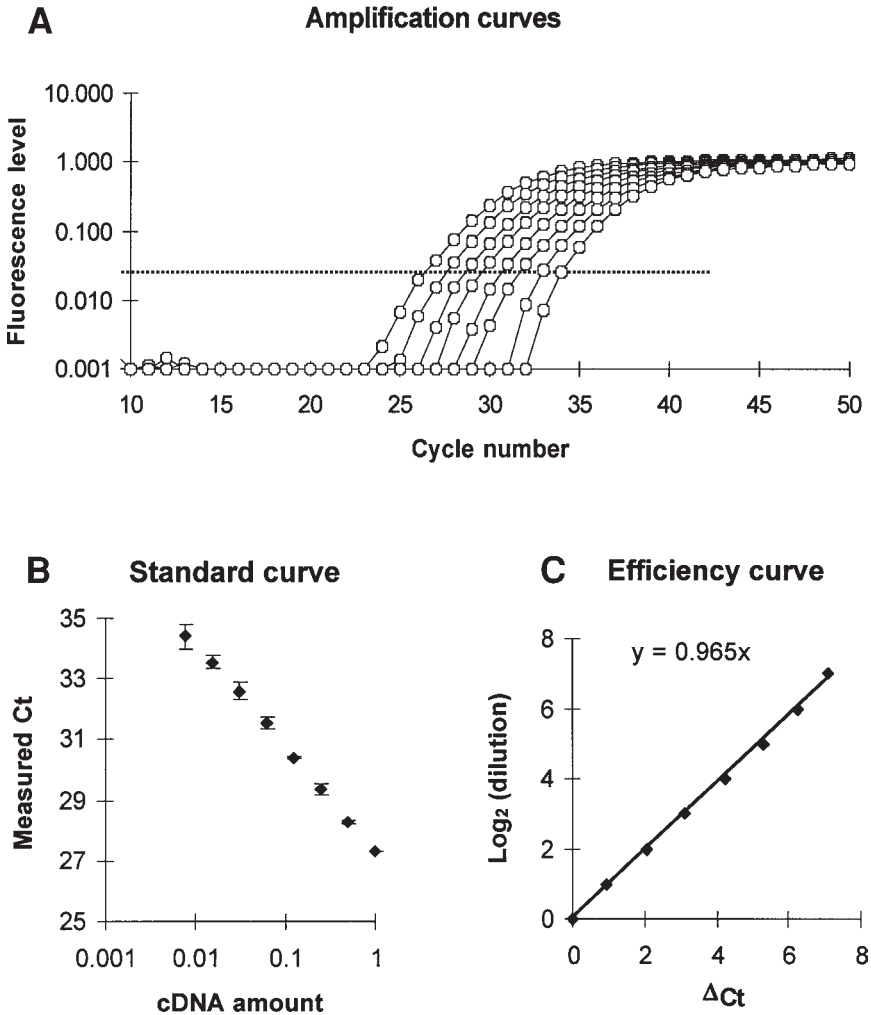
A **Amplification curves**

B **Standard curve**   **C** **Efficiency curve**

Fig. 1. Typical amplification, standard, and efficiency curves obtained by real-time PCR. (**A**) Amplification plots obtained by serial dilutions of cDNA, starting from 1 ng (*leftmost curve*) to 0.0078 ng (1:128 dilution, *rightmost curve*). C_t is defined as the fractional cycle number at which the fluorescent signal reaches the selected threshold (indicated by a dotted line). In the graph, values lower than 0.001 were set to 0.001. (**B**) Standard curve obtained by plotting the measured C_t vs the starting cDNA amount. (**C**) Efficiency curve obtained by plotting the measured increase in C_t after each 1:2 dilution (ΔCt) vs the expected increase in C_t (e.g., the logarithm in base 2 of the dilution factor). The amplification efficiency for each target sequence is calculated as the slope of the best linear fit of the corresponding efficiency curve (e.g., 0.965 in this case). An ideal efficiency of 1 (or 100%) corresponds to one additional cycle required to reach the same threshold after a 1:2 dilution.

for the two probes have different emission wavelength maxima and there is no competition between the two parallel reactions. The latter condition is satisfied if the exponential phases of amplification in the two reactions are not overlapping: this is typically achieved by using rRNA as an endogenous reference (the concentration is always greater than the concentration of any target mRNA), and by limiting the concentration of primers of the rRNA sequence (so that the reaction reaches a plateau before the exponential phase of the target gene reaction) (PE-ABI; Sequence Detector User Bulletin 2).

8. Values derived using the formula $2^{\Delta Ct}$ can be used to compare the relative amount of target gene in different samples, but cannot be considered as absolute expression levels of the target gene (e.g., fold expression of the housekeeping gene), since the intensity of fluorescence emissions from different probes may vary (PE-ABI; Sequence Detector User Bulletin 2). The choice of a reference sample (calibrator) and the use of the formula $2^{\Delta \Delta Ct}$ allows a more straightforward expression of the amount of the target gene mRNA, normalized to the housekeeping gene, as fold difference relative to the selected reference.

References

1. Gibson, U. E., Heid, C. A., and Williams, P.M. (1996) A novel method for real time quantitative RT-PCR. *Genome Res.* **6,** 995–1001.
2. Martin, I., Jakob, M., Schafer, D., Dick, W., Spagnoli, G., and Heberer, M. (2001) Quantitative analysis of gene expression in human articular cartilage from normal and osteoarthritic joints. *Osteoarthritis Cartilage* **9,** 112–118.
3. Jakob, M., Démarteau, O., Schäfer, D., Hintermann, B., Dick, W., and Martin, I. (2001) Specific growth factors during the expansion and redifferentiation of adult human articular chondrocytes enhance chondrogenesis and cartilaginous tissue formation in vitro. *J. Cell. Biochem.* **81,** 368–377.
4. Frank, O., Heim, M., Jakob, M., et al. (2002) Real-time quantitative RT-PCR analysis of human bone marrow stromal cells during osteogenic differentiation in vitro. *J. Cell Biochem.* **85,** 737–746.
5. Bustin, S. A. (2000) Absolute quantification of mRNA using real-time reverse transcription polymerase chain reaction assays. *J. Mol. Endocrinol.* **25,** 169–193.

19

Mechanical Testing of Cell-Material Constructs

A Review

John Kisiday, Alex Kerin, and Alan Grodzinsky

1. Introduction

The exponential growth in basic research and clinical trials involving tissue-engineered materials has generated a corresponding need for the evaluation of the material properties and functional performance of these constructs during development and/or after implantation. Applications focusing on musculoskeletal tissues, in particular, require detailed assessment of the biomechanical properties of neo-tissue constructs in vitro and in vivo *(1)*. Based on the known properties of normal tissues, investigators have identified a range of biological, biochemical, and biophysical end-point parameters that must be quantified to determine the potential for success of a particular tissue-engineering methodology. Such end-point assessment is critical to our understanding of the basic scientific approaches underlying tissue engineering. In addition, biomechanical assessment is crucial for the implementation of regulatory processes that are coupled to clinical practice.

When creating musculoskeletal tissue constructs, it is important to determine whether the constructs are capable of withstanding the forces associated with locomotion in vivo, and whether construct properties compare to the corresponding native tissue *(1,2)*. In some instances, it is required that the construct should be bioabsorbable, and measurement of material properties may help to quantify the mechanisms and kinetics of biodegradability. For tissue-engineering approaches in which cells must re-synthesize a functional extracellular matrix (ECM) within a scaffold, the mechanical properties of the construct will indicate whether the native structure is being replicated *(3)*. The ability to quantify the intrinsic mechanical properties of tissue constructs is

also necessary to compare alternative techniques used to synthesize specific tissues and to compare approaches used by different research groups. Finally, the ability to monitor the mechanical properties of implanted constructs *in situ* can help to evaluate the degree of successful repair of injured or diseased tissues and organs *(4)*.

1.1. Native Tissue Properties Motivate Construct Evaluation

Musculoskeletal tissues are composed of cells surrounded by a porous, hydrated ECM (including a mineralized phase in the case of hard tissues). Biomechanical characterization of such tissues must reflect a variety of material properties, including the equilibrium behavior of the ECM and the time-dependent viscoelastic and poroelastic behavior of the tissue following deformation. For example, articular cartilage is often modeled as a poroelastic or biphasic material *(5,6)* with a porous solid phase and mobile interstitial fluid containing ionic *(7)* and other solutes. The mechanical properties are dependent on the behavior of the solid phase—which may be modeled as intrinsically elastic or viscoelastic *(8)*—as well as fluid–solid interactions that may accompany tissue deformation, limited by matrix porosity and electrical charge effects *(6,7)*. These fluid solid interactions give the tissue increased stiffness to loads that occur at higher rates (higher frequencies) *(9)*, a property that is critical to functional behavior in vivo. Therefore, investigators who study the biomechanical behavior of tissue-engineered cartilage constructs look to these cartilage-like properties as hallmarks of the potential for success upon implantation *(10–12)*.

1.2. Characterization of Constructs In Vitro

Cell-seeded constructs for tendon, ligament, meniscus, cartilage, and bone are being studied with the use of a variety of cell sources (e.g., primary cells, cell lines, stem cells) cultured in natural and synthetic scaffold materials *(13–15)*. Motivated by the tissue type and desired properties, methodologies have been developed to quantify construct properties in compression (confined and unconfined), tension, and shear. Although destructive non-sterile measurement techniques can be used to advantage, several incubator-housed testing instruments have recently been developed. Such devices enable the investigator to measure the time-dependent evolution of living construct material properties over a period of days, weeks, or even months in culture. These instruments can also be used for mechanical stimulation of cell-seeded constructs as a means of improving the functional mechanical properties of the end product.

1.3. Characterization of Repair Tissue In Situ

The use of tissue engineered constructs for musculoskeletal applications in vivo has necessitated the development of methods for quantifying the func-
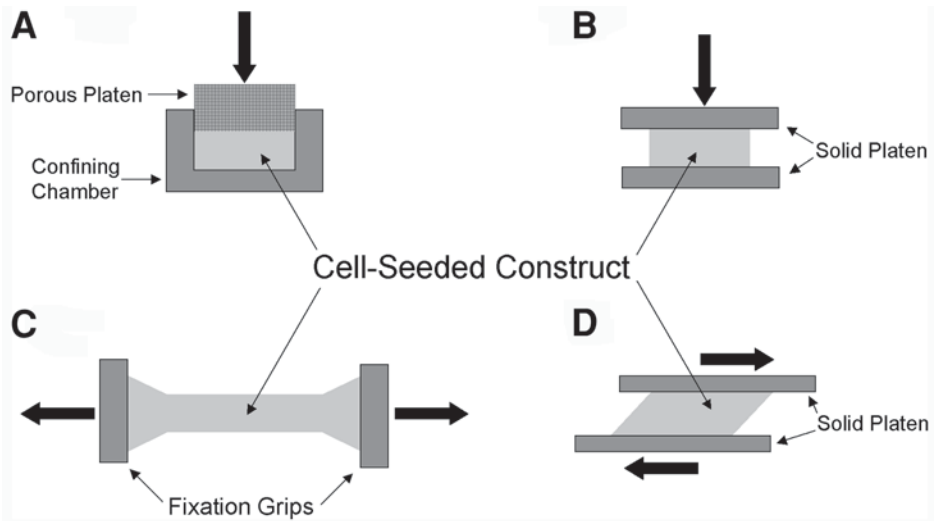
Fig. 1. Four testing configurations for measurement of intrinsic material properties of tissue-engineered constructs and cellular deformation in vitro: **(A)** Uniaxial confined compression. **(B)** Uniaxial unconfined compression. **(C)** Tension. **(D)** Shear.

tional biomechanical properties of the resulting implants as repair or unwanted degeneration ensues. After implantation into animals, it is often desirable to compare the properties of the repair tissue to those of adjacent normal tissue. Histological examination can provide valuable, qualitative information regarding the biochemical composition of the implant and tissue integration into the host. Non-destructive imaging modalities such as magnetic resonance imaging (MRI) can also provide compositional data during stages of construct development in vivo. However, it is extremely useful to have direct quantitative measurements of the biomechanical properties of the repair tissue that cannot yet be obtained by other modalities. Several new devices are now under various stages of development for direct *in situ* measurement of material properties, as summarized here.

2. Overview of In Vitro Biomechanical Evaluation

Upon implantation, tissue engineered constructs may be subjected to a complex physical environment. The objective of biomechanical testing in vitro is not to directly mimic *in situ* loading. Instead, mechanical tests utilizing compression, tension, or shear loading (**Fig. 1**) may be conducted *(2)* to establish the baseline intrinsic material properties of the construct (e.g., **Table 1** for cartilage). These values may be compared to those of native tissues to estimate whether the construct is suitable for implantation. The material properties of

Table 1
Mechanical Properties of Acellular and Chondrocyte-Seeded Constructs

Scaffold	Test mode	Time in culture	Modulus
Collagen-GAG Sponge *(22)*	Unconfined compression (equilibrium)	Acellular Type I Collagen Acellular Type II Collagen	145–730 Pa 730 Pa
Chondrocyte-seeded Agarose *(3)*	Confined compression (equilibrium)	0 d 70 d	20 kPa 150 kPa
Chondrocyte-seeded PGA *(20,21,30)*	Confined compression (equilibrium)	6 wk 7 mo	52 kPa 930 kPa
	Dynamic shear (frequency - 1 Hz)	7 d 56 d	0.8 kPa 15 kPa
PVA hydrogel *(25)*	Unconfined compression, (transient strain rate -1000%/min)	Acellular	1 MPa @ 10% strain 18 MPa @ 60% strain
	Shear (transient strain rate - 75%/min)		100 MPa @ 10% strain 450 MPa @ 60% strain
Scaffold-free monolayer *(28)*	Tension (transient strain rate - 12%/min)	8 wk	1.3 MPa

Values are summarized for examples of compressive, tensile, and shear testing in both equilibrium and dynamic modes.

various constructs may also be compared to evaluate the relative advantages of a particular scaffold material (*see* **Note 1**).

2.1. Equilibrium Biomechanical Properties

The equilibrium stress-strain behavior of constructs is determined by measuring the stress (load normalized to construct cross-sectional area) in response to an applied strain (change in tissue dimension normalized to the original dimension), or vice versa. Equilibrium properties may be evaluated by applying very slow ramps of load or displacement (e.g., at a low strain rate). Alternatively, a series of small increments in load (*or displacement*) may be applied, and the final steady-state displacement (*load*) attained after creep (*stress relaxation*) is used to compute the equilibrium stress-strain behavior. This stress-strain plot is used to calculate the equilibrium modulus. The simplicity of this testing protocol allows for measurements to be made using a simple-load cell and displacement system.

Constructs may exhibit an elastic region in which scaffold geometry is completely restored upon unloading. Native biological tissues are likely to be inhomogeneous and anisotropic, and may exhibit highly nonlinear stress-strain behavior. The initial deformation of tendons, for example, results in nonlinear increases in stress, the so-called "toe" region. The equilibrium stress-strain behavior beyond this toe region may be approximately linear, and is of interest in defining an equilibrium elastic modulus of the tissue—the slope of the linear stress/strain plot *(16)*. Similar behavior may be expected from cell-seeded constructs, although construct properties may be initially more homogeneous if cells are evenly seeded throughout the scaffold, especially at early stages of matrix deposition.

2.2. Dynamic Biomechanical Properties

Dynamic biomechanical measurements are important in characterizing construct response to periodic loading environments, such as that experienced by musculoskeletal tissues during locomotion. Thus, the rate or frequency of testing is motivated by physiological loading rates. The complex nature of dynamic testing requires more sophisticated instruments capable of feedback control of applied displacement or load. Sinusoidal, saw-tooth, pulse-like, or other waveforms are often used. Because of the poroelastic and viscoelastic properties of cell-seeded constructs, dynamic properties will depend on specimen geometry and testing conditions. In particular, dynamic properties are expected to depend on strain rate or frequency *(6)*. Rapid deformation also creates a proportional increase in hydrostatic pressure within a fluid-filled cell-seeded construct. In addition, the viscoelastic relaxation properties of the ECM are limited by rapid deformation, thereby increasing material stiffness. Test sample geometry may

also complicate the measurement of biomechanical properties. Cell-seeded constructs are often limited in size. As a result, clamping of the construct by the testing grips of the instrument can cause nonuniform strain distributions within the sample. Gardiner et al. *(17)* demonstrates an example of the effects of sample geometry on shear properties. Guidelines for optimal sample geometry are available from the American Society for Testing and Materials (ASTM).

2.3. Failure Testing

In addition to evaluating constructs in a non-destructive manner, failure testing may be used to identify the maximum load or strain that the construct may endure. For example, the strain at which a construct undergoes permanent deformation, and will not return to the original geometry upon unloading, is known as the yield strain, and the accompanying stress, the yield stress (or strength). Constructs tested in tension or shear may be deformed to the point when macroscopic fractures occur *(16)*, corresponding to the ultimate stress (or strength). Compressive ultimate strength testing is possible, but it is sometimes difficult to define failure, especially in softer tissues. Failure properties may be compared to the mechanical environment encountered in vivo in order to predict the structural stability of the implant.

Determining which failure parameter is the most relevant depends on the expected loading as well as the tissue surrounding the construct. For example, implantation of constructs into focal defects in articular cartilage can create an interface between native and construct materials with very different compressive stiffness. Without adequate integration at the interface, joint loading forces *(18)* can lead to failure at the interface, a very challenging problem for cartilage tissue engineering. Similarly, implantation of constructs for bone regeneration that occupy the entire cross-section of the bone must support total structural loading. Variation in construct strain can be predicted from applied stress. Construct failure analysis is based on the understanding of subfailure and failure properties of the material, utilizing the testing configurations outlined here.

3. In Vitro Biomechanical Methods

3.1. Confined and Unconfined Compression

Specimen geometry for compression testing (*see* **Notes 2–4**) is typically cylindrical disk or slab structures, with parallel surfaces to ensure even load distribution. Compressive testing is performed with samples held in a radially unconfined or confined geometry. In unconfined compression (**Fig. 1B**), samples are allowed to freely expand radially during uniaxial compression (*see* **Note 5**). Under ideal conditions, the slope of the measured equilibrium stress/

strain curve in the linear region gives the equilibrium compressive Young's modulus, E, of the construct. Specimen geometry is limited to a range of aspect ratios of sample height/width to prevent testing artifacts such as buckling.

Confined compression (**Fig. 1A**) requires specimens to be tested in a tight-fitting chamber to prevent any radial expansion. Typically, the specimen is compressed by a porous platen to allow free draining of the construct fluid at the platen-construct interface during compression (*see* **Notes 6,7**). Both the equilibrium-confined compression modulus, H, and the dynamic stiffness can be measured in this configuration. The dynamic stiffness includes contributions from hydrostatic pressurization within the construct associated with fluid-ECM frictional forces *(6,7)*. Extensive descriptions of methodological details are available in confined *(3,19,20–23)* and unconfined *(9,24,25)* geometries.

3.2. Tension

Tensile properties of constructs may be determined from both equilibrium and time-varying stress-strain measurements. The equilibrium Young's modulus, E, can be calculated from the linear region of the equilibrium stress-strain curve. Samples must be appropriately fixed within testing grips to prevent artefactual failure at the sample/grip interface. If the specimen size allows, test samples may be cut in a "dogbone" geometry (**Fig. 1C**) such that a large grip area relative to the working length *(26)* minimizes stress concentrations at the grip. Other fixation strategies are available for specific sample geometries (*16,27–29*). In all cases, failure of the sample within the working length is indicative of a properly fixed sample.

Tensile test sample lengths must be significantly greater than cross-sectional dimensions (*see* **Note 1**) to ensure uniform strain through the working length; *see* ASTM guidelines summarized in **ref.** *(2)*. Large working lengths may also minimize bending effects resulting from irregular samples or improper alignment in the testing apparatus. When a working length has not been defined, evaluation of strain must be representative of the working length. Extensometers, optical scanning, or other devices may be necessary to accurately evaluate strain in the region of interest.

3.3. Shear

Specimen geometry for shear measurements is similar to that for compression, in which flat, parallel surfaces are necessary for accurate testing. Samples are fixed between parallel platens so that shear deformation may be performed using rotational *(30,31)* or translational *(25,31–34)* displacement (*see* **Note 8**) (**Fig. 1D**). Translational displacements result in shear stress equal to the force normalized to specimen surface area. For rotational displacement, stress is calculated from the applied torque, sample radius, and surface polar moment of
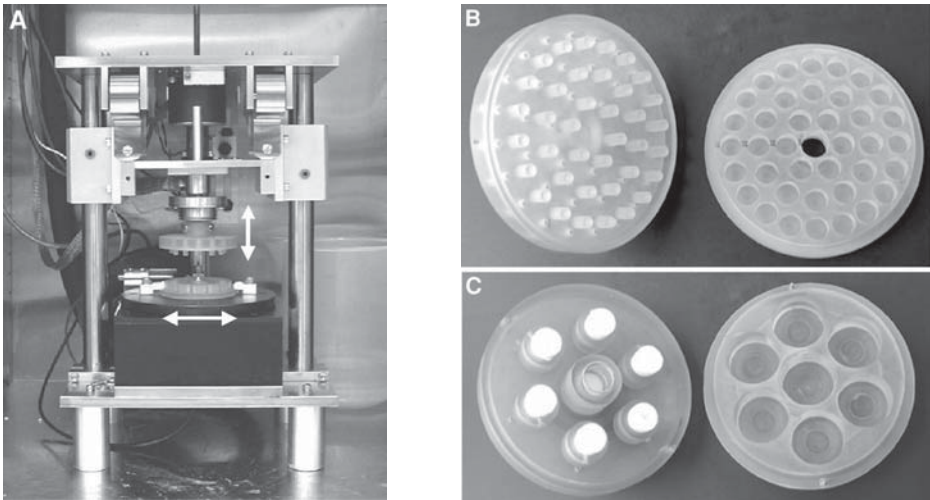
Fig. 2. (**A**) Example of an incubator-housed material testing instrument capable of measuring compressive, shear, and tensile properties, as well as studying the effects of applied mechanical loads on the development of tissue-engineered constructs *(31)*. A testing chamber capable of loading 12 plugs in shear and/or compression is installed. (**B**) Loading chamber capable of testing or stimulating up to 38 samples in individual wells. Different well radii from the center allow three different levels of shear strain to be applied during a single loading event. (**C**) Chamber capable of compressive loading of up to six large cell-material constructs. A central spring ensures that the platen lifts off the samples during the unloading part of the cycle. Platens to compress the samples are porous to ensure adequate transport of feed media to center of constructs during prolonged loading.

inertia (e.g., *see* **ref. 32**), and shear strain is defined as the angle of deformation divided by the height of the sample. Both equilibrium and dynamic shear measurements are important for construct characterization. Under steady-state conditions, the equilibrium shear modulus G is calculated from the linear region of the stress-strain curve. The dynamic complex shear modulus, G*, includes the so-called storage (in phase) and loss (out of phase) moduli. For ideal, infinitesimal shear deformation, there is no fluid flow within the construct, and therefore, no fluid-solid frictional interactions. Thus, the dynamic G* reflects the frequency-dependent intrinsic viscoelastic properties of the ECM *(34)*.

3.4. Biomechanics at the Cell and Nano-Molecular-Length Scales

Mechanical properties of cell-seeded tissue-engineered constructs are likely to be minimally influenced by the presence of cells. Cells typically occupy a
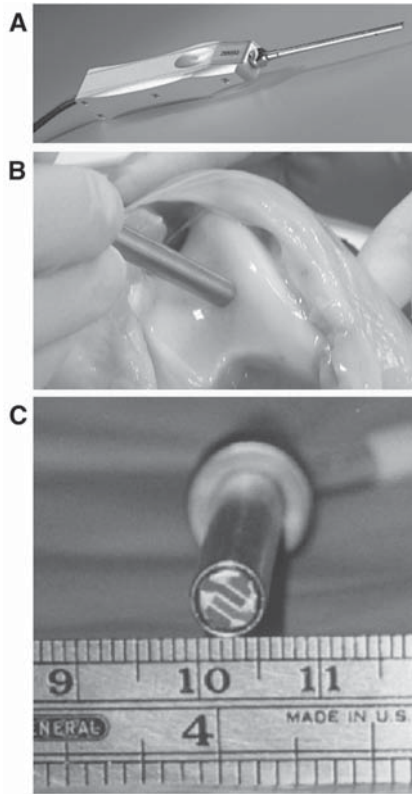
Fig. 3. **(A,B)** Devices capable of measuring material properties of constructs *in situ*. Artscan (Helsinki, Finland) probe capable of measuring cartilage compressive stiffness *(4,49)*. **(C)** End view of sensors of surface electromechanical spectroscopy probe *(51,52)* capable of measuring impedance (electrical resistance) in cartilage. The impedance changes with tissue swelling and with changes in the content of charged GAGs. This probe is also capable of measuring electrical straming potentials and mechanical stress generated by a small electric currents (related to tissue content of GAG, tissue stiffness, hydraulic permeability, and other material properties).

small volume relative to overall scaffold geometry, and cell stiffness is typically low compared to that of the scaffold or newly synthesized. For example, a micropipet aspiration technique has been used to evaluate the elastic modulus of isolated chondrocytes, giving E ~ 0.6 kPa *(35)*. Atomic force microscopy (AFM) indentation analysis *(36)* and magnetic bead rheometry *(37)* have provided values of fibroblast moduli E ~ 3–5 kPa and G ~ 20 kPa. In comparison, the moduli of cartilage *(38)* and ligament and tendon *(39)* are at least two orders of magnitude greater than that of the individual cells because of the

presence of ECM. Scaffold material properties vary, but are likely to be greater than that of the cells for practical handling. Therefore, material properties of cell-seeded constructs are likely to be dominated by accumulated ECM, with contributions from stiffer scaffold materials. Consequently, scaffold-ECM strain will be transmitted to the seeded cells in proportion to the deformation of the localized pericellular environment. Cell deformation has been visualized in chondrocyte-seeded agarose scaffolds. With no accumulation of ECM, compressive scaffold strains of 5–15% produced axial compression and lateral extension of the cells, changing cell morphology from spherical to elliptical *(40)*. Mechanical strain has also been observed to increase cell surface area and deform the nucleus of agarose-seeded chondrocytes *(41)*. These experiments illustrate the potential for regulation of biosynthesis in cell-seeded constructs by mechanotransduction. Static compression *(42,43)*, dynamic compression *(43)*, and dynamic shear loading *(44)* have been found to modulate ECM biosynthesis in cartilage explant culture. Static and dynamic compression is also a potent regulator of cell metabolism in chondrocyte-seeded agarose *(11,45)* and alginate *(46)*. Therefore, mechanical loading applied in vivo or during in vitro conditioning prior to implantation may be an important factor in the stimulation of an appropriate repair response using cell-seeded constructs.

3.5. Fatigue Testing

The mechanical tests previously described focus on testing of constructs in a nondestructive manner. However, in many instances it is important to know how a construct will perform over repeated loading cycles as well as the maximum stress it will bear before failure. Fatigue tests are common in the study of soft tissues and tissue replacements that are loaded in tension, such as tendons *(47)*. Fatigue during shear and compressive loading have also been addressed in detail *(34,47)*. A nominal target stress or strain in the physiological range is typically selected, and the sample is cycled between an initial state and the target value until rupture occurs. The number of cycles to failure is the fatigue life, and is usually dependent on the stress or strain applied each cycle as well as the frequency of loading (strain rate). If enough samples are tested using a range of target values, then a graph of "load vs number of cycles to failure" can be constructed (referred to as an S-N curve). This will allow researchers to predict the fatigue life of a tissue or construct given the expected loading regimen. Tissue failure for materials such as bone or bone substitutes may be obvious. For soft tissues, a clear definition of failure must first be identified. In cartilage constructs, for example, failure could be defined as the appearance of surface fissures. Tests to failure, rather than fatigue, are characterized by a single application of load at a desired strain rate, increased until failure occurs in tension, compression, or shear.

3.6. In Situ *Characterization of Graft-Repair Tissue*

The ultimate goal of tissue engineering is the implantation of the cell-material constructs into the body. If the construct becomes well-integrated with surrounding tissue and progressively achieves functionality like the original native tissue, it can be deemed a success. Assessment of the biomechanical properties of the evolving graft, as well as other measures (e.g., histological examination) is important for documenting the ultimate success of the repair. For clinical applications, there is a critical need for the development of nondestructive, minimally invasive biomechanical measurement techniques. In the case of bone-replacement constructs, X-rays can be used to evaluate trabecular structure. However, soft-tissue structure is not so easily imaged. Although MRI technology has advanced dramatically during the past decade, biomechanical assessment is not possible with this modality, and it is necessary to use minimally invasive contact methods for such *in situ* measurements.

Several indentation probes have been developed for clinical biomechanical assessment of cartilage during routine arthroscopic examination *(4,48)* (**Fig. 3A**). These probes are designed to characterize the mechanical stiffness of cartilage repair grafts and for the diagnosis of cartilage degeneration in osteoarthritis. The use of *in situ* indentation instruments for the estimation of the tissue's Young's modulus has recently been described *(49)*. Another probe that measures dynamic compressive and shear stiffness of cartilage has also been developed *(50)*. The choice of such a probe and the use of an indentation modality must be made with caution, since developing tissue constructs may not be able to withstand the force of indentation testing (*see* **Note 9**).

Other probes under development focus on the electromechanical and electrical impedance properties of tissue *(51,52)* (**Fig. 3B,C**). Tissue impedance is influenced by the concentration of charged molecules within the ECM (e.g., proteoglycans) and the tissue's porosity and water content, properties that change with construct growth, repair, and degeneration. Probe application of a small electrical current into tissue constructs may also induce a mechanical stress within the ECM that is measurable by the probe. The current induces intratissue fluid flow and micromechanical motions of the developing ECM, causing a current-generated stress that also depends on ECM charge density, hydraulic permeability, and mechanical properties. Multiple electrode contacts on such probes (**Fig. 3C**) allow current application at several spatial wavelengths across the construct surface, thus enabling evaluation of tissue properties at various depths into the tissue.

3.7. Summary

Material testing is a fundamental tool for evaluating the mechanical functionality of cell-seeded constructs with respect to development of neo-tissue,

or predicting structural stability when placed in a loading environment. The methods outlined in this chapter are designed to first allow the reader to select testing parameters that best represent the ultimate functional mode of the cell-seeded construct. Then, simple testing in compression, tension, shear, indentation, or electromechanical means may be performed to establish tissue stiffness and other physical properties associated with normal tissue function. Evaluation of mechanical properties *in situ* extends the characterization of construct development to environments in which ultimate failure or success will be determined. In this manner, cell-seeded construct development or degradation may be closely monitored at all time-points as an indicator of neo-tissue accumulation or remodeling in the cell/scaffold system. Diagnostic testing protocols may also be modified to apply non-destructive loading as a means of conditioning cell-seeded constructs in vitro. Cell signaling via mechanotransduction may be utilized to increase or modify biosynthesis, controlling ECM accumulation prior to implantation.

4. Notes

1. In vitro measurements may be performed using living tissue immersed in culture medium. Testing of previously frozen specimens requires the use of protease inhibitors to prevent degradation of the ECM during testing.
2. Micrometers or calipers may be used for dimensioning samples. However, accuracy may be compromised when samples are deformable. Feedback devices (e.g., resistance or voltage sensors) will help to identify when the measuring device is in contact with sample surfaces. The diameter of small cylindrical samples may be determined via a laser micrometer.
3. Sample thickness may also be determined using the testing apparatus. Zero strain can be defined by the position at which the testing platens produce a tare load in the specimen. Specimens must be completely immersed in appropriate medium or buffer for mechanical testing.
4. The upper platen may be fixed to the load cell if the weight of the platen affects the response of the sample to dynamic compression.
5. Unconfined compression: Test platens should be rigid and impermeable; low friction between specimen and platen will allow for appropriate radial expansion.
6. Confined compression: The upper platen must be porous, but should not deform during testing. Porous high-density or ultra-high mol-wt polyethylene (pore sizes of ~50–100 µm) are sufficient for most constructs.
7. Confined compression: Displacement control has an advantage over load control —stress relaxation is 4× quicker than creep. Although load control may mimic physiologic loading conditions, displacement and load control are equivalent for deriving intrinsic material properties.
8. For shear measurements, specimens are sometimes glued to platens to prevent slipping. However, glues are often toxic to cell-seeded constructs. Therefore, platens with a rough surface will be useful. In addition, a 5–10% static offset compression may be needed to grip the specimen.

9. Indentation tests may be needed for complex, in vivo tissue geometry (e.g., cartilage on bone in the intact joint). However, when using small-diameter indentors with non-ideal construct geometries, interpretation of time-dependent indentation data to derive intrinsic material properties may be difficult. The ability to remove specimens for in vitro testing is advantageous when possible.

References

1. Butler, D. L., Goldstein, S. A., and Guilak, F. (2000) Functional tissue engineering: the role of biomechanics. *J. Biomech. Eng.* **122(6),** 570–575.
2. Athanasiou, K. A., Zhu, C., Lanctot, D. R., Agrawal, C. M., and Wang, X. (2000) Fundamentals of biomechanics in tissue engineering of bone. *Tissue Eng.* **6(4),** 361–381.
3. Buschmann, M. D., Gluzband, Y. A., Grodzinsky, A. J., Kimura, J. H., and Hunziker, E. B. (1992) Chondrocytes in agarose culture synthesize a mechanically functional extracellular matrix. *J. Orthop. Res.* **10(6),** 745–758.
4. Lyyra, T., Jurvelin, J., Pitkanen, P., Vaatainen, U., and Kiviranta, I. (1995) Indentation instrument for the measurement of cartilage stiffness under arthroscopic control. *Med. Eng. Phys.* **17,** 395–9.
5. Mak, A. F., Lai, W. M., and Mow, V. C. (1987) Biphasic indentation of articular cartilage—I. Theoretical analysis. *J. Biomech.* **20(7),** 703–714.
6. Frank, E. H. and Grodzinsky, A. J. (1987) Cartilage electromechanics—II. A continuum model of cartilage electrokinetics and correlation with experiments. *J. Biomech.* **20(6),** 629–639.
7. Lai, W. M., Hou, J. S., and Mow, V. C. (1991) A triphasic theory for the swelling and deformation behaviors of articular cartilage. *J. Biomech. Eng.* **113(3),** 245–258.
8. Ehlers, W. and Markert, B. (2001) A linear viscoelastic biphasic model for soft tissues based on the theory of porous media. *J. Biomech. Eng.* **123(5),** 418–424.
9. DiSilvestro, M. R., Zhu, Q., and Suh, J. K. (2001) Biphasic poroviscoelastic simulation of the unconfined compression of articular cartilage: II—Effect of variable strain rates. *J. Biomech. Eng.* **123(2),** 198–200.
10. Chang, S. C., Rowley, J. A., Tobias, G., Genes, N. G., Roy, A. K., Mooney, D. J., et al. (2001) Injection molding of chondrocyte/alginate constructs in the shape of facial implants. *J. Biomed. Mater. Res.* **55(4),** 503–511.
11. Mauck, R. L., Soltz, M. A., Wang, C. C., Wong, D. D., Chao, P. H., Valhmu, W. B., et al.(2000) Functional tissue engineering of articular cartilage through dynamic loading of chondrocyte-seeded agarose gels. *J. Biomech. Eng.* **122(3),** 252–260.
12. Kisiday, J. D., Jin, M., Hung, H., Kurz, B., Semino, C., Zhang, S., and et al. (2002) Self-assembling peptide hydrogel fosters chondrocyte extracellular matrix production and cell division: implications for cartilage tissue repair. *PNAS* **99(15),** 9996–10,001.
13. Glowacki, J. (2000) In vitro engineering of cartilage. *J. Rehabil. Res. Dev.* **37(2),** 171–177.
14. Goldstein, S. A., Patil, P. V., and Moalli, M. R. (1999) Perspectives on tissue engineering of bone. *Clin. Orthop.* **367 Suppl,** S419–S423.

15. Woo, S. L., Hildebrand, K., Watanabe, N., Fenwick, J. A., Papageorgiou, C. D., and Wang, J. H. (1999) Tissue engineering of ligament and tendon healing. *Clin. Orthop.* **367 Suppl,** S312–S323.

16. Donahue, T. L., Gregersen, C., Hull, M. L., and Howell, S. M. (2001) Comparison of viscoelastic, structural, and material properties of double-looped anterior cruciate ligament grafts made from bovine digital extensor and human hamstring tendons. *J. Biomech. Eng.* **123(2),** 162–169.

17. Gardiner, J. C. and Weiss, J. A. (2001) Simple shear testing of parallel-fibered planar soft tissues. *J. Biomech. Eng.* **123(2),** 170–175.

18. Eckstein, F., Reiser, M., Englmeier, K. H., and Putz, R. (2001) In vivo morphometry and functional analysis of human articular cartilage with quantitative magnetic resonance imaging—from image to data, from data to theory. *Anat. Embryol.* **203(3),** 147–173.

19. Frank, E. H. and Grodzinsky, A. J. (1987) Cartilage electromechanics—I. Electrokinetic transduction and the effects of electrolyte pH and ionic strength. *J. Biomech.* **20(6),** 615–627.

20. Vunjak-Novakovic, G., Martin, I., Obradovic, B., Treppo, S., Grodzinsky, A. J., Langer, R., and et al. (1999) Bioreactor cultivation conditions modulate the composition and mechanical properties of tissue-engineered cartilage. *J. Orthop. Res.* **17(1),** 130–138.

21. Freed, L. E., Langer, R., Martin, I., Pellis, N. R., and Vunjak-Novakovic, G. (1997) Tissue engineering of cartilage in space. *Proc. Natl. Acad. Sci. USA* **94(25),** 13,885–13,890.

22. Lee, C. R., Breinan, H. A., Nehrer, S., and Spector, M. (2000) Articular cartilage chondrocytes in type I and type II collagen-GAG matrices exhibit contractile behavior in vitro. *Tissue Eng.* **6(5),** 555–565.

23. Klisch, S. M. and Lotz, J. C. (2000) A special theory of biphasic mixtures and experimental results for human annulus fibrosus tested in confined compression. *J. Biomech. Eng.* **122(2),** 180–188.

24. Fortin, M., Soulhat, J., Shirazi-Adl, A., Hunziker, E. B., and Buschmann, M. D. (2000) Unconfined compression of articular cartilage: nonlinear behavior and comparison with a fibril-reinforced biphasic model. *J. Biomech. Eng.* *122*(**2**), 189–195.

25. Stammen, J. A., Williams, S., Ku, D. N., and Guldberg, R. E. (2001) Mechanical properties of a novel PVA hydrogel in shear and unconfined compression. *Biomaterials* **22(8),** 799–806.

26. Catanese, J. 3rd, Featherstone, J. D., and Keaveny, T. M. (1999) Characterization of the mechanical and ultrastructural properties of heat-treated cortical bone for use as a bone substitute. *J. Biomed. Mater. Res.* **45(4),** 327–336.

27. Cartmell, J. S. and Dunn, M.G. (2000) Effect of chemical treatments on tendon cellularity and mechanical properties. *J. Biomed. Mater. Res.* **49(1),** 134–140.

28. Fedewa, M. M., Oegema, Jr, T. R., Schwartz, M. H., MacLeod, A., and Lewis, J. L. (1998) Chondrocytes in culture produce a mechanically functional tissue. *J. Orthop. Res.* **16(2),** 227–236.

29. Guilak, F., Ratcliffe, A., Lane, N., Rosenwasser, M. P., Mow, V. C. (1994) Mechanical and biochemical changes in the superficial zone of articular cartilage in canine experimental osteoarthritis. *J. Orthop. Res.* **12(4),** 474–484.

30. Stading, M. and Langer, R. (1999) Mechanical shear properties of cell-polymer cartilage constructs. *Tissue Eng.* **5(3),** 241–250.

31. Frank, E. H., Jin, M., Loening, A. M., Levenston, M. E., and Grodzinsky, A. J. (2000) A versatile shear and compression apparatus for mechanical stimulation of tissue culture explants. *J. Biomech.* **33(11),** 1523–1527.

32. Jin, M. and Grodzinsky, A. J. (2001) The effect of electrostatic interactions between glycosaminoglycans on the shear stiffness of cartilage: a molecular model and experiments. *Macromolecules* **34,** 8330–8339.

33. Anderson, D. R., Woo, S. L., Kwan, M. K., and Gershuni, D. H. (1991) Viscoelastic shear properties of the equine medial meniscus. *J. Orthop. Res.* **9(4),** 550–558.

34. Simon, W. H., Mak, A. F., and Spirt, A. A. (1989) The effect of shear fatigue on bovine articular cartilage. *J. Orthop. Res.* **8(1),** 86–93.

35. Jones, W. R., Ting-Beall, H. P., Lee, G. M., Kelley, S. S., Hochmuth, R. M., and Guilak, F. (1999) Alterations in the Young's modulus and volumetric properties of chondrocytes isolated from normal and osteoarthritic human cartilage. *J. Biomech.* **32(2),** 119–127.

36. Rotsch, C., Jacobson, K., and Radmacher, M. (1999) Dimensional and mechanical dynamics of active and stable edges in motile fibroblasts investigated by using atomic force microscopy. *Proc. Natl. Acad. Sci. USA* **96(3),** 921–96.

37. Bausch, A. R., Ziemann, F., Boulbitch, A. A., Jacobson, K., and Sackmann, E. (1998) Local measurements of viscoelastic parameters of adherent cell surfaces by magnetic bead microrheometry. *Biophys. J.* **75(4),** 2038–2049

38. Eisenberg, S. R. and Grodzinsky, A. J. (1985) Swelling of articular cartilage and other connective tissues: electromechanochemical forces. *J. Orthop. Res.* **3(2),** 148–159.

39. Danto, M. I. and Woo, S.-L. (1993) The mechanical properties of skeletally mature rabbit anterior cruciate ligament and patellar tendon over a range of strain rates. *J. Orthop. Res.* **11(1),** 58–67.

40. Freeman, P. M., Natarajan, R. N., Kimura, J. H., and Andriacchi, T. P. (1994) Chondrocyte cells respond mechanically to compressive loads. *J. Orthop. Res.* **12(3),** 311–320.

41. Lee, D. A., Knight, M. M., Bolton, J. F., Idowu, B. D., Kayser, M. V., and Bader, D. L. (2000) Chondrocyte deformation within compressed agarose constructs at the cellular and sub-cellular levels. *J. Biomech.* **33(1),** 81–95.

42. Gray, M. L., Pizzanelli, A. M., Grodzinsky, A. J., and Lee, R. C. (1988) Mechanical and physiochemical determinants of the chondrocyte biosynthetic response. *J. Orthop. Res.* **6(6),** 777–792.

43. Sah, R. L., Kim, Y. J., Doong, J. Y., Grodzinsky, A. J., Plaas, A. H., and Sandy, J. D. (1989) Biosynthetic response of cartilage explants to dynamic compression. *J. Orthop. Res.* **7(5),** 619–636.

44. Jin, M., Frank, E. H., Quinn, T. M., Hunziker, E. B., and Grodzinsky, A. J. (2001) Tissue shear deformation stimulates proteoglycan and protein biosynthesis in bovine cartilage explants. *Arch. Biochem. Biophys.* **395(1),** 41–48.

45. Buschmann, M. D., Gluzband, Y. A., Grodzinsky, A. J., and Hunziker, E. B. (1995) Mechanical compression modulates matrix biosynthesis in chondrocyte/ agarose culture. *J. Cell Sci.* **108(Pt 4),** 1497–1508.

46. Ragan, P. M., Chin, V. I., Hung, H. H., Masuda, K., Thonar, E. J., Arner, E. C., et al. (2000) Chondrocyte extracellular matrix synthesis and turnover are influenced by static compression in a new alginate disk culture system. *Arch. Biochem. Biophys.* **383(2),** 256–264.

47. Ker, R. F. (1999) The design of soft collagenous load-bearing tissues. *J. Exp. Biol.* **202 Pt 23,** 3315–3124.

48. Niederauer, M. Q., Cristante, S., Niederauer, G. M., Wilkes, R. P., Singh, S. M., Messina, D. F., et al. (1998) A novel instument for quantitatively measuring the stiffness of articular cartilage. New Orleans, LA, ORS. Transactions of the Orthopaedic Research Society.

49. Toyras, J., Lyyra-Laitinen, T., Niinimaki, M., Lindgren, R., Nieminen, M. T., Kiviranta, I., et al. (2001) Estimation of the Young's modulus of articular cartilage using an arthroscopic indentation instrument and ultrasonic measurement of tissue thickness. *J. Biomech.* **34,** 251–256.

50. Appleyard, R. C., Swain, M. V., Khanna, S., and Murrell, G. A. (2001) The accuracy and reliability of a novel handheld dynamic indentation probe for analyzing articular cartilage. *Phys. Med. Biol.* **46,** 541–550.

51. Berkenblit, S. I., Frank, E. H., Salant, E. P., and Grodzinsky, A. J. (1994) Nondestructive detection of cartilage degeneration using electromechanical surface spectroscopy. *J. Biomech. Eng.* **116,** 384–392.

52. Treppo, S., Berkenblit, S. I., Bombard, D. L., Frank, E. H., and Grodzinsky, A. J. (1999) Physical diagnostics of cartilage degeneration, in *Advances in Osteoarthritis* (Tanaka, S. and Hamanishi, C., eds.), Springer-Verlag, Tokyo, pp. 59–73.